



University  
of Glasgow

Kremer, Katrin (2013) *Vesicular trafficking in Toxoplasma gondii*. PhD thesis.

<http://theses.gla.ac.uk/4753/>

Copyright and moral rights for this thesis are retained by the author

A copy can be downloaded for personal non-commercial research or study, without prior permission or charge

This thesis cannot be reproduced or quoted extensively from without first obtaining permission in writing from the Author

The content must not be changed in any way or sold commercially in any format or medium without the formal permission of the Author

When referring to this work, full bibliographic details including the author, title, awarding institution and date of the thesis must be given

# **Vesicular Trafficking in *Toxoplasma gondii***

by

Dipl.Biol.

Katrin Kremer

Submitted in fulfilment of the requirements for the  
Degree of Doctor of Philosophy

Institute of Infection, Immunity & Inflammation  
College of Medical, Veterinary & Life Science  
University of Glasgow

## Abstract

*Toxoplasma gondii* is an obligate intracellular protozoan parasite with a worldwide prevalence. Together with the causative agent of malaria (*Plasmodium falciparum*) and other medically important pathogenic parasites it belongs to the phylum of the Apicomplexa. Besides identifiable eukaryotic organelles, apicomplexan parasites differ from other eukaryotic cells by an extra set of specialised secretory organelles (micronemes, rhoptries and dense granules), that are sequentially secreted during invasion of the host cell. Upon host cell contact the apically located micronemes are the first organelles to be released and contain crucial virulence factors that are secreted.

In order to systematically analyse vesicular traffic with a special focus on the secretory pathway of rhoptry and microneme proteins the ddFKBP system was used to perform a systematic analysis of Rab proteins in *Toxoplasma gondii*. Rab proteins are small GTP-binding proteins that are involved in targeting and fusion of vesicles from a donor to an acceptor membrane. Whereas higher eukaryotes like human cells encode more than 60 different Rab proteins apicomplexan parasites possess only a reduced core set of Rab proteins.

Performing co-localisation studies with generated parasite lines expressing ddFKBPMyc-tagged versions of Rab1A, 1B, 2, 4, 5A, 5C, 7, 18 and Rab5B-ddFKBPHA revealed, that all these Rabs localise to the early secretory pathway (Rab1B, 2 and 18), the Golgi (Rab4), or the late secretory pathway (Rab5A, Rab5B, Rab5C and Rab7). No exact localisation could be defined for Rab1A.

Rab5A and Rab5C, normally involved in endocytic uptake, were identified as important regulators of traffic to micronemes and rhoptries in *Toxoplasma gondii*, using an overexpression screen of Rabs and the analysis of trans-dominant mutants of promising candidates.

Intriguingly, some microneme proteins could be found to traffic independently on functional Rab5A and Rab5C, indicating the existence of independent transport routes to micronemes, which again indicates that apicomplexans have remodelled Rab5-mediated vesicular traffic into a secretory system that is essential for host cell invasion.

By using two-colour super-resolution stimulated emission depletion (STED) microscopy, distinct localisations of independent microneme proteins could be verified. This demonstrated that micronemal organelles are organised in distinct subsets or subcompartments.

Given these results, it can be assumed that apicomplexan parasites modify classic regulators of the endocytic system to carry out essential parasite-specific roles in the biogenesis of their unique secretory organelles.

# Table of Contents

Title page .....	.....
Abstract .....	ii
List of Tables .....	vii
List of Figures .....	vii
Acknowledgements .....	x
Author's Declaration .....	xii
Abbreviations/ Definitions .....	xiii
1. Introduction .....	1
1.1. Overview about <i>Toxoplasma gondii</i> .....	1
1.1.1 Clinical relevance of <i>T.gondii</i> .....	1
1.1.2. The life cycle of <i>T.gondii</i> .....	2
1.1.3. <i>Toxoplasma gondii</i> as a model organism .....	4
1.2. The ddFKBP system .....	5
1.3. Morphology and organelles of <i>T.gondii</i> .....	7
1.3.1. Endosymbiotic organelles: Mitochondrion and Apicoplast .....	7
1.3.2. Acidocalcisome-like organelles .....	8
1.3.3. Endosomal-like compartments (ELCs): proM2AP, VP1 and CPL compartment .....	8
1.3.4. Apical structure and secretory organelles: Apical complex, IMC, micronemes, rhoptries and dense granules .....	10
1.4. The lytic cycle of <i>T.gondii</i> .....	13
1.4.1. Gliding and Invasion .....	13
1.4.2. Replication and Egress .....	16
1.5. Vesicular transport in higher eukaryotes .....	17
1.5.1. Vesicle formation, transport and fusion .....	18
1.5.2. The endocytic pathway .....	19
1.5.3. Biosynthetic/Secretory pathway .....	20
1.6. Rab proteins .....	22
1.6.1 G-proteins and the functional cycle of Rab proteins .....	22
1.6.2. Conserved domains of Rab proteins .....	24
1.6.3. The role of selected Rab GTPases in higher eukaryotes .....	25
1.6.4. How Rab proteins fulfil their functions .....	29
1.7. Secretory proteins in <i>T.gondii</i> .....	32
1.7.1. Microneme proteins .....	32
1.7.2. Rhoptry proteins .....	35
1.7.3. Dense Granule proteins .....	36
1.8. Protein transport in <i>T.gondii</i> .....	36
1.8.1. Protein transport to the endosymbiotic organelles .....	36
1.8.2. Protein transport to the secretory organelles .....	37
1.9. Rab GTPases in Apicomplexan parasites .....	41
1. 10. Aim of this study .....	42
2. Materials and Methods .....	43
2.1. Consumables, biological and chemical reagents .....	43
2.2. Equipment .....	44
2.3. Buffers, Solutions and Media .....	46
2.3.1 General Buffers .....	46
2.3.2. DNA analysis .....	47
2.3.3. Protein analysis .....	47
2.3.4. Bacteria culture .....	48
2.3.5. Tissue culture .....	48
2.3.6. IFA .....	49

2.3.7. Electron microscopy .....	49
2.4. Organisms:.....	49
2.4.1. <i>T.gondii</i> strains .....	49
2.4.2. Cell lines used in tissue culture.....	50
2.4.3. Bacteria strains.....	50
2.5. Enzymes and Kits .....	50
2.6. Antibodies .....	51
2.6.1. Primary Antibodies.....	51
2.6.2. Secondary Antibodies.....	51
2.7. Plasmids.....	52
2.8. Oligonucleotide Primers.....	52
2.9. Molecular Biology.....	53
2.9.1. Purification of genomic DNA of extracellular <i>T.gondii</i> tachyzoites ...	53
2.9.2. Purification of RNA of extracellular <i>T.gondii</i> tachyzoites .....	54
2.9.3. Reverse Transcription .....	54
2.9.4. Polymerase Chain Reaction.....	54
2.9.5. Agarose gel electrophoresis .....	57
2.9.6. Extraction of DNA fragments from Agarose gel or out of solution ....	58
2.9.7. Ethanol precipitation of DNA.....	58
2.9.8. Determination of nucleic acid concentrations .....	58
2.9.9. Restriction endonuclease digests.....	59
2.9.10. Dephosphorylation of DNA fragments at the 5' end .....	59
2.9.11. Ligation of DNA fragments .....	59
2.9.12. Transformation of <i>E. coli</i> cells .....	59
2.9.13. Isolation of plasmid DNA from <i>E.coli</i> .....	60
2.10. Biochemistry .....	61
2.10.1. Preparation of parasite cell lysates for SDS page .....	61
2.10.2. Sodium dodecyl sulphate polyacrylamide gel electrophoreses (SDS-PAGE).....	61
2.10.3. Western blotting .....	62
2.10.4. Ponceau-S- staining.....	62
2.10.5. Immunoblotting .....	62
2.11. Cell biology .....	63
2.11.1. Culturing of <i>T.gondii</i> and host cells .....	63
2.11.2. Trypsin/EDTA treatment of host cells.....	64
2.11.3. Freezing and defrosting of <i>T.gondii</i> parasite stabilates.....	64
2.11.4. Determination of amount of parasites with Neubauer counting chamber .....	65
2.11.5. Transient transfection of <i>T.gondii</i> .....	65
2.11.6. Stable transfection of <i>T.gondii</i> .....	66
2.11.7. Isolation of single <i>T.gondii</i> tachyzoite clones via limited dilution...	67
2.11.8. Plaque-Assay.....	67
2.11.9. Replication assay .....	68
2.11.10. Invasion Assay.....	68
2.11.11. Egress Assay .....	69
2.11.12. Immunofluorescence assay .....	69
2.11.13. Stimulated emission depletion microscopy (STED) .....	70
2.11.14. Preparation of samples for electron microscopy.....	70
2.11.15. Pulse-chase analysis .....	70
2.12. Bioinformatics .....	71
2.12.1. Sequencing and sequence alignment .....	71
3. Localisation of Rab proteins in <i>T.gondii</i> .....	72
3.1. Introduction .....	72

3.2. 12 Rab GTPases are expressed in <i>T.gondii</i> tachyzoites .....	73
3.3. Amplification and verification of the amino acid sequence of TgRab1A, TgRab1B, TgRab2, TgRab4, TgRab5A, TgRab5B, TgRab5C, TgRab7 and TgRab18 .....	74
3.4. Generation of inducible parasite lines overexpressing TgRab proteins...	76
3.5. Screening for inducibility of ddFKBP tagged TgRab proteins .....	77
3.6. Localisation of TgRab1A,B,2,4,5A,B,C,7 and TgRab18 .....	80
3.6.1. Localisation of TgRab1B, TgRab2 and TgRab18 in pre-Golgi regions .	81
3.6.2. Localisation of TgRab4 mainly at the Golgi region .....	84
3.6.3. Localisation of TgRab1A.....	85
3.6.4. Localisation of TgRab5A,B,C and TgRab7 in post-Golgi regions .....	86
3.7. Summary and Conclusion.....	91
3.7.1. 12 Rab proteins are expressed in <i>T.gondii</i> tachyzoites .....	91
3.7.2. Localisation of TgRab1A,B,2,4,5A,B,C,7 and TgRab18 .....	91
4. Systematic phenotypisation of overexpressed RabGTPases and mutants .....	94
4.1. Introduction .....	94
4.2. Overexpression screen part I: Growth analysis .....	95
4.3. Overexpression screen part II: Secretory organelles .....	97
4.4. Generation and analysis of inducible parasite strains expressing trans-dominant Rab proteins. ....	99
4.4.1. Generation of inducible parasite lines expressing trans-dominant Rab proteins .....	99
4.4.2. Characterisation of dominant negative TgRab1A .....	101
4.4.3. Characterisation of dominant negative and constitutively active TgRab7 .....	103
4.4.4 Characterisation of dominant negative TgRab5B .....	115
4.5. Summary and Conclusions.....	117
4.5.1. Overexpression screens .....	117
4.5.2. Analysis of inducible parasite strains expressing trans-dominant Rab proteins .....	118
5. Characterisation of TgRab5A and TgRab5C.....	121
5.1. Introduction .....	121
5.2. Inducibility and proliferation ability of parasites expressing dominant negative TgRab5A and TgRab5C .....	121
5.2.1. Growth analysis.....	122
5.3. Phenotypic characterisation of parasites expressing ddFKBPMycRab5A(wt), 5C(wt), 5A(N158I) and 5C(N153I) .....	123
5.3.1. Replication .....	123
5.3.2. Egress .....	124
5.3.3. Invasion .....	125
5.3.4. Analysis of secretory organelles .....	127
5.4. Further characterisation of TgRab5A(N158I).....	136
5.4.1. MIC3 processing in ddFKBPRab5A(N158I) expressing parasites.....	136
5.4.2. Other organelles.....	139
5.4.3. Organellar effects on ultrastructural level .....	141
5.5. Summary and Conclusions.....	146
6. Stimulated Emission Depletion (STED) microscopy on RH <sup>hxgprt</sup> - parasites to investigate, if subpopulations of micronemes exist .....	149
6.1. Introduction .....	149
6.2. Single-colour STED analysis.....	150
6.3. Two-colour STED analysis .....	152
6.3. Two-colour STED analysis with thin- sectioned samples.....	154
6.4. Summary and conclusions.....	156

7. Discussion .....	158
7.1 Rab proteins and their potential functions in <i>T.gondii</i> .....	159
7.1.1. Rab proteins of the early secretory pathway and the Golgi.....	159
7.1.2. Rab proteins of the late secretory pathway .....	161
7.2. Distinct transport routes to the micronemes .....	166
7.3 Future work .....	170
7.3.1. Investigating TgRab functions .....	170
7.3.2. Functionally different microneme subset .....	171
References .....	<b>Error! Bookmark not defined.</b>

## List of Tables

Table 2-1: Reaction mix of a general PCR reaction .....	55
Table 2-2: Thermocycler-program for general PCR reactions. ....	55
Table 2-3: PCR reaction using the megaprimer .....	56
Table 2-4: Thermocycler-program for mutagenic PCR reactions using the megaprimer. ....	57
Table 3-1: The 15 predicted Rab proteins in <i>T.gondii</i> and their orthologs in other apicomplexan species. ....	74

## List of Figures

Figure 1-1: Life cycle of <i>Toxoplasma gondii</i> . ....	4
Figure 1-2: Mode of operation of the ddFKBP system.....	6
Figure 1-3: The origin of the apicoplast. ....	8
Figure 1-4: Morphology of <i>Toxoplasma gondii</i> . ....	12
Figure 1-5: The lytic cycle of a <i>T.gondii</i> tachyzoite.. ....	13
Figure 1-6: The glideosome at the moving junction (MJ).. ....	15
Figure 1-7: Steps of Invasion.....	16
Figure 1-8: Vesicular trafficking cycle. ....	19
Figure 1-9: Vesicular transport between the organelles of a eukaryotic cell. ....	22
Figure 1-10: The functional Rab cycle.....	23
Figure 1-11: Putative domains of YPT7.....	24
Figure 1-12: Localisation of selected Rab proteins in vesicular trafficking in a mammalian cell. ....	29
Figure 1-13: Rab proteins within the vesicular trafficking. ....	31
Figure 1-14: Toxoplasma microneme protein domains and their interactions. ....	34
Figure 1-15: Hypothised model of microneme protein maturation and transport to their target organelles, modified from: (Parussini, Coppens et al. 2010). ....	39
Figure 1-16: Hypothised model of microneme and rhoptry protein maturation and transport to their target organelles, modified from: (Sloves, Delhaye et al. 2012).. ....	40
Figure 3-1. Alignment of the nine amplified Rab-like proteins in <i>T. gondii</i> .....	75
Figure 3-2: Overview of parasite strains expressing ddFKBP-tagged Rab proteins.. .....	79

Figure 3-3: Overview of antibodies and marker proteins applied to analyse the localisation of TgRab proteins in <i>T. gondii</i> tachyzoites. ....	81
Figure 3-4: Localisation of Rab1B, Rab2 and Rab18.....	83
Figure 3-5: Localisation of Rab4.....	84
Figure 3-6: Localisation of Rab1A.....	85
Figure 3-7: Localisation of TgRab7.....	86
Figure 3-8: Localisation of Rab5A, Rab5B and Rab5C.....	89
Figure 3-9: Co-localisation analysis of TgRab5A with TgRab5C and TgRab5B....	90
Figure 4-1: Parasite growth is inhibited by overexpression of TgRab2,4,5A,B and C. ....	96
Figure 4-2: Overexpression of TgRab5A and C causes mislocalisation of only a subset of microneme proteins. ....	98
Figure 4-3: Diagram showing the sequence site of setting the point mutation to generate a dominant negative (DN) version of a Rab protein and its cellular consequence. ....	100
Figure 4-4: Regulation and growth analysis of ddFKBPmycRab1A(N126I).....	102
Figure 4-5: The presence of ddFKBPmycRab7(G18E) or ddFKBPmycRab7(N124I) within <i>T. gondii</i> tachyzoites is regulable. ....	104
Figure 4-6: ddFKBPmyc tagged constitutively active TgRab7 is localised at the ELC region.....	105
Figure 4-7: Parasites expressing the constitutively active version of TgRab7 showed a defect in their growth ability.....	106
Figure 4-8 : Parasites expressing ddFKBPmycRab7(G18E) were affected in their replication ability.....	107
Figure 4-9: Neither overexpression of wild type Rab7 (wt) nor expression of its constitutively active version (G18E) was affecting the ability to egress host cells. ....	109
Figure 4-10. Parasites expressing the constitutively active version of TgRab7 showed a reduced invasion ability. ....	110
Figure 4-11: Expression of the constitutively active version of TgRab7 was not affecting micronemes or rhoptries.....	111
Figure 4-12: Expression of ddFKBPmycRab7(G18E) led to a small effect on CPL localisation.....	112
Figure 4-13: CPL processing is unaffected in ddFKBPmycRab7(G18E) expressing parasites.....	114
Figure 4-14: Parasites expressing ddFKBPmycRab5B(N152I) showed a defect in their growth ability. ....	116
Figure 4-15: Expression of dominant negative TgRab5B causes no mislocalisation of microneme and rhoptry proteins.....	117
Figure 5-1: The presence of ddFKBPmycRab5A(N158I) or ddFKBPmycRab5C(N153I) within <i>T. gondii</i> tachyzoites is regulable. ....	122
Figure 5-2 : Expression of ddFKBPmycRab5A(N158I) and ddFKBPmycRab5C(N153I) results in a severe growth phenotype. ....	123
Figure 5-3 : No significant differences in replication were detected when parasites expressing ddFKBPmycRab5A(wt),5C(wt),5A(N158I) and 5C(N153I) were analysed.....	124

Figure 5-4 : Both overexpression and dominant negative expression of TgRab5A and TgRab5C led to a decrease in the egress ability.....	125
Figure 5-5: Both overexpression and dominant negative expression of TgRab5A and TgRab5C led to a severe invasion defect. ....	127
Figure 5-6: Parasites overexpressing ddFKBPmycRab5A, ddFKBPmycRab5C, ddFKBPmycRab5A(N158I) or ddFKBPmycRab5C(N153I) led to mislocalisation of only a subset of microneme proteins (MIC3, MIC8 and MIC11). ....	130
Figure 5-7: Time course analysis of parasites expressing ddFKBPmycRab5A, ddFKBPmycRab5C, ddFKBPmycRab5A(N158I) and ddFKBPmycRab5C(N153I)....	134
Figure 5-8: Expression of the dominant negative version of TgRab5A or TgRab5C is causing mislocalisation of rhoptry proteins.....	135
Figure 5-9: Microneme processing and organisation of the ELC, CPL, is unaffected in ddFKBPmycRab5A(N158I) expressing parasites. ....	138
Figure 5-10 : Expression of dominant negative ddFKBPmycRab5A(N158I) shows no negative effects on organelle formation and distribution. ....	141
Figure 5-11: Less micronemes and no rhoptries were detectable in ddFKBPmycRab5A(N158I) parasites grown in presence of Shield-1 in electron microscopic samples. ....	143
Figure 5-12: Over 50% less micronemes were detected when expressed ddFKBPmycRab5A(N158I) is stabilised in <i>T.gondii</i> tachyzoites.. ....	144
Figure 5-13: M2AP distribution in ddFKBPmycRab5A(N158I) expressing parasites imaged with ImmunoEM. ....	145
Figure 6-1: STED-microscopy.....	150
Figure 6-2: Single-colour STED analysis reveals different localisation patterns of microneme proteins in RH <sup>hxgprt-</sup> parasites.....	152
Figure 6-3: Two-colour STED analysis reveals different localisations of microneme proteins in RH <sup>hxgprt-</sup> parasites.....	153
Figure 6-4: Two-colour STED images of typical microneme co-localisation patterns in 100nm ultrathin sections. ....	155
Figure 7-1: Model of Rab locations and potential functions in <i>T.gondii</i> . ....	169

## Acknowledgements

First of all I am grateful to my supervisor Dr. Markus Meissner for giving me the opportunity to do my PhD in his laboratory. Thanks to his supervision I could experience the creativity and enthusiasm research is about. I am also thankful for his support and sympathy especially during the last three years.

The Meissner labs, both in Heidelberg and in Glasgow, were great groups to be part of and I want to thank all present and past members for their help and support whenever it was needed. Together with the past members of the Frischknecht group I enjoyed the time inside and outside the lab. Thank you.

Special thanks to Manuel, Manuela, Carolina, Saskia, Nicole, Jo, Gurman, Caroline, Alli and also to Markus for looking after my parasites whenever I was away and for helping out whenever I wasn't allowed to get in contact with substances or parasites.

I also want to thank Sabine Mahler, Joanne Heng, Halley Flammer, Dirk Kamin and Eva Rittweger who contributed to some of the data presented in this work.

Thank you to the people from the Department of Parasitology in Heidelberg from way back when and to everyone on level 6 of the GBRC especially Jim and Fiona.

Many thanks to Clare, Jo and Gurman for proofreading parts of my thesis.

I am thankful to my former assessors from Heidelberg Prof. Michael Lanzer and Prof. Christine Clayton and my assessors from Glasgow Prof. Jeremy Mottram and Dr. Sonya Taylor for their sound advices and valuable suggestions.

Ein großes Dankeschön an Iwona, Hedda und Heiko Kremer für die enorme Unterstützung besonders in den schreibintensiven Monaten meiner Doktorarbeit. Auch Julia möchte ich hier dankend erwähnen, besonders für's Babysitten wenn Not am Mann war.

Ganz besonders möchte ich mich bei meinen Eltern und bei meinem Bruder bedanken ohne deren Unterstützung und Liebe ich nicht so weit gekommen wäre. DANKE!

Last but definitely not least I want to thank you Clemens for all your support and love and for giving me the most important "projects" of my life. THANK YOU!

## Author's Declaration

I, Katrin Kremer hereby declare that I am the sole author of this thesis and performed all of the work presented, with the following exceptions:

### Chapter 3:

- Sabine Mahler generated p5RT70DDmycRab1B-HXGPRT, p5RT70DDmycRab2-HXGPRT and p5RT70DDmycRab18-HXGPRT expressing parasite strains and performed fluorescence analyses and western blots with them under my supervision
- The construct p5RT70Rab5BHADD-HXGPRT was designed by Christopher Tonkin from the Walter and Eliza Hall Institute of Medical Research, Australia

### Chapter 4:

- Growth analyses of Rab1B, Rab2, Rab4 and Rab18 overexpressing parasites were done by Sabine Mahler under my supervision
- Some fluorescence analyses and pulse chase experiments were performed by Halley Flammer in collaboration with the group of Vernon Carruthers from the University of Michigan School of Medicine, USA
- Some fluorescence analyses of Rab5B were done by Joanne Heng

### Chapter 5:

- Pulse chase experiments were performed by Halley Flammer in collaboration with the group of Vernon Carruthers
- IEM and EM analysis was performed in collaboration with David Ferguson from the University of Oxford, United Kingdom.

### Chapter 6:

- STED analyses were performed by Eva Rittweger and Dirk Kamin in collaboration with the group of Stefan Hell from the Max Planck Institute for Biophysical Chemistry Göttingen, Germany and the German Cancer Research Center / BioQuant Heidelberg, Germany

## Abbreviations/ Definitions

A	ATPase
AMP	Adenosine monophosphat
ATP	Adenosine triphosphat
BLAST	Basic-Local-Alignment-Search-Tool
Ca	Calcium
CPL	Cathepsin-L-like protease
COP	Coat protein complex
dd	Destabilisation domain
DG	Dense granule
DMEM	Dulbecco's Modified Eagle's Medium
DN	Dominant negative
DNA	Deoxyribonucleic acid
ECF	East coast fever
EE	Early endosome
e.g.	Exempli gratia (for example)
EGF	Epidermal growth factor
ELC	Endosomal-like compartment
EM	Electron microscopy
ER	Endoplasmatic reticulum
GalNac	UDP-N-acetyl-D-galactosamine:polypeptide N-acetylgalactosaminyltransferase T1
GAP	GTPase activating protein
GDF	GDI dissociation factor
GDI	Guanine nucleotide dissociation inhibitor
GDP	Guanosine diphosphate
GEF	Guanine exchange factor
GGT	Geranylgeranyl tranferase
GMP	Guanosin monophosphat
GRASP	Golgi re-assembly stacking protein
GTP	Guanosine triphospate
HA	Hemagglutinin
HPM	Host plasma membrane
IEM	Immuno electron microscopy
IFA	Immunofluorescence analysis
ILV	Intralumenal vesicle
IMC	Inner membrane complex
IMP	Inosine monophosphat
ISG	Immature secretory granule
K	Potassium
kDa	Kilodalton
Kb	Kilobase
LDL	Low-density lipoprotein
LE	Late endosome

Mb	Megabase
MCS	Membrane contact sites
Mg	Magnesium
MJ	Moving junction
MLC	Myosin light chain
MPA	Mycophenolic acid
MT	Microtubule
Myo A	Myosin A
M2AP	MIC2 associated protein
NCBI	National Center for Biotechnology Information
nm	Nanometer
PBS	Phosphate buffered saline
PFA	Paraformaldehyde
PFP	Pore forming proteins
PI	Phosphoinositide
PLC	Plant like vacuole
PLP	Perforin-like protein
PM	Plasma membrane
POI	Protein of interest
PPM	Parasites plasma membrane
PVM	Parasitophorous membrane
PV	Parasitophorous vacuole
REP	Rab escort protein
RFP	Red fluorescent protein
RNA	Ribonucleic acid
SAG	Surface antigen
SDS-PAGE	Sodium dodecyl sulfate polyacrylamide gel electrophoresis
SRP	Signal recognition particle
SRS	SAG related sequence
Tg	Toxoplasma gondii
TGN	Trans-golgi network
TIM	Transporter inner membrane
TM	Transmembrane
TOC/TIC	Translocon at outer/inner envelope membrane of Chloroplast
TOM	Transporter outer membrane
VAC	Vacuolar compartment
VP1	Vacuolar-type H <sup>+</sup> -pyrophosphatase
WHO	World health organisation
wt	Wild type
XMP	Xanthosine monophosphat
YFP	Yellow fluorescent protein
μM	Micromolar
μm	Micrometer

# 1. Introduction

## 1.1. Overview about *Toxoplasma gondii*.

*Toxoplasma gondii* is a single-celled intracellular parasite first found over 100 years ago in the North African comb rat (Gundi; *Ctenodactylus gundi*) by Nicolle and Manceaux (1908) (Nicolle and Manceaux 1908). In 1932 it was discovered that *Toxoplasma gondii* (*T.gondii*) was the causative agent of an infectious disease (Robert-Gangneux and Darde 2012) and fifty years later the whole life cycle was fully understood (Dubey, Miller et al. 1970). *T.gondii* infections have been found in birds and warm blooded animals including humans all over the world and new host species are found constantly down to the present day (Hill, Chirukandoth et al. 2005). The prevalence of this highly successful parasite ranges from ordinary farm animals such as sheep, cows and pigs to the more exotic Australian Wallabies, Brazilian Agoutis (rodent) and sea mammals (Ashton 1979; Dubey, Sundberg et al. 1981; Oksanen, Tryland et al. 1998; Soares, Minervino et al. 2011). In contrast to the many species *T.gondii* is able to infect, under the current taxonomy only one species is reported for the *Toxoplasma* genus itself (Sibley and Boothroyd 1992). *T.gondii* belongs to the phylum of Apicomplexa, which comprise over 5000 species of protozoa. All of them have a unique organelle complex at the apical tip, named the apical complex, which gives the phylum its name (Tilney and Tilney 1996). The most clinically relevant representative of this phylum is *Plasmodium falciparum*, the causative agent of malaria in humans and every year over half a million people fall victim to this pathogen (WHO 2012). Because of its relatedness to *Plasmodium* and the ease of culturing and genetic manipulation, *T.gondii* is applied as a model organism for malaria research world-wide (see chapter 1.1.3.).

### 1.1.1 Clinical relevance of *T.gondii*

*T.gondii* is the causative agent of Toxoplasmosis and roughly one-third of the world's human population is infected with this parasite (Hill, Chirukandoth et al. 2005). In most cases infection is harmless and asymptomatic for healthy individuals although occasionally influenza-like symptoms have been observed. After the first immune reaction, *T.gondii* hides from the immune system by forming tissue cysts in the central nervous system and musculature. These cysts

can remain inactive for a lifetime within the infected person's body or can be reactivated at any time. Infection or cyst reactivation has major implications for immunocompromised patients, such as those with HIV or organ transplants (Robert-Gangneux and Darde 2012). In those individuals, the parasite can multiply without hindrance and damage the affected tissue. Without any treatment, lesions in the brain can lead to death. Furthermore, primary infection during pregnancy can be dangerous, if the parasite is transmitted from the mother to her unborn child. Depending on the point of time of the infection during pregnancy, the parasite can cause miscarriage or severe damage of the unborn child such as Chorioretinitis or Hydrocephalus (Martin 2001; Vutova, Peicheva et al. 2002). Infection with *Toxoplasma gondii* can be treated with a combination of pyrimethamin and sulfadoxin however, this treatment is not successful against encysted parasites. A vaccine for sheep is commercially available, which is based on the infection of an attenuated *Toxoplasma* strain (Toxovax®). Despite intense study, no drugs against tissue cysts and no vaccination, are currently available for humans.

### **1.1.2. The life cycle of *T.gondii***

Like many parasites, *T.gondii* can have a direct or an indirect life cycle and can replicate by asexual cell division or through a sexual cycle. This means, the parasite can complete its life cycle in its primary host (direct life cycle), but most often it infects intermediate hosts to gain a broader distribution and to increase the probability to be taken up by its primary host (indirect life cycle). The sexual reproduction is restricted to felids (primary host) (Figure 1-1). After ingestion of tissue cysts from an intermediate host or uptake of oocysts, sporozoites are released by destroying the cyst wall by gastric enzymes. After several generations of asexual replication within intestinal cells, differentiation into female macrogametes and male microgametes (Figure1: Gamogony) follows. They fuse into diploid zygotes with further development to oocysts, which are released with the feces of the cat. Oocysts can persist for several months with no drop in infectivity. Oocysts are approximately 10 µm x 15 µm and, after sporogony, contain two sporocysts with two sporozoites (6 µm x 8 µm) in each case. After an intermediate host ingests oocyst-contaminated food, sporozoites are released and penetrate intestinal cells allowing access to the bloodstream. This allows *T.gondii* to quickly reach target tissues where it invades and

replicates within cells of the central nervous tissue or musculature. This asexual replication is via an unusual method named endodyogeny (Figure 1-1), where two daughter cells form within one parental cell. The motile stages involved in this fast invasion/replication process are named tachyzoites (greek: tachos = fast). Tachyzoites are 8  $\mu\text{m}$  x 4  $\mu\text{m}$  and have a crescent shape (greek: toxon = bow). They are morphologically similar to sporozoites, however sporozoites have a higher number of unique apicomplexan secretory organelles at the apical tip (micronemes and rhoptries) (see 1.3.4.). Upon activation of the host's immune response, tachyzoites develop into bradyzoites, which are persistent tissue cyst forms. Within these tissue cysts *T.gondii* evades the host immune system. If the host immune system later becomes suppressed, bradyzoites can re-develop into tachyzoites. Bradyzoites replicate more slowly than tachyzoites (greek: brady = slowly), but possess energy reserves in the form of amylopectin granules (storage polysaccharide). Cyst formation occurs preferentially in the brain, eyes and musculature of the heart and skeleton. Uptake of these cysts by consumption by the definitive or an intermediate host completes the life cycle.

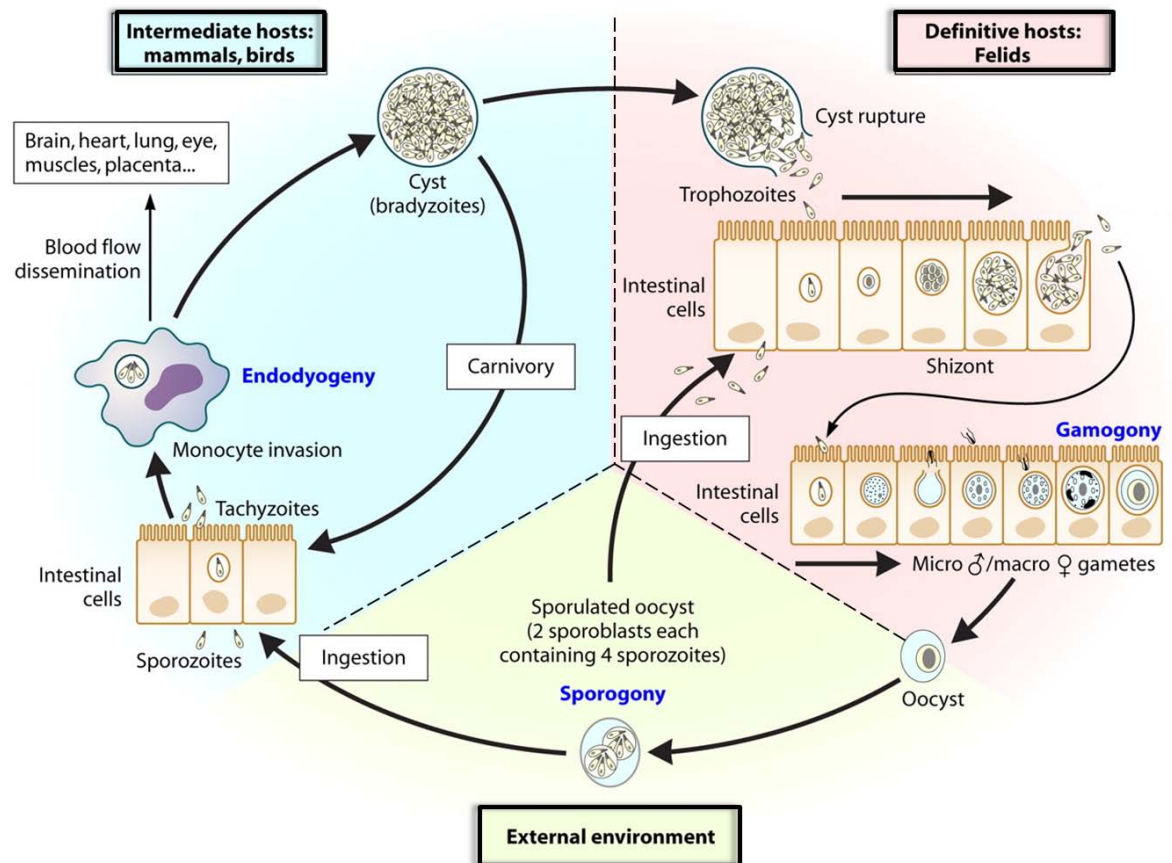


**Figure 1-1: Life cycle of *Toxoplasma gondii*.** After ingestion of oocysts from contaminated food or tissue cysts from infected animals, the parasite first multiplies asexually and then sexually (Gamogony) within intestinal cells of the definitive host (pink). Oocysts are released into the environment by the feces (grey) and taken up by the definitive host itself or by intermediate hosts. Within the intermediate host the parasites undergo multiple asexual replication cycles (Endodyogeny) within intestinal cells and via the blood and lymph system within cells of the central nervous system, heart, lungs placenta etc (blue). To evade the immune system of a healthy host, parasites (tachyzoites) develop into less reproductive stages (bradyzoites) and form persistent tissue cysts. The image is modified from: (Robert-Gangneux and Darde 2012).

### 1.1.3. *Toxoplasma gondii* as a model organism

*T. gondii* is widely used as a model organism in apicomplexan research. The parasite has several advantages over other members of this family. *T. gondii* replicates every 6-8 hours within the nucleated cells of warm blooded animals, making it very easy to culture compared to *Plasmodium*, which is restricted to certain cell types (e.g. hepatocytes, erythrocytes). Furthermore, *T. gondii* tachyzoites are five times bigger than *P. falciparum* which, in combination with reporter genes, makes intracellular localisation of a protein of interest (POI) and organellar biogenesis easy to analyse. Characterisation of the apical complex and the proteins of the invasion machinery in *T. gondii* have given insight into the mechanisms of gliding and active invasion in apicomplexan parasites. The

Toxoplasma genome has 80 Mb arranged on 14 chromosomes and it is fully sequenced. Since the asexual stage (tachyzoite) genome is haploid, phenotypisation of generated mutants or knock outs of certain genes is simplified. With the successful establishment of both transient and stable transfections with different selection markers in *T.gondii* (Donald and Roos 1993; Kim, Soldati et al. 1993; Sibley, Messina et al. 1994; Messina, Niesman et al. 1995; Soldati and Boothroyd 1995; Donald, Carter et al. 1996) this parasite has become the preeminent model organism in Apicomplexa research. Stable integration of plasmids into a gene locus is based on random integration via homologous recombination or integrative mutagenesis. Recently, the efficiency of this procedure has been increased through the generation of  $\Delta$ KU80 parasites (Fox, Ristuccia et al. 2009; Huynh and Carruthers 2009). Together with Ku70, Ku80 forms a heterodimer, which binds to double strand break ends and repairs DNA through non-homologous end joining. Deletion of Ku80 ( $\Delta$ Ku80) enables the integration of plasmid constructs into the genome exclusively by homologous recombination. Within the  $\Delta$ Ku80 parasite line, epitope tags or gene knock outs can be generated with relative ease. Since tachyzoites are haploid, essential genes cannot be directly removed requiring the construction of conditional expression systems. The tetracycline inducible system (Meissner, Schluter et al. 2002) has been successfully applied for several investigations. Another system proven to be useful for the characterisation of cytosolic proteins is the ddFKBP system (Herm-Goetz, Agop-Nersesian et al. 2007). A most recent new established recombination system in *T.gondii* is combining the advantages of the  $\Delta$ Ku80 and conditional systems (Andenmatten, Egarter et al. 2013). Here the two inactive fragments of a Cre recombinase are fused with rapamycin binding proteins FRB and FKBP. This allows the activity of Cre, which catalyses the excision of loxP site flanked DNA fragments, to be regulated.

## 1.2. The ddFKBP system

The ddFKBP system from Herm-Goetz, Agop Nersesian and co-workers is based on the interaction of rapamycin with FKBP (FK506 binding protein). Rapamycin is an immunosuppressant drug derived from bacteria (Vezina, Kudelski et al. 1975). Within cells it forms a complex with FKBP-12 and together they bind to the

rapamycin-binding domain of mTOR, FRB, (FKBP\*rapamycin\*FRB ternary complex) inhibiting its function (Banaszynski, Liu et al. 2005). mTOR regulates essential functions within the cell such as cell growth and proliferation by regulating protein synthesis (Hay and Sonenberg, 2004). In 2006 Banaszynski and colleagues engineered mutants of the human FKBP-12 which destabilise rapidly and constitutively in mammalian cells (Banaszynski, Chen et al. 2006). Additionally, they synthesized a rapamycin derivative called Shield-1 (Shld1), which is unable to bind mTOR. This system allows a protein of interest to be fused to the FKBP-12 mutant (destabilisation domain) and degraded as long as the ligand for this domain is missing. However, in presence of Shield-1 the fusion protein will not be targeted to the proteasome and is protected (shielded) from degradation (Figure 1-2). With the establishment of the ddFKBP system in *T.gondii* (Herm-Gotz, Agop-Nersesian et al. 2007) and *P.falciparum* (Armstrong and Goldberg 2007) a rapid and reversible method is available to analyse functions of essential genes in apicomplexan parasites.

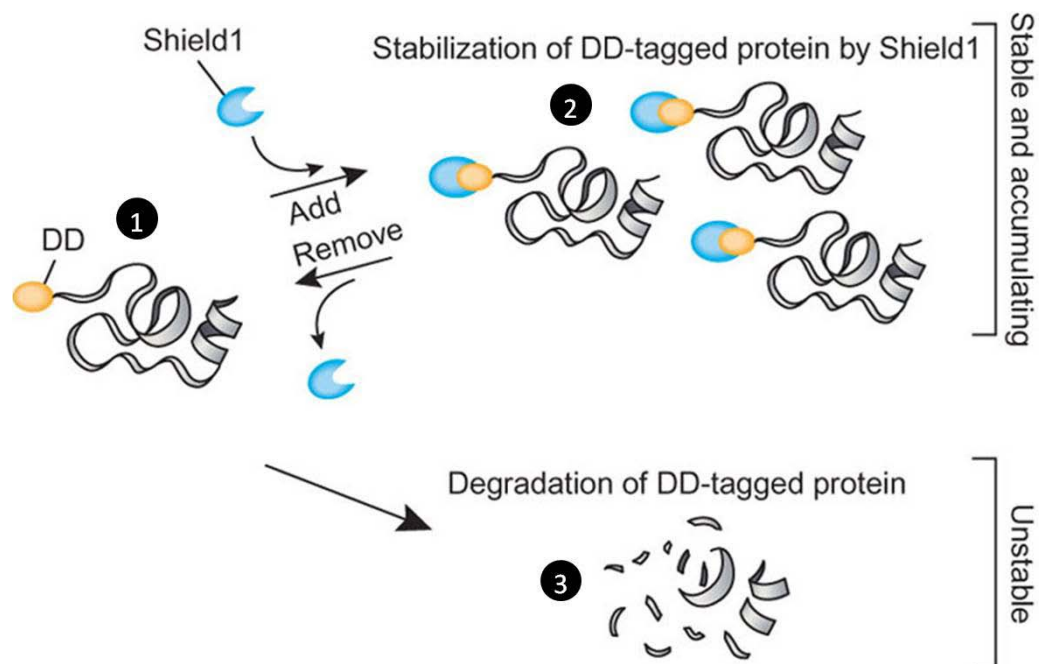


**Figure 1-2: Mode of operation of the ddFKBP system.** 1.) A protein of interest is fused to the destabilisation domain (DD). 2.) By adding the DD-ligand, Shield-1, the fusion protein becomes stabilised by protecting it from degradation. 3.) In the absence of Shield-1 the fusion protein is unstable and becomes degraded. The Figure is modified from: (Haugwitz, Nourzaie et al. 2008).

### **1.3. Morphology and organelles of *T.gondii*.**

Like other eukaryotic cells, *T.gondii* has a basic set of organelles including the nucleus, endoplasmic reticulum (ER), Golgi and mitochondrion. In addition, *T.gondii* has a number of specialised organelles which will be introduced here.

#### **1.3.1. Endosymbiotic organelles: Mitochondrion and Apicoplast**

Apicomplexans have two organelles originated from endosymbiosis, the mitochondrion and the apicoplast (Gardner, Hall et al. 2002; Parsons, DeRocher et al. 2007; Seeber and Soldati 2007). The *T.gondii* mitochondrion has, like other higher eukaryotes, two membranes and is believed to originate from primary endosymbiosis of an alpha - proteobacterium (Miyagishima 2005). The apicoplast in turn has 4 membranes and originated from two endosymbiosis events (secondary endosymbiosis) as described in Figure 1-3 (Köhler, Delwiche et al. 1997; Foth, Ralph et al. 2003; Waller, Keeling et al. 2003). Both organelles are semi-autonomous and have a circular genome (Wilson, Denny et al. 1996; Gray, Lang et al. 2004). At 6 - 7 kb, the apicomplexan mitochondrion genome is the smallest mitochondrion genome (Gray, Lang et al. 2004; Seeber, Limenitakis et al. 2008) and the apicoplast genome is, at 35 kb, the most reduced plastid genome discovered so far (Wilson and Williamson 1997). Furthermore, the apicoplast encodes only few proteins compared to its predicted proteome. For example, 32 protein encoding genes are found in the apicoplast of *P.falciparum*, however more than 450 proteins are predicted for the apicoplast proteome (Foth, Ralph et al. 2003; Sheiner and Striepen 2012). Although essential processes like fatty acid beta-oxidation, [Fe-S] biosynthesis, haem and pyrimidine biosynthesis and the citric acid cycle are found in the apicomplexan mitochondrion, it differs from the host mitochondria in some details (Seeber and Soldati 2007; Seeber, Limenitakis et al. 2008). The apicoplast has lost its photosynthetic ability, however some metabolic pathways are still present and essential for apicomplexa including the biosynthesis of fatty acids, haem and isoprenoids (Gardner, Hall et al. 2002; Vaishnava and Striepen 2006; Seeber and Soldati 2007). These processes are similar to their prokaryotic origin and different to higher eukaryotic cells like human cells. This makes these organelles and their metabolic pathways promising drug targets.

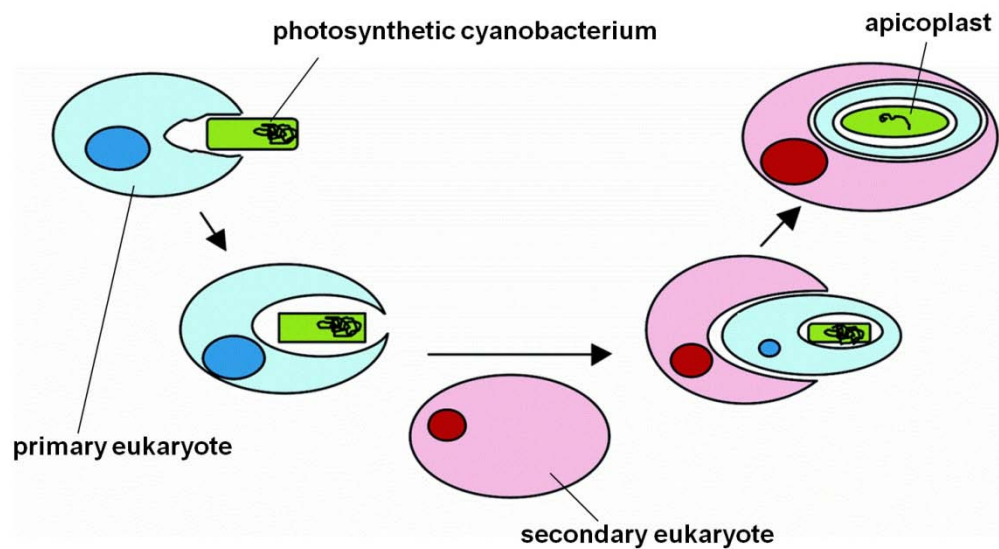


**Figure 1-3: The origin of the apicoplast.** During the primary endosymbiosis event, a primary eukaryote (blue) is taking up a photosynthetic cyanobacterium (green). The newly formed organism is then ingested by a secondary eukaryote (red) during a secondary endosymbiosis event. After that, the original primary eukaryote, with its cyanobacterium derived organelle, becomes the apicoplast by gene transfer and protein import. Modified from: (Surolia, Ramya et al. 2004).

### 1.3.2. Acidocalcisome-like organelles

Acidocalcisomes are electron-dense acidic organelles, rich in calcium and polyphosphate, which can be found in all kinds of cells, from bacteria to higher eukaryotes including human cells (Docampo, de Souza et al. 2005). In *T.gondii*, organelles have been purified which feature characteristics of acidocalcisomes. These acidocalcisome-like organelles show high concentrations of phosphorus, calcium and magnesium (Rodrigues, Ruiz et al. 2002). Additionally sodium, potassium, zinc, pyrophosphate and enzymes including  $\text{Ca}^{2+}$ -ATPase (TgA1), vacuolar-type  $\text{H}^{+}$ -pyrophosphatase (TgVP1), polyphosphatase and bafilomycin  $\text{A}_1$ -sensitive ATPase could be shown to present (Luo, Vieira et al. 2001; Rodrigues, Ruiz et al. 2002; Drozdowicz, Shaw et al. 2003). Besides the ER, acidocalcisome-like organelles are thought to be the major centres for intracellular calcium storage, which is an important regulator of secretory protein secretion and host cell invasion (Carruthers, Moreno et al. 1999).

### 1.3.3. Endosomal-like compartments (ELCs): proM2AP, VP1 and CPL compartment

In eukaryotes, endosomes are a central intersection between protein transport from the surface (endocytosis) and the secretory pathway from the Golgi. Intriguingly, no convincing evidence of endocytosis has been found in *T.gondii*,

but several reports describe the presence of endosomal-like compartments (ELCs).

### **1.3.3.1. TgVP1**

In 2003, a type I vacuolar proton translocating pyrophosphatase (TgVP1) was isolated in *T.gondii* (Drozdowicz, Shaw et al. 2003). Its function and localisation was assumed to be acidocalcisome related (see 1.3.2). Three years later, the localisation of TgVP1 was assumed to be the post-Golgi compartment where microneme protein (MIC) processing takes place (Harper, Huynh et al. 2006). However, recent data about TgVP1 suggests that this enzyme is a homologue to a vacuolar plant pump and is localised in a new apicomplexan organelle. Since a plant like aquaporin water channel (TgAQP1) was also localised to this "TgVP1 compartment", it was assumed to be a plant-like vacuole (PLV) (Miranda, Pace et al. 2010).

### **1.3.3.2. proM2AP**

Harper and colleagues analysed 2006 the precursor of the microneme protein M2AP (proM2AP) (Harper, Huynh et al. 2006). They found that fractions of proM2AP co-localised with the trans-Golgi network (TGN) marker TgGalNac-YFP [UDP-*N*-acetyl-D-galactosamine:polypeptide *N*-acetylgalactosaminyltransferase T1 fused to yellow fluorescent protein (Nishi and Roos, unpublished)] and TgRab51-HA [assumed to be an early endosome marker (Robibaro, Stedman et al. 2002)]. This led to the assumption that proM2AP localises to the TGN and early endosomes.

### **1.3.3.3. TgCPL**

In 2006 Harper and colleagues also described the enzyme Cathepsin-L-like protease (TgCPL), which partially co-localises with proM2AP and TgVP1 (Harper, Huynh et al. 2006). This protein, called TgCPL, is a homologue of cathepsin L, a lysosomal cysteine protease in higher eukaryotes (Spira, Stypmann et al. 2007). TgCPL was recently characterised as a maturase for the microneme proteins TgMIC3 and TgM2AP, which functions at low pHs (Parussini, Coppens et al. 2010). This led to the hypothesis that TgCPL marks a lysosome-like compartment [vacuolar compartment (VAC)].

### **1.3.4. Apical structure and secretory organelles: Apical complex, IMC, micronemes, rhoptries and dense granules**

*Toxoplasma gondii* tachyzoites are polarised and have a crescent shape. Maintenance of this shape is determined by a structure called the apical complex (Dubey, Lindsay et al. 1998; Hu, Roos et al. 2002; Morrissette and Sibley 2002; Hu, Johnson et al. 2006) and by specialised, uniquely-apicomplexa, secretory organelles such as micronemes and rhoptries (Carruthers and Sibley 1997; Dubey, Lindsay et al. 1998; Dubremetz, Garcia-Reguet et al. 1998).

#### **1.3.4.1 The apical complex**

The apical complex is positioned around the conoid (Figure 1-4) and consists of 14 spiral left-turning tubulin fibres (Hu, Roos et al. 2002). These fibres arise from pre-conoidal rings and both structures surround two intraconoid microtubules (MT), which are probably involved in secretory vesicle transport (Carruthers and Sibley 1997; Hu, Johnson et al. 2006). Furthermore, 22 subpellicular MT originate in a so called polar ring, a microtubule organizing centre found at the apical tip of the parasite (Nichols and Chiappino 1987). These microtubules extend subpellicularly and spiral down over two thirds of the parasite. They are crucial in maintaining the shape, stability and polarity of the parasite (Hu, Johnson et al. 2006).

#### **1.3.4.2. The inner membrane complex (IMC)**

Apicomplexans are grouped in the alveolata infrakingdom. One morphological feature of these organisms is the presence of membrane sacs beneath the plasma membrane (PM), named alveoli. In apicomplexan parasites these alveoli, together with the underlying network of subpellicular microtubules, is termed the IMC (Morrissette, Murray et al. 1997; Mann and Beckers 2001). Recently, a protein family was identified which determines the arrangement of the IMC into three sub-compartments: an apical cap, a central region and a central plus basal region (Beck, Rodriguez-Fernandez et al. 2010). The study of IMC proteins provides greater insights into cytokinesis, how daughter cells develop and divide (Beck 2010; Anderson-White 2011; Fung 2012). Furthermore, the IMC is linked with an actin/myosin based gliding machinery, named the glideosome (Gaskins, Gilk et al. 2004). The glideosome is located between the IMC and the PM and is traditionally thought to control the parasites motility, migration, host cell egress

and invasion (Figure 1-6) however its role in invasion has recently come under question (Andenmatten, Egarter et al. 2013).

#### **1.3.4.3. Micronemes**

Micronemes are ellipsoidal organelles located at the apical tip of the parasite (Figure 1-4). They represent the smallest secretory organelles in apicomplexans with an internal dimension of 75 nm - 150 nm (Carruthers and Tomley 2008). The number of micronemes within one organism varies between species and developmental stages and is correlated with the parasite's motility, migration and invasion (Carruthers and Tomley 2008). The contents of the micronemes are secreted in a regulated manner upon external or internal stimuli. Microneme proteins can be transmembrane (TM) or soluble and function mainly in complexes to enable host cell attachment, by binding to host cell receptors, and invasion (Carruthers and Tomley 2008; Sheiner, Santos et al. 2010).

#### **1.3.4.4. Rhoptries**

Also located at the apical tip are the club-shaped rhoptries. Between apicomplexan species, rhoptries vary in size, electron density and number (Boothroyd and Dubremetz 2008). Approximately 8-12 rhoptries can be found in *T.gondii* tachyzoites and each is approximately 2 to 3  $\mu\text{m}$  long (Dubey, Lindsay et al. 1998). Like micronemes, rhoptries store secretory proteins, these proteins can be subdivided by location within the rhoptry organelle. Most identified rhoptry proteins are located in the rhoptry bulb (Figure 1-4) and named ROP proteins. Some proteins are present in the rhoptry neck region (Figure 1-4) and are called RON proteins. Some RON proteins, such as RON2, 4, 5 and 8 are involved in the formation of the moving junction (MJ), a complex between the parasite and the host cell PM. Currently it is believed that the microneme protein AMA1 plays a crucial function in MJ formation (Alexander, Mital et al. 2005; Lebrun, Michelin et al. 2005; Besteiro, Michelin et al. 2009; Lamarque, Besteiro et al. 2011; Straub, Peng et al. 2011; Tonkin, Roques et al. 2011; Tyler, Treeck et al. 2011), although opposing studies suggest that AMA1 is not required for MJ formation on host cells (Giovannini, Spath et al. 2011). ROPs can play diverse roles in host cell infection. Some have been shown to be involved in the formation of a parasitophorous vacuole (PV) (Boothroyd and Dubremetz 2008) while others are secreted directly into the host cell and interfere with host

innate immune pathways (see 1.7.2.). Rhoptries also contain lipids including cholesterol and phospholipids (Foussard, Leriche et al. 1991). The lipid content is potentially involved in the transport of ROP proteins into the host cell via vesicles (Boothroyd and Dubremetz 2008).

#### 1.3.4.5. Dense granules (DG)

DGs are the third class of apicomplexan specific secretory organelles. They are electron dense compartments of around 200nm in diameter which are distributed throughout the parasite. Like micronemes and rhoptries, the number and composition vary depending on the stage and apicomplexan species (Mercier, Cesbron-Delauw et al. 1998). 12 proteins of dense granules have been identified thus far (Nam 2009) and are thought to be constitutively secreted into the extracellular environment (Chaturvedi, Qi et al. 1999). These proteins have been shown to have functions in the biogenesis and modification of the PV (Ossorio, Dubremetz et al. 1994; Cesbron-Delauw, Gendrin et al. 2008).

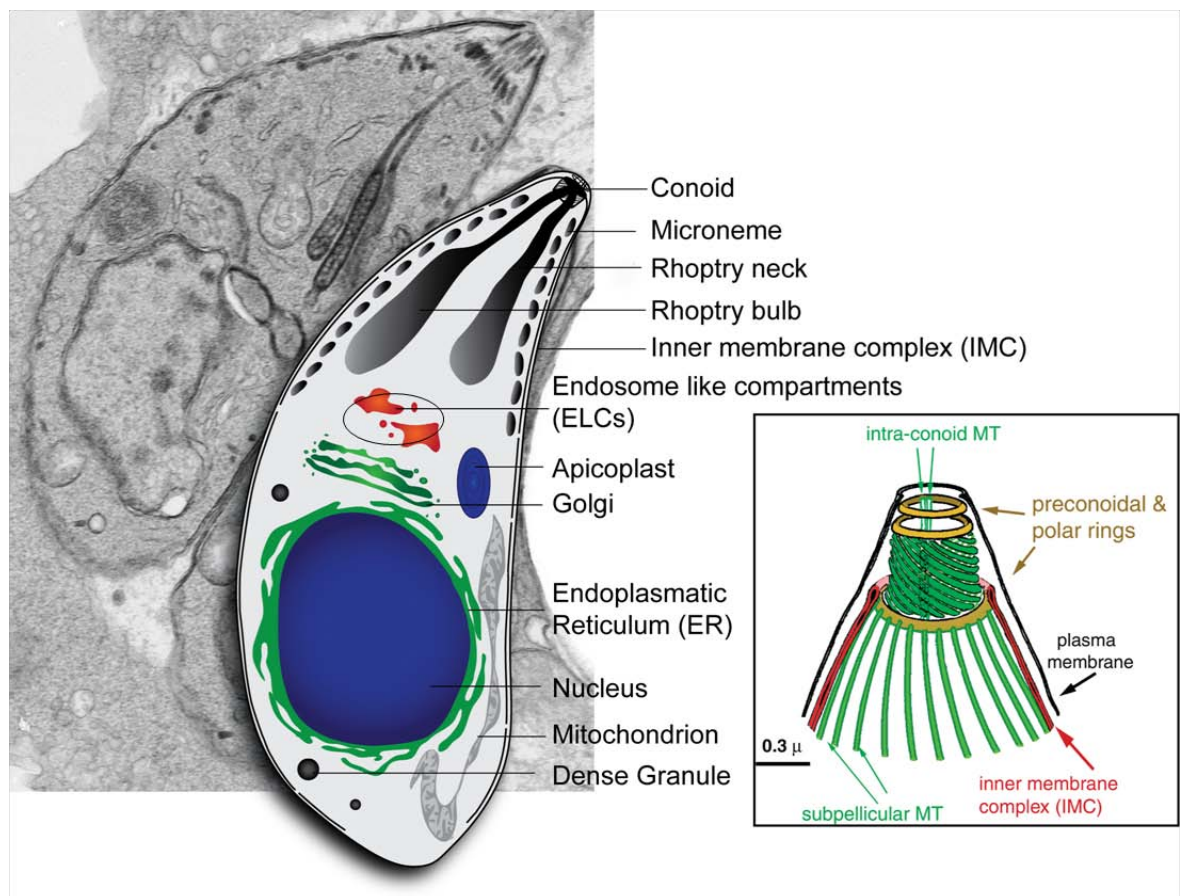


**Figure 1-4: Morphology of *Toxoplasma gondii*.** EM image (David Ferguson) and schematic overview of the organelles in *T.gondii*. The image in the box shows a schematic illustration of the apical complex and is modified from: (Hu, Johnson et al. 2006).

## 1.4. The lytic cycle of *T.gondii*

As mentioned in chapter 1.1., *Toxoplasma* tachyzoites can infect and replicate within any nucleated cell. In immunocompromised individuals, *T.gondii* can destroy whole tissues when left untreated. The lytic cycle begins when (Figure 1-5) one tachyzoite invades a host cell and forms a surrounding PV. Within this protected environment, the parasite undergoes several rounds of replications. When host cell nutrients become limiting, newly developed tachyzoites lyse the host cell. These extracellular tachyzoites are now free to glide and invade a neighbouring cell. Due to the high concentration of parasites escaping the host cell, it is not unusual for neighbouring cells to be multiply infected.

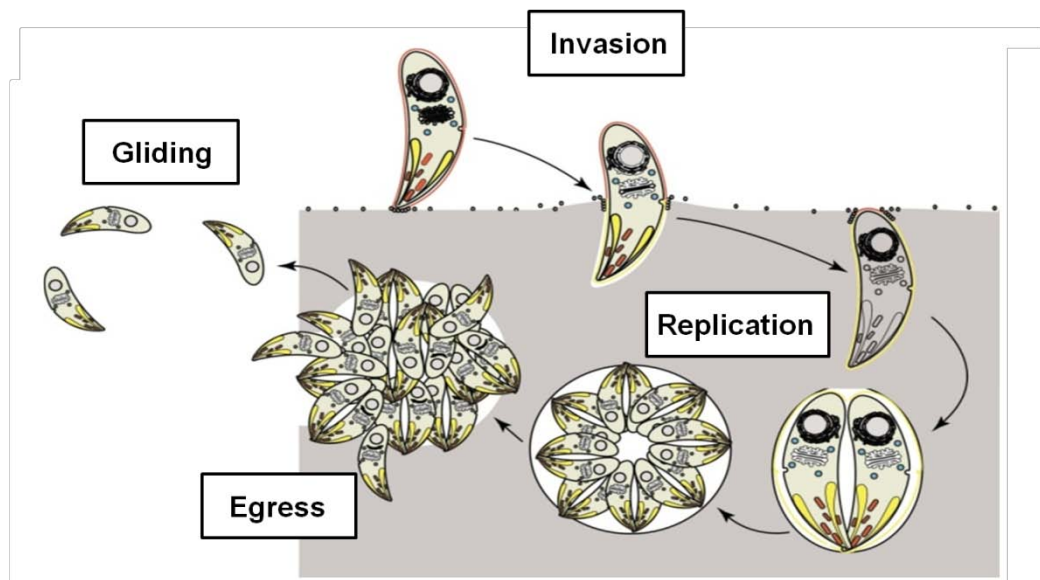


**Figure 1-5: The lytic cycle of a *T.gondii* tachyzoite.** One tachyzoite invades a host cell (grey) and replicates within a parasitophorous vacuole. After several rounds of replication, the tachyzoites egress the host cell by lysis and move by gliding motility to the next host cell. Modified by M.Meissner from: (Soldati and Meissner 2004).

### 1.4.1. Gliding and Invasion

Until recently, it was believed that gliding motility and host cell invasion required the same machinery. The traditional invasion model predicted that the parasite uses its own actin-myosin system to actively penetrate the host cell. Although an alternative, an actin-myosin-independent invasion mechanism has been recently demonstrated (Andenmatten, Egarter et al. 2013), the molecular mechanisms involved in this uptake are unknown at this point. This makes it

difficult to predict if two independent invasion mechanisms operate or if the current model needs to be substantially modified.

According to the current model, surface antigens (SAGs) and SAG related sequence (SRS) proteins are evenly distributed over the whole parasite surface and thought to make a low-affinity, lateral contact (Figure 1-7) with the host cell surface (Carruthers and Boothroyd 2007). After this initial attachment, which is thought to be reversible, the parasite secretes microneme proteins accompanied by conoid extrusion in a calcium dependent manner (Werk 1985; Morisaki, Heuser et al. 1995; Dobrowolski, Carruthers et al. 1997; Carruthers 1999; Wetzel, Hakansson et al. 2003; Carruthers and Boothroyd 2007). In general, the parasite migrates through tissue and invades host cells by a substrate-dependent, active process called gliding motility (Keeley and Soldati 2004). Instead of cilia or flagella, apicomplexan parasites possess a unique actin/myosin based gliding machinery, powered by the glideosome (Gaskins, Gilk et al. 2004; Soldati and Meissner 2004). Within the traditional model, the glideosome is located between the IMC and the PM and is connected to the host cell surface via microneme proteins (Figure 1-6). After the parasite's apical tip with the glideosome moves closer to the host cell surface, active penetration of the host cell occurs. During invasion, a complex, called the moving junction (MJ) (Figure 1-6), between the parasite and host cell cytoskeleton is established. This ring of contact is thought to move down the parasite as invasion progresses (Figure 1-7) (Alexander, Mital et al. 2005; Tyler, Treeck et al. 2011). The moving junction is traditionally assumed to be formed by a complex of RON proteins (RON 2,4,5, and 8) and the microneme protein AMA-1 (Alexander, Mital et al. 2005; Lebrun, Michelin et al. 2005; Besteiro, Michelin et al. 2009; Lamarque, Besteiro et al. 2011; Straub, Peng et al. 2011; Tonkin, Roques et al. 2011; Tyler, Treeck et al. 2011). However AMA1's role in this complex has recently been questioned (Giovannini, Spath et al. 2011), AMA1 is secreted at the parasite surface and RON2,4,5 and 8 are secreted into the host cell.

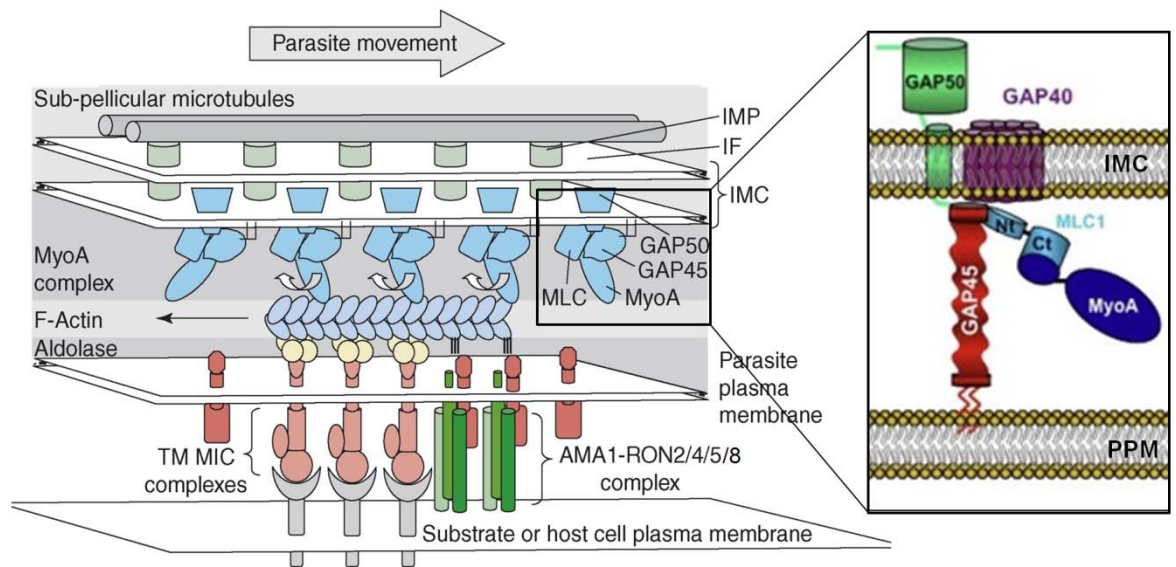


**Figure 1-6: The glideosome at the moving junction (MJ).** These schematic models show the components of the glideosome and its interaction partners during gliding on substrate or at the MJ. The myosin A (MyoA) complex consisting of MyoA, the myosin light chain (MLC) and the IMC interacting proteins GAP50 and GAP45, is connected to the IMC and F-Actin. The mechanical forces of the glideosome are transferred to the substrate or host cell plasma membrane via microneme protein complexes (TM MIC complexes), which bind substrate or host cell receptors and which are connected with F-Actin via Aldolase. At the MJ, an additional connection between the parasite's and host cell's PM is formed via the AMA-1-RON2/4/5/8 complex. To update this model, which was modified from: (Carruthers and Boothroyd 2007), the right box, modified from: (Frenal, Polonais et al. 2010), shows a more recent model of the glideosome. In this model GAP45 interacts directly with the parasite's plasma membrane (PPM).

Rhoptry bulb proteins (ROPs) are then secreted and promote the formation of the PV around the invading parasite (Figure 1-7, Rhoptry discharge). Some of the ROPs are secreted directly into the host cell and transported further into the nucleus, where they interfere with the transcription of several host cell genes (see 1.7.2.). Other ROPs are transported into the lumen or the membrane of the forming PV. These are either involved in the formation of the PV or interfere with host cell signalling pathways, for example to prevent degradation of the PVM by the host cell (see 1.7.2.) (Boothroyd and Dubremetz 2008). By using the actin/myosin motor of the glideosome and its connection to the host cell surface at the moving junction, the parasite is traditionally thought to move into the host cell surrounded by the simultaneously formed PVM (Figure 1-7, Invasion). It is assumed that for both gliding motility and invasion, shedding and consequently maintenance of an apical-posterior gradient of micronemal proteins by intramembrane proteolysis is important (Buguliskis, Brossier et al. 2010). Several proteases located both in rhoptries and micronemes are thought to be secreted at the same time as ROPs and MICs to fulfil their function (see 1.7.1.2.). The last

step in host cell invasion is the process of pinching off from the host PV. The mechanism of this is currently unknown however; this appears to be the slowest step in invasion (Figure 1-7).

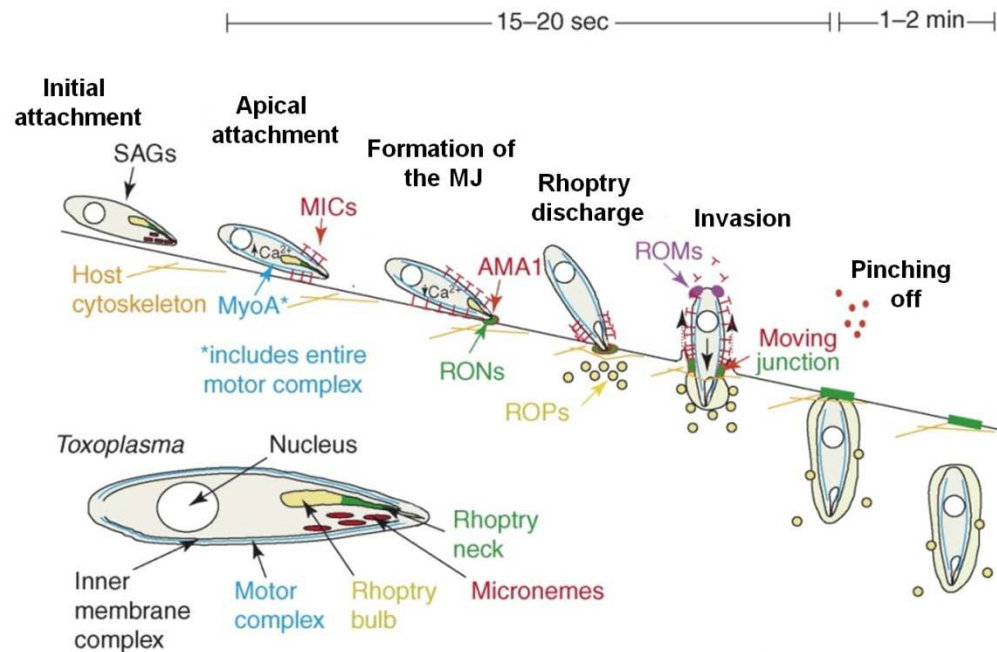


**Figure 1-7: Steps of Invasion.** A schematic model of the different activities within the invasion process [modified from: (Carruthers and Boothroyd 2007)]. Initial attachment: recognition of receptors by surface antigens (SAGs). Apical attachment: microneme proteins MICs (red, T shaped) are secreted in a calcium- dependent manner. This connects the glideosome with its motor complex (only MyoA is shown in blue) with the host cell surface. Formation of the MJ: A complex of the microneme protein AMA1 and rhoptry neck proteins (RONS, green) connects, together with the glideosome, the parasite's cytoskeleton with the host's cytoskeleton. Rhoptry discharge: Rhoptry bulb proteins (ROPs, yellow) are secreted into the host cell and into the lumen or membrane of the developing parasitophorous vacuole (PV). Invasion: Actual penetration of the host cell takes place with involvement of the MJ (upward pointing, lateral arrow) and the glideosome (downward pointing, lateral arrow). Shedding of micronemal proteins at the posterior end is carried out by rhomboid proteases (ROM, purple). Pinching off: Closure and separation of the PV are the steps, which are taking the longest of the time (indicated by the time scale at the top).

### 1.4.2. Replication and Egress

Once the parasite has entered the host cell, it starts to replicate by endodyogeny (Sheffield and Melton 1968; Striepen, Jordan et al. 2007; Nishi, Hu et al. 2008) (Figure 1-5). The secretory organelles are synthesised *de novo* (Dubremetz 2007; Striepen, Jordan et al. 2007), whereas all the other organelles divide synchronously with the nucleus. The mother cell's components of the invasion machinery are depleted only after the invasion machinery, including the apical complex, is completely assembled in the two daughter cells. After several

rounds of replication, when host cell nutrients become limiting, it is possible that the parasites sense extrinsic signals, including host  $K^+$ , to promote egress (Roiko and Carruthers 2009). Additionally, the intracellular  $Ca^{2+}$  level increases through release from intracellular compartments (Lovett and Sibley 2003). This leads to activation of the parasites motility machinery and secretion of egress effector proteins including the pore forming proteins (PFP) such as perforin-like protein (TgPLP1) (Kafsack, Pena et al. 2009) or protein proteases like subtilisin1 (TgSUB1) (Zhou, Kafsack et al. 2005). Disruption of the parasitophorous vacuole membrane (PVM) follows (Roiko and Carruthers 2009), freeing the parasites into the cytoplasm. Parasite and host proteins such as the calcium-dependent protease Calpain1 and TgPLP-1 act to disrupt host cytoskeleton and host plasma membrane (HPM) (Chandramohanadas, Davis et al. 2009; Kafsack, Pena et al. 2009; Kafsack and Carruthers 2010). Once the HPM is destroyed, parasites use their motility system to escape the lysed host cell.

## 1.5. Vesicular transport in higher eukaryotes

One of the key distinguishing features of eukaryotes is the division of cellular functions into distinct, membrane-bound organelles such as the nucleus, Golgi and mitochondrion. The physical separation of these organelles requires trafficking systems to move molecules into and between compartments. These mechanisms can be divided into gated, transmembrane and vesicular transport. Gated transport is the transport of cytosolic molecules into the nucleus via a nuclear pore complex (Zuleger, Kerr et al. 2012). The transmembrane transport is the translocation of proteins from the cytosol into organelles such as the ER lumen or mitochondria via protein translocators located within the organelle membrane (Köhler, Delwiche et al. 1997; Shao and Hegde 2011). In vesicular transport, molecules/proteins are transported within membrane-bound vesicles. A vesicle buds off from a donor membrane and travels within the cell to its target membrane (acceptor membrane) and fuses with it (Figure 1-8) (Bonifacino and Glick 2004). The cargo can be soluble, within the lumen of the vesicle, or membrane integrated molecules/proteins. The vesicular protein transport (traffic) can be sub-divided into the endocytic and biosynthetic/secretory transport. To keep the plasma membrane (PM) and organelles intact from where

vesicles bud off, retrograde/retrieval vesicle transport can be found in both transport pathways.

### **1.5.1. Vesicle formation, transport and fusion**

As mentioned above, vesicles bud off from a donor compartment and travel within the cytosol to its acceptor membrane, where they fuse with it. Membrane budding is controlled by membrane-associated GTPases which recruit coating proteins to the vesicle budding. The cargo either binds to membrane integrated receptors (transmembrane (TM) cargo proteins) or is localised within the budding membrane (Figure 1-8). They become concentrated at the vesicle budding site, together with R/v-SNAREs (R = arginine, v= vesicle-SNAREs) and Rab-GTPases (see 1.6.4.) (Kirchhausen 2000; Bonifacino and Lippincott-Schwartz 2003). Variation between protein coats and sorting signals allow differentiation between the exocytic or endocytic pathways. Vesicles budding from the PM, secretory granules, the TGN and endosomes are coated with Clathrin (Rothman 1986) (Figure 1-9). The coat protein complex (COP) II is found in vesicles trafficking from the ER to the ER-Golgi intermediate compartment (ERGIC) or within the Golgi complex itself (Figure 1-9) (Barlowe, Orci et al. 1994). COPI protein coating is found in intra-Golgi transport and retrograde transport from the Golgi to ER (Figure 1-9) (Letourneur, Gaynor et al. 1994).

Once the vesicle has budded, the coat is shed and coating proteins are released into the cytosol to be reused (Figure 1-8). Uncoated vesicles are then transported to their acceptor membrane by motor protein complexes and microtubules. For example, the transport of secretory vesicles is mainly enabled by microtubules and actin filaments (Bonifacino and Glick 2004). When the vesicle approaches its acceptor membrane, tethering proteins such as Rab effector proteins establish a first contact between the membrane and vesicle (Whyte and Munro 2002). This is followed by R/v-SNAREs and Q/t-SNAREs (Q= glutamine, target-SNAREs), located at the acceptor membrane forming a complex and supporting the docking process (Figure 1-8). The formation of a trans-SNARE complex promotes the fusion of the vesicle with its acceptor membrane (Rothman 1994).

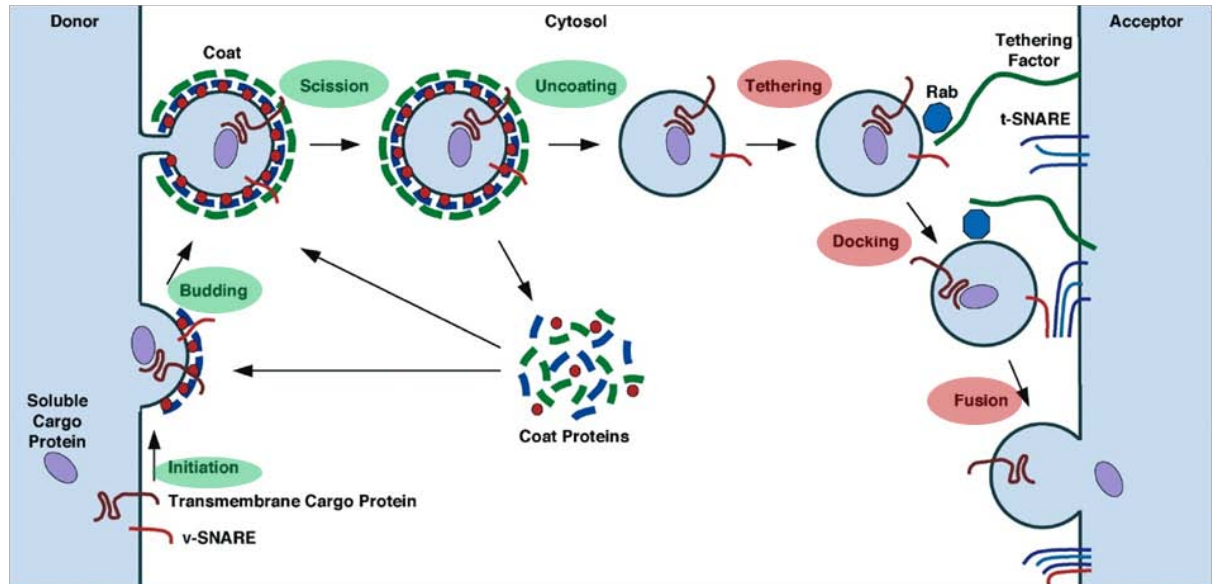


**Figure 1-8: Vesicular trafficking cycle.** Vesicular trafficking can be regulated at seven different steps: 1. Initiation, 2. Budding, 3. Scission, 4. Uncoating, 5. Tethering, 6. Docking and 7. Fusion. In the first part (green) the vesicle is formed by the recruitment of cytosolic coat proteins and pinches off. In the second part (red), the budded vesicle becomes uncoated, transported through the cytosol and fuses with its acceptor membrane. Modified from: (Bonifacino and Glick 2004).

### 1.5.2. The endocytic pathway

Trafficking of cargos from the PM to degradation within the cell is controlled by the endocytic pathway. This pathway can be divided into the early endosomes (EE), late endosomes (LE) and lysosomes (Figure 1-9). During endocytosis, these compartments exchange contents and undergo structural alterations. Typically, extracellular molecules are ingested by endocytosis, transported via endosomes to lysosomes and degraded. For example, in receptor-mediated endocytosis, LDL (low-density lipoprotein) or the growth hormone EGF (epidermal growth factor) binds extracellularly to their receptor. A vesicle buds off from the PM, is transported to the EE and fuses with its membrane. The lower pH within the EE can cause the dissociation of the cargo, for instance, LDL is released from its receptor into the EE lumen (Brown and Goldstein 1979). Unbound receptors are then recycled back to the PM. This can be fast and direct or slowly via recycling endosomes (Figure 1-9) (Maxfield and McGraw 2004; Grant and Donaldson 2009). In the case of EGF and its receptor, both molecules are further transported to LEs (Carpenter 1987). The transition from EE to LE is gradual and various intermediates of EEs and LEs are distinguishable (Saftig and Klumperman 2009). LEs have both tubular and multivesicular areas with different protein and lipid contents (Gruenberg 2003; Russell, Nickerson et al. 2006). Membrane

invagination and budding into the endosomal lumen [intralumenal vesicles (ILVs)] forms multivesicular endosomes/bodies. Late endosomes then fuse with lysosomes where trafficked molecules and proteins are degraded and their components become accessible to the cell (Piper and Katzmann 2007; Pryor and Luzio 2009). In addition, newly synthesised endo-lysosomal proteins are transported from the trans-Golgi network (TGN) to endosomes and from there to lysosomes. For example, the mannose 6-phosphate receptor (M6PR) binds lysosomal enzymes in the TGN, delivers them to the endosomes and then cycles back to the TGN (Kornfeld 1987; Ghosh, Dahms et al. 2003). Vesicles are constantly cycling between EEs, LEs, lysosomes, the TGN and the PM, but there is no gradual transport chain within the endocytic pathway and the interactions between these pathways have been a focus of intensive research and debate for many years (Gruenberg and Stenmark 2004; van der Goot and Gruenberg 2006; Luzio, Pryor et al. 2007; Saftig and Klumperman 2009).

### ***1.5.3. Biosynthetic/Secretory pathway***

Secreted proteins, membrane proteins of the PM and endo-lysosomal proteins initially follow the same pathway. Synthesis and post-translational modifications occurs at or in the ER (Hebert and Molinari 2007). From there they are transported to the Golgi where further modifications take place such as glycosylation (Griffiths and Simons 1986; Saraste and Svensson 1991). As described above, freshly synthesised and modified endo-lysosomal proteins are then transported to endosomes (Kornfeld 1987; Ghosh, Dahms et al. 2003). Proteins targeted to the PM and secretory proteins are further transported to the PM. This takes place through a constitutive or a regulated pathway (Burgess and Kelly 1987; Gerdes 2008). The constitutive secretory pathway is found in all cells and is the direct vesicular transport of plasma membrane and secretory proteins from the TGN to the PM. This way, soluble proteins are constantly secreted and the PM is provided with newly synthesised lipids and proteins (Burgess and Kelly 1987; Ponnambalam and Baldwin 2003). The regulated secretory pathway is mainly a feature of polarised cells and well-studied in neurons, endocrine and exocrine cells (Vazquez-Martinez, Diaz-Ruiz et al. 2012). Regulated exocytosis (discharge of intracellular molecules into the extracellular environment) is usually triggered by external signals which activate intracellular signal cascades, leading to the fusion of secretory vesicles (Palade 1975; Burgess

and Kelly 1987; Bonifacino and Glick 2004). It is possible that regulated secretory proteins are transported from the TGN via recycling endosomes to the PM (Rodriguez-Boulan and Musch 2005). However, the classical model of the secretory pathway postulates that transport from the TGN occurs via secretory granules to specific regions of the PM. There they become secreted by exocytosis (Figure 1-9) (Palade 1975; Burgess and Kelly 1987). Since many studies have been done on various cell types, different exocytosis regulations at different steps were observed. There are a number of hypotheses and models which attempt to explain the regulated secretory pathway in detail. For example, two main models try to explain how secretory or plasma membrane proteins are sorted for the constitutive or regulated pathway in the TGN or post-Golgi region (Vazquez-Martinez, Diaz-Ruiz et al. 2012). In the "sorting-for-entry" hypothesis, regulated secretory proteins bind at sorting receptors in the TGN before forming immature secretory granules (ISGs, Figure 1-9) (Kuliawat and Arvan 1994; Arvan and Castle 1998; Tooze 1998). Another model hypothesised that sorting happens one step later, within the ISGs. Only regulated secretory proteins form aggregates within these granules and non-secretory proteins are removed later, because of their inability to aggregate (Arvan, Kuliawat et al. 1991; Arvan and Castle 1998). Due to retrograde transport of Golgi components from the ISGs back to the TGN, the granule's content becomes increasingly concentrated. The resulting mature secretory granules show an electron dense structure in the EM and are termed dense core vesicles. These store secretory proteins until extracellular signals trigger their fusion with the PM via intracellular signals such as the rise of intracellular  $Ca^{2+}$  concentration (Katz and Miledi 1967), cAMP (Fujita-Yoshigaki, Dohke et al. 1999; Takahashi, Kadowaki et al. 1999) or protein kinase activity (e.g. PKA) (Hilfiker, Czernik et al. 2001).

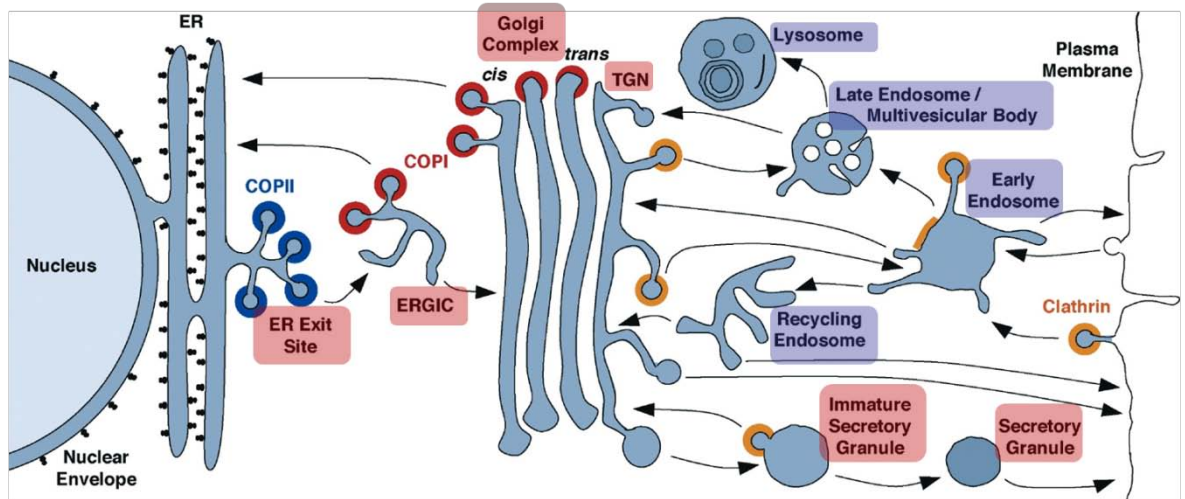


**Figure 1-9: Vesicular transport between the organelles of a eukaryotic cell.** Endocytic pathways are underlined in blue and Biosynthetic/secretory pathways in red. ERGIC= ER/Golgi intermediate compartment. Modified from (Bonifacino and Glick 2004).

## 1.6. Rab proteins

Rab (Ras analog in the brain) proteins are the largest family of the Ras superfamily. Ras proteins are small GTP binding proteins (G-proteins), which are monomeric and have a size of 20-40 kDa. They are essential regulators of signal transductions within all kind of eukaryotic and even prokaryotic cells (Mittenhuber 2001). More than 100 soluble G-proteins have been reported to date in eukaryotes, including proteins of the Ras, Rho, Sar1/Arf1, Ran and Rab families. Rab proteins chiefly regulate targeting and fusion of vesicles from a donor to an acceptor membrane.

### 1.6.1 G-proteins and the functional cycle of Rab proteins

Like all G-proteins, Rab proteins function as molecular switches which cycle between an inactive, cytosolic GDP-bound form and an active, membrane-linked GTP-bound form (Figure 1-10). Before activation, most Rab proteins are post-translationally prenylated. Immediately, the synthesized Rab protein interacts with a Rab escort protein (REP). This presents the Rab to a Rab geranylgeranyl transferase (RabGGT), which catalyses the addition of geranylgeranyl groups to the C-terminus of the Rab protein. REP also escorts the Rab to its target membrane (Figure 1-10). The resulting inactive Rab protein can be integrated directly into

the appropriate donor membrane. GDP dissociation inhibitor (GDI) dissociation factors (GDF) can be involved to support this process. Once the Rab protein is inserted into the donor membrane, a guanine nucleotide exchange factor (GEF) activates it by replacing the GDP by a GTP nucleotide. The resulting conformational change makes the Rab protein accessible to effector proteins. Rab proteins regulate the transport, targeting, tethering/docking and fusion of vesicles solely via the interaction with their specific effectors (Stenmark 2009). After fusion of the vesicle with the acceptor membrane, a GTPase activating protein (GAP) promotes the hydrolysis of GTP to GDP and the Rab protein becomes inactive and cytosolic (Figure 1-10). A GDP dissociation inhibitor (GDI) stabilises the inactive Rab protein in the cytosol until it becomes membrane inserted to restart the cycle.

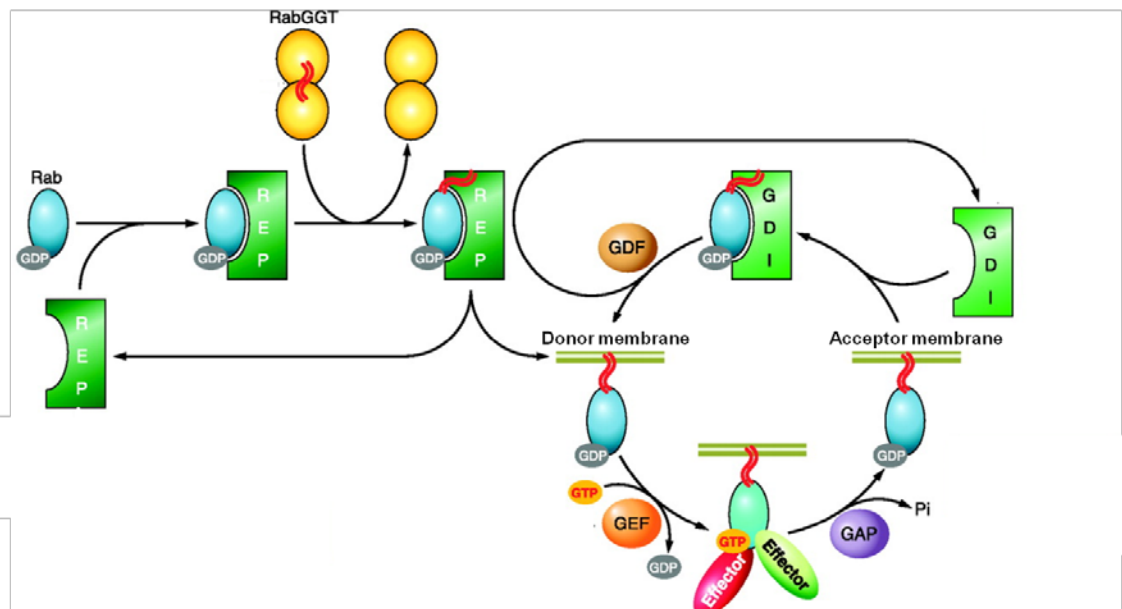


**Figure 1-10: The functional Rab cycle.** The synthesised Rab protein is escorted via a Rab escort protein (REP) to the donor membrane. Additionally the REP presents the Rab protein to a Rab geranylgeranyl transferase (RabGGT), where it becomes prenylated. The prenylated Rab protein is directly integrated into the donor membrane. The Rab protein remains in its GDP bound state until a guanine nucleotide exchange factor (GEF) catalyses an GDP to GTP exchange, which activates the Rab protein. Effector proteins bind to the activated Rab protein and together they regulate the transport, traffic and fusion of the vesicle to the membrane of an acceptor organelle. At the acceptor membrane the GTP of the Rab protein is hydrolysed to GDP, which is catalysed by a GTPase activating protein (GAP). The re-inactivated Rab protein is removed from the membrane by a guanine nucleotide dissociation inhibitor (GDI). With the assistance of a GDI dissociation factor (GDF) the Rab protein can be escorted or directly integrated into the donor membrane again. The cartoon is modified from: (Hutagalung and Novick 2011).

### 1.6.2. Conserved domains of Rab proteins

Like all small GTPases, Rab proteins possess a GTPase domain, a GTP/Mg<sup>2+</sup> binding site where GDP or GTP can bind with the help of the bound cofactor Mg<sup>2+</sup>. Most Rab proteins have a C-terminal hypervariable region followed by CAAX (C= prenylated cysteine residue, a= aliphatic amino acid) boxes, which contain two cysteine residues. At these cysteine residues geranylgeranyl tails can be added, which enables membrane integration of the Rab protein (see 1.6.1). Furthermore, all Rab proteins exhibit a switch I and switch II region (Figure 1-11), which undergo conformational changes when GTP is bound (Pfeffer 2005; Lee, Mishra et al. 2009). Conserved sequence motifs for nucleotide binding have also been identified. The G1 box within the phosphate binding loop (p-loop), the G2 box in the switch I region, the G3 box in the switch II region, the G4 and G5 box for interaction with the guanine base (Itzen and Goody 2010). Domains for GDI and effector interaction, Rab family (RabF) regions (which are unique under the Rab proteins within the Ras superfamily) and Rab subfamily specific (RabSF) regions (which are conserved among the Rab subfamily) have also been identified (Pereira-Leal and Seabra 2000).

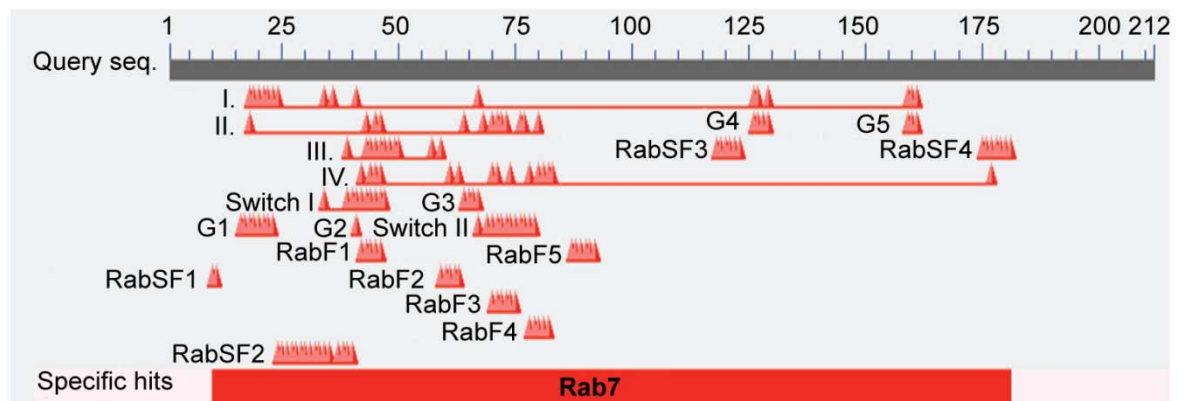


**Figure 1-11: Putative domains of YPT7.** A graphic summary of NCBI search and blast of the GTPase YPT7 (spIO94655.1) in yeast as an example to display putative conserved domains (red) of Rab proteins. I. GTP/Mg<sup>2+</sup> binding site, II. GDI interaction site, III. putative GEF interaction site, IV. putative effector interaction site, G boxes 1-5, Rab subfamily motifs RabSF1-4, Rab family motifs (RabF) 1-5.

### **1.6.3. The role of selected Rab GTPases in higher eukaryotes**

The number of Rab proteins found in higher eukaryotes varies greatly. Over 60 Rab proteins have been identified from human cells while only 11 Rab proteins are present in yeast (Pereira-Leal and Seabra 2000; Seabra, Mules et al. 2002). Below, selected Rab proteins which are highly conserved in most eukaryotes and their activity in higher eukaryotes are introduced.

#### **1.6.3.1. Rab1A and Rab1B**

Rab1A and Rab1B are highly conserved at the sequence level (Touchot, Zahraoui et al. 1989). Both proteins are involved in the regulation of the anterograde transport between ER and cis-Golgi in higher eukaryotes including plant cells (Batoko, Zheng et al. 2000) and mammalian cells (Plutner, Cox et al. 1991; Tisdale, Bourne et al. 1992). Recently an additional involvement in early endosome to Golgi trafficking and a function within endocytic processing was reported for Rab1A (Sclafani, Chen et al. 2010; Mukhopadhyay, Nieves et al. 2011). Furthermore, in yeast, Rab1 also participates in the regulation of vesicle transport within the Golgi apparatus from cis- to medial- Golgi (Jedd, Richardson et al. 1995).

#### **1.6.3.2. Rab2**

Rab2 regulates vesicular traffic between the ER and Golgi. It is primarily involved in COPI vesicle trafficking to the pre-Golgi ER-Golgi intermediate compartment (ERGIC, Figure 1-9) in mammalian (Tisdale, Bourne et al. 1992; Tisdale and Jackson 1998) and plant cells (Cheung, Chen et al. 2002). Interestingly, an additional role of Rab2 in the maturation of dense core vesicles was described in the nematode *Caenorhabditis elegans* (Nematoda) (Edwards, Charlie et al. 2009).

#### **1.6.3.3. Rab4**

Rab4 is principally associated with early endosomes in higher eukaryotes. It has been shown to be involved in transferrin- and oxytocin receptor recycling (Van Der Sluijs, Hull et al. 1991; Conti, Sertic et al. 2009). Transferrin is an iron-binding glycoprotein and oxytocin is a hormone, both are molecules, which are endocytosed and their receptors are immediately recycled back to the PM. Rab4

has a potential role in endosome formation and recycling in mammalian cells (van der Sluijs, Hull et al. 1992; Pagano, Crottet et al. 2004; Yudowski, Puthenveedu et al. 2009). Interestingly, in the single celled parasite *Trypanosoma brucei*, a new role of Rab4 was reported in lysosomal traffic, without involvement of the endocytosis or recycling pathways (Hall, Pal et al. 2004).

#### **1.6.3.4. Rab5**

All three isoforms of Rab5 (Rab5A, Rab5B and Rab5C) have been shown to be involved in endocytosis and homotypic fusion of early endosomes in mammalian cells. Through regulation of the assembly of clathrin-coated pits at the PM, Rab5 is involved in endocytosis of the transferrin receptor (McLauchlan, Newell et al. 1998). It was also recently demonstrated that Rab5 is a master regulator of endosome biogenesis in mammalian cells (Zeigerer, Gilleron et al. 2012). The yeast Rab5 homologues Vps21/Ypt51p, Ypt52p, Ypt53p can be grouped together due to sequence similarity. These are involved in endocytic membrane traffic and are also responsible for correct sorting of vacuolar hydrolases (Singer-Kruger, Stenmark et al. 1994). In plants, Rab5 proteins are mainly involved in vesicular trafficking to the vacuole, which is an organelle of the secretory pathway with several functions including turgor pressure maintenance and protein storage (Sohn, Kim et al. 2003; Bolte, Brown et al. 2004; Kotzer, Brandizzi et al. 2004; Bottanelli, Gershlick et al. 2011). Two classes of Rab5 proteins have been defined in plants, Rha1 and Ara7, which share a very high sequence homology (Sohn, Kim et al. 2003), and Ara6, a Rab5 protein found only in plant cells. In contrast to Rha1 and Ara7, which are C-terminally lipid anchored, Ara6 is characterized by N-terminal myristoylation (Ueda, Yamaguchi et al. 2001). Both Rab5 classes are thought to function differently, since they show partial but not identical co-localisation in endosomes (Ebine, Fujimoto et al. 2011).

Aside its key role in endocytosis, Rab5 was recently also shown to be involved in exocytosis. In *C.elegans* Rab5 and Rab10 mutants showed defects in dense core vesicle secretion (Sasidharan, Sumakovic et al. 2012).

### 1.6.3.5. Rab6

Rab6 has also been well characterised. It is localised at the Golgi in various cell types (Goud, Zahraoui et al. 1990). Rab6 regulates the retrograde transport from the Golgi to the ER. A COPI independent transport was reported to be Rab6 dependent and is used for Golgi glycosylation enzymes (Girod, Storrie et al. 1999). Even in *Aspergillus nidulans*, where the Golgi is not stacked, the mammalian Rab6 ortholog RabC is localised in the Golgi demonstrating the conserved role of this protein (Pantazopoulou and Penalva 2011). Recently a new role was reported in trans-Golgi trafficking of clathrin coated and COPI-coated vesicles and in maintenance of Golgi homeostasis (Storrie, Micaroni et al. 2012).

### 1.6.3.6. Rab7

Rab7 is involved in the regulation of vesicles between endosomes and lysosomes (Chavrier, Parton et al. 1990; Meresse, Gorvel et al. 1995; Bucci, Thomsen et al. 2000; Vanlandingham and Ceresa 2009). It also recruits the VPS35/29/26 trimer, a cargo-selective retromer sub-complex, which is required for retrieval of transmembrane proteins from endosomes to the TGN [shown in HeLa cells by (Seaman, Harbour et al. 2009)]. The yeast homologue Ypt7 was shown to regulate the traffic from endosomes to the vacuole and to have a role in vacuole fusion (Kashiwazaki, Iwaki et al. 2009). In the protozoan parasite *Entamoeba histolytica* Rab7 was shown to be involved in lysosome and phagosome biogenesis (Saito-Nakano, Mitra et al. 2007). Additionally, it was reported that Rab7 is involved in the regulation of autophagy in CHO (Chinese hamster ovary) cells (Gutierrez, Munafo et al. 2004). Autophagy is a “self digesting” cell process, where cytosolic components are sequestered in vesicles (autophagosomes), delivered to lysosomes and become degraded.

### 1.6.3.7. Rab11

In most eukaryotic cells, Rab 11 is involved in the “slow” endocytic recycling via recycling endosomes (Grant and Donaldson 2009). In mammalian cells it was shown to regulate PM recycling via the Rab11 family interacting protein 2 (Rab11-FIP2) (Hales, Vaerman et al. 2002). In this context it was also reported that Rab11 is involved in the regulation of cytokinesis (cell division). During cytokinesis a cleavage furrow is formed at the PM, where the final splitting and

formation of daughter cells starts. In *C.elegans* and *Drosophila* it was shown, that Rab11 containing vesicles are required for this furrow formation (Skop, Bergmann et al. 2001; Pelissier, Chauvin et al. 2003). The Rab11 yeast homologs (Ypt31/32) are reported to recruit type V myosin, Myo2, for the transport of secretory vesicles to the site of secretion (Casavola, Catucci et al. 2008; Lipatova, Tokarev et al. 2008).

#### **1.6.3.8. Rab18**

The main appearance of Rab18 in mammalian cells is in vesicle transports between the ER and Golgi (Dejgaard, Murshid et al. 2008). Rab18 was also found to interact with lipid droplets (lipid storage organelles) in human liver cells (Hep G2 cells) and could play an important role in lipid transport between these two organelles (Martin, Driessen et al. 2005; Ozeki, Cheng et al. 2005). In neuroendocrine cells, Rab18 is also involved in the secretion of secretory granules (Vazquez-Martinez, Cruz-Garcia et al. 2007). In plant cells (*Arabidopsis*) it was additionally found that the expression of Rab18 is involved in the abscissic acid (ABA)-transduction cascade. ABA is a plant hormone, which induces an increase in cytosolic  $Ca^{2+}$ , which is important for turgor regulation of the plant cell (Ghelis, Dellis et al. 2000).



phosphate receptor (M6PR) from the LE to the TGN, recruits its effector (M6PR binding protein 1) to the LE. This interaction increases the affinity of the effector with its cargo (1 in Figure 1-13) (Carroll, Hanna et al. 2001). Additionally, Rab5-GDI was shown to be essential for the formation of transport vesicles by ligand sequestration into clathrin-coated pits (McLauchlan, Newell et al. 1998).

#### **1.6.4.2. Uncoating**

Once the vesicle is coated and pinched off from its donor membrane, vesicle uncoating is necessary for further intracellular transport. Rab5 is involved in the removal of the cargo adaptor protein complex (AP2) from clathrin-coated vesicles (2 in Figure 1-13). Rab5 recruits class I PI3-kinases (PI3K) (Christoforidis, Miaczynska et al. 1999) or phosphatases (Shin, Hayashi et al. 2005) to the vesicle. This causes dephosphorylation of a subunit of AP2 and increases PtdIns(4,5)P<sub>2</sub> turnover, which in turn destabilises the interaction of the AP2 complex with the vesicle (Semerdjieva, Shortt et al. 2008).

#### **1.6.4.3. Motility**

After uncoating, the vesicle establishes interactions with actin filaments and microtubules (3 in Figure 1-13). For example the Rab11 family-interacting protein 2 (RAB11-FIP2) connects Rab11A vesicles to myosin Vb (Hales, Vaerman et al. 2002). Rab proteins can interact with kinesins either directly or indirectly. For example, Rab6 interacts directly with its effector protein, rabkinesin 6 (KIF20A). However, Rab5 recruits phosphatidylinositol-3-OH kinase (hVPS34) which increases the concentration of PtdIns-3phosphate (PtdIns(3)P) in the endosomal membrane. This lipid then recruits kinesin 3 (KIF16B), demonstrating indirect association of a Rab and kinesin (Hoepfner, Severin et al. 2005).

#### **1.6.4.4. Tethering and Fusion**

Once the transported vesicle approaches its target compartment, tethering, docking and fusion of the vesicle needs to be triggered and regulated (4,5 in Figure 1-13). Rab proteins are involved in the recruitment of tethering complexes. An example of this is the EE antigen (EEA1) and rabenosyn 5, which are both Rab5 effector proteins (Stenmark 2009). EEA1 and rabenosyn 5 can interact directly with SNAREs like syntaxin 6,7,13 (McBride, Rybin et al. 1999) to

regulate vesicle fusion. Alternatively, rabenosyn 5 can interact with the vacuolar sorting protein sorting-associated protein 45 (hVPS45), a SNARE regulator (Nielsen, Christoforidis et al. 2000).

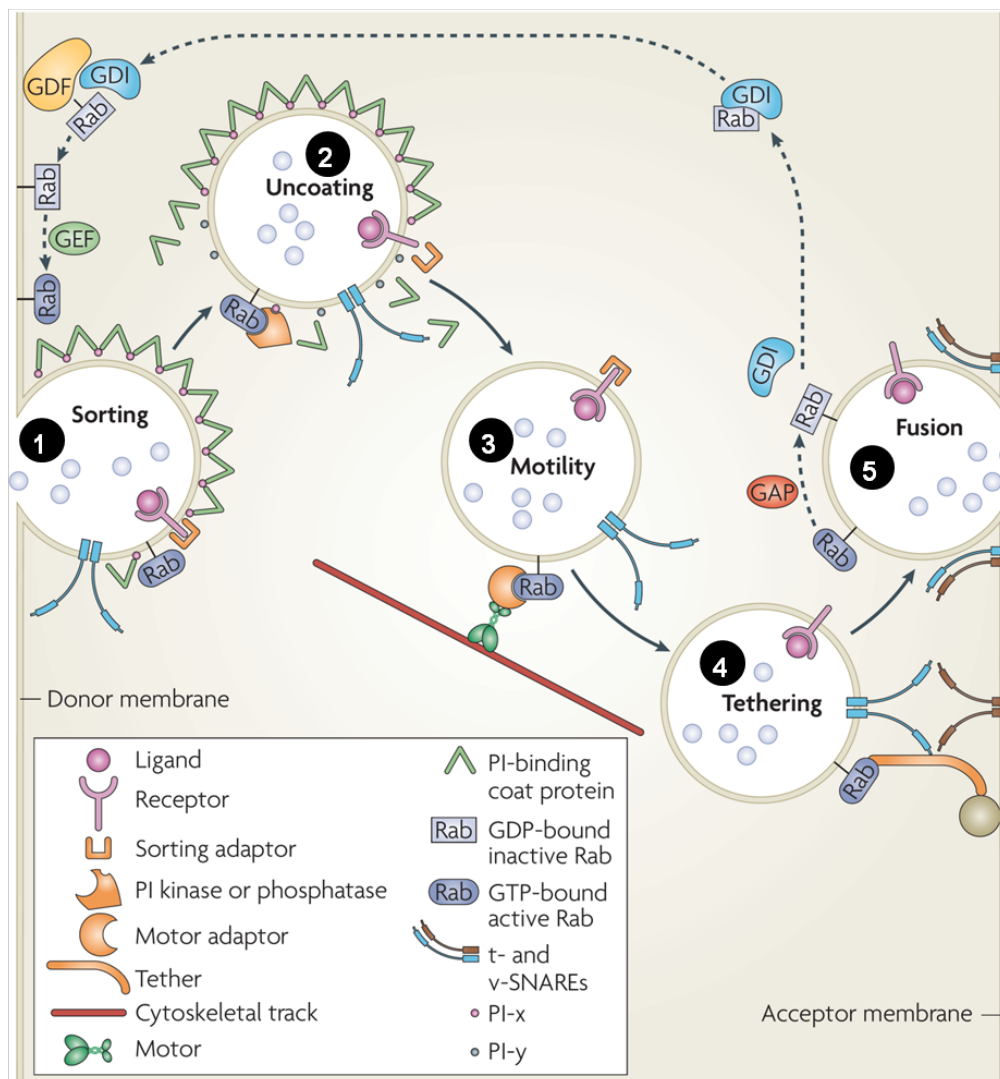


**Figure 1-13: Rab proteins within the vesicular trafficking.** 1. A Rab protein activates a sorting adaptor to sort a receptor with its ligand (purple) into the vesicle. 2: Recruitment of phosphoinositide (PI) kinases or phosphatases (orange) could change the PI composition of the vesicle. Dissociation of PI-binding coat proteins or uncoating respectively would be the consequence. 3: For example, by interacting with motor adaptors (orange), Rab proteins mediate the transport of the vesicles along actin filaments or microtubules (= cytoskeletal track). 4: Recruitment of tethering factors (orange) which interact with molecules at the acceptor membrane (grey) mediates tethering of the vesicle. 5: Formation of a SNARE complex (red and blue) mediates the fusion of the vesicle with its acceptor membrane. The Rab protein becomes inactivated and cycles back to its donor membrane. The cartoon is modified from: (Stenmark 2009).

## **1.7. Secretory proteins in *T.gondii***

### **1.7.1. Microneme proteins**

#### **1.7.1.1. Microneme proteins with adhesive functions**

Most microneme proteins have adhesive domains such as thrombospondin (TSR)-like, lectin or epidermal growth factor to allow interactions with proteins or carbohydrates on the host cell surface (Carruthers and Tomley 2008). Often these proteins function in complexes which consist of at least one transmembrane (TM) and one soluble protein (Sheiner, Santos et al. 2010). Several microneme protein complexes were shown to undergo proteolytic processing either by removal of an N-terminal or internal propeptide including TgMIC3 (Cerede, Dubremetz et al. 2002), TgAMA1 (Donahue, Carruthers et al. 2000), TgMIC4 (Brecht, Carruthers et al. 2001), TgMIC5 (Brydges, Sherman et al. 2000), TgMIC11 (Harper, Zhou et al. 2004) and TM2AP (Rabenau, Sohrabi et al. 2001). For example, the TSR-like domain in the soluble microneme protein TgMIC1 enables the recruitment and interaction with another soluble microneme protein, TgMIC4. TgMIC4 is proteolytically processed and binds to the host cell surface and TgMIC6 (Brecht, Carruthers et al. 2001; Carruthers and Tomley 2008). TgMIC6 is a transmembrane protein thought to be an escorter for TgMIC1 and essential for the complex to leave the early secretory pathway (ER/Golgi) (Reiss, Viebig et al. 2001; Saouros, Edwards-Jones et al. 2005; Carruthers and Tomley 2008). The TgMIC1/4/6 complex (Figure 1-14) has been shown to be involved in host cell attachment (Reiss, Viebig et al. 2001). Another microneme complex, which is important for gliding and invasion, is the TgMIC2-TgM2AP complex. Together with the soluble TgMIC2 associated protein (TgM2AP), the TM protein TgMIC2 is classically thought to interact with host cell receptors and the parasites actin/myosin motor (Jewett and Sibley 2004). Mutated parasites in which TgM2AP could not be processed were unable to form a stable complex between TgM2AP and TgMIC2. As a consequence, these parasites were less invasive (Harper, Huynh et al. 2006). Nevertheless, recent data has been published questioning TgMIC2's role in invasion (Andenmatten, Egarter et al. 2013).

The soluble dimeric microneme protein TgMIC3 with its lectin-like domain is assumed to be responsible for binding to the surface of all nucleated host cells

(Garcia-Reguet, Lebrun et al. 2000). N-terminal processing of TgMIC3 and dimer formation are essential for receptor binding and *T.gondii*'s virulence (Cerede, Dubremetz et al. 2002). The propeptide together with an EGF domain is necessary for trafficking to the micronemes (El Hajj, Papoin et al. 2008). TgMIC3 is believed to form a complex with the microneme TM protein, TgMIC8, (Sheiner, Santos et al. 2010), although knock down of TgMIC8 did not affect TgMIC3 and this interaction remains controversial (Kessler, Herm-Gotz et al. 2008). TgMIC3 has been shown to be essential for host cell attachment (Cerede, Dubremetz et al. 2002), whereas TgMIC8 could be shown to be essential for invasion, before the formation of the moving junction (Kessler, Herm-Gotz et al. 2008). Replication, gliding and egress are not affected in parasites where TgMIC8 is conditionally knocked down (Kessler, Herm-Gotz et al. 2008). Interestingly, RON4, which is involved in MJ-formation, could not be secreted by these parasites. Another TM microneme protein essential for host cell attachment and invasion is TgAMA1, (Donahue, Carruthers et al. 2000; Hehl, Lekutis et al. 2000; Mital, Meissner et al. 2005). As previously described (1.4.1.), TgAMA1 was thought to interact with rhoptry neck proteins to form a complex leading to the formation of the MJ. Whether TgAMA1 is directly involved in MJ formation is not clear. Recent published (Collins and Blackman 2011; Giovannini, Spath et al. 2011) and unpublished data from our group indicate that TgAMA1 is not involved in MJ formation in the traditional manner and is not essential for invasion. In addition, the suggested involvement of TgAMA1 in switching from an invasion to a replication mode of zoites by intramembrane cleavage (Santos, Ferguson et al. 2011) is highly controversial (Parussini, Tang et al. 2012). Future research will attempt to confirm the role of this key secreted protein.

#### **1.7.1.2. Microneme proteins without adhesive functions**

TgMIC11 is a soluble microneme protein which undergoes two proteolytic events to remove an internal propeptide during its maturation. As with other microneme proteins, TgMIC11 is secreted in a calcium dependent manner, but does not interact with the parasite surface during invasion (Harper, Zhou et al. 2004). Its function is currently unknown, however a central role in microneme content organisation by homotypic ionic interaction has been hypothesised (Harper, Zhou et al. 2004). Another microneme protein without adhesive properties is the perforin-like protein (TgPLP1). TgPLP1 is secreted in a calcium

dependent manner and shown to be crucial for egress (Kafsack, Pena et al. 2009). Kafsack and colleagues demonstrated that TgPLP1 KO parasites were entrapped within the host cell due to an inability to permeabilize the PVM (see egress, section 1.4.2. for more details).

Shedding of microneme proteins from the surface is crucial for motility and active invasion in *T. gondii* (Carruthers and Tomley 2008). Several rhomboid-like proteins (TgROMs) including micronemal protein protease 1-3 (MPP1-3), with their rhomboid-like protease activity, have been identified (Santos, Graindorge et al. 2012). MPPs are involved in intramembrane cleavage of TgMIC2, TgMIC6 and TgAMA1 (Opitz, Di Cristina et al. 2002; Brossier, Jewett et al. 2003; Howell, Hackett et al. 2005; Santos, Ferguson et al. 2011; Santos, Graindorge et al. 2012). A protease found in micronemes named subtilisin-like serine protease TgSUB1 is probably required for MPP2 and MPP3 activity and involved in surface processing of TgMIC2-TgM2AP (Lagal, Binder et al. 2010).

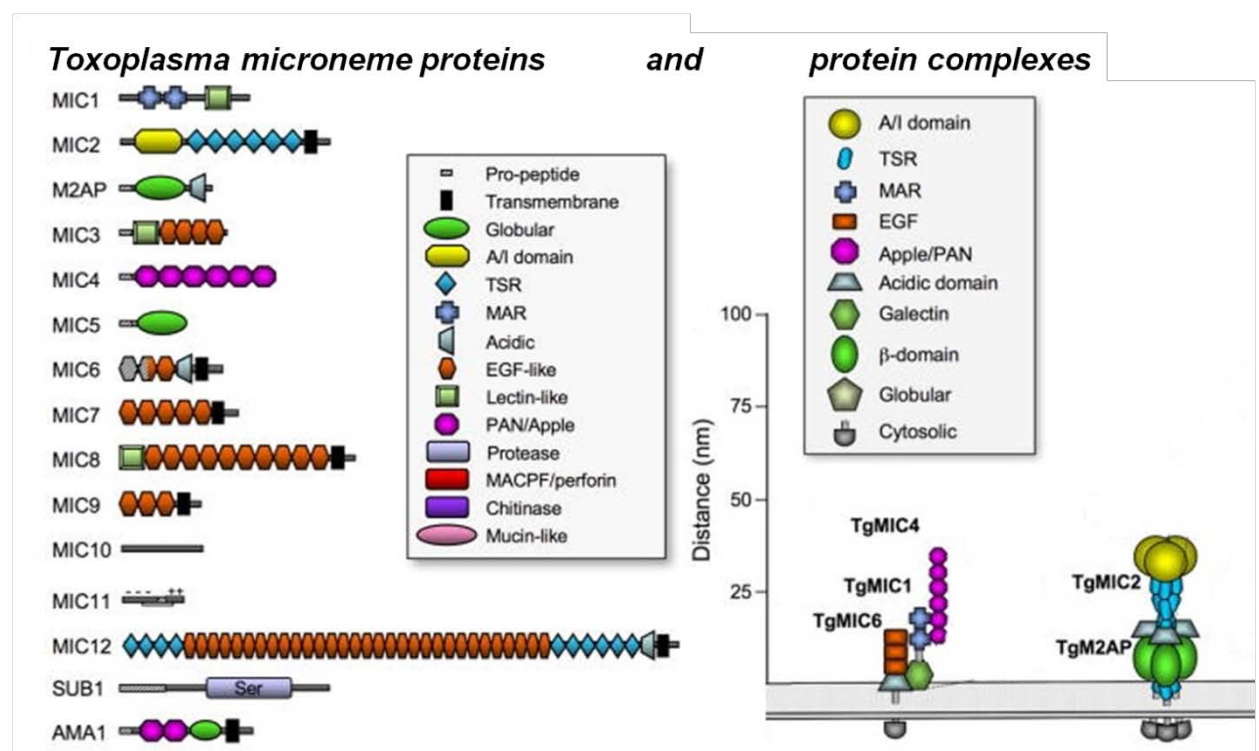


**Figure 1-14: Toxoplasma microneme protein domains and their interactions.** Identified microneme proteins and their domains in *T. gondii* (left). Complex formation of TgMIC1/4/6 and TgMIC2/M2AP (right). Modified from: (Carruthers and Tomley 2008).

### **1.7.2. Rhoptry proteins**

More than 40 rhoptry proteins have been identified in *T.gondii* (Bradley, Ward et al. 2005). As described in chapter 1.4. RON2,4,5,8 are secreted during invasion and are involved in the formation of the MJ (Alexander, Mital et al. 2005; Lebrun, Michelin et al. 2005; Besteiro, Michelin et al. 2009; Lamarque, Besteiro et al. 2011; Straub, Peng et al. 2011; Tonkin, Roques et al. 2011; Tyler, Treeck et al. 2011). ROPs are secreted after RONs during invasion (Riglar, Richard et al. 2011). Some ROPs are secreted directly into the host cell and function there either within the cytosol such as Toxofilin (Hakansson, Charron et al. 2001) and ROP13 (Turetzky, Chu et al. 2010), or the nucleus such as ROP16 (Saeij, Boyle et al. 2006) and PP2C (Gilbert, Ravindran et al. 2007). Other ROPs are secreted into the lumen or the membrane of the PV including ROP1 (Ossorio, Schwartzman et al. 1992). Many ROPs belong to the ROP2 family; proteins of this family are localised directly to the PV membrane (PVM). ROP18, for example, is a ROP2 member and was found to locate at the host cytosolic side of the PVM. ROP18 is thought to be involved in preventing the host innate immune pathway from destroying the PVM (Fentress, Steinfeldt et al. 2012). ROP5 is a pseudokinase of the ROP2 family and also located at the PVM. Its C-terminus is facing the host cell cytosol and it is secreted during invasion (El Hajj, Lebrun et al. 2007). Several ROP2 proteins have lost their enzymatic activities, however may regulate other ROPs with kinase activities (Boothroyd and Dubremetz 2008) although this is still under investigation. ROP4, another member of the ROP2 family, is released during invasion, localised to the PVM and becomes phosphorylated in the infected host cell (Carey, Jongco et al. 2004). Recombinant ROP2 and ROP4 are currently being used for vaccination development (Dziadek and Brzostek 2012) since their inhibition of activity was shown to prevent parasites from replicating.

Several rhoptry proteins including ROP1,2,4,8 and RON2,4,5,8 are processed before they are secreted (Beckers, Wakefield et al. 1997; Soldati, Lassen et al. 1998; Sinai and Joiner 2001; Miller, Thathy et al. 2003; Bradley, Li et al. 2004; Besteiro, Michelin et al. 2009). Processing, usually involving the removal of a prodomain, is believed to either enable the correct targeting toward the rhoptries or regulate the activity of the rhoptry protein.

### **1.7.3. Dense Granule proteins**

Comparatively little is known about dense granule proteins, however they are thought to interact with a variety of host cell proteins (Ahn, Kim et al. 2006). Currently over 23 GRA proteins have been identified, however few have been functionally characterised. It has been reported that GRA7 interacts with ROP2 and ROP4 in infected host cells (Dunn, Ravindran et al. 2008) and that GRA4 and GRA6 form a complex with GRA2, within an intravacuolar network for nutrient or protein transport (Labruyere, Lingnau et al. 1999) illustrating crosstalk between rhoptry and dense granule secretion. GRA3 and GRA10 are released into the PV during or shortly after the invasion and are associated with the PV membrane (Ahn, Kim et al. 2005). As with ROPs, selected dense granule proteins have been identified to modulate signalling cascades within the host cell. GRA15 was shown to interfere with the host immunity response by modulating the NF- $\kappa$ B pathway (Rosowski, Lu et al. 2011) and GRA16 was recently identified to be exported through the PV membrane to reach the host nucleus, where it interferes with host gene expression (Bougdour, Durandau et al. 2013).

## **1.8. Protein transport in *T.gondii***

### **1.8.1. Protein transport to the endosymbiotic organelles**

The protein transport in *T.gondii* to the endosymbiotic organelles is probably via transmembrane transport like in higher eukaryotes (Köhler, Delwiche et al. 1997; Shao and Hegde 2011). Nucleus-encoded mitochondrion proteins are synthesised on cytoplasmic ribosomes and transported via organellar translocation machinery like TIMs (Transporter inner membrane) and TOMs (transporter outer membrane) into the mitochondrion (Sheiner and Soldati-Favre 2008). Similarly, most apicoplast proteins are encoded in the nucleus and so must be trafficked to the organelle and a Golgi-independent pathway is thought to be most likely (Tonkin 2006; DeRocher 2005). Apicoplast proteins are thought to have a dual targeting signal consisting of a signal peptide to enter the secretory pathway and a transit peptide to direct proteins into the apicoplast (Waller, Keeling et al. 1998; Roos 1999; Waller, Reed et al. 2000). Components of the TIC/TOC (Translocon at outer/inner envelope membrane of Chloroplast)

machinery of plants such as Tic20, has been identified in *T.gondii* (van Dooren, Tomova et al. 2008)] and *P.falciparum* (known as Tic22) (Kalanon, Tonkin et al. 2009)]. Tonkin and colleagues showed in *P.falciparum* that apicoplast proteins could still be targeted to the apicoplast in presence of Brefeldin A, a drug known to block trafficking between the ER and Golgi. Additionally, they found the apicoplast to be located on a small extension of the ER. This could also be seen as membrane contact sites (MCS) in *T.gondii* (Tomova, Humbel et al. 2009). These MCS are thought to be lipid trafficking points, which are probably protein mediated. They are not permanent and no fusion between the ER and apicoplast has been detected. Since the apicoplast is an important location of fatty acid biosynthesis, MCS are thought to be established depending on the parasite's lipid requirements. Vesicular transport of apicoplast proteins via endosome-like organelles could also be a scenario, since phosphatidylinositol 3-monophosphate (PI3P) was detected both at the apicoplast and at apicoplast protein-shuttling vesicles (Tawk, Chicanne et al. 2010; Tawk, Dubremetz et al. 2011). Inhibition of the PI3P synthesising kinase interfered with apicoplast biogenesis. In higher eukaryotes, PI3P synthesising kinase is also known as VPS34 and an effector protein of Rab5, demonstrating a divergent role for this kinase in *T.gondii* (Murray and Backer 2005).

### **1.8.2. Protein transport to the secretory organelles**

Dense granule proteins are synthesised in the ER and modified in the Golgi as seen for secretory proteins in other higher eukaryotes. No regulated vesicular transport has been shown for dense granule proteins thus far and it is assumed that all GRAs are constitutively secreted as has been shown for GRA 10 (Ahn, Kim et al. 2005) and GRA3 (Chaturvedi, Qi et al. 1999) (see 1.7.3.). It is thought that GRA proteins are released via a calcium-independent mechanism with involvement of Rab-triggered SNARE complex formation (see 1.5.1. and 1.6.4.) (Karsten, Qi et al. 1998; Chaturvedi, Qi et al. 1999; Kaasch and Joiner 2000; Liendo, Stedman et al. 2001; Stedman, Sussmann et al. 2003).

Microneme and rhoptry proteins are also synthesised in the ER and modified in the Golgi. Signal recognition particles (SRPs) for co-translational translocation are conserved in apicomplexa (Sheiner and Soldati-Favre 2008). All microneme and rhoptry proteins are regulatively secreted in a calcium-dependent manner. Biogenesis of micronemes and rhoptries and how their proteins are sorted to the

organelles is still not fully understood. Recent studies indicate that microneme and rhoptry proteins are transported to their apical compartments via endosomal-like compartments (ELCs) (Ngo, Yang et al. 2003; Harper, Huynh et al. 2006; Breinich, Ferguson et al. 2009; Miranda, Pace et al. 2010; Parussini, Coppens et al. 2010; Sloves, Delhaye et al. 2012). A dynamin (DrpB) has been identified in *T.gondii* which was shown to be essential in the biogenesis of secretory organelles (Breinich, Ferguson et al. 2009). In higher eukaryotes, dynamin is involved in formation of clathrin coated vesicles. In *T.gondii* it is located close to the Golgi and is suggested to be involved in formation of vesicles for the regulatory secretory pathway via transport to the ELCs (Breinich, Ferguson et al. 2009; Sloves, Delhaye et al. 2012). For rhoptry biogenesis it is also thought, that immature, pre-rhoptries are transported from the Golgi to the apical tip during rhoptry biogenesis of *T.gondii*. Several rhoptry proteins become processed during the transition from immature to mature rhoptries including ROP4 (Carey, Jongco et al. 2004), ROP1 (Bradley and Boothroyd 2001) and ROP13 (Turetzky, Chu et al. 2010).

As mentioned in chapter 1.7.1., most microneme proteins function in complexes, which consist of at least one transmembrane (TM) and one soluble protein. Targeting signals within the cytoplasmic domain of the TM protein are responsible for targeting to the micronemes, potentially via interaction with a clathrin-associated adaptor protein (AP) complex (Di Cristina, Spaccapelo et al. 2000; Harper, Huynh et al. 2006; Sheiner, Santos et al. 2010). This does not rule out an important role of soluble proteins in trafficking. The best studied example of microneme proteins trafficking via ELCs is the TgMIC2/TgM2AP complex. It was shown that TgCPL is involved in cleavage of recombinant proM2AP and that proM2AP and TgCPL partially co-localise with TgVP1 (Harper, Huynh et al. 2006; Parussini, Coppens et al. 2010). Harper and colleagues found a fraction of proM2AP also co-localising with TgGalNac-YFP and TgRab51-HA, which led them to assume that the proM2AP-MIC2 complex traffics from the TGN to the EE. Deletion of the M2AP propeptide resulted in a defect in trafficking of the MIC2-M2AP complex within endosomal-like compartments and consequently the inability to process or secrete MIC2. In M2AP knockout parasites, MIC2 expression was affected and retained in the ER/Golgi region (Huynh, Rabenau et al. 2003). On the other hand, reduction of MIC2 expression results in mislocalisation of M2AP to dense granules and its secretion into the PV (Huynh

and Carruthers 2006). It is possible that uncleaved proM2AP or the propeptide could take another secretory pathway (Karsten, Qi et al. 1998).

Post Golgi, there are currently two opposing models of the mechanism of protein trafficking. The first model from Parussini and colleagues in 2010, suggested that micronemes derive from the endocytic system (LE or VAC) instead of the TGN. Proteolytic maturation of proMICs takes place in the LE or VAC (Parussini, Coppens et al. 2010).

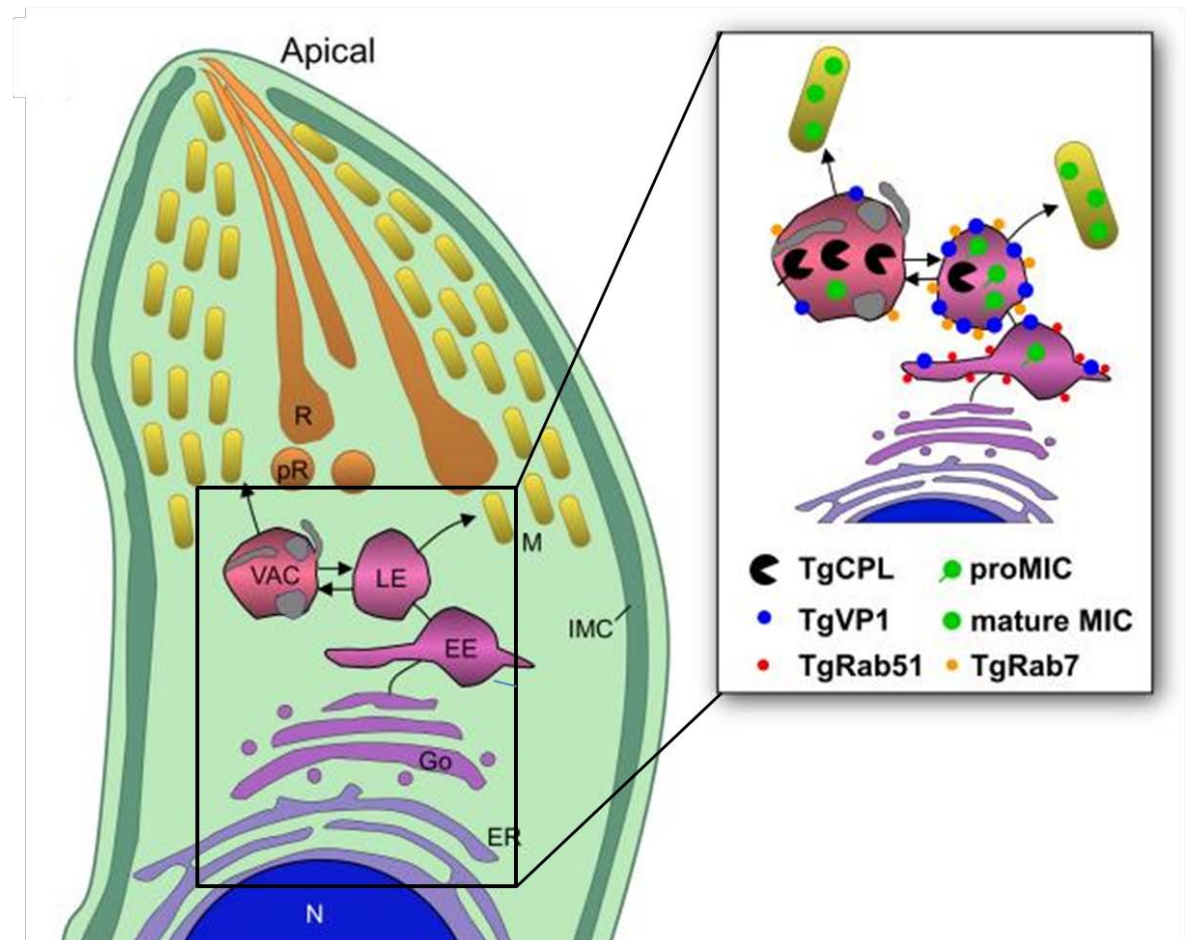


**Figure 1-15: Hypothesised model of microneme protein maturation and transport to their target organelles, modified from: (Parussini, Coppens et al. 2010).** After synthesis in the ER and posttranslational modifications in the Golgi microneme proteins are transported to their final organelles via EE, LE and probably the lysosome-like VAC. TgRab51 localises and indicates the EE. Localisation of TgRab7 is believed to indicate the LE compartment. TgVP1 is concentrated at the LE membrane and also present in the EE and VAC membranes. Maturation of microneme proteins (cleavage of a propeptide) mediated by TgCPL is thought to take place within the VAC and LE. M= microneme, R= rhoptry, pR= pre-rhoptry

The second model is based on the identification of a sortilin-like receptor (TgSORTLR) *T.gondii* (Sloves, Delhaye et al. 2012). Sortilin (VPS10) in yeast functions in mannose-6-phosphate independent transport to the endosomal

system. No mannose-6-phosphate receptor could be identified in apicomplexans and TgSORTLR was shown to be essential for protein traffic and biogenesis of secretory organelles. Sloves and colleagues hypothesise a similar trafficking pathway in *T. gondii* for microneme and rhoptry proteins. In this case, TgSORTLR binds to rhoptry or microneme proteins in the lumen of the Golgi and recruits AP adaptins, clathrins and vacuolar sorting proteins (VPS). TgSORTLR vesicles with microneme and rhoptry proteins as their cargo are further transported through the EE and probably LE to pre-rhoptries or immature micronemes. After that, TgSORTLR is assumed to recruit a retromer complex for retrograde transport to the Golgi (Sloves, Delhaye et al. 2012).

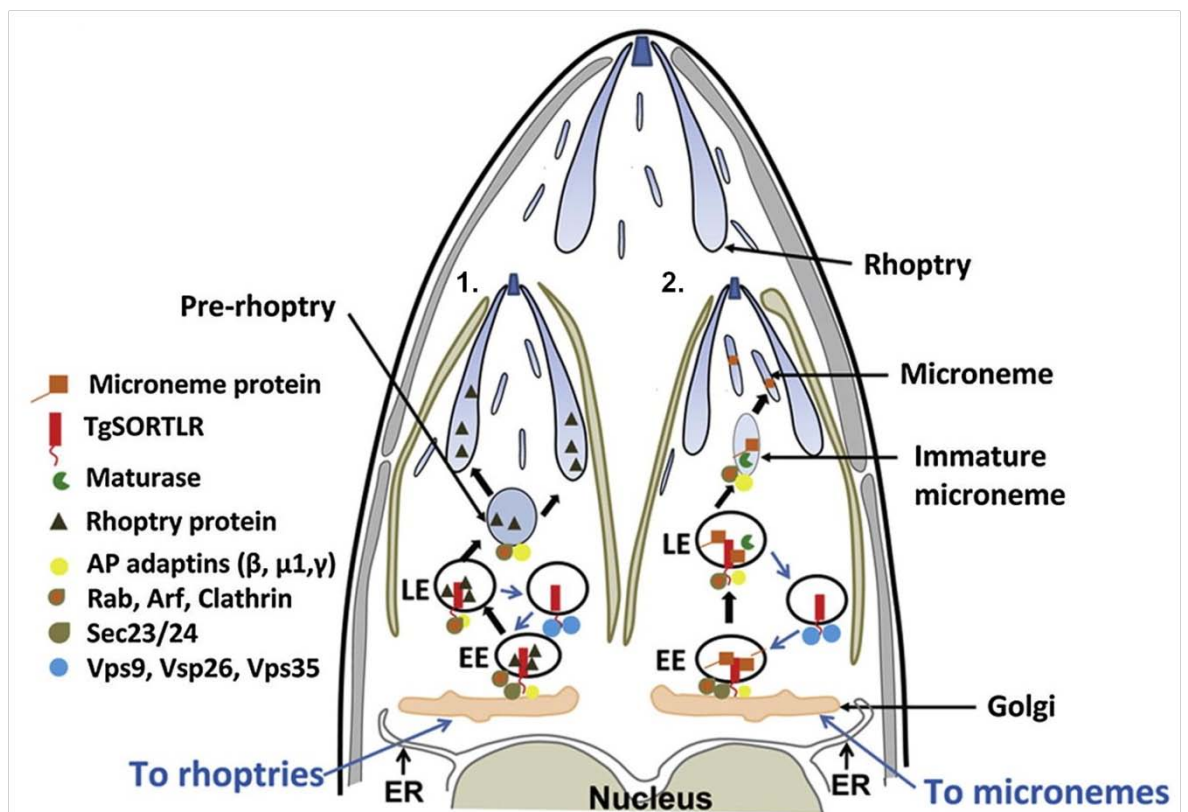


**Figure 1-16: Hypothesised model of microneme and rhoptry protein maturation and transport to their target organelles, modified from: (Sloves, Delhaye et al. 2012).** (1.) Rhoptry proteins are transported to pre-rhoptries via EE and LE. (2.) Microneme proteins are transported via EE and LE to immature micronemes. Maturation of microneme proteins takes place in the LE and immature micronemes. In both cases TgSORTLR is thought to bind the transported secretory proteins. With its cytosolic tail TgSORTLR is thought to interact with vesicle formation/ coating and transport regulators like coat complex transport proteins (Sec23/24), retromer associated vacuolar sorting proteins (Vps9, Vps26, Vps23), AP adaptins, Rabs, Arfs and Clathrin.

## 1.9. Rab GTPases in Apicomplexan parasites

Rab proteins in higher eukaryotes have been intensively investigated for the past 20 years. Although apicomplexan parasites possess only a reduced core set of Rab proteins (Langsley, van Noort et al. 2008) few detailed studies have been performed. One Rab protein in *Theileria parva*, a tick transmitted causative agent of East Coast Fever (ECF), which is a lymphoproliferative disease of cattle in sub-Saharan Africa, has been described. The Rab1 homologue in *T. parva* is thought to regulate the vesicular traffic between ER and the cis Golgi (Janoo, Musoke et al. 1999). In a genome analysis of *Cryptosporidium hominis*, the cause of acute diarrhoea in humans, proteins of the NSF/SNAP/SNARE/Rab machinery have been identified (Xu, Widmer et al. 2004) however has not been further characterised. Rab proteins and their effectors are better described in *Plasmodium*. In *Plasmodium*, 11 Rab proteins have been identified (Quevillon, Spielmann et al. 2003). This study demonstrated that PfRab1B functioned in ER/Golgi transport and PfRab2 and PfRab7 are probably involved in vacuole formation. Furthermore, PfRab6 was shown to be involved in intra-Golgi traffic, also co-localising with an ER marker (anti-Pf39) (de Castro, Ward et al. 1996; Quevillon, Spielmann et al. 2003) and being a trans-Golgi marker in *P. falciparum* research (Struck, Herrmann et al. 2008). More recently, PfRab1A was identified as a unique *paralogue* in chromalveolates and rhizarians, potentially with a novel function (Elias, Patron et al. 2009) and a more detailed analysis of *Plasmodium* Rab11A revealed its role in cytokinesis (Agop-Nersesian, Naissant et al. 2009). Currently, the function of four Rab-GTPases has been analysed in greater detail in *Toxoplasma gondii*. Rab5A has been demonstrated to localise adjacent to the Golgi, where it might play a role in formation of endosomal-like compartments (ELCs) and cholesterol acquisition (Robibaro, Stedman et al. 2002). Rab6 has been localised close to the Golgi and has been demonstrated that it plays a role in retrograde transport from post-Golgi secretory granules to the Golgi (Stedman, Sussmann et al. 2003). TgRab11A has been shown to localise to the Inner Membrane Complex (IMC) during replication, where it is required for maturation of the IMC and consequently for cytokinesis (Agop-Nersesian, Naissant et al. 2009). Interestingly Rab11B is an alveolate specific GTPase and also plays a role in IMC biogenesis and appears to act prior to Rab11A during replication (Agop-Nersesian, Egarter et al. 2010). Another *T. gondii* Rab protein,

which is described in the literature, but is not functionally characterised, is TgRab7. In connection with studies about a new organelle (plant like vacuole or a putative late endosome) in *T.gondii*, TgRab7 was found to co-localise with markers of the ELC (Miranda, Pace et al. 2010; Parussini, Coppens et al. 2010).

## **1.10. Aim of this study**

In the following project, the ddfKBP system is used to perform a systematic analysis of the Rab proteins and the connected secretory traffic in *Toxoplasma gondii*. As recently shown for Rab11A (Agop-Nersesian, Naissant et al. 2009) and Rab11B (Agop-Nersesian, Egarter et al. 2010), regulated overexpression of Rab wild type (wt) and dominant negative (DN) (setting a point mutation within the highly conserved GTPase domain) of the respective Rab allows for localisation and functional studies of Rab proteins in this parasite and analysis of effects on organellar trafficking and biogenesis. As TgRab11A, TgRab11B and TgRab6 are described in detail in the literature (Stedman, Sussmann et al. 2003; Agop-Nersesian, Naissant et al. 2009; Agop-Nersesian, Egarter et al. 2010), the remaining predicted TgRab proteins will be analysed in this work.

Here, analysis of Rab protein localisation will allow a first impression of Rab-regulated vesicular trafficking in *T.gondii*. As previously mentioned all microneme and rhoptry proteins characterised thus far are secreted in a regulated manner, however, the mechanism of sorting is unclear. Using a TgRab overexpression screen, Rab proteins will be identified and their function in the biogenesis of organelles such as micronemes and rhoptries will be investigated. Further characterisation of trans-dominant mutants of these candidates should give us a better understanding of how the late secretory system is organised.

## 2. Materials and Methods

### 2.1. Consumables, biological and chemical reagents

Acetic acid:	VWR
Acetone:	AppliChem
Agarose:	Invitrogen
Ammonium persulfate (APS):	Roth
Ampicillin sodium salt:	Roth
Bacto-Agar:	BD
Bacto-Trypton:	BD
Bacto-Yeast:	BD
Bovine serum albumin:	AppliChem, Roth
Bromophenol blue sodium salt:	Merck
CaCl <sub>2</sub> *2H <sub>2</sub> O:	Merck
Coomassie Brilliant Blue R250:	Fluka
DAPI:	Calbiochem-Novabiochem GmbH
Dabco <sup>®</sup> 33-LV:	Sigma
D-(+)-Glucose:	Merck
Dimethyl sulfoxide (DMSO):	AppliChem
Dithiothreitol (DTT):	AppliChem
Dulbecco's Modified Eagle Medium (DMEM):	c.c.pro GmbH
Ethanol 100%:	Sigma
Ethanol 96%:	Sigma
Ethidium bromide:	Roth
Ethylenediaminetetraacetic acid (EDTA):	Acros Organics
Ethylene glycol tetraacetic acid (EGTA):	Serva
Fetal calf serum (FCS):	c.c.pro GmbH
Fluoromount G:	Southern Biotech
Gentamicin:	c.c.pro GmbH
Glycerol:	Roth
Glycine:	Acros Organics
HEPES:	Gerbu Biochemicals GmbH
Isopropyl β-D-1-thiogalactopyranoside (IPTG):	AppliChem
Methanol:	J.T. Baker
MgCl <sub>2</sub> * 6H <sub>2</sub> O:	Merck
MgSO <sub>4</sub> * 7H <sub>2</sub> O:	Merck
Milk powder:	Roth
Monopotassium phosphate (KH <sub>2</sub> PO <sub>4</sub> ):	Merck
MnCl <sub>2</sub> *4H <sub>2</sub> O:	AppliChem
Mowiol <sup>®</sup> :	Sigma
Natrium chloride (NaCl):	Merck
NaH <sub>2</sub> PO <sub>4</sub> :	Riedel-de Haën GmbH
Na <sub>2</sub> HPO <sub>4</sub> :	Riedel-de Haën GmbH

NaOH:	Merck
Paraformaldehyde (PFA):	AlliedSignal Riedel-de Haën GmbH
Phosphate buffered saline (PBS):	c.c.pro GmbH
Potassium chloride (KCl):	Merck
Potassium hydroxide (KOH):	AlliedSignal Riedel-de Haën GmbH
PIPES:	Sigma
Ponceau S:	AppliChem
Pyrimethamine:	Sigma
RNase free water:	AppliChem
Sodium carbonate:	Sigma
Sodium dodecyl sulfate (SDS):	Roth
Tetracycline:	Sigma
Tetramethylethylenediamine (TEMED):	AppliChem
Tris-Acetate:	Roth
Tris-HCl:	Roth
Triton X-100:	Merck
Tryptone/Peptone/Casein Hydrolysate:	Sigma
X-Gal:	Neolab
Xylene Cyanol:	AppliChem

## 2.2. Equipment

Agarose gel electrophoresis equipment:	CTI GmbH; BioRad
Analytical balances (TE 124S-OCE):	Sartorius GmbH
Autoclave sterilizer:	Holzner
Cell scraper 300 mm:	Neolab
Centrifuges:	
Bench top 5417C:	Eppendorf
Bench top 5417R:	Eppendorf
Labofuge 400E:	Heraeus Instruments
Rotanta/RR:	Hettich
Refrigerated centrifuge Beckman J2-21M/E:	Beckman Coulter GmbH
Multifuge 1 s-R:	Heraeus Instruments
Refrigerated centrifuge Sorvall Legend XFR:	Thermoscientific
Large bench centrifuge 6K15:	Sigma
Cover slips for IFA:	Hölzer
Cryo tubes:	Greiner Bio-One
Electroporation cuvettes:	BTX
Electroporation systems:	
Electro Square Pore 830:	BTX
Gene pulser Xcell:	BioRad

Gel Documentation Systems:	Herolab, BioRad
Hyperprocessor Automatic Film Processor:	Amersham Pharmacia
Incubators:	
Incubator 60°C and 37°C:	Heraeus Instruments
Shaking incubator HT:	Infors AG
Shaking incubator Innova 4000:	New Brunswick Scientific
CO <sub>2</sub> - incubator tissue culture, MCO-17AI:	Sanyo
CO <sub>2</sub> - incubator tissue culture, InnovaCo/170:	New Brunswick Scientific
CO <sub>2</sub> - incubator tissue culture, Heracell 240i:	Thermoscientific
Magnetic stirrer:	Starlab
Immersion oil: Immersol™ 518 F:	Zeiss
Microscopes:	
Light microscope Diavert:	Leitz
Stereo microscope Nikon SMZ 1500 with:	Nikon
Nikon Coolpix 5400 camera	
Nikon MXA 5400 Objectiv	
Leica DMIL with:	Leica Microsystems
Leica DFC 320 camera	
Leica LAS Version 2.20 R1 software	
Zeiss Axioscope 2 microscope with:	Carl Zeiss
Zeiss AxioCam MRm CCD camera	
Zeiss Axiovision Version software	
Nikon TE2000 Inverted microscope with:	Nikon
Perkin Elmer Spinning Disc confocal System	
ERS	Perkin Elmer
UltraView software	Perkin Elmer
Delta vision Core system with:	Applied Precision
SoftWoRx suite software	
Microscope slides for IFA:	Menzel GmbH, Thermoscientific
Needles(0,7 mm x 30 mm; 0,4 mm x 19 mm):	BD
Neubauer counting chambers:	Marienfeld
Nitrocellulose membrane:	Bioscience Schneider & Schnell,
Parafilm:	Amersham
Petri dishes:	Pechiney
Plastic pipettes sterile (5 ml, 10 ml, 25 ml):	Greiner Bio-One
Pipette tips:	Greiner Bio-One
SDS-PAGE equipment:	CTI GmbH or BioRad
Semidry-Blot equipment:	CTI GmbH or BioRad
Syringes (sterile) BD:	BD
Software for DNA or Protein sequence analysis:	
BioEdit:	Tom Hall, Ibis Biosciences

pDraw32:	AcaClone software
CLC Genomics Workbench 4:	CLCBio
Software for Image editing:	
Adobe Photoshop CS4:	Adobe Systems Inc.
Adobe Illustrator CS4:	Adobe Systems Inc.
ImageJ 1.40 g:	National Institutes of Health.
ImageJ 1.46r:	Wayne Rasband National Institutes of Health
Software for operating systems and word processing:	
Windows XP, 7:	Microsoft Corportion, CA,USA
Microsoft Office 2007:	Microsoft Corportion, CA,USA
Endnote X4:	Thomson Scientific, USA
Spectrophotometer:	Nanodrop
Thermocycler: Mastercycler Eppgradient	Eppendorf
Thermo mixer compact:	Eppendorf
Tissue culture hollow-ware Cellstar:	Greiner Bio-One
Culture flasks (T25, T75, T175)	
6-cm dishes	
24 well plate	
96 well plate	
Vortexer:	
Vortex Reaxtop:	Heidolph
Vortex Wizard:	Starlab
Water baths:	
Whatman <sup>TM</sup> 3MM:	Julabo; Grant
X-ray film cassette:	Whatman Paper Company
X-ray film (BioMax MR):	Kodak
	Kodak

## 2.3. Buffers, Solutions and Media

### 2.3.1 General Buffers

10x PBS:	137 mM NaCl, 2.7 mM KCl, 8 mM Na <sub>2</sub> HPO <sub>4</sub> , 1.8 mM KH <sub>2</sub> PO <sub>4</sub> (pH 7.4)
----------	--

### **2.3.2. DNA analysis**

50x TAE:	2 M Tris/Acetate (pH 8.0), 0.5 M Na <sub>2</sub> EDTA
5x DNA loading buffer:	30% Gluceronol, 5x TAE, Brom-Phenolblue, Xylencyanolblue, H <sub>2</sub> O
DNA ladder:	150 µl 1kb-Ladder plus (1 µg/µl), 300 µl 5x DNA loading buffer, 1050 µl H <sub>2</sub> O

### **2.3.3. Protein analysis**

PAA stock solution:	30% PAA, 0.8% Bis-AA
Seperating gel buffer 4x :	1.5 M Tris/ HCl (pH 8.8), 0.4% SDS (w/v), filtered sterile
Stacking gel buffer 4x:	0.5 M Tris/HCl (pH 6.8), 0.4% SDS (w/v), filtered sterile
Seperating gel:	8-15% PAA (v/v), 25% 4x Seperating gel buffer, 0.1% APS 10% (v/v), 0.2% TEMED (v/v)
Stacking gel:	4% PAA (v/v), 25% 4x Stacking gel buffer (v/v), 0.1% APS 10%(v/v), 0.2% TEMED (v/v)
5x SDS-PAGE running buffer :	33 mM Tris/HCl (pH 6.8), 190 mM Glycine, 0.1 % SDS
4x SDS-PAGE sample buffer :	50% 4x Stacking gel buffer (v/v), 40% Glycerol (v/v), 8 % SDS (w/v), 0.2 % Bromphenol blue (w/v), 400 mM DTT (w/v)
Towbin buffer for semi-dry blot:	48mM Tris, 39mM glycine, 20% methanol (v/v)
Towbin buffer for wet-blot:	25mM Tris, 190mM glycine, 20% methanol (v/v)
Ponceau-S staining solution 10x:	2% Ponceau S (w/v), 30% TCA (v/v), 20% sulfosalicylic acid (w/v)
Blocking solution:	0.2% Tween (v/v), 3% milk powder (w/v) in PBS
Washing solution:	0.2% Tween (v/v) in PBS

**2.3.4. Bacteria culture**

IPTG (100 µl/petri dish):	100 mM IPTG in H <sub>2</sub> O
X-Gal (20 µl/petri dish):	50 mg/ml in N,N-dimethylformamide
50x PIPES:	0.5 M PIPES with 5 mM KOH (pH 6.7), sterile filtered
Transformation buffer:	55 mM MnCl <sub>2</sub> *4H <sub>2</sub> O, 15 mM CaCl <sub>2</sub> *2H <sub>2</sub> O, 250 mM KCl, 1x PIPES (10 mM) (pH 6.7), sterile filtered
Lysogeny broth (LB) medium:	1% Bacto-Trypton (w/v), 0.5% Yeast extract (w/v), 1% NaCl (w/v), autoclaved
LB-Agar:	1.5% Bacto-Agar (w/v) in LB-Medium, autoclaved
Super optimal broth (SOB) medium:	2% Bacto-Trypton (w/v), 0.5% Bacto-Yeast (w/v), 0.05% NaCl (w/v), 2.5 mM KCl, autoclaved
SOB with Catabolite repression (SOC) medium:	2% Trypton/Pepton/Caseinhydrolysate (w/v), 0.5% Bacto-Yeast (w/v), 10 mM NaCl, 2.5 mM KCl, autoclaved, 20 mM Glucose, 10 mM MgCl <sub>2</sub> * 6H <sub>2</sub> O, 10 mM MgSO <sub>4</sub> * 7H <sub>2</sub> O added sterile
Ampicilin (1000x):	100mg/ml in ddH <sub>2</sub> O
Tetracycline (1000x):	5mg/ml in 70% ethanol

**2.3.5. Tissue culture**

DMEM <sub>complete</sub> :	500 ml DMEM, 10% FCS (v/v), 1% Glutamine (v/v), 1x Gentamicin (20 µg/ml)
Trypsin/EDTA:	1x H <sub>2</sub> O, autoclaved
Freezing solution:	25% FCS (v/v), 10% DMSO (v/v) in DMEM <sub>complete</sub>
Elektroporation buffer/ Cytomix:	10 mM K <sub>2</sub> HPO <sub>4</sub> /KH <sub>2</sub> PO <sub>4</sub> , 25 mM HEPES and 2 mM EGTA pH 7.6, 120 mM KCl, 0.15 mM CaCl <sub>2</sub> , 5 mM MgCl <sub>2</sub> with 5 mM KOH to pH 7.6, 2 mM ATP, 3 mM GSH
ATP (30 µl/ml):	100 mM in H <sub>2</sub> O

GSH (30 µl/ml):	100 mM in H <sub>2</sub> O
Giemsa staining solution:	10x Giemsa stain, diluted 1:10 in H <sub>2</sub> O
Egress buffer:	1 µM A23187 in DMEM
Chloramphenicol (1000x):	10mg/ml in ethanol
MPA (500x):	12.5mg/ml methanol
Xanthine (500x):	20mg/ml, 1M KOH
Pyrimethamine (1000x):	1mM in ethanol
Gentamycine (500x):	10mg/ml in ddH <sub>2</sub> O
Shield-1 (1000x):	1mM in 70% ethanol
Calcium ionophore (1000x):	1mM in DMSO

### **2.3.6. IFA**

PFA fixing solution:	4% PFA (w/v) in PBS
Permeabilisation solution:	0.2% Triton X-100 in PBS
Blocking solution:	2% BSA in Permeabilisation solution
DAPI 5000x (stock -20°C):	50 µg/µl in PBS
DAPI-staining solution 500x (stock 4°C):	DAPI 5000x diluted 1:10 in PBS

### **2.3.7. Electron microscopy**

Phosphate buffer (0.1 M):	10.9g Na <sub>2</sub> HPO <sub>4</sub> , 3.2 g NaH <sub>2</sub> PO <sub>4</sub> in 500 ml H <sub>2</sub> O, pH 7.4
EM fixation solution:	2.5% Glutaraldehyde (v/v) in Phosphate buffer 0.1 M, pH 7.4
IEM fixation solution:	4% Paraformaldehyde (w/v) in Phosphate buffer 0.1 M, pH 7.4

## **2.4. Organisms:**

### **2.4.1. T.gondii strains**

RH<sup>hxgprt-</sup> (Donald, Carter et al. 1996) kindly provided by Dominique Soldati-Favre (University of Genève, Switzerland)

### **2.4.2. Cell lines used in tissue culture**

Human Foreskin Fibroblasts (HFF) kindly provided by Dominique Soldati-Favre (University of Genève, Switzerland) and purchased from ATCC.

Vero cells (African green monkey kidney cells) kindly provided by Dominique Soldati-Favre (University of Genève, Switzerland)

### **2.4.3. Bacteria strains**

XL1 Blue (Stratagene)

XL 10 Gold (Stratagene)

## **2.5. Enzymes and Kits**

Alkaline Phosphatase, Calf Intestinal:	New England Biolabs
DNeasy Blood & Tissue Kit:	QIAGEN
ECL bzw. ECL Plus Western blotting detection reagents:	Amersham Biosciences
EuroTaq:	EuroClone
Expand High Fidelity <sup>PLUS</sup> PCR System:	Roche Diagnostics GmbH
High Pure PCR Product Purification Kit:	Roche Diagnostics GmbH
Nucleobond-AX-System:	Machery-Nagel
Platinum Taq DNA Polymerase High Fidelity:	Invitrogen
QIAprep Spin Miniprep Kit:	QIAGEN
QIAquick Gel Extraction Kit:	Roche Diagnostics GmbH
Restriction endonucleases:	New England Biolabs
RNAagents Total RNA Isolation Kit:	Promega
T4-DNA-Ligase:	New England Biolabs
Titan One Tube RT-PCR System:	Roche Diagnostics GmbH

Transcriptor One-Step RT-PCR Kit:	Roche Diagnostics GmbH
Transcriptor Reverse Transcriptase:	Roche Diagnostics GmbH
Trypsin/EDTA 10x:	c.c.pro GmbH

## 2.6. Antibodies

### 2.6.1. Primary Antibodies

Antibodies	raised in	Dilution	Source
AMA1	mouse	1:300	Gary Ward
Catalase	rabbit	1:3000	Dominique Soldati
c-myc (A-14)	rabbit	1:250	Santa Cruz
c-myc SC-40	mouse	1:5000	Sigma
c-myc SC-40 (9E10)	mouse	1:250	Santa Cruz
CPL	rabbit	1:100	Vern Carruthers
FKBP12	rabbit	1:500	Abcam
GRA9	rabbit	1:500	Didier Desleea
HA	rat	1:1000	Roche
IMC	rabbit	1:1500	Con Beckers
MIC2	mouse	1:300	Vern Carruthers
M2AP	rabbit	1:1000	Vern Carruthers
MIC3	mouse	1:300	Maryse Lebrun
MIC8	rabbit	1:300	Markus Meissner
MIC11	rabbit	1:300	Vern Carruthers
proM2AP	rabbit	1:500	Vern Carruthers
Rop2-4	mouse	1:1000	Jean F. Dubremetz
Rop5	mouse	1:1000	Jean F. Dubremetz
Sag1	mouse	1:100	Lloyd Kasper
Ty	rabbit	1:250	GenScript
VP1	rabbit	1:500	Vern Carruthers

### 2.6.2. Secondary Antibodies

Antibodies	Dilution	Source
Alexa Fluor 488 goat anti-rabbit	1:3000	Invitrogen
Alexa Fluor 488 goat anti-mouse	1:3000	Invitrogen
Alexa Fluor 594 goat anti-rabbit	1:3000	Invitrogen
Alexa Fluor 594 goat anti-mouse	1:3000	Invitrogen
ATTO 565 anti-mouse	1:200-1:1000	Stefan Hell
ATTO 594 anti-mouse	1:100	Stefan Hell

ATTO 594 anti-rabbit	1:100	Stefan Hell
ATTO 647N anti-mouse	1:100	Stefan Hell
ATTO 647N anti-rabbit	1:100	Stefan Hell
Dyomics 485 anti-rabbit (DY 485 XL)	1:20-1:150	Stefan Hell
Peroxidase-conjugated AffiniPure goat anti-rabbit IgG	1:5000	Dianova
Peroxidase-conjugated AffiniPure donkey anti-mouse IgG	1:5000	Dianova

## 2.7. Plasmids

Vector and expression plasmids	Source or Reference
pGEM-T Easy Vector System	Promega
p5RT70DDmycGFP-HXGPRT	(Herm-Gotz, Agop-Nersesian et al. 2007)
RnGRASP-RFP-CAT	(Pflugger, Goodson et al. 2005)
TgGalNac-YFP-CAT	(Nishi and Roos DS, not published)
FNR-RFP-CAT	(Striepen, Crawford et al. 2000)
TgERD2-GFP	(Pflugger, Goodson et al. 2005)
HSP60-RFP-CAT	(van Dooren, Reiff et al. 2009)
p5RT70Rab5BHADD-HXGPRT	Chris Tonkin (Kremer, Kamin et al. 2013)
p5RT70TyRab5A-HXGPRT	(Kremer, Kamin et al. 2013)
p5RT70DDmycRab1A-HXGPRT	(Kremer, Kamin et al. 2013)
p5RT70DDmycRab1A(N126I)-HXGPRT	(Kremer, Kamin et al. 2013)
p5RT70DDmycRab1B-HXGPRT	(Kremer, Kamin et al. 2013)
p5RT70DDmycRab2-HXGPRT	(Kremer, Kamin et al. 2013)
p5RT70DDmycRab4-HXGPRT	(Kremer, Kamin et al. 2013)
p5RT70DDmycRab5A-HXGPRT	(Kremer, Kamin et al. 2013)
p5RT70DDmycRab5A(N158I)-HXGPRT	(Kremer, Kamin et al. 2013)
p5RT70DDmycRab5B-HXGPRT	(Kremer, Kamin et al. 2013)
p5RT70DDmycRab5B(N152I)-HXGPRT	(Kremer, Kamin et al. 2013)
p5RT70DDmycRab5C-HXGPRT	(Kremer, Kamin et al. 2013)
p5RT70DDmycRab5C(N153I)-HXGPRT	(Kremer, Kamin et al. 2013)
p5RT70DDmycRab7-HXGPRT	(Kremer, Kamin et al. 2013)
p5RT70DDmycRab7(N124I)-HXGPRT	(Kremer, Kamin et al. 2013)
p5RT70DDmycRab7(G18E)-HXGPRT	(Kremer, Kamin et al. 2013)
p5RT70DDmycRab18-HXGPRT	(Kremer, Kamin et al. 2013)

## 2.8. Oligonucleotide Primers

To design primers BioEdit and pDraw were used as software and generated by *Thermo Fisher Scientific* or Eurofins. In the following sense (s) and antisense (as) primers used in this work are listed.

### Primer in 5'-3' orientation

Rab1A-s: CCATGCATGCGGCAGGCAGACCACGG  
 Rab1A-as: GCGTTAATTAACATGAACAGTTGCCAGTCCGCTGTGCCATAGCCC  
 GGTTGTCAGCAC  
 Rab1A(N126)-as: TCGTCTGCCTTCTCGCATTGATTCTACGAGGATCTTGC  
 Rab1B-s: GCGATGCATAAGCCTGAATACGACTATCTTTTCAAGCTGCTTCTCA  
 TTGGCGACTC  
 Rab1B-as: GCGTTAATTAACAACAACCCGAAGAGACGCTGCGAACCGGCTGG  
 Rab2-s: GCGATGCATATGCCGTACCAGTATCTCTTCAAGTATATCATCA  
 Rab2-as: GCGTTAATTAACAGCAACTTGCAGACCGCTG  
 Rab4-s: GCGATGCATGACTCCAGCAAGGACCTG  
 Rab4-as: GCGTTAATTAACACGAGCAACTCGATGGCGG  
 Rab5A-s: GCGATGCATGGTTTTCGAATCTGCTGAGG  
 Rab5A-as: GCGTTAATTAACTTTTGCCTCCACATGCACACC  
 Rab5A(N158I)-as: CGCGGGGATCAAAGAGG  
 Rab5B-s: GCGATGCATGGATGCACCGCGAGCTCCAC  
 Rab5B-as: GCGTTAATTAATCACAACCTCCATCATGCTCTGCTTCAGC  
 Rab5B(N142I)-as: GCTGCGATCAAGAGCG  
 Rab5C-s: GCGATGCATTCTTTCTCGCAAGCTTACAGTTC  
 Rab5C-as: GCGTTAATTAATCAACTGTTTCCGCCGCAAC  
 Rab5C(N153I)-as: GCAGCCATCAAGATGG  
 Rab7-s: GCGATGCATCCCAAGAAGAAGGCTCTCTTGAAAG  
 Rab7-as: GCGTTAATTAACAGCAGCCGCCGCTGC  
 Rab7(N124I)-as: CGTTGGCATCAAAGTCG  
 Rab7(G18E)-s: GCGATGCATCCCAAGAAGAAGGCTCTCTTGAAAGTCATCATC  
 CTCGGGGACAGCGAGGTAGGCAAGACCTCGCTGATGAACCAGT  
 Rab18-s: GCGATGCATGGTCGCGCAGGA  
 Rab18-as: GCGTTAATTAACAGGAACACCCGGCGG

## 2.9. Molecular Biology

### 2.9.1. Purification of genomic DNA of extracellular *T.gondii* tachyzoites

To purify genomic DNA from extracellular parasites the DNeasy Blood & Tissue Kit from QIAGEN was used. Freshly egressed tachyzoites from HFF cells, which were cultured on a 24 well plate, were separated from host cell debris by centrifugation (1000xg for 5 minutes at 4°C). The parasite pellet was then washed with ice cold PBS. Purification of genomic DNA from animal and human cells was performed following the manufacturer's protocol. In summary parasites are lysed with Proteinase K and genomic DNA (gDNA) isolated with Silica gel technology. The genomic DNA could be purified quickly and efficiently and used

for PCR-based analyses. The gDNA was eluted with 50µl ddH<sub>2</sub>O and the received eluate was used for a second elution step to increase the yield of eluted DNA.

### **2.9.2. Purification of RNA of extracellular *T.gondii* tachyzoites**

To purify RNA the RNAagents Total RNA Isolation Kit from Promega was used. Parasites were cultured in confluent Vero cells in a T75 cell culture flask or in confluent HFF cells in a T175 cell culture flask. Freshly egressed tachyzoites (ca.  $1 \times 10^9$ ) were separated from host cell debris by centrifugation (1000xg for 5 minutes at 4°C) and washed with ice cold PBS up to two times. Phenol-Chloroform-extraction was performed to isolate the RNA. To purify the RNA from  $1 \times 10^9$  parasites, the protocol of the manufacturer was followed by using a fivefold standard reaction mix. The purified RNA was dissolved in 50µl RNase free H<sub>2</sub>O and immediately processed or stored at -80°C.

### **2.9.3. Reverse Transcription**

To generate cDNA the *Transcriptor Reverse Transcriptase* (Roche Diagnostics) was applied following manufacturers instruction to transcribe purified RNA (2.9.2.) into complementary DNA (cDNA). The cDNA was stored at -20°C or directly used for standard PCR to amplify specific cDNA sequences. Besides this so called Two-Step-RT-PCR, One-Step-RT-PCR was applied too, to get specific cDNA sequences. This was done with the *Titan One Tube RT-PCR System* or the *Transcriptor One-Step RT-PCR Kit* (Roche Diagnostics) following manufacturer's instructions.

### **2.9.4. Polymerase Chain Reaction**

#### **2.9.4.1. From *T.gondii* genomic DNA, cDNA or plasmid DNA templates**

Polymerase Chain Reaction (PCR) allows for the *in vitro* amplification of defined nucleotide sequences. This process takes place in three steps: First the double stranded DNA is denatured with heat and split into single strands; then the primer hybridises with the complementary target sequence through Watson-Crick base-pairing and finally the DNA polymerase synthesises a complimentary copy of the sequence. This cycle doubles the target sequence and is repeated many times, leading to an exponential amplification. *Eurotag* and *EuroClone* polymerase were used for analytical sequencing while *Expand High Fidelity<sup>PLUS</sup>*

*PCR System* (Roche Diagnostics GMBH) or *Platinum Taq DNA Polymerase High Fidelity* (Invitrogen) was used in case the sequence was needed for further processing. The latter two were used because of their improved proof-reading activity (6x reduced error rate).

Table 2-1: Reaction mix of a general PCR reaction

Components	Final concentrations
DNA	50-100 ng
Reaction buffer	1x
MgCl <sub>2</sub> <sup>a, b</sup> bzw. MgSO <sub>4</sub> <sup>c</sup>	1-5 mM
dNTP mix	à 200 µM
Forward Primer	0.4 µM <sup>b, c</sup> - 0.8 µM <sup>a</sup>
Reverse Primer	0.4µM <sup>b, c</sup> - 0.8 µM <sup>a</sup>
Polymerase	0.1U <sup>a, c</sup> - 2.5 U <sup>a, b</sup>

ddH<sub>2</sub>O was added up to a volume of 50 µl

<sup>a</sup> *EuroTaq*, <sup>b</sup> *Expand High Fidelity<sup>PLUS</sup> PCR System*,

<sup>c</sup> *Platinum Taq DNA Polymerase High Fidelity*

For analytical reactions, a final volume of 25µl was prepared. The reaction was performed in a Thermocycler (Eppendorf) with following programmes:

Table 2-2: Thermocycler-program for general PCR reactions.

Cycles	Steps	Temperature	Time
1x	Initial Denaturation	94°C	2-5 min
25x -35x**	Denaturation	94°C	30 s
	Annealing	45-65°C*	30 s
	Elongation	68°C <sup>b, c</sup> - 72°C <sup>a, b</sup>	1 min/kb

1x	Final Elongation	68°C <sup>b, c</sup> - 72°C <sup>a, b</sup>	7 min
1x	Cooling-down	4°C	∞

\* the optimum annealing temperature for the primers used were dependent on their respective melting temperatures

\*\* Alternatively only 10x and 15-20x with 10 seconds (s) time increment for the elongation<sup>b</sup>.

<sup>a</sup> *EuroTaq*, <sup>b</sup> *Expand High Fidelity<sup>PLUS</sup> PCR System*,

<sup>c</sup> *Platinum Taq DNA Polymerase High Fidelity*

#### 2.9.4.2. Site-directed mutagenesis by using the mega primer method

Site directed mutagenesis to generate dominant negative Rab proteins were carried out by using the mega primer method. Two PCR steps were performed and plasmids containing the respective wild type Rab cDNA were used as a template. Within the first PCR step a megaprimer was produced. The procedure is performed within a standard PCR (2.9.4.1.) with a forward primer complementary to the 5' end of the desired Rab cDNA and a mutagenic primer containing the desired point mutation. The resulting PCR fragment was then analysed on and extracted from an agarose gel. The purified megaprimer was then used as a forward primer for the second PCR step (Table 2-3, 2-4) together with a reverse primer, which is complementary to the 3' end of the Rab cDNA.

Table 2-3: PCR reaction using the megaprimer

Components	Final concentrations
DNA	200 ng
Reaction buffer	1x
MgCl <sub>2</sub>	1.25 mM
dNTP mix	à 200 µM
Megaprimer	0.4 µM
flanking Primer	4µM

Polymerase	0.25U <sup>a</sup> - 2.5 U <sup>b</sup>
------------	---

ddH<sub>2</sub>O was added up to a volume of 100 µl

<sup>a</sup> *Platinum Taq DNA Polymerase High Fidelity*

<sup>b</sup> *Expand High Fidelity<sup>PLUS</sup> PCR System*

Table 2-4: Thermocycler-program for mutagenic PCR reactions using the megaprimer.

Cycles	Steps	Temperature	Time
1x	Denaturation	94°C	4 min
	Annealing	45-55°C	60 s
	Elongation	68°C <sup>a,b</sup> - 72°C <sup>b</sup>	30 s
20x	Denaturation	94°C	40 s
	Annealing	45-55°C	60 s
	Elongation	68°C <sup>a,b</sup> - 72°C <sup>b</sup>	30 s
1x	Denaturation	94°C	40 s
	Annealing	45-55°C	60 s
	Elongation	68°C <sup>a,b</sup> - 72°C <sup>b</sup>	5 min
1x	Cooling-down	4°C	∞

<sup>a</sup> *Platinum Taq DNA Polymerase High Fidelity*,

<sup>b</sup> *Expand High Fidelity<sup>PLUS</sup> PCR System*

### 2.9.5. Agarose gel electrophoresis

For gel electrophoresis, agarose was dissolved at concentration between 0.8 and 2 % (w/v) in 1 x TAE buffer. Ethidium bromide or Sybr<sup>®</sup> Safe DNA Gel stain (Invitrogen) were used to visualise the DNA. DNA samples were mixed with 6 x DNA loading dye. Electrophoresis was performed in 1x TAE and according to the gel size following the instructions of the manufacturer (BioRad). To determine the size of DNA fragments 1 kb ladder or 1kb plus DNA ladder (Invitrogen) was run simultaneously with the samples. After electrophoresis, the DNA was

visualized on a transilluminator.

### **2.9.6. Extraction of DNA fragments from Agarose gel or out of solution**

For the DNA extraction from agarose gels or out of solutions the QIAquick Gel Extraction Kit or the High Pure PCR Product Purification Kit from Roche Diagnostics GmbH was applied. Following the instructions of the manufacturer DNA fragments were purified based on silica gel purification and by making use of a bench top centrifuge. The DNA fragments were eluted with 30 to 50µl ddH<sub>2</sub>O and the received eluate was used for a second elution step to increase the yield of eluted DNA fragments.

### **2.9.7. Ethanol precipitation of DNA**

To concentrate plasmid DNA or to exchange buffers before transfecting into *T.gondii*, precipitation of DNA was performed. The DNA containing solution was mixed with 1/10 volume of 3 M sodium acetate (pH 5.2) and 2.5 volume of 100% ethanol (stored at -20°C). The mixture was then incubated for at least 20 minutes at -80°C before centrifugation for 15 minutes at 15,000 g at 4°C. The supernatant was removed and the DNA pellet, was washed with 70% ethanol (-20°C) and centrifuged for 10 minutes at 15,000 g at 4°C. This step was performed twice to remove all excessive salts from the DNA pellet. After the last washing step the supernatant was removed and the pellet air dried under a sterile category 2 tissue culture hood. The dried pellet was then dissolved in Cytomix transfection buffer.

### **2.9.8. Determination of nucleic acid concentrations**

Concentrations of DNA and RNA solutions were determined by measuring the absorbance (A) at 260 nm. An absorbance of 1 correlates with 50µg/µl double stranded (ds) DNA, 40µg/µl RNA and 33µl/µg single stranded (ss) DNA. The absorbance of aromatic amino acids (tyrosine, phenylalanine, and tryptophan) at 280nm was additionally measured to estimate the concentration of proteins in the sample. Typically 1:100 or 1:200 dilutions in ddH<sub>2</sub>O were used to measure both absorbances in a quartz cuvette with a UV-visible spectroscope. The purity of the nucleic acid sample was determined by calculating the ratio of  $A_{260}/A_{280}$ .

Values should be between 1.8 and 2.0 to have a pure nucleic acid sample.

Alternatively the nucleic acid concentration of a sample was determined using the Nanodrop following the instructions of the manufacture.

### **2.9.9. Restriction endonuclease digests**

For all restriction endonuclease digests in this study endonucleases were purchased from New England Biolabs. Manufacturer's instructions were followed to use the appropriate NEB buffer and BSA when required. The digests were performed either in a heating block or in an incubator at 37°C. To analyse plasmids 0.2-1µg of DNA were digested. For a preparative digest 1-5µg of DNA and for vector linearization 30-60µg of DNA was taken.

### **2.9.10. Dephosphorylation of DNA fragments at the 5'end**

To minimise the risk of self-ligation of compatible ends of a linearised vector-DNA, 5'-phosphate residues were removed. This was done by using the *Alkaline phosphatase, Calf Intestinal* (NEB) following manufacturer's instructions.

### **2.9.11. Ligation of DNA fragments**

For ligations of PCR products into a cloning vector via TA (Thymine, Adenine) cloning the pGEM-T Easy Vector System (Promega) was used following manufacturer's instructions.

For PCR products into *T.gondii* expression vectors a T4-DNA Ligase (NEB) was applied with the respective buffer also following the manufacturer's instructions. Usually 100-200ng of vector-DNA was used. The amount of insert-DNA was between a ratio of 1:3 to 1:7 to the vector-DNA. The ligation mix was incubated either at room temperature for 1 hour or over night at 16°C.

### **2.9.12. Transformation of *E. coli* cells**

#### **2.9.12.1. Preparation of chemically competent cells**

A 5 ml pre-culture of XL-blue1 cells was grown overnight in LB medium and used to inoculate 500 ml fresh medium the next day. Cells were grown at 37°C in a

shaking incubator. When the OD600 of the culture reached an optical density of 0.55, the bacterial culture was cooled on ice for 10 minutes. After that, the bacterial culture was transferred into sterile tubes and centrifuged at 2500 g for 10 minutes at 4°C. The supernatant was discarded and the cells were resuspended in 20 ml transformation buffer with 1.5 ml DMSO. The cells were incubated on ice for 10 minutes, aliquoted into 1.5 ml Eppendorf tubes and snap-frozen on dry ice. Chemically competent cells were stored at -80°C.

#### **2.9.12.2. Transformation of chemically competent cells**

To transform chemically competent cells, 50µl of prepared competent cells (XLblue1) or XL-10 gold cells were defrosted and incubated on ice for 10 minutes. 5 µl of a ligation mix or 10-15ng plasmid DNA were added to the bacteria suspension and incubated for 30 minutes on ice. After that heat shock at 42°C for 90 seconds or according to the manufacturers' instructions was performed. Incubation for 2 minutes on ice followed and 200µl pre-warmed (37°C) SOC or LBmedium was added. After that the suspension was spread onto a LB agar plate with ampicillin and incubated over night at 37°C. For blue/white screening IPTG and X-Gal were additionally added to the final suspension.

#### **2.9.13. Isolation of plasmid DNA from *E.coli***

To isolate plasmid DNA from *E.coli* two methods were applied, depending on the desired amount of plasmid. Both methods are based on alkaline lysis of bacteria followed by precipitation of most bacterial proteins and genomic DNA with SDS and a final purification step with silica columns.

##### **2.9.13.1. Small scale plasmid purification (Miniprep)**

To prepare small amounts of plasmid DNA (10 to 30 µg), 3 ml of LB medium containing ampicillin for plasmid selection were inoculated with single bacteria colonies picked from agar plates. Bacteria cultures were grown at 37°C overnight with constant shaking at 200 rpm. Next day, plasmid DNA was isolated using the Qiaprep Spin Miniprep Kit (Qiagen) and following manufacturer's instructions. Plasmid DNA was eluted with 30 µl sterile water.

### **2.9.13.2. Large scale plasmid purification (Maxiprep)**

To prepare higher amounts of plasmid DNA (up to 1mg) single bacterial colonies were picked from fresh agar plates and added directly to 500 ml of LB medium with ampicillin or to 5ml LB medium to set up pre-cultures. The pre-cultures were incubated for 6-8 hours at 37°C and then diluted 1:100 into 500ml LB medium with ampicillin. After incubation at 37°C overnight with constant shaking at 200 rpm, plasmid DNA was purified using the Nucleo Bond Xtra Maxi Plus Kit from Machery and Nagel following manufacturer's instructions. Plasmid DNA was eluted with 350 µl sterile water.

## **2.10. Biochemistry**

### **2.10.1. Preparation of parasite cell lysates for SDS PAGE**

To prepare a cell lysate of parasites for a SDS-PAGE the amount of extracellular parasites (either freshly egressed or mechanically extracted from host cells) was determined by using a Neubauer counting chamber. Then the appropriate volume was centrifuged at 1000xg for 5 minutes at 4°C and the pellet resuspended with ice-cold PBS afterwards and centrifuged again. The resulting pellet was then stored at -80°C or directly resuspended with 1x SDS-PAGE-sample buffer or resuspended with in 4x LDS loading buffer with 1x reducing agent (Invitrogen) in PBS. This mixture was either stored at -20°C for later usage or incubated directly for 5 minutes at 95°C and centrifuged at 14000 rpm for 5 minutes at room temperature before loading on a SDS-polyacrylamide gel.

### **2.10.2. Sodium dodecyl sulphate polyacrylamide gel electrophoreses (SDS-PAGE)**

According to Laemmli (Laemmli 1970), proteins were separated by SDS-PAGE. Here the SDS polyacrylamide gels consisted of a running and a stacking gel. The percentage of the running gels contained 8-15% acrylamide. SDS-PAGE was performed with the Trans-Blot Cell or Mini-Trans-Blot Cell system from BioRad according to the manufacturer's instruction. For all buffers and solutions see

manufacturer's instructions or chapter 2.3.3.. 10-40µl of parasite lysate (see 2.5.1.) and 8 µl of *Page Ruler Plus Prestained Protein Marker* (Fermentas) were loaded and the gels ran in 1 x SDS PAGE running buffer first at 35 mA for the stacking gel and then at 70mA for the running gel at a maximum of 200 V. Following electrophoresis, gels were used for western blots.

### **2.10.3. Western blotting**

After proteins were separated within SDS-PAGEs, proteins were transferred onto Protran nitrocellulose membranes (Laemmli 1970; Towbin, Staehelin et al. 1979; Burnette 1981). A Transblot semidry transfer system or a Wet/Tank blotting system, both from BioRad, were used according to manufacturer's instructions.

For the semi-dry procedure, blots were set up as a sandwich of two pieces thick whatman filter paper, the membrane, the gel and another two pieces of thick whatman filter paper and run at 15 V for 30 minutes.

For the wet-blot procedure blots were set up as sandwiches of 3 pieces whatman filter paper, membrane, gel and another three pieces of whatman filter paper. Ice-cold transfer buffer was used and the blot was run at 300-500mA or 70-100V for 30-60 minutes on ice.

### **2.10.4. Ponceau-S- staining**

To check if proteins were transferred onto the membrane during the western-blotting and if one should continue with the immuno-blotting, positively charged amino acids were stained with *Ponceau-S solution*. Therefore the membrane was incubated for few minutes in Ponceau-S-staining solution and washed with ddH<sub>2</sub>O until red protein bands could be detected.

### **2.10.5. Immunoblotting**

Blotted membranes were blocked in 3 % (w/v) skimmed milk in PBS/ 0.2 % Tween20 (v/v) on a shaker, either for 1 hour at room temperature or overnight at 4°C. Primary antibodies were diluted to the required concentration in blocking solution and added to the membrane after blocking. Therefore the membrane was placed within a "wet chamber", which is a petri dish (150mm x15mm) with a wet paper towel at the bottom. The membrane is between two

pieces of parafilm and 1ml of antibody solution is sufficient to cover the membrane. The membrane was incubated with the primary antibodies for at least 60 minutes at room temperature. After that the membrane was rinsed twice and washed three times in PBS/ 0.2 % Tween20 (v/v). Horseradish peroxidase (HRP) labelled secondary antibodies were diluted 1:50000 in 3 % (w/v) skimmed milk in PBS / 0.4 % (w/v) Tween20 and incubated with the membranes for two hours. The membranes were rinsed twice and washed three times for 5 minutes again in PBS / 0.2% Tween20. HRP conjugated secondary antibodies were detected with the Amersham ECL plus kit and visualized by exposing the western blots to X-ray films.

## **2.11. Cell biology**

### **2.11.1. *Culturing of T.gondii and host cells***

#### **2.11.1.1. Host cells**

The virulent *T.gondii* RH strain (RHhxgprt) was used as the parent strain to generate the parasite strains used for the research work described here. This strain features a short doubling time (6-8hrs) and an efficient host cell lysis. By that, extracellular parasites could be gained in a huge amount without too much contamination of host cell debris. *T.gondii* infects adherent growing cells more efficiently than cells floating in a suspension. For that reason HFF (human foreskin fibroblasts) and transformed Vero cells (from African green monkey kidney) were chosen as host cells. The Vero cells used in this work are transformed. Being potentially immortal and having lost their contact inhibition ability these Vero cells grow in many layers, which results in a higher rate of yield of parasites per cell culture dish. Vero cells were used for culturing stable parasite lines. HFF cells are primary cells with contact inhibition and limited growth. Splitting is only possible up to thirty passages. Due to their ability to grow only in monolayers HFF cells were mainly used for immunofluorescence and all kinds of phenotypic analyses as well as for selection and subcloning of stably transfected parasites. Both host cell lines were cultured in DMEM<sub>complete</sub> at 37°C in 5% CO<sub>2</sub> and humid environment. HFF were passaged once a week in a 1:3 ratio and Vero cells passaged every five days at a 1:10 ratio.

### **2.11.1.2. *T.gondii* tachyzoites**

To maintain *T.gondii* tachyzoites in culture extracellular parasites were inoculated on confluent host cell layers until their complete lysis. The growth conditions are as described above for host cell cultures. *T.gondii* tachyzoites are able to survive 12 to 24 hours extracellularly after host cell lysis. Within this time frame the extracellular parasites need to be re-inoculated on fresh confluent host cells. Alternatively intracellular parasites could be used for inoculation. For this purpose host cell layers were destroyed by scratching with a cell scraper. The parasites, which are still intracellular, are released from host cells by destroying the host cells and parasites extracted from host cells by disruption of the host cells by syringing with a small bore needle (0.7mm).

### **2.11.2. *Trypsin/EDTA treatment of host cells***

This technique was applied for maintaining host cell cultures or for freezing host cells or intracellular parasites. Instead of scratching the host cells a gentle technique to detach host cells from culture dish cell-cell surfaces Trypsin/EDTA was applied. Cell layers growing on the bottom of a culture flask were washed with PBS to remove FCS, which is in the media and inactivates Trypsin. Cell layers were then covered with 1xTrypsin/EDTA and incubated for 5 to 10 minutes at 37°C. Tapping of the culture flask helped to detach the cells from the surface. The cell solution was then resuspended and transferred into new culture dishes or culture flasks.

### **2.11.3. *Freezing and defrosting of T.gondii parasite stabilates***

For long term storage of parasites, intracellular parasites were frozen within host cells either HFF or Vero cells. Infected host cells were detached from the dish surface by scratching or by trypsin/EDTA treatment (0.5ml). Detached host cells carrying the parasites within, were gently resuspended in 1ml freezing media and transferred into a 2ml cryotube and immediately frozen at -20°C. As soon as the solution was frozen it was transferred to -80°C, where it could be stored for several months. For a longer time storage frozen stocks were transferred to liquid nitrogen. The same procedure could be applied for freezing host cells without parasites. Typically host cells in 75cm<sup>2</sup> culture flask were frozen in 1ml freezing media.

To thaw frozen uninfected or infected host cells back into culture they were defrosted at 37°C water bath. To dilute the DMSO, which is a component of the freezing medium, 1ml of the thawed stabilate was added to 10ml DMEM<sub>complete</sub> and gently centrifuged. The resulting pellet was resuspended in fresh DMEM<sub>complete</sub> and transferred onto new HFFs, ready to infect fresh host cells. Uninfected host cells were added to a fresh 75cm<sup>2</sup> culture flask. Alternatively, defrosted stabilates with infected host cells were immediately transferred on a 6 cm culture dish with a HFF monolayer. After 2 hours the medium was exchanged to remove the diluted freezing medium.

#### **2.11.4. Determination of amount of parasites with Neubauer counting chamber**

To determine the number of tachyzoites or host cells per ml a Neubauer counting chamber was employed. 10- 20µl (concentrated or diluted depending on the amount of parasites) of cell suspension was placed between the chamber and a coverslip. Cleaning the chamber and coverslip before and after use with 70% ethanol made sure, that no remaining cells or dirt interferes with the counting. Cells within a defined area were counted by placing the chamber under a light microscope. Afterwards the amount of cells per 1ml could be calculated according to the manufacturer's specifications.

#### **2.11.5. Transient transfection of *T.gondii***

For transient transfection, plasmid DNA was introduced into *T.gondii* tachyzoites and remained extra-chromosomal and was lost over subsequent cell divisions. Parasites were transfected with DNA via electroporation (Soldati and Boothroyd 1993). Freshly egressed or mechanically extracted parasites were washed with Cytomix and centrifuged. Afterwards the cell pellet was resuspended in 850µl Cytomix. Circa 10<sup>7</sup> parasites were used for one transfection. 60µg of ethanol precipitated plasmid DNA were dissolved in 50µl Cytomix. 25µl ATP (100mM), 25µl GSH (100mM) and 700 µl of the parasite/cytomix suspension were added to this mixture. The resulting 800µl transfection mix was transferred into an electroporation cuvette. The electroporation was performed with the Electro Square Por 830 of BTX with a two times pulse at 1.7kV for 176µs. The transfected parasites were immediately transferred onto confluent HFF cells

grown on glass coverslips and cultured under normal growth conditions. After 16-24 hours the transfected parasites had enough time to invade the host cells and undergo at least two replication rounds. The infected host cells were then fixed and immunofluorescence analysis could be performed.

### **2.11.6. Stable transfection of *T.gondii***

Stable transfections (Donald and Roos 1993) involved random integration of linearised Plasmid DNA into the parasite's genome. The amount of copies integrated into the genome is variable. To gain stable parasites, the application of selection marker genes is essential. The selection marker gene can be either on the same plasmid as the expressed gene of interest, or on a second plasmid. Transfection of two plasmids is called a co-transfection. The performance of a stable transfection is the same as for a transient transfection. Instead of circular plasmid DNA, the DNA was previously treated with a single cutting restriction enzyme to linearise the plasmid. 10 Units of the same restriction enzyme were also added to the transfection mix. This cuts the genomic DNA randomly and by that the DNA repairing machinery of the cell is probably activated. This procedure is called Restriction Enzyme Mediated Insertion (REMI) and increases the probability of integration of exogenous DNA into the *T.gondii* genome up to 400 times (Black, Seeber et al. 1995). It is important to choose a restriction enzyme, that does not cut within the gene, which should be integrated into the genome or within its promoter region, within the 3'UTR of the DHFR<sup>TS</sup> or within the selection marker gene. Similar to a transient transfection 60µg of ethanol precipitated DNA was used per stable transfection. In case of a co-transfection additional 30µg of the second plasmid was used. After transfection the electroporated parasites were selected according to their integrated selection marker. Therefore fresh transfected parasites were transferred on HFF monolayers and cultured for 12-24 hours under normal growth conditions. Afterwards the "drug" for the respective selection was added to the medium. Within this work, the *dhfrts* (dihydrofolate reductase-thymidylate synthase) gene for pyrimethamine resistance (Donald and Roos 1993) and the *hxgprt* (hypoxanthine-xanthine-guanine phosphoribosyltransferase) gene for mycophenolic acid (MPA) resistance (Donald, Carter et al. 1996) were used. The following concentrations of the selection "drugs" were applied: 1 µM of pyrimethamine or 40 µg/ml Xanthine and 25 µg/ml MPA. A treatment of 3 days

with pyrimethamine and of circa 5 days with Xanthin/MPA should result in a pool with stable parasites.

### ***2.11.7. Isolation of single *T.gondii* tachyzoite clones via limited dilution***

To produce a parasite line with clonal parasites stably expressing the gene of interest, the parasite pool was subcloned via limited dilution in a 96 well plate. This 96 well plate contained a confluent monolayer of HFF cells. The parasite suspension was diluted, so that some wells received only one parasite. After 5-7 days parasites will have invaded the host cells, replicated within, lysed them and invaded the next one and so on. This process forms plaques of destroyed host cells within the monolayer. Wells with only one plaque indicated a single parasite clone, because only one parasite was originally present in this well. The parasites within this well were isolated and transferred onto new HFF cells in a 24 well plate and cultured under normal growth conditions. Once enough parasites were gained the clonal parasite line was checked with immunofluorescence analyses and further characterisations followed.

### ***2.11.8. Plaque-Assay***

Within their lytic cycle (host cell invasion, intracellular replication, host cell egress and gliding motility), *T.gondii* tachyzoites lyse their infected host cell. Having a monolayer of host cells and infecting it with parasites would result in spots of destroyed host cells. These spots are called plaques. The size and the quantity of these plaques reflect the infectivity of the respective parasite strain. For a plaque assay, HFF monolayers within a 6 well plate well were inoculated with 50 to 100 parasites. After 5-6 days incubation under normal growth conditions plaque containing cell layer was fixed with 100% Methanol for 5-10 minutes and then Giemsa stained. The plaque assays were analysed and imaged with a binocular or a light microscope. By measuring the area of the plaques with an image process program (ImageJ), plaque sizes were analysed and quantified.

### **2.11.9. Replication assay**

The replication assay was used to analyse the ability of *T.gondii* tachyzoites to undergo normal intracellular replication within infected host cells. Confluent monolayers of HFF cells grown on a glass coverslip within a 24 well plate well were used. One monolayer was infected with  $1 \times 10^6$  per 1ml freshly egressed or mechanically extracted extracellular parasites. After 24 to 30 hours incubation under normal growth conditions the glass coverslip was fixed with 4% paraformaldehyde (PFA). An immunofluorescence assay was performed with  $\alpha$ -IMC or  $\alpha$ -Sag1 to detect single parasites, fluorescence microscopy (60x or 100x magnification) was used to visualise single parasites within one vacuole. For each assay 10-20 fields per view containing over 100 vacuoles were counted to determine the number of parasites.

### **2.11.10. Invasion Assay**

The invasion assay was used to analyse the ability of extracellular *T.gondii* tachyzoites to invade host cells. Two ways to perform an invasion assay were applied in this work: the "normal" invasion assay [modified from (Kessler, Herm-Gotz et al. 2008)] and the Red/green invasion assay (Huynh, Rabenau et al. 2003). For both assays intracellular parasites were extracted from host cells by scratching and passage through a needle (0.7mm) three times. HFF monolayers, growing on glass cover slips on 24 well plate wells, were infected with an equal amount of the resulting fresh extracellular parasites. The parasites were allowed to invade host cells under normal growth conditions for 1-2 hours.

Within the normal invasion assay, extracellular parasites were removed by washing the coverslips five times with PBS prior to fixation with 4% PFA. Immunofluorescence analysis was followed using  $\alpha$ -IMC to label intracellular parasites. For each cover slip, the amount of invaded intracellular single parasites were counted within 10 fields of view under a fluorescence microscope and normalised with the amount of RH<sup>hxgprt</sup> parasites.

For the Red/Green invasion assay, coverslips were fixed immediately after 1-2 hours invasion time. After that Immunofluorescence assay without the permeabilisation step was performed for extracellular parasites using  $\alpha$ -Sag1-  $\alpha$ -mouse Alexa Fluor 594 antibody combination. For invaded intracellular parasites

a second standard immunofluorescence assay was performed with permeabilisation and with  $\alpha$ -IMC- $\alpha$  rabbit Alexa Fluor 488 antibody combination.  $\alpha$ -Sag1 bound to the outer surface of the parasite and does not require a permeabilisation step, whereas  $\alpha$ -IMC bound to the inner membrane complex (IMC) after permeabilisation. Consequently extracellular parasites (stained with  $\alpha$ -Sag-1 and  $\alpha$ -IMC) appeared yellow and intracellular parasites (only stained with  $\alpha$ -IMC) appeared green under the fluorescent microscope. The ratios of yellow versus green fluorescent parasites were calculated and normalised with RH<sup>hxgprt</sup>- parasites.

### **2.11.11. Egress Assay**

To analyse the ability of intracellular parasites to egress the infected host cell, egress assays were performed. Confluent HFF monolayers were infected with an equal amount of parasites and intracellular growth was allowed for 36 hours. After that a Calcium ionophore (A 23187; 1 $\mu$ M) was added to the medium 5-10 minutes prior to fixation. A 23187 was shown to trigger egress of intracellular *T.gondii* tachyzoites (Endo, Sethi et al. 1982; Black, Arrizabalaga et al. 2000; Arrizabalaga and Boothroyd 2004). After fixation, immunofluorescence assays were performed using  $\alpha$ -IMC or  $\alpha$ -Sag1 to enable counting of freshly lysed host cells (accumulation of extracellular parasites) and intact vacuoles under a fluorescence microscope. Vacuoles within 10 fields of view were analysed and normalised with RH<sup>hxgprt</sup>- parasites.

### **2.11.12. Immunofluorescence assay**

Confluent HFF monolayers on glass coverslips in 24 well plate wells were infected with *T.gondii* tachyzoites strains to be analysed. Invasion, Egress or intracellular growth was allowed for the respective time. Cells were fixed with 4% paraformaldehyde for 20 minutes washed for 5 minutes with PBS and permeabilized with 0.2% Triton X-100 in PBS (20 minutes.). After blocking with 2% bovine serum albumin in PBS or 0.2% Triton X-100 in PBS for additional 20 minutes immunolabelling was performed with the respective primary antibodies for 30-60 minutes. Washing the coverslips three times for 5 minutes with PBS followed. After that, treatment with respective secondary antibodies (Alexa-Fluor 594/ Alexa-Fluor 488 conjugated goat-anti rabbit or anti mouse) for another 45-60 minutes in the dark was performed. Finally the coverslips were

washed three times for 5 minutes with PBS and mounted with Fluoromount-G™ (with DAPI) on glass slides.

### **2.11.13. Stimulated emission depletion microscopy (STED)**

Thin sectioning, STED and two-colour STED measurements were performed by the group of Stefan Hell as described in (Kremer, Kamin et al. 2013).

#### **2.11.13.1. Immunofluorescence assay for STED**

The procedure for the immunofluorescence assay for STED samples was for the most part the same as for standard IFAs (chapter 2.11.12.). After fixation an additional treatment for 20 minutes with 100 mM NH<sub>4</sub>Cl was added to quench auto-fluorescence of the host cells. After labelling with the secondary antibodies an additional washing step was performed, where the coverslips were treated three times for 5 minutes with high salt PBS (PBS with 500mM NaCl). Instead of mounting the samples with Fluoromount-G™, samples were mounted with Mowiol 4-88/ DABCO mounting media.

### **2.11.14. Preparation of samples for electron microscopy**

HFF monolayers were infected with tachyzoites of the strains to be analysed and cultured for 24 hours before trypsinisation of the infected host cells. The following procedure was performed by David Ferguson as described in (Breinich, Ferguson et al. 2009).

### **2.11.15. Pulse-chase analysis**

Pulse-chase analyses have been performed by the group of Vern Carruthers as described in detail in: (Brydges, Sherman et al. 2000).

## 2.12. Imaging

The immunofluorescence images presented in this work were either taken with the Axioscope 2 microscope, the Nikon TE2000 Inverted microscope or the Delta Vision Core System. For Imaging with the Nikon TE2000 Inverted microscope (NIKON Center, Heidelberg) a 100x oil immersion lens (NA 1.6) was used, Z- stack images were taken with an increment of 0.15  $\mu\text{m}$  and deconvolution was applied by using standard parameters of the "Huygens-Software". For Imaging with the Delta Vision Core System a 100x oil immersion lens (UPlanSApo, NA 1.40) was used, Z-stack images were taken with an increment of 0.2  $\mu\text{m}$  and deconvolution was applied by using automatic setups of the softWoRx Suite 2.0 software. All images were further processed with the Adobe Photoshop CS4 software. For co-localisation analyses, the Pearson correlation coefficient of 10-16 imaged parasites was calculated by using ImageJ 1.46r (Wayne Rasband National Institute of Health). Here, one image layer was taken to compare dual color stains. The ImageJ 1.46r software has a plugin for colocalisation analysis to determine the Manders Coefficients and the Pearson correlation coefficient.

## 2.13. Bioinformatics

### 2.13.1. Sequencing and sequence alignment

DNA sequencing was performed by *Geneart GmbH* in Regensburg, *GATC* in Konstanz and *DNA Sequencing & Service* in Dundee.

To analyse sequenced data the ClustalW-function of the BioEdit Alignment editor was applied. For the comparison of DNA or protein sequences of different proteins or organisms the Basic-Local-Alignment-Search-Tool (BLAST) algorithm (Altschul, Gish et al. 1990) of NCBI (<http://www.ncbi.nlm.nih.gov/>) or ToxoDB (<http://ToxoDB.org/>) was applied.

### 3. Localisation of Rab proteins in *T.gondii*

#### 3.1. Introduction

Higher eukaryotic cells have a highly elaborate and complex endomembrane system with hundreds of regulatory proteins. For example, 71 Rab proteins which are involved in vesicular transport, have been identified in humans (Colicelli 2004). *T.gondii* and other apicomplexan parasites have only a reduced set of these regulatory proteins. Although organelles were identified, where protein transport from the Golgi takes place, no organelles involved in endocytosis (endosomes or lysosomes) could be classified in apicomplexans. Interestingly, apicomplexans feature additional unique secretory organelles (micronemes, rhoptries, dense granules). Especially in *T.gondii*, these organelles are essential for the lytic cycle (see 1.4.) and the infectivity of this obligate intracellular parasite. How these organelles develop and how their secretory proteins are transported to them is widely unknown. Studying the localisation of Rab proteins in *T.gondii* should give a first idea of in which pathway TgRab proteins are involved. This could give first indications of their functions compared to higher eukaryotic cells.

In this chapter orthologs of Rab proteins in *T.gondii* were identified by using different databases and compared with earlier investigations. TgRab proteins, which are not characterised so far in the literature or which are potentially involved in the secretory pathway of microneme and rhoptry proteins were overexpressed in *T.gondii* tachyzoites using the ddFKBP system. The localisation of these regulatable fusion proteins will be analysed by using different antibodies and marker proteins for different organelles in *T.gondii*.

### 3.2. 12 Rab GTPases are expressed in *T.gondii* tachyzoites

Previously 15 genes encoding Rab-like proteins have been identified in the genome of *T.gondii*, whereas analyses of other apicomplexan genomes indicated the presence of 9 Rab proteins in *Theileria*, *Cryptosporidium* and *Babesia* and 11 in *Plasmodium* (Langsley, van Noort et al. 2008). This could be confirmed in this work by sequence analyses of *Toxoplasma gondii* (Tg)Rab proteins shown in Table 3-1. Therefore amino acid sequences of Rab proteins from other organisms (e.g. human; *Homo sapiens*) were taken from the National Center for Biotechnology Information (NCBI) database ([www.ncbi.nlm.nih.gov](http://www.ncbi.nlm.nih.gov)) to search for orthologs in *Toxoplasma gondii* on ToxoDB ([www.toxodb.org](http://www.toxodb.org)) using the Basic-Local-Alignment-Search-Tool (BLAST) (Altschul, Gish et al. 1990). Together with the OrthoMCL database ([www.orthomcl.org](http://www.orthomcl.org)) orthologs of TgRab proteins in other apicomplexan parasites were identified. In Table 3-1, Rab proteins of some medically relevant representatives of the apicomplexan genera (*Toxoplasma gondii*, *Neospora caninum*, *Cryptosporidium parvum*, *Theileria parva*, *Babesia bovis* and *Plasmodium falciparum*) and their Gene IDs on ToxoDB, PlasmoDB and OrthoMCL are displayed. As already identified, only Rab1A,B,2,5A,6,11A and 11B are conserved among the analysed apicomplexan species (Langsley, van Noort et al. 2008) (Table 3-1). No existence of Rab4 could be found in *P.falciparum*, *B.bovis* and *T.parva*. Rab5B and Rab18 are absent in *C.parvum*, *T.parva* and *B.bovis* and Rab5C is also absent in *C.parvum*.

Furthermore it is important to mention that the classification of *T.gondii* Rab proteins within this work relies on the sequence homology with other eukaryotic Rab proteins, which again depends on the applied algorithm. The classification of the TgRab proteins presented in this work is based on phylogenetic analysis performed by Jonathan Wilkes (Kremer, Kamin et al. 2013).

Rab	<i>T.gondii</i>	<i>N.caninum</i>	<i>C.parvum</i>	<i>T.parva</i>	<i>B.bovis</i>	<i>P.falciparum</i>
1A	TGME49_258130	NCLIV_028240	cgd6_3830	TP04_0644	XP_001611865.1	PFE0690c
1B	TGME49_214770	NCLIV_051820	cgd6_3220	TP03_0775	XP_001611213.1	PFE0625w
2	TGME49_312050	NCLIV_055690	cgd1_2060	TP01_0877	XP_001610821.1	PFL1500w
4	TGME49_257340	NCLIV_029730	cgd8_1040	no	no	no
5A	TGME49_267810	NCLIV_038540	cgd3_3150	TP04_0575	XP_001611807.1	PFB0500c
5B	TGME49_207460	NCLIV_002540	no	no	no	MAL13P1.51
5C	TGME49_219720	NCLIV_060890	no	TP01_0639	XP_001609456.1	PFA0335w
6	TGME49_310460	NCLIV_054540	cgd2_1940	TP02_0799	XP_001611576.1	PF11_0461
7	TGME49_248880	NCLIV_065010	cgd7_1680	TP03_0666	XP_001611307.1	PFI0155c
11A	TGME49_289680	NCLIV_041930	cgd4_320	TP01_1204	XP_001610582.1	PF13_0119
11B	TGME49_320480	NCLIV_009790	cgd7_4380	TP02_0559	XP_001610116.1	MAL13P1.205
18	TGME49_313190	NCLIV_056520	no	no	no	PF08_0110
23	TGME49_283530	NCLIV_015390	no	no	no	no
8/10 like	TGME49_243450	NCLIV_018180	no	no	no	no
Rab-like	TGME49_239855	no	no	no	no	no

**Table 3-1: The 15 predicted Rab proteins in *T.gondii* and their orthologs in other apicomplexan species.** Gene IDs of Rab orthologs from ToxoDB, PlasmoDB and OrthoMCL for *Toxoplasma gondii*, *Neospora caninum*, *Cryptosporidium parvum*, *Theileria parva*, *Babesia bovis* and *Plasmodium falciparum* are displayed.

### 3.3. Amplification and verification of the amino acid sequence of TgRab1A, TgRab1B, TgRab2, TgRab4, TgRab5A, TgRab5B, TgRab5C, TgRab7 and TgRab18

Since TgRab11A, TgRab11B and TgRab6 have already been characterised in detail in the literature (Stedman, Sussmann et al. 2003; Agop-Nersesian, Naissant et al. 2009; Agop-Nersesian, Egarter et al. 2010), the full length cDNA of the remaining 13 TgRab proteins was amplified by PCR. Only for TgRab1A, TgRab1B, TgRab2, TgRab4, TgRab5A, TgRab5B, TgRab5C, TgRab7 and TgRab18 full-length cDNA could be amplified and their predicted amino acid sequences were verified. Analyses of TgRab proteins in ToxoDB revealed no expression data for TgRab23 and TgRab-like. Additionally, no cDNA could be amplified for their genes as for TgRab8/10 as well. These Rab proteins were excluded from further analysis. By using the CLUSTAL W alignment (Thompson, Higgins et al. 1994) protein sequences of TgRab1A, TgRab1B, TgRab2, TgRab4, TgRab5A, TgRab5B, TgRab5C, TgRab7 and TgRab18 were aligned and depicted in Figure 3-1. Here, amino acids are displayed in their single-letter code and highlighted in grey when they were similar (50%) and red when they were identical (80%). In all displayed TgRab proteins the GTP/Mg<sup>2+</sup> binding domain with its p-loop, switch I and switch II domains (see 1.6.2.) are highly conserved as expected. With the exception of

TgRab5B, the presented TgRab proteins feature a C-terminal prenylation motif likely required for correct localisation (green Figure 3-1). This prenylation motif has two cysteine residues, where geranylgeranyl tails can be added for integration into the donor membrane (see 1.6.2.). TgRab5B has no such cysteine residues at its C-terminus. Instead a N-terminal myristoylation motif (blue Figure 3-1) was identified, which may be important for correct membrane integration.

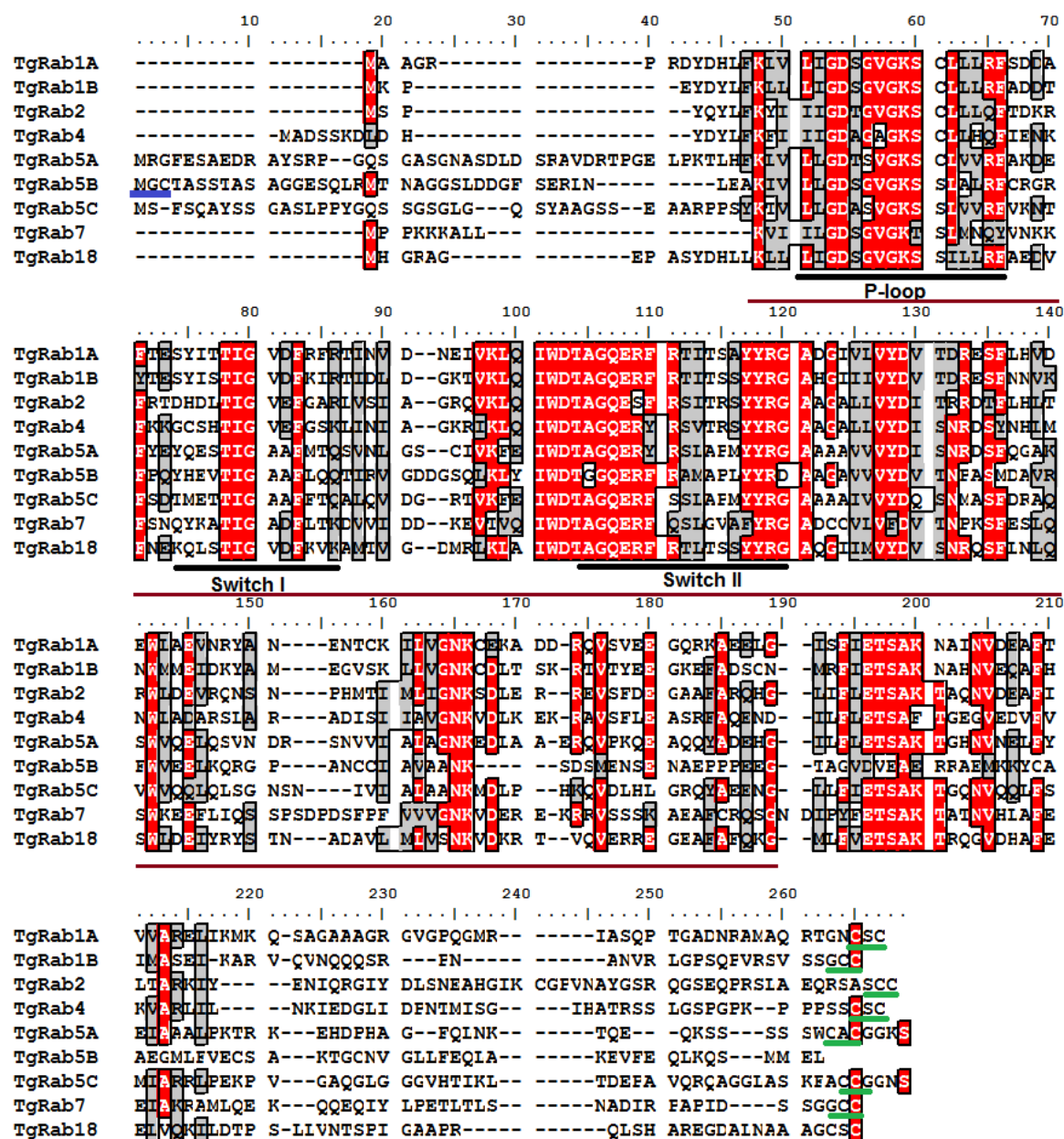


**Figure 3-1. Alignment of the nine amplified Rab-like proteins in *T. gondii*.** Amino acids are displayed in a single-letter code. Highly conserved regions are indicated in red (80% similarity) and grey (50% similarity). Putative motifs for C-terminal prenylation (green) and N-terminal myristoylation (blue) (only Rab5B) are indicated. The conserved GTP/Mg<sup>2+</sup> binding site is indicated in purple and p-loop, switch I and switchII domain in black.

### 3.4. Generation of inducible parasite lines overexpressing TgRab proteins

After the full-length cDNA was amplified for TgRab1A,1B,2,4,5A,5B,5C,7 and 18, parasites overexpressing the respective Rab proteins were generated for localisation analyses. As overexpression of a Rab protein could lead to deleterious effects on the parasite, similar to higher eukaryotes (Bucci, Parton et al. 1992; van der Sluijs, Hull et al. 1992), the ddFKBP system was employed to allow for regulated TgRab overexpression. The ddFKBP system is based on a destabilisation domain (a mutant of the human rapamycin binding protein FKBP12) fused to a protein of interest (POI). In the absence of the ligand, Shield-1 (Shld-1, a rapamycin derivative) the destabilisation domain (ddFKBP) is responsible for the degradation of the fusion protein. In presence of Shld-1, the fusion protein will not be targeted to the proteasome and is protected from degradation (see 1.2.). The ddFKBP system has successfully been applied in *T.gondii* for TgRab11A and 11B (Herm-Gotz, Agop-Nersesian et al. 2007; Agop-Nersesian, Naissant et al. 2009; Agop-Nersesian, Egarter et al. 2010).

Together with an additional myc tag, TgRab1A,1B,2,4,5A,5B,5C,7 and 18 were N-terminally tagged with the destabilisation domain, ddFKBP. This was done by amplifying the cDNA of the respective Rab protein with a 5' primer containing an NsiI site and a 3' primer with a PaeI restriction site (see 2.8.). To gain a higher amount of the respective Rab DNA, the resulting PCR product was ligated into a pGEM-T Easy vector and chemically transformed into *E.coli* cells. After culturing of the transformed *E.coli* cells, the respective plasmid DNA was purified and NsiI/PaeI digested. Rab cDNA was then ligated into the NsiI/PaeI linearised and dephosphorylated p5RT70DDmycGFP-HXGPRT vector plasmid (Herm-Gotz, Agop-Nersesian et al. 2007). Thereby the GFP was exchanged with the respective Rab full length cDNA. The final construct (p5RT70DDmycRab-HXGPRT) contained selection genes for bacteria ampicillin and parasite MPA/Xanthin positive selection. The p5RT70 promoter is a tubulin promoter and guarantees a constant high expression rate of the attached gene. For Rab5B, an additional construct was designed, where the ddFKBP domain together with a HA tag was C-terminally added. This was done by the group of Christopher Tonkin. The provided construct (p5RT70Rab5BHADD-HXGPRT) also contained genes for ampicillin and MPA/Xanthin selection.

The final constructs were linearised with *NotI* for stable transfection into the RH<sup>hxgprt-</sup> parasite strain. Plasmid linearization and addition of the respective restriction enzyme during transfection increases the probability of random integration into the *Toxoplasma* genome by up to 400 times (Black, Seeber et al. 1995). The RH<sup>hxgprt-</sup> parasite strain is a *Toxoplasma gondii* strain lacking the gene for hypoxanthine-xanthine-guanine phosphoribosyl transferase (*hxgprt*). This enzyme represents an essential part of an alternative guanine monophosphate (GMP) synthesis pathway. GMP is normally obtained from AMP (adenosine MP) via IMP (inosine MP) via XMP (xanthosine MP). Alternatively GMP can be obtained from hypoxanthine and guanine with the help of HXGPRT. If the first pathway is blocked e.g. by mycophenolic acid (MPA), parasites of the RH<sup>hxgprt-</sup> strain would die. By adding MPA and Xanthin to the medium circa 24 hours after transfection, parasites that integrated the plasmid into their genome could be positively selected. The resulting stable parasite pools were then subcloned via limited dilution to obtain clonal parasite strains expressing the fusion protein ddFKBPmycRab1A,B,2,4,5A,5B,5C,7 or 18 or Rab5BHAddFKBP. Since ddFKBP is a destabilisation domain the fusion protein is constantly degraded within the parasite, the addition of Shld-1 protects the fusion protein from degradation and “switches” the overexpression of the respective Rab protein on. This allows an analysis of localisation and of overexpression phenotypes of Rab proteins even if their additional overexpression is lethal.

### **3.5. Screening for inducibility of ddFKBP tagged TgRab proteins**

Immunofluorescence analyses (IFAs) and western blots were performed for each strain. For the IFA, two monolayers of HFF cells were infected with parasites of the respective Rab overexpression strain +/- Shld-1 for 18 hours. Following this, host cell monolayers with intracellular parasites were fixed and immuno-stained within an IFA. For western blotting, HFF monolayers were infected with parasites of the respective Rab overexpression strain and incubated for 24 to 48 hours until host cell lysis. After counting of freshly egressed extracellular parasites one half was incubated with and the other one without Shld-1 for 4 hours under normal growth conditions. Equal amounts of parasites were loaded on an SDS-

PAGE and immunoblotting was performed to detect expression levels. To detect the ddFKBpmycRab or Rab5BHAddFKBP fusion protein within the IFA,  $\alpha$ -myc or  $\alpha$ -HA antibodies were used. For western blot analysis  $\alpha$ -ddFKBP was employed to detect the ddFKBPRab fusion protein and  $\alpha$ -Catalase was used as an internal loading control. Parasites were induced with varying Shld-1 concentrations to investigate the upregulation without generating overexpression artefacts. These artefacts can be seen sometimes in transient transfections of essential proteins. Abnormal localisation patterns of the inner membrane complex (IMC) could be an indicator for that. Therefore co-immunostaining was performed with  $\alpha$ -IMC. The results for +/- 1 $\mu$ M Shld-1 treatment of the indicated Rab overexpression strain are displayed in Figure 3-3. Although background expression could be detected for most of the Rab proteins on IFA level without Shld-1, this was also detectable by western blot for Rab5BHAddFKBP. This indicated that the addition of 1 $\mu$ M Shld-1 was suitable to upregulate the overexpression of the respective Rab protein to detect it intracellularly by 18 hours within IFAs and extracellularly by 4 hours within western blots. No abnormal IMC stains or abnormal nucleus signals could be detected, when TgRab1A,B,2,4,5A,B,C,7 or 18 were overexpressed.

In the case of Rab5B, two different localisation patterns were detected. In IFAs for the N-terminal tagged version of Rab5B a diffuse and vesicular distribution in the whole parasite was observed. Whereas for the C-terminal tagged version an accumulation within a particular region could be identified. This could confirm the assumption, that the N-terminal myristoylation motif is responsible for Rab5Bs membrane integration and by that for its localisation. Therefore for further localisation analyses only the C-terminal tagged version of Rab5B (Rab5BHAddFKBP) was used.

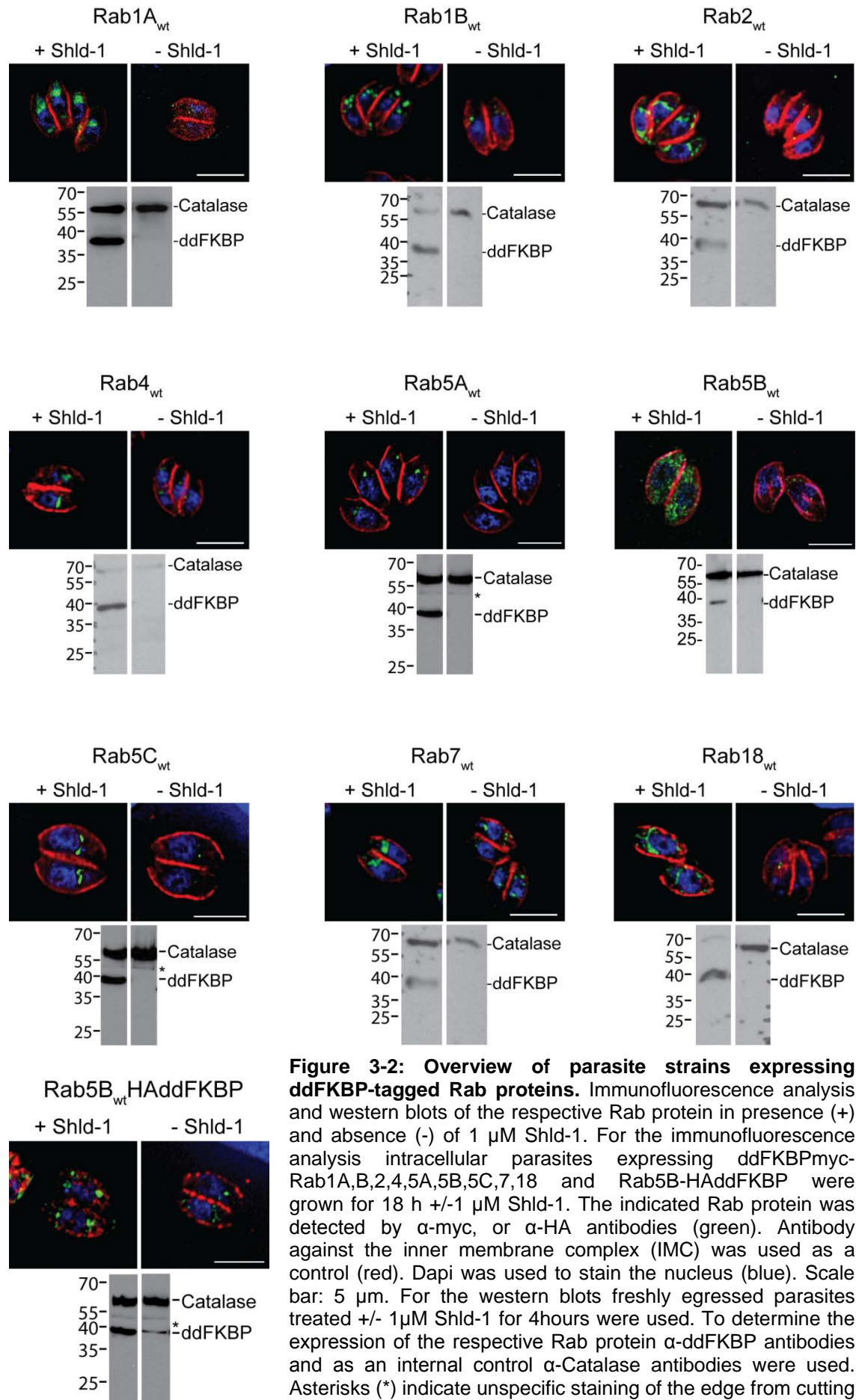


**Figure 3-2: Overview of parasite strains expressing ddFKBP-tagged Rab proteins.** Immunofluorescence analysis and western blots of the respective Rab protein in presence (+) and absence (-) of 1  $\mu$ M Shld-1. For the immunofluorescence analysis intracellular parasites expressing ddFKBpmyc-Rab1A,B,2,4,5A,5B,5C,7,18 and Rab5B-HAddFKBP were grown for 18 h +/- 1  $\mu$ M Shld-1. The indicated Rab protein was detected by  $\alpha$ -myc, or  $\alpha$ -HA antibodies (green). Antibody against the inner membrane complex (IMC) was used as a control (red). Dapi was used to stain the nucleus (blue). Scale bar: 5  $\mu$ m. For the western blots freshly egressed parasites treated +/- 1  $\mu$ M Shld-1 for 4 hours were used. To determine the expression of the respective Rab protein  $\alpha$ -ddFKBP antibodies and as an internal control  $\alpha$ -Catalase antibodies were used. Asterisks (\*) indicate unspecific staining of the edge from cutting the membrane. IFAs and western blots of Rab1B, 2, 4 and 18 were performed under my supervision by Sabine Mahler. Except for the images of Rab5BwtHAddFKBP (Delta Vision Core System), the images were taken with the Nikon TE 2000 inverted microscope.

### 3.6. Localisation of TgRab1A,B,2,4,5A,B,C,7 and TgRab18

After it was assured that a Shld-1 concentration of 1 $\mu$ M is suitable to detect ddFKBPmycRab1A,B,2,4,5A,B,C,7,18 and Rab5BddFKBP proteins in *T.gondii*, the localisation of the Rab proteins was determined by IFAs. Therefore the generated stable parasite lines (3.4.) were added to HFF monolayers and incubated with 1 $\mu$ M Shld-1 over night (18 hours). After fixation, IFAs were performed with various organellar markers within *T.gondii*. As illustrated in Figure 3-3, antibodies against rhoptry proteins (Rop5, Rop2,3,4), microneme proteins (M2AP, MIC2, MIC3, MIC8, AMA1, MIC11), the inner membrane complex (IMC), dense granule protein GRA9 and endosomal-like organelles, TgVP1, TgCPL and proM2AP were applied in this work. Alternatively, the analysed parasite strains were transiently co-transfected with marker proteins for different organelles (Figure 3-3) e.g. GRASP (Golgi re-assembly stacking protein) -RFP, TgERD2 (Pfluger, Goodson et al. 2005), TgGalNAC-YFP [UDP-*N*-acetyl-D-galactosamine:polypeptide *N*-acetylgalactosaminyltransferase T1 (TgGalNac) fused to yellow fluorescent protein (YFP), (Nishi and Roos, unpublished)] or RFP-FNR. Together with  $\alpha$ -myc or  $\alpha$ -HA antibodies, to detect the expressed ddFKBP-Rab fusion protein, the localisation of the respective Rab protein was analysed. Co-localisation signals of 10 to 16 imaged parasites were also quantified by calculation of the Pearson correlation coefficient. The images were analysed with WCIF ImageJ and the Manders coefficient plugin was applied.

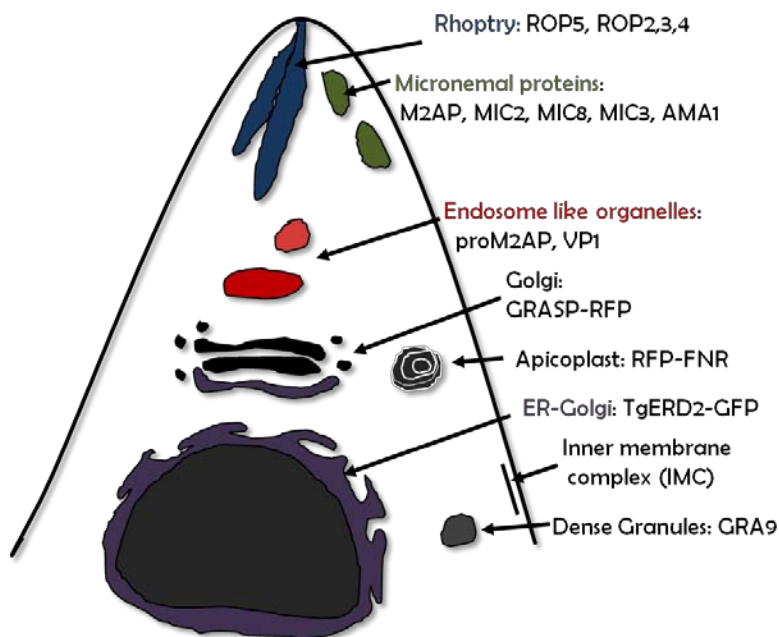
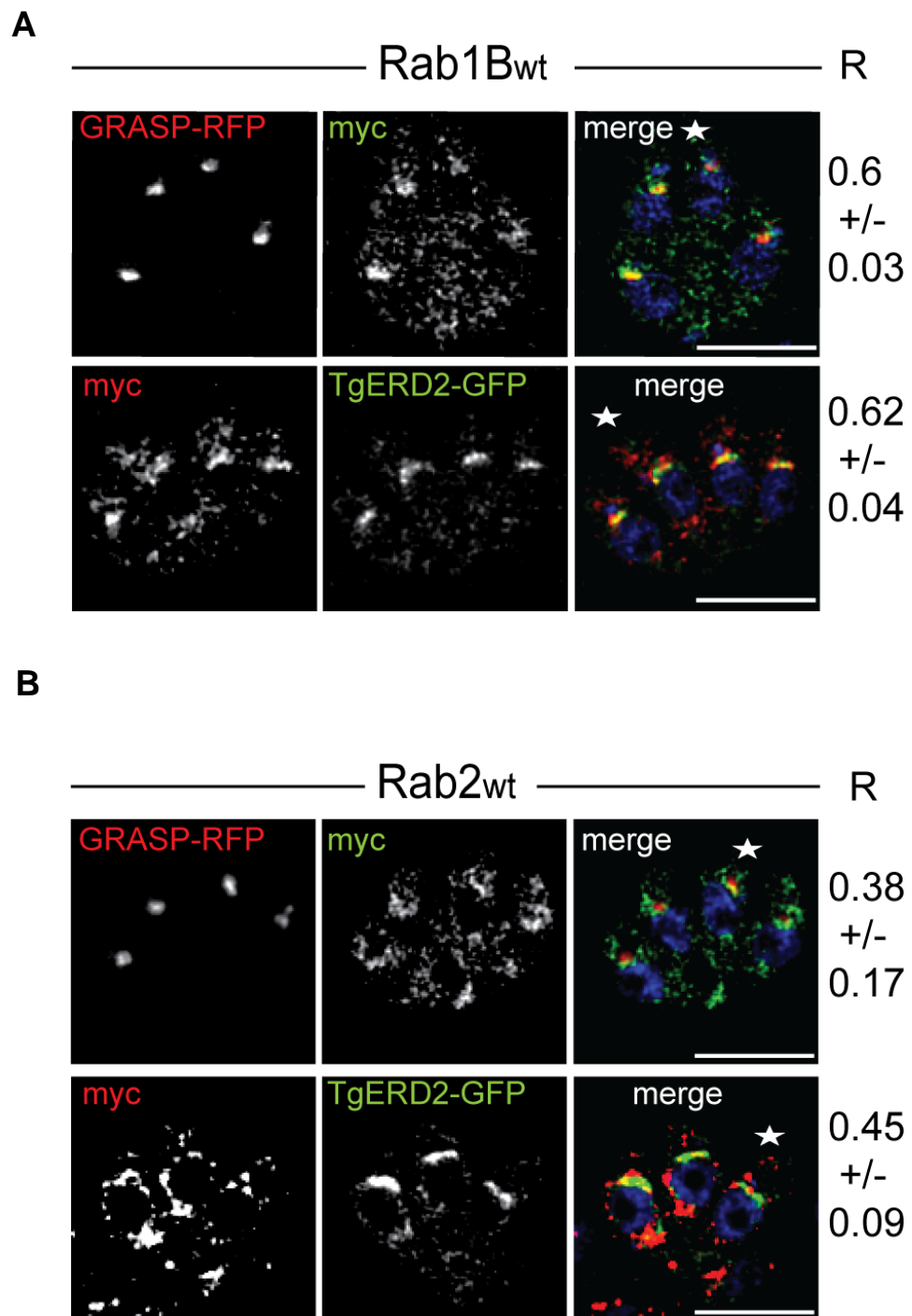


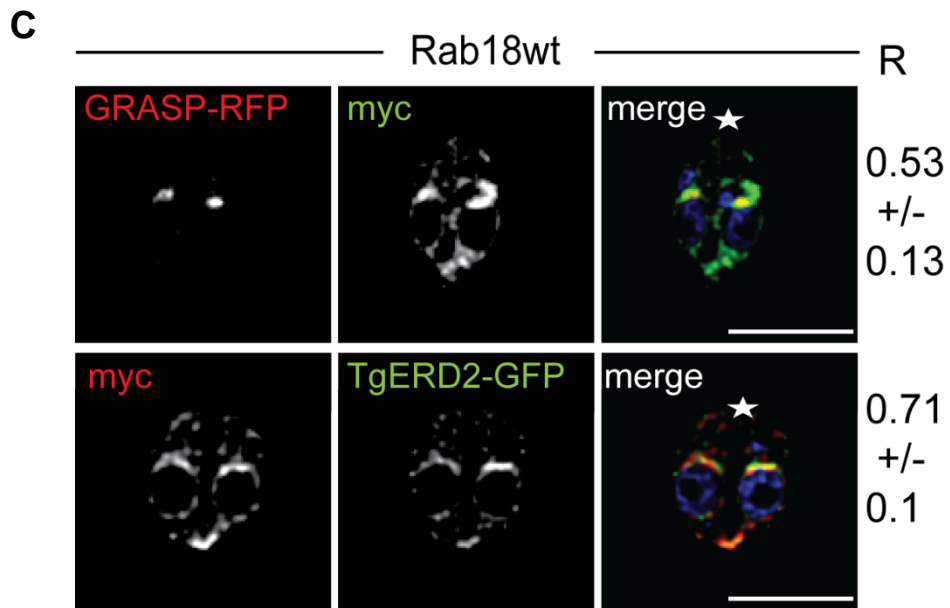
**Figure 3-3: Overview of antibodies and marker proteins applied to analyse the localisation of TgRab proteins in *T.gondii* tachyzoites.** Antibodies: ROP5; ROP2,3,4; M2AP; MIC2; MIC8; MIC3; AMA1; proM2AP; TgVP1; TgCPL; IMC; GRA9. Marker proteins: GRASP-RFP; TgGalNAC-YFP; RFP-FNR

### **3.6.1. Localisation of TgRab1B, TgRab2 and TgRab18 in pre-Golgi and partially in Golgi regions**

Figure 3-4 displays IFAs of intracellular parasites expressing stabilised ddFKBPmycRab1B, 2 and 18 co-transfected with TgERD2-GFP (involved in ER/Golgi transport) and GRASP-RFP [located at the Golgi (Pflugger, Goodson et al. 2005)]. Rab1B showed a diffuse cytosolic localisation with a clear concentration at the Golgi/ER region. This could be defined by co-localisation with GRASP-RFP and TgERD2-GFP (Figure 3-4A). Rab18 also exhibited a concentration at the ER/Golgi region, shown by co-localisation with GRASP-RFP and TgERD2-GFP. An additional presence of Rab18 around the nucleus up to the basal half of the parasite could be also detected (Figure 3-4C). It is possible that this area belongs to the ER as well, but since no marker or antibodies were available within this work no statement can be made. Rab2 showed a diffuse cytosolic localisation with some accumulation at the Golgi/ER region, where only partial co-localisation with GRASP-RFP and TgERD2 was detected (Fig3-4B). Similar to Rab18, accumulation around the nucleus and in the basal half of the parasites could be detected. In summary, ddFKBPmycTgRab1B and ddFKBPmycTgRab18 are mainly localised at the ER/Golgi (pre-Golgi) region. ddFKBPmycRab2 showed a

weaker accumulation in this area, but due to the lack of antibodies or marker proteins, a localisation at the ER region can only be speculated.

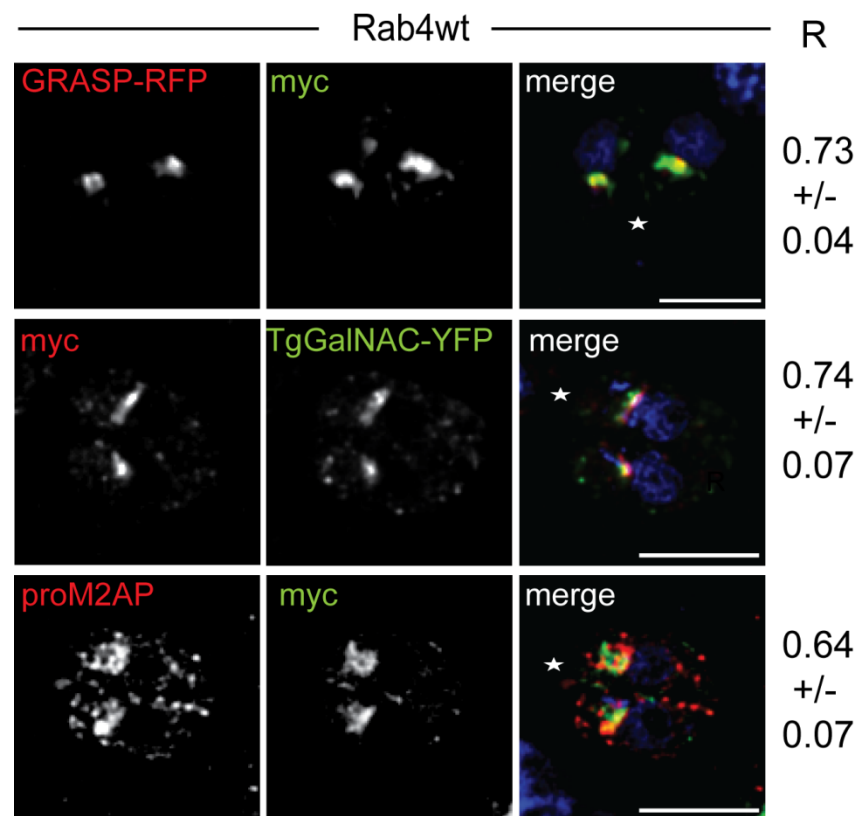




**Figure 3-4: Localisation of Rab1B, Rab2 and Rab18.** (A-C) Intracellular parasites stably expressing the indicated ddFKBPmycRab-construct were grown for 18hours in the presence of 1  $\mu$ M Shld-1 prior to fixation. Co-expression of the Golgi marker GRASP-RFP and the Golgi/ER marker TgERD2-GFP were performed. To indicate the localisation of the respective Rab  $\alpha$ -myc antibodies were used. Dapi is shown in blue. The scale bars represent 5 $\mu$ m. Rab1B and Rab18 are mainly located at the ER/Golgi region, whereas Rab2 has a broad localisation signal with concentration at the ER/Golgi region, shown by partial co-localisation with GRASP and TgERD. Co-localisation was quantified by calculating the Pearson's correlation coefficient (R). Mean values and respective standard deviation of 10-16 parasites are indicated next to the respective image. Stars indicate the parasites orientation, where the apical part is pointing towards the star. IFAs were performed under my supervision by Sabine Mahler. The images were taken with the Nikon TE 2000 inverted microscope.

### 3.6.2. Localisation of TgRab4 mainly at the Golgi region

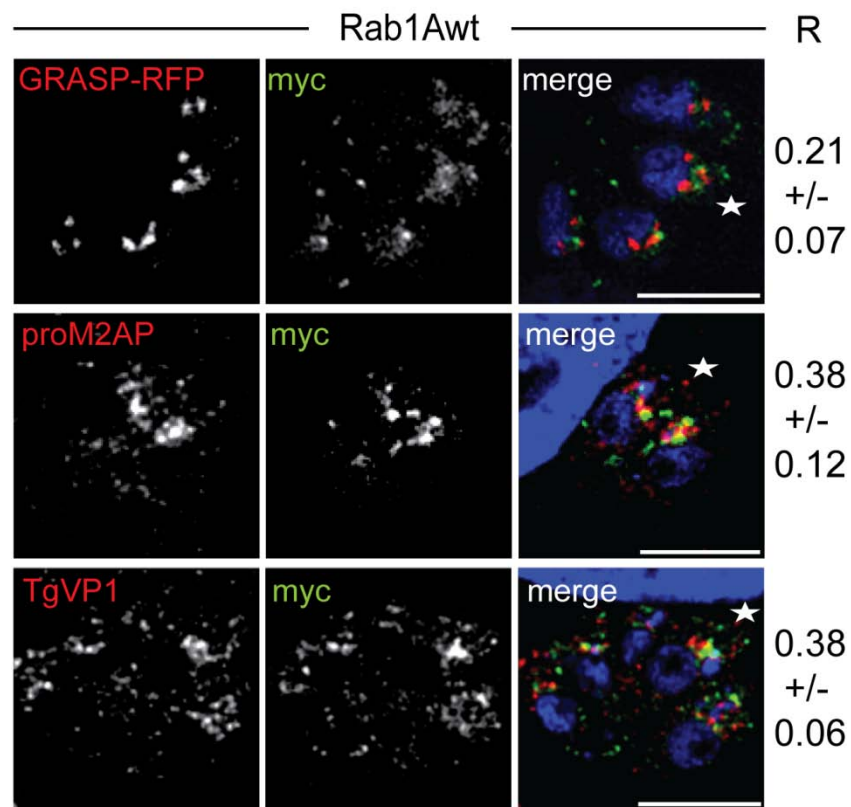
Figure 3-5 displays IFAs of intracellular parasites expressing stabilised ddFKBPmycRab4 co-transfected with the Golgi marker proteins GRASP-RFP and TgGalNAC-YFP or immunostained with  $\alpha$ -proM2AP (Harper, Huynh et al. 2006), a marker for an endosomal-like compartment (ELC, see 1.3.3.). Beside weak cytosolic distribution of ddFKBPmycRab4, a clear accumulation at the Golgi region, indicated by co-localisation with GRASP-RFP and TgGalNAC-YFP, could be detected in all IFAs. In some parasites, especially where the  $\alpha$ -myc signal was less concentrated, a co-localisation with proM2AP could also be detected (Figure 3-5). In summary, ddFKBPmycRab4 was mainly detected at the Golgi region.



**Figure 3-5: Localisation of Rab4.** Intracellular parasites stably expressing the ddFKBPmycRab4-construct were grown for 18hours in the presence of 1  $\mu$ M Shld-1 prior to fixation. Co-expression of the Golgi marker GRASP-RFP, TgGalNac-YFP and co-staining with the  $\alpha$ -proM2AP antibody to label endosomal-like compartments (ELCs) were performed. To localise TgRab4  $\alpha$ -myc antibody was used. Dapi is shown in blue. The scale bars represent 5 $\mu$ m. Rab4 is almost exclusively localised to the Golgi, as indicated by co-localisation with GRASP and TgGalNac. However, in some occasions partial co-localisation of Rab4 with  $\alpha$ -proM2AP was also detected. Co-localisation was quantified by calculating the Pearson's correlation coefficient (R). Mean values and respective standard deviation of 10-16 parasites are indicated next to the respective image. Stars indicate the parasites orientation, where the apical part is pointing towards the star. IFAs were performed under my supervision by Sabine Mahler. The images were taken with the Nikon TE 2000 inverted microscope.

### 3.6.3. Localisation of TgRab1A

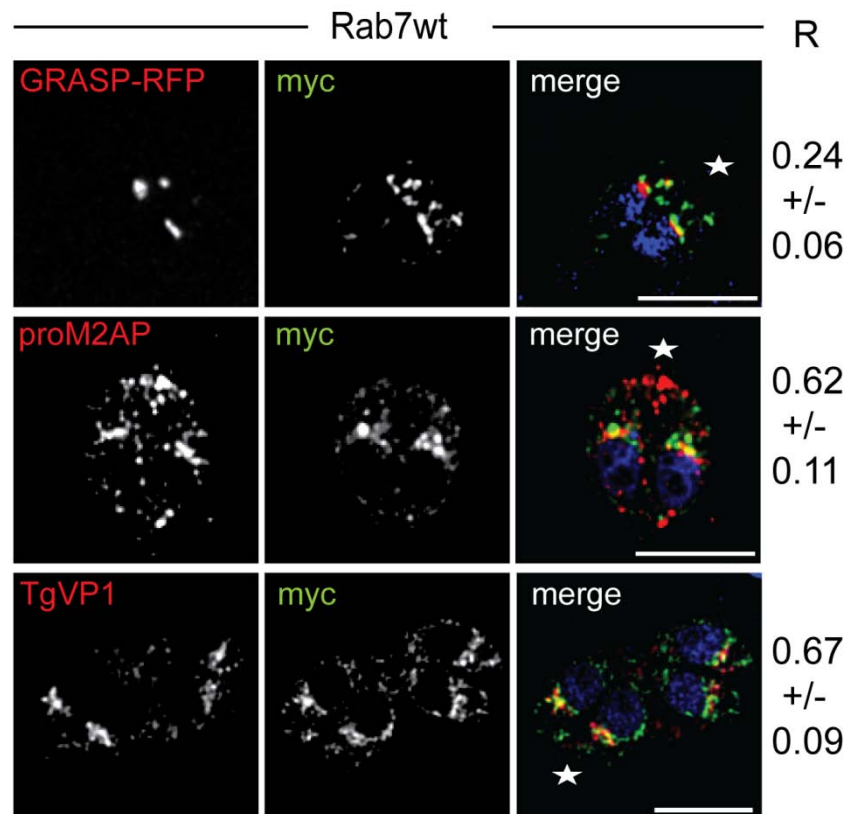
Figure 3-6 displays IFAs of intracellular parasites expressing stabilised ddFKBpmycRab1A co-transfected with the Golgi marker GRASP-RFP or immunostained with  $\alpha$ -proM2AP or  $\alpha$ -TgVP1 (Harper, Huynh et al. 2006). TgRab1A showed a very dynamic localisation pattern (different localisation pattern in different IFAs) with some accumulation at the post-Golgi region, seen relative to the GRASP-RFP signal. Weak partial co-localisation with proM2AP and TgVP1 was detectable. One can say, that Rab1A is mainly localised around the post-Golgi region, but no reliable localisation to a specific compartment was evident.



**Figure 3-6: Localisation of Rab1A.** Intracellular parasites stably expressing a ddFKBpmycRab1A-construct were grown for 18hours in the presence of 1  $\mu$ M Shld-1 prior to fixation. Co-expression of the Golgi marker GRASP-RFP or co-staining with  $\alpha$ -proM2AP, or  $\alpha$ -TgVP1 antibodies were performed. To indicate the localisation of TgRab1A  $\alpha$ -myc was used. Dapi is shown in blue. The scale bars represent 5 $\mu$ m. Rab1A has a very broad localisation signal, but is mainly concentrated at the post-Golgi region, as indicated by partial co-localisation with GRASP, proM2AP and TgVP1. Co-localisation was quantified by calculating the Pearson's correlation coefficient (R). Mean values and respective standard deviation of 10-16 parasites are indicated next to the respective image. Stars indicate the parasites orientation, where the apical part is pointing towards the star. The images were taken with the Nikon TE 2000 inverted microscope.

### 3.6.4. Localisation of TgRab5A,B,C and TgRab7 in post-Golgi regions

Figure 3-7 displays IFAs of intracellular parasites expressing stabilised ddFKBPmycRab7 co-transfected with the Golgi marker GRASP-RFP or immunostained with  $\alpha$ - proM2AP or TgVP1. Compared with the GRASP-RFP signal, Rab7 could be clearly detected at the post-Golgi region of *T.gondii*. Beside a diffuse localisation pattern throughout the parasites, TgRab7 is concentrated at the ELC area. This could be detected by co-localisation with proM2AP and TgVP1. Comparing the Pearson's correlation coefficients for the co-stains, no preferred localisation for one of these two compartments were indicated.

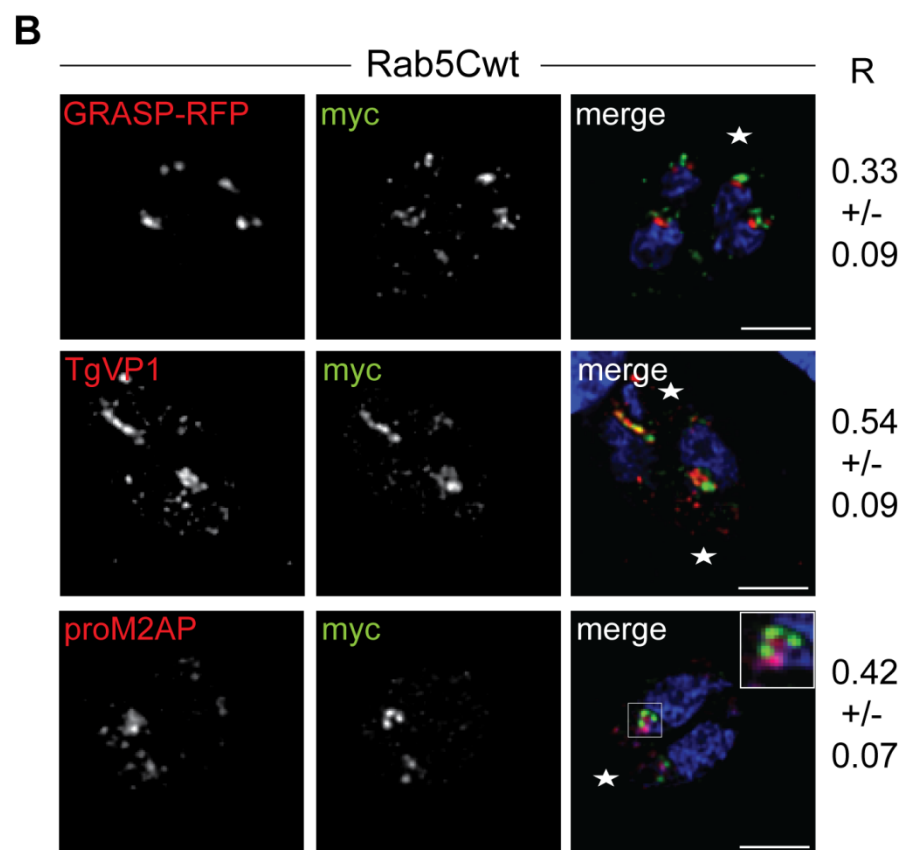
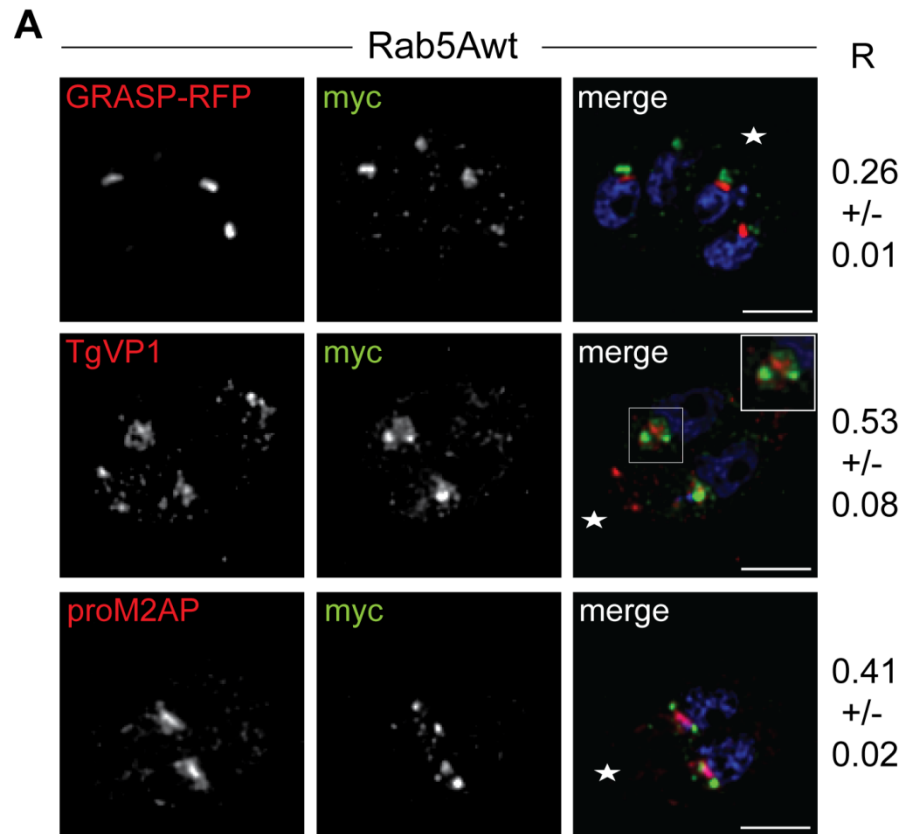


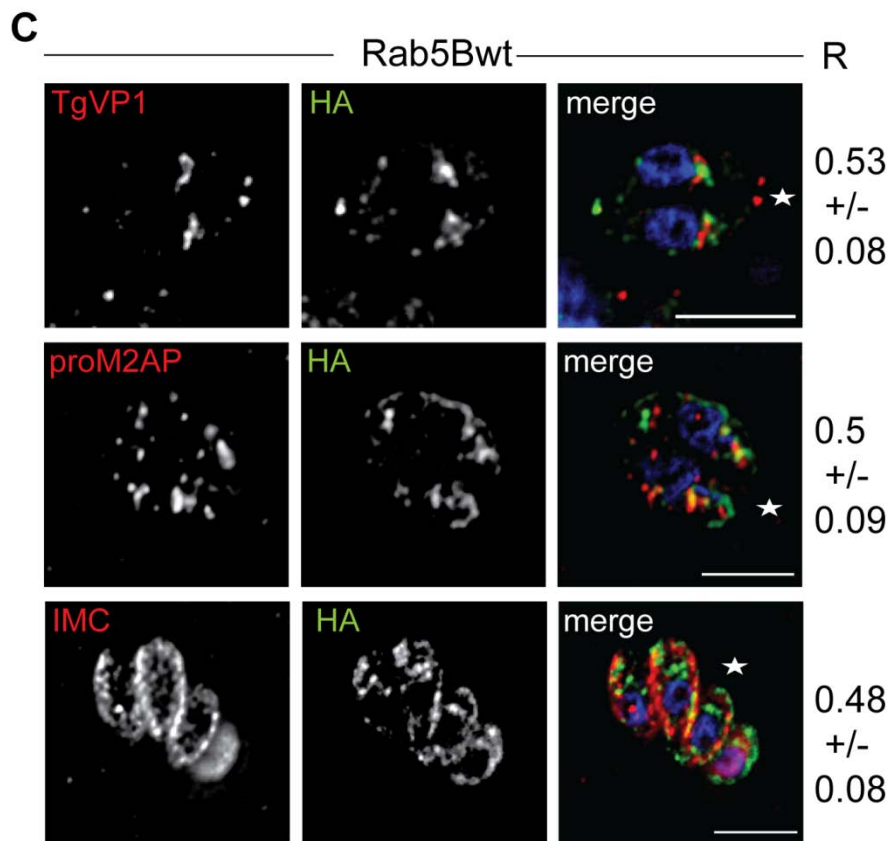
**Figure 3-7: Localisation of TgRab7.** Intracellular parasites stably expressing the ddFKBPmycRab7-construct were grown for 18hours in the presence of 1  $\mu$ M Shld-1 prior to fixation. Co-expression of the Golgi marker GRASP-RFP or co-staining with  $\alpha$ -proM2AP, or  $\alpha$ -TgVP1 antibodies were performed. To indicate the localisation of the respective TgRab7  $\alpha$ -myc was used. Dapi is shown in blue. The scale bars represent 5 $\mu$ m. TgRab7 shows partial co-localisation with both ELCs antibodies ( $\alpha$ -proM2AP and  $\alpha$ -TgVP1). Co-localisation was quantified by calculating the Pearson's correlation coefficient (R). Mean values and respective standard deviation of 10-16 parasites are indicated next to the respective image. Stars indicate the parasites orientation, where the apical part is pointing towards the star. The images were taken with the Nikon TE 2000 inverted microscope.

Figure 3-8 displays IFAs of intracellular parasites expressing stabilised ddFKBPmycRab5A, 5C and Rab5BHAddFKBP co-transfected with the Golgi marker GRASP-RFP or immunostained with  $\alpha$ -proM2AP,  $\alpha$ -TgVP1 or  $\alpha$ -IMC. Compared with the GRASP-RFP signal, Rab5A and C could be clearly detected in the post-Golgi region of *T.gondii*. Besides a weak diffuse cytosolic staining, the main localisation signal for TgRab5A and C was strongly concentrated at the ELC region. This could be detected by co-localisation studies with proM2AP and TgVP1. Interestingly, no clear co-localisation with the ELC markers (proM2AP and TgVP1) was detectable, as seen for TgRab7 (Figure 3-7). Both Rab5A and Rab5C appeared to be localised around or between the ELC compartments (close ups in Figure 3-7 A and B). Both Rab5A and 5C were found to co-localise with TgVP1.

For TgRab5B an irregular localisation pattern was detected. Co-localisation with TgVP1 and proM2AP is indicating an accumulation at the ELC region. But additional localisation at the PM could be observed and detected with partial co-localisation with  $\alpha$ -IMC.

In summary, all three Rab5 proteins are mainly detected at the ELC region. In this connection, Rab5A and C showed a similar localisation, which could indicate an identical occurrence of these two proteins. The localisation pattern of Rab5B clearly differs from Rab5A and Rab5C.





**Figure 3-8: Localisation of Rab5A, Rab5B and Rab5C.** Intracellular parasites expressing the indicated ddFKBpmycRab5A, 5C and Rab5BHAddFKBP-construct were grown for 18hours in presence of 1  $\mu$ M Shld-1 prior to fixation. Co-expression of the Golgi marker GRASP-RFP, or co-staining with  $\alpha$ -proM2AP,  $\alpha$ -TgVP1 or  $\alpha$ -IMC was performed. To indicate the localisation of the respective Rab protein  $\alpha$ -myc, or  $\alpha$ -HA antibodies were used. Dapi is shown in blue. Scale bar: 5  $\mu$ m. Co-localisation was quantified by calculating the Pearson's correlation coefficient (R). Mean values and respective standard deviation of 10-16 parasites are presented in a table beneath the respective image set. Stars indicate the parasites orientation, where the apical part is pointing towards the star. The images for Rab5A and 5C were taken with the Nikon TE 2000 inverted microscope and the images for Rab5B were taken with the Delta Vision Core System.

To analyse the extent the three TgRab5 proteins co-localise with each other, an additional construct where TgRab5A was N-terminally tagged with a Ty tag, was designed. Therefore the ddFKBpmyc tag in the construct ddFKBpmycRab5A was exchanged for a Ty-tag using EcoRI/NsiI. The resulting plasmid DNA (p5RT70TyRab5A-HXGPRT) was purified and transiently transfected into extracellular parasites of the parasite strains expressing ddFKBpmycRab5C or Rab5BHAddFKBP. Within a transient transfection, the plasmid DNA is not linearised and no selection is applied. The protein will be expressed from the plasmid itself and one to two replication rounds (each 8-10 hours) should be allowed to detect the protein in the parasites.

After inoculation of HFF monolayer and incubation for 20 hours with Shld-1, intracellular parasites were fixed and an IFA, using  $\alpha$ -Ty and  $\alpha$ -myc or  $\alpha$ -HA respectively was performed. The results are displayed in Figure 3-9. Comparing the signals for  $\alpha$ -Ty and  $\alpha$ -myc in the ddFKBPmycRab5C parasite line, a nearly identical localisation for TgRab5A and C could be detected. Less co-localisation of  $\alpha$ -Ty and  $\alpha$ -HA in the Rab5BHAddFKBP parasite line was detected. This confirmed the observation made in Figure 3-8.

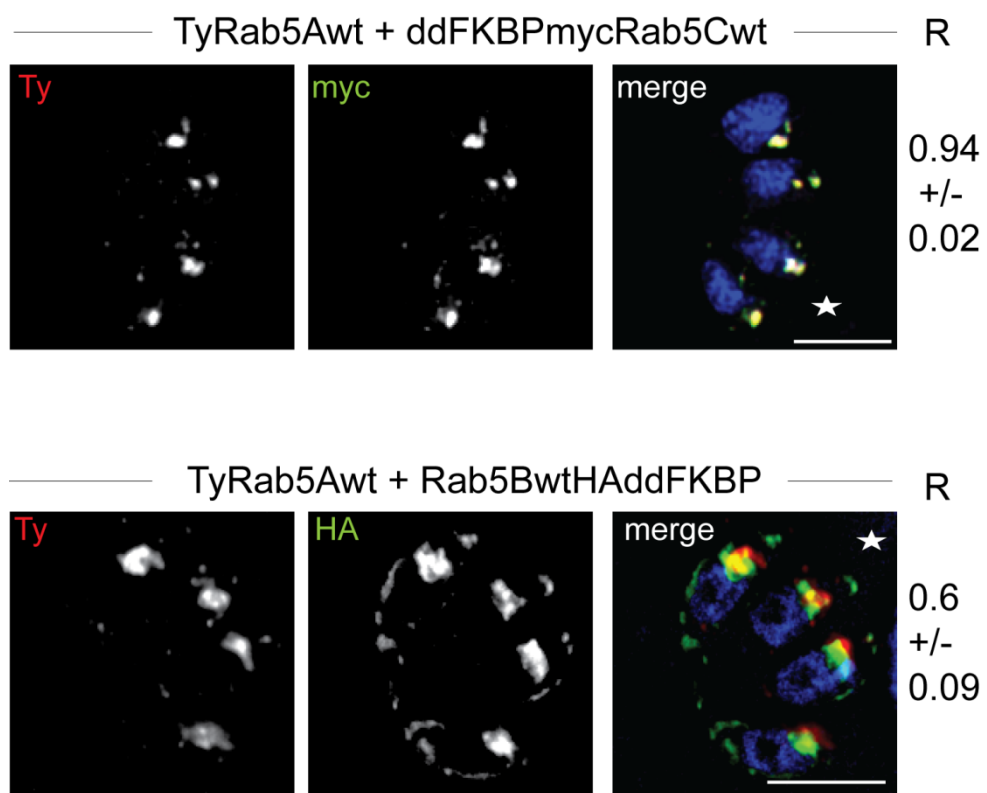


**Figure 3-9: Co-localisation analysis of TgRab5A with TgRab5C and TgRab5B.** Parasites co-expressing TyRab5A and ddFKBPmycRab5C were probed with  $\alpha$ -Ty and  $\alpha$ -myc antibodies. Rab5A and Rab5C show complete co-localisation. Scale bar: 5  $\mu$ m. Co-localisation was quantified by calculating the Pearson's correlation coefficient (R). Mean values and respective standard deviation of 10-16 parasites are presented in a table beneath the respective image set. Stars indicate the parasites orientation, where the apical part is pointing towards the star. The image for TyRab5Awt+ddFKBPmycRab5Cwt was taken with the Nikon TE 2000 inverted microscope and the image for TyRab5Awt+Rab5BwtHAddFKBP was taken with the Deltra Vision Core System.

## 3.7. Summary and Conclusion

### 3.7.1. 12 Rab proteins are expressed in *T.gondii* tachyzoites

The earlier identification of 15 Rab proteins (Tg1A,B,2,4,5A,B,C,7,18,8/10,23 and TgRab-like protein) in *T.gondii* (Langsley, van Noort et al. 2008) was confirmed within this work. TgRab6, TgRab11A and TgRab11B were expressed and characterised in earlier studies (Stedman, Sussmann et al. 2003; Agop-Nersesian, Naissant et al. 2009; Agop-Nersesian, Egarter et al. 2010). Three of the previous identified putative Rab-GTPases in *T.gondii* were excluded from further analyses mainly because of the inability to amplify cDNA for the respective genes (*tgrab23*, *tgrab-like* and *tgrab8/10*). For 9 Rab proteins (TgRab1A,B,2,4,5A,B,C,7 and 18), cDNA could be amplified within this work. When this study was performed, synthesising DNA for cloning was not as affordable as it is today. For this reason only TgRab1A,B,2,4,5A,B,C,7 and 18 were further analysed.

### 3.7.2. Localisation of TgRab1A,B,2,4,5A,B,C,7 and TgRab18

To investigate potential functions of these Rab proteins, localisation analyses were performed. The ddFKBP system, which was already applied for Rab11A and Rab11B in *Toxoplasma*, was used to create a regulated overexpression of the respective Rab protein. Within immunofluorescence analyses and with the application of antibodies and marker proteins of different organelles in *T.gondii* tachyzoites, the localisation of each Rab protein was determined.

Using this approach it was found that all analysed Rabs are localised to the early-late secretory system of the parasite, but not to the apical secretory organelles.

**Rab1B,2,18:** Rab1B and 18 were found to localise predominantly to organelles of the early secretory pathway, the ER and the Golgi (Figure 3-4) as demonstrated by co-localisation with the marker proteins TgERD2 and GRASP (Pflugger, Goodson et al. 2005). Rab 2 displayed accumulation at the ER/Golgi region (Figure 3-4B), however the co-localisation is not as clear as it is for Rab1B and 18. This could suggest that Rab1B and Rab2 have a similar role in the transport of vesicles

between the ER and the Golgi, as observed in other eukaryotes (Tisdale, Bourne et al. 1992; Dhir, Goulding et al. 2004), but a different function within apicomplexans for Rab2 cannot be ruled out. Rab18 has been identified in several eukaryotic lineages, indicating that this Rab was present in the LCEA (Elias, Brighouse et al. 2012). However, in contrast to Rab1 and 2 it has been lost in several species, including some apicomplexan parasites, where it is missing in case of *Cryptosporidium*, *Theileria* and *Babesia* (Langsley, van Noort et al. 2008). Rab18 has been implicated in diverse roles, including ER-Golgi-traffic (Dejgaard, Murshid et al. 2008), formation of lipid droplets (Martin, Driessen et al. 2005; Ozeki, Cheng et al. 2005) or regulation of secretion in neuroendocrine cells (Vazquez-Martinez, Cruz-Garcia et al. 2007), indicating that this protein does not show a strict functional conservation.

**Rab4:** Rab4 can be identified in diverse eukaryotic lineages, but has been lost on several occasions (Brighouse, Dacks et al. 2010). Similarly, in apicomplexans Rab4 is present in *Toxoplasma* and *Cryptosporidium* but absent in *Plasmodium* and *Theileria* (Langsley, van Noort et al. 2008). Rab4 had been first characterised in human cells and shown to be essential for endocytosis and the formation of early endosomes (van der Sluijs, Hull et al. 1992). In contrast it was found within this study, that *T.gondii* Rab4 is almost exclusively localised to the Golgi (Figure 3-5), as indicated by co-localisation with GRASP-RFP and TgGalNac fused to yellow fluorescent protein. On some occasions a partial co-localisation of Rab4 with proM2AP, a marker for endosomal-like compartments (Figure 3-5) was found.

**Rab1A:** A recent phylogenetic analysis suggests that apicomplexan Rab1A defines a unique paralog shared by alveolates (Elias, Patron et al. 2009) and phylogenetic analysis of Jonathan Wilkes supports this view (Kremer, Kamin et al. 2013). When parasites expressing a ddFKBpmyc-tagged version of Rab1A were analysed, it was found that this protein concentrated within the post-Golgi region, as indicated by co-localisation with the Golgi marker GRASP-RFP and ELC marker proM2AP and TgVP1. Due to different localisation pattern in the post-Golgi region in different IFAs, the location of Rab1A is assumed to be highly dynamic and no specific localisation could be defined (Figure 3-6). For future work time lapse imaging could be applied to gain more information about the

location of Rab1A.

**Rab7:** Rab7 has been previously localised to the ELCs in *T.gondii* (Miranda, Pace et al. 2010; Parussini, Coppens et al. 2010). In this study, co-localisation of Rab7 with ELCs (proM2AP and TgVP1) (Figure 3-7) was confirmed, consistent with a conserved role of Rab7 in trafficking from early to late endosomes (Vanlandingham and Ceresa 2009).

**Rab5A,B,C:** Three Rab5-GTPases could be identified in the genome of apicomplexan parasites (Table 3-1). While Rab5A and Rab5C appear to be derived from a lineage-specific gene duplication event, Rab5B belongs to a unique class that is only conserved in apicomplexan parasites (Langsley, van Noort et al. 2008; Kremer, Kamin et al. 2013). Interestingly this protein lacks the typical prenylation motif at the C-terminus. Instead a potential myristoylation motif at the N-terminus could be identified. Therefore Rab5B was C-terminally tagged with ddFKBPHA for localisation studies and it was found that this protein showed a concentration at ELCs (Figure 3-8C) and to a lesser extent at the surface of the parasite, possibly the inner membrane complex (IMC). Consistent with earlier studies (Robibaro, Stedman et al. 2002), Rab5A was identified at ELCs and an identical location for Rab5C was found (Figure 3-9). Co-localisation analysis of Rab5A and Rab5B exhibited small overlapping but no identical localisation signals of these two Rab proteins (Figure 3-9). This indicates that Rab5B might have a different function than Rab5A and 5C in *T.gondii*, which are most likely involved in the organisation and function of the ELCs.

## 4. Systematic phenotypisation of overexpressed RabGTPases and mutants

### 4.1. Introduction

After localisation of the 9 Rab proteins TgRab1A,B,2,4,5A,B,C,7 and 18 as a first step to obtaining information regarding their potential functions in *T.gondii* tachyzoites (see chapter 3), further functional analyses were performed and are presented in this chapter. Since overexpression is widely used in different eukaryotes to analyse the function of Rab proteins (Bucci, Parton et al. 1992; van der Sluijs, Hull et al. 1992), the generated parasite strains overexpressing the respective Rab protein were screened for their general proliferation ability. A decrease in proliferation could indicate that secretory organelles (micronemes and rhoptries) are affected, since their proteins are involved in the lytic cycle of *T.gondii* tachyzoites. Therefore parasites showing a significant decrease in proliferation were analysed for their localisation of microneme and rhoptry proteins.

In chapter 3, TgRab5A,B,C and 7 proteins were found to localise within the post-Golgi region, indicating a function in the late secretory pathway. While the localisation of TgRab1A could not be determined, a potential function in the late secretory pathway cannot be excluded. To analyse the direct function of these Rab proteins in the vesicular traffic of secretory proteins (microneme and rhoptry proteins) to their target organelles, trans-dominant mutants were generated and analysed. Only the results for TgRab1A, TgRab5B and TgRab7 are presented in this chapter.

## 4.2. Overexpression screen part I: Growth analysis

To investigate if overexpression of the 9 Rab proteins affected the infectivity of *T. gondii*, growth analyses were performed with ddFKBPmycRab1A,1B,2,4,5A,5C,7,18 and Rab5B-ddFKBPHA expressing parasites. This was done by plaque assays. HFF monolayers were inoculated with an equal number of parasites expressing the respective Rab protein and incubated with or without Shld-1 for 5 to 6 days under normal growth conditions. Due to the lytic cycle of *T. gondii* tachyzoites (host cell invasion, intracellular replication, host cell egress and gliding motility) spots of destroyed host cells (plaques) are detectable, when parasites are not affected in their infectivity. This means, if the analysed parasite strain was affected in its general ability to grow (undergoing several lytic cycles) it was reflected in the plaque sizes within a plaque assay. By measuring the area of the plaques with image processing software (ImageJ), plaque sizes were analysed and quantified (Figure 4-1). As expected, normal plaque formation could be detected in absence of the inducer Shld-1, since the respective Rab protein is not overexpressed. In contrast, no plaques could be detected if parasites were overexpressing TgRab2,4,5B and C (Figure 4-1). For the strain overexpressing TgRab5A, growth was severely decreased or almost blocked. Compared to the plaque sizes of uninduced ddFKBPmycRab5A parasites, incubation with Shld-1 resulted in over 90% smaller plaques sizes. Overexpression of TgRab1A and 1B resulted in plaques, which were circa 50% smaller than plaques from uninduced parasites of the same strains (Figure 4-1). No significant effect on plaque sizes could be seen for parasites overexpressing TgRab7 and TgRab18.

In summary, only overexpression of TgRab2,4,5A,B and C was severely affecting the parasites's ability to undergo several rounds of its complete lytic cycle.

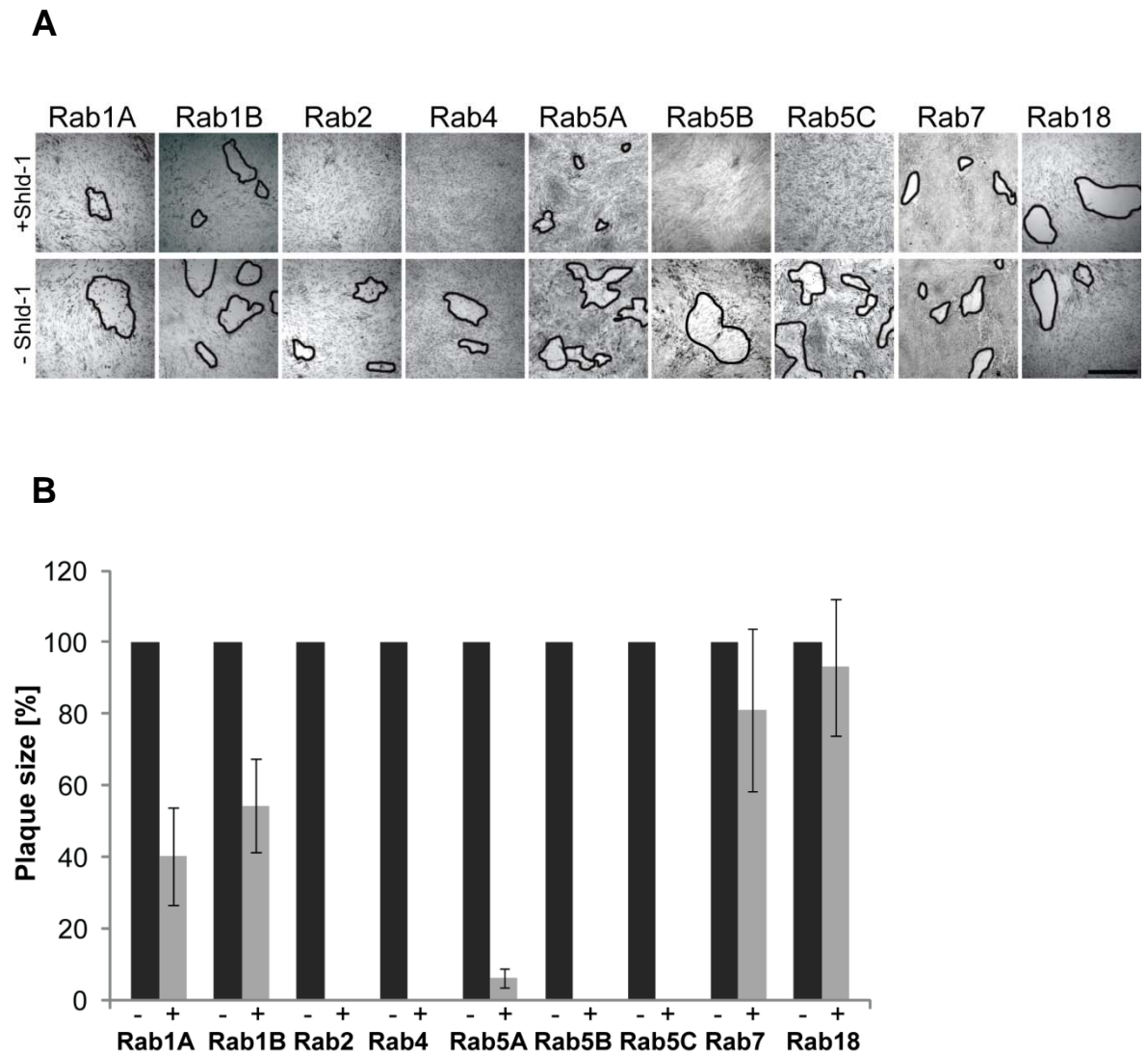


**Figure 4-1: Parasite growth is inhibited by overexpression of TgRab2,4,5A,B and C.** (A,B) Growth analysis (plaque assays): 50 parasites expressing ddFKBPmycRab1A,B,2,4,5A,C,7,18 or Rab5BHAddFKBP, were inoculated on HFF cells growing in a “6 well plate” well and cultured with (+) and without (-) 1 $\mu$ M Shld-1 for 5-6 days. (A) Light microscopic images of the respective HFF monolayers after 5-6 days, fixed and stained with Giemsa. Single plaques are indicated by black edging (bordered with ImageJ). The scale bar represents 1 mm. (B) Normalised quantification of the plaque sizes of one representative plaque assay out of 3. In each case, the mean area and standard deviation of 10 plaques was determined. The data was normalised relative to the plaque size of the respective uninduced (-) parasite strain. The images were taken from (Kremer, Kamin et al. 2013).

### 4.3. Overexpression screen part II: Secretory organelles

A detected growth phenotype as seen for the overexpression of TgRab2,4,5A,B and C, could mean that parasites cannot replicate, glide, invade or egress properly. For gliding, invasion and egress, intact secretory organelles containing the secretory proteins are essential (see 1.4.). Focussing on the traffic of regulated secretory proteins and the biogenesis of their organelles in *T.gondii*, the effect on rhoptry and microneme proteins in ddFKBPmycRab2,4,5A,C and Rab5BHAddFKBP expressing strains were analysed. HFF monolayers were infected with the respective parasite strain, incubated for 24 hours with Shld-1, fixed and immunostained within immunofluorescence analyses (IFAs). Antibodies against different rhoptry and microneme proteins [MIC3 (soluble), MIC2 (TM) and ROP 2-4] involved in invasion (see 1.7.) were used to detect effects on the respective secretory organelles. The *T.gondii* strain: RH<sup>hxgprt-</sup> was used as a control for a normal rhoptry or microneme protein localisation signal. In Figure 4-2 only vacuoles with 8 parasites, detectable by the nucleus stain with Dapi, are presented. The apical, cap-like signal of microneme proteins and the more or less apical elongated signal of rhoptry proteins in RH<sup>hxgprt-</sup> parasites indicated the normal localisation of these proteins (Figure 4-2). Compared with the localisation signals of RH, overexpression of TgRab5B, TgRab2 and TgRab4 showed normal localisation of rhoptry and microneme proteins (Figure 4-2). Interestingly, for the parasites overexpressing TgRab5A and TgRab5C a mislocalisation of MIC3 and ROP2-4 was detected. Instead of its normal apical localisation signals, MIC3 and ROP2-4 were localised mainly outside of the parasite, accumulating within the parasitophorous vacuole (PV). Surprisingly, the localisation of MIC2 remained unaffected under TgRab5A or C overexpressions, indicating different transport routes of MIC2 and MIC3 to the micronemes.

In summary, only overexpression of TgRab5A or TgRab5C caused mislocalisation of some secretory proteins and only a subset of microneme proteins was affected.

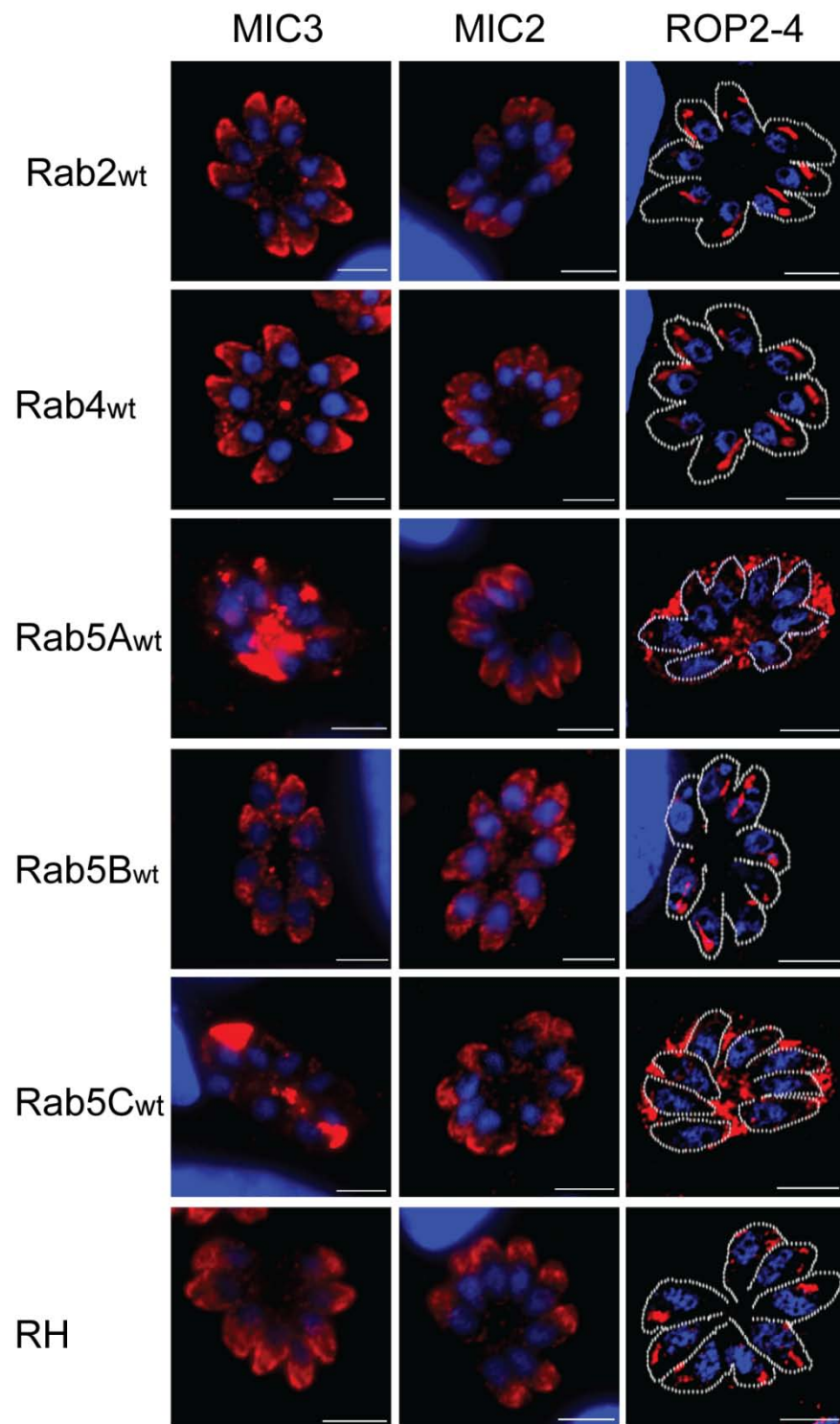


**Figure 4-2: Overexpression of TgRab5A and C causes mislocalisation of only a subset of microneme proteins.** Immunofluorescence analysis of intracellular parasites expressing ddFKBpmycRab2,4,5A,C or Rab5BHAddFKBP and wild type parasites RH<sup>hxgprt</sup> treated for 24 hours with 1µM Shld-1 and probed with α-MIC3, α-MIC2 or α-ROP2-4 antibody (red) and Dapi (blue). The dashed line in the ROP2-4 images is indicating the parasites surface within the vacuole performed from differential interference contrast (DIC) images merged with the fluorescence image of the same vacuole and outlined in Photoshop CS4. Scale bars represent 5µm. The images were taken with the Delta Vision Core System.

## 4.4. Generation and analysis of inducible parasite strains expressing trans-dominant Rab proteins.

### **4.4.1. Generation of inducible parasite lines expressing trans-dominant Rab proteins**

To study the regulated secretory pathway in *T.gondii*, all Rab proteins localising at the Golgi or post-Golgi region were further analysed. Trans-dominant versions of TgRab1A,7,5A,5B and 5C were thus generated. Overexpression of a dominant negative (non-functional) version of a protein leads to competition between the endogenous and the mutated version. This affects the function of the endogenous protein, which can be then analysed. Within this study, dominant negative versions of TgRab1A,7,5A,5B and 5C were generated using the same strategy as employed for TgRab11A and TgRab11B (Agop-Nersesian, Egarter et al. ; Agop-Nersesian, Naissant et al. 2009). Here an amino acid exchange [from asparagine (N) to isoleucine (I)] was introduced in the third conserved region for GNP-binding of the highly conserved GTPase domain. This changes the binding affinity for GDP and GTP in GDP's favour. GDP becomes locked and the Rab protein cannot be activated and remains in its cytosolic conformation. To generate the dominant negative version of the respective Rab protein, site-directed mutagenesis was employed by using the "megaprimer" method (Sarkar and Sommer 1990). The resulting PCR fragment was integrated into the p5RT70DDmycGFP-HXGPRT expression vector (Herm-Gotz, Agop-Nersesian et al. 2007), using the same cloning strategy as for the wild type Rab protein version (see chapter 3.4.). Stable transfection and subcloning clonal parasite strains expressing ddFKBPmycRab1A(N126I), ddFKBPmycRab7(N124I), ddFKBPmycRab5A(N158I), ddFKBPmycRab5B(N152I) or ddFKBPmycRab5C(N153I) were obtained.



#### **4.4.2. Characterisation of dominant negative TgRab1A**

In higher eukaryotes Rab1A is involved in the retrograde vesicle transport between ER and Golgi (see 1.6.), but in *Plasmodium* it was found to be a unique paralog to chromalveolates with a likely distinct function (Elias, Patron et al. 2009). Together with the observation that TgRab1A's localisation is different from higher eukaryotes (3.6.3.) further analyses with a dominant negative version were undertaken.

As described in the previous paragraph, a clonal parasite strain expressing the dominant negative version of TgRab1A [ddFKBPMycRab1A(126I)] was generated and showed the expected GDP-locked cytosolic localisation pattern (Figure 4-4). To test if the expression of Rab1A(N126I) is regulatable with the ddFKBP system, a western blot and IFA were performed as described for the wild type TgRab1A (see chapter 3.5.) The results are displayed in Figure 4-4A. Detection of ddFKBPMycRab1A(N126I) occurred via  $\alpha$ -ddFKBP (western blot) and  $\alpha$ -myc (IFA) antibodies. As expected, no signal could be detected in absence of Shld-1, but a clear upregulation of the ddFKBPRab1A(N126I) fusion protein was apparent in presence of Shld-1 (Fig4-4A). According to this, a regulation of the dominant negative Rab1A version with the ddFKBP system could be confirmed to continue with its further analysis.

To test if expression of the dominant negative TgRab1A is affecting proliferation of tachyzoites, growth analysis (plaque assay) was conducted. The procedure of the plaque assay was the same as described for wild type TgRab1A (see chapter 4.2.). Compared with the effect on plaque formations in host cell monolayers infected with RH<sup>hxppt</sup> parasites, parasites expressing the dominant negative version incubated for 5 days with and without Shld-1 displayed no significant differences (Figure 4-4B).

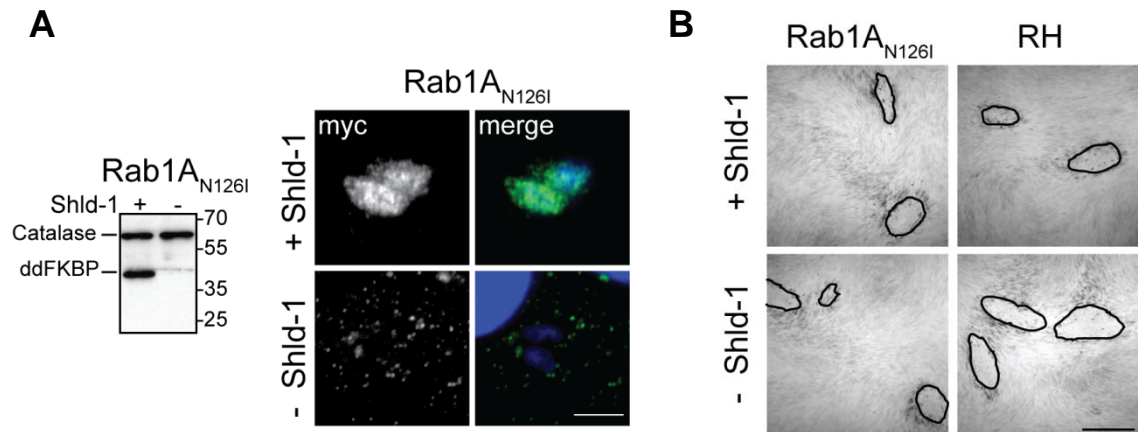


**Figure 4-4: Regulation and growth analysis of ddFKBpmycRab1A(N126I).** (A) Western blot and IFA of ddFKBpmycRab1A(N126I) expressing parasites. For the western blot freshly egressed parasites were treated for 4hours +/- 1  $\mu$ M Shld-1 and for the IFA intracellular parasites were treated for 18hours +/- 1  $\mu$ M Shld-1. The regulation of the mutant was detected either by  $\alpha$ -ddFKBP (western blot) or  $\alpha$ -myc antibodies (IFA, green). As an internal control for the western blot  $\alpha$ -catalase antibodies were used. Dapi is shown in blue. The scale bar represents 5  $\mu$ m. (B) Growth analysis of the indicated parasite strains for 5 days +/- 1  $\mu$ M Shld-1. The scale bar represents 1 mm. The IFA images were taken with the Zeiss Axioscope 2 microscope.

### **4.4.3. Characterisation of dominant negative and constitutively active TgRab7**

In higher eukaryotes Rab7 plays an essential role in endosome-lysosome traffic (see introduction). No lysosomes could be identified so far in *T.gondii*, but TgRab7 could be shown to localise within the ELC region (Figure 3-7). Since Rab7 is highly conserved in eukaryotes and is probably involved in vesicular transport to a plant-like vacuole and/or secretory organelles (Miranda, Pace et al. 2010; Parussini, Coppens et al. 2010), a clonal parasite strain expressing an inducible dominant negative version of TgRab7 (Rab7N124I) was generated as described in chapter 4.4. Additionally a clonal strain with a constitutively active version of TgRab7 was generated, ddFKBPmycRab7(G18E). In this case a point mutation within the phosphate binding (p-loop) motif of the GTPase domain (see 1.6.2.) was introduced. As shown for other GTPases (Schmidt, Rose et al. 2005; Heasman and Ridley 2008), a mutation within this motif produces a mutated Rab protein, which cannot hydrolyse GTP. This mutant would remain constitutively active and sequesters effector proteins. Overexpression of constitutively active TgRab7 would result in an inhibition of the signalling cascade of endogenous TgRab7. To generate parasites expressing ddFKBPmycRab7(G18E), a mutagenic primer with the containing point mutation, Glycine (G) to Glutamic acid (E) at position 18 (see 2.8.), was used to amplify the mutated cDNA. The resulting PCR product was cloned into the p5RT70DDmycGFP-HXGPRT expression vector via pGEM-T Easy vector cloning and NsiI/PacI restriction sites as described for the wild type TgRab7 (see chapter 3.4.). The final vector was linearised with NotI and transfected into RH<sup>hxgprt</sup>- parasites as described in chapter 3.4..

To test if the expression of both trans-dominant TgRab7 mutants was regulatable with the ddFKBP system, a western blot and IFA were performed as described for the wild type TgRab7 (3.5.) The results are displayed in Figure 4-5. Detection of ddFKBPmycRab7(N124I) and ddFKBPmycRab7(G18E) occurred via  $\alpha$ -ddFKBP (western blot) and  $\alpha$ -myc (IFA) antibodies. No signal could be detected in absence of Shld-1 for the dominant negative TgRab7 parasite line within western blot and IFA, but a clear upregulation of the fusion protein was apparent in presence of Shld-1 (Figure 4-5). Some background expression of the constitutively active TgRab7 mutant could be detected in parasites treated with Shld-1 free medium. This could be seen within the western blot and IFAs.

Compared to the strong expression signal of ddFKBpmycRab7(G18E) in presence of Shld-1, detectable in western blot and IFA, one can say, that expression of the constitutively active TgRab7 mutant could be also regulated with the ddFKBP system. Further analyses to investigate the role of TgRab7 in post-Golgi vesicular traffic in *T.gondii* are followed.

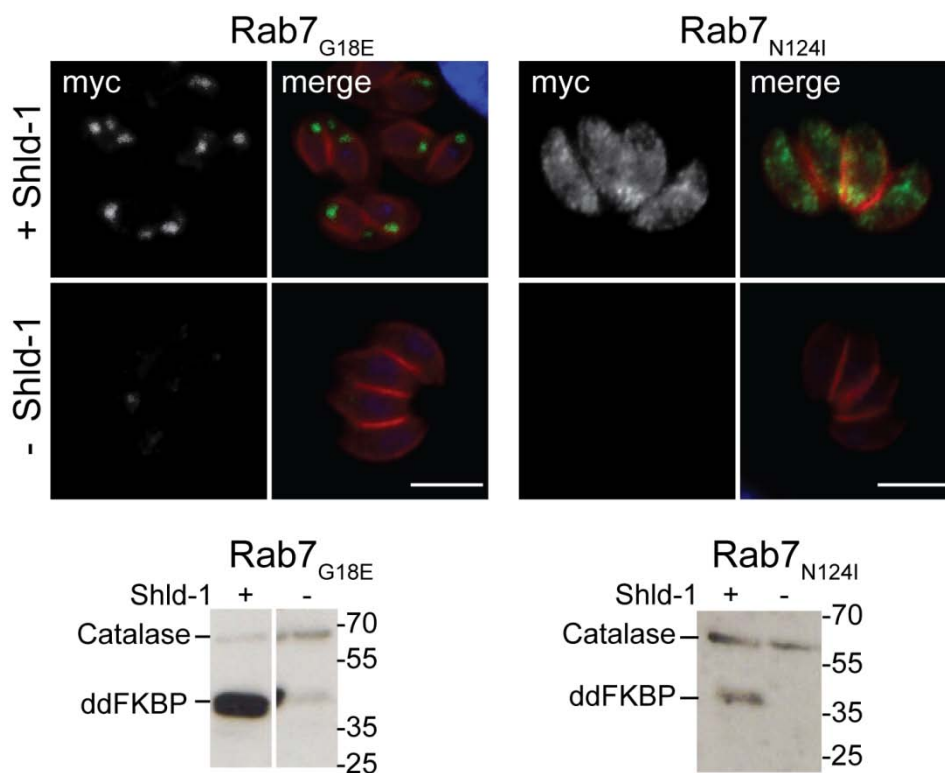


**Figure 4-5: The presence of ddFKBpmycRab7(G18E) or ddFKBpmycRab7(N124I) within *T.gondii* tachyzoites is regulable.** Western blot (lower panel) and immunofluorescence analyses (upper panel) of ddFKBpmycRab7(G18E) and ddFKBpmycRab7(N124I) expressing parasites. For the western blots freshly egressed parasites were treated for 4 h +/- 1  $\mu$ M Shld-1 and for the immunofluorescence analyses intracellular parasites were treated for 18 hours +/- 1  $\mu$ M Shld-1. To detect expression of the respective fusion protein  $\alpha$ -myc was applied for the IFA and  $\alpha$ -ddFKBP for the western blot. As an internal control for the western blot  $\alpha$ -catalase antibodies were used. To detect parasites  $\alpha$ -IMC (red) was used in IFAs. The merged images exhibit additionally the DAPI stain. The scale bars represent 5  $\mu$ m. The IFA images were taken with the Axioscope 2 microscope.

Besides the regulation of both mutants, one can also see in Figure 4-5, that both mutants display a different localisation signal. As expected for the dominant negative (GDP locked) version, a cytosolic signal within the whole parasite could be detected. For the constitutively active version (GTP locked) an accumulation at the target membrane was expected. In Figure 4-5 an accumulation within the post-Golgi region was already identifiable for ddFKBpmycRab7(G18E). Co-localisation analyses with  $\alpha$ -prom2AP showed clearly (Figure 4-6) that the

constitutively active TgRab7 is localised in the ELC region as its wild type version.

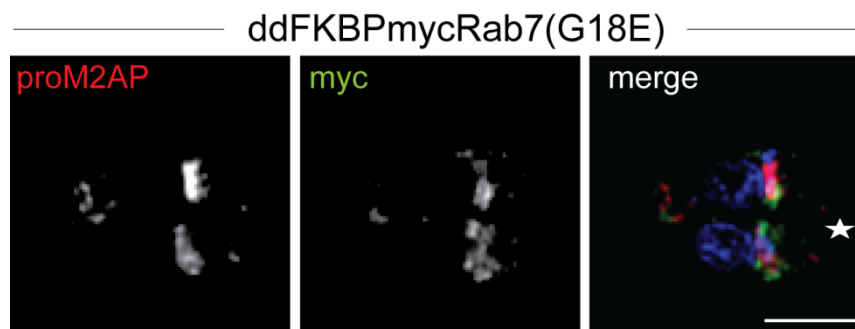


**Figure 4-6: ddFKBPmyc tagged constitutively active TgRab7 is localised at the ELC region.** Intracellular parasites expressing ddFKBPmycRab7(G18E) were grown for 18hours in presence of 1  $\mu$ M Shld-1 prior to fixation. Co-staining with  $\alpha$ -proM2AP was performed within a immunofluorescence analysis. To indicate the localisation of the fusion protein  $\alpha$ -myc antibody was used. Dapi is shown in blue. The scale bar represents 5  $\mu$ m. The star indicates the parasites orientation, where the apical part is pointing towards the star. The image was taken with the Delta Vision Core System.

#### 4.4.3.1. Growth analysis

Since overexpression of TgRab7 did not result in a growth phenotype (Figure 4-1), plaque assays with the wild type, the dominant negative and the constitutively active versions of TgRab7 were performed. Figure 4-7 displays one representative result out of 3 independent experiments. The procedure of the plaque assay was the same as described for the overexpression screen of TgRab proteins in the beginning of this chapter (4.2.). No differences in plaque formation after 5 days of growth with and without Shld-1 could be detected and confirmed for the overexpression of TgRab7. For parasites expressing the dominant negative version, no differences could be detected (Figure 4-7). Parasites expressing the constitutively active version of TgRab7 showed a clear defect in plaque formation. Comparing the ability to grow for all three parasite lines in absence of Shld-1, it was observed that the constitutively active mutant could not form plaques to the same size as parasites expressing the dominant negative or wild type version. This could be the cause of background expression already observed in IFAs and western blots (Figure 4-5). Comparing the plaque sizes of the ddFKBPmycRab7(G18E) expressing parasites with and without Shld-1, fewer and smaller plaques were detected when treated with Shld-1.

In summary, constitutive expression of the active version of TgRab7 affects the infectivity of *T.gondii* tachyzoites however overexpression of dominant negative TgRab7 does not.

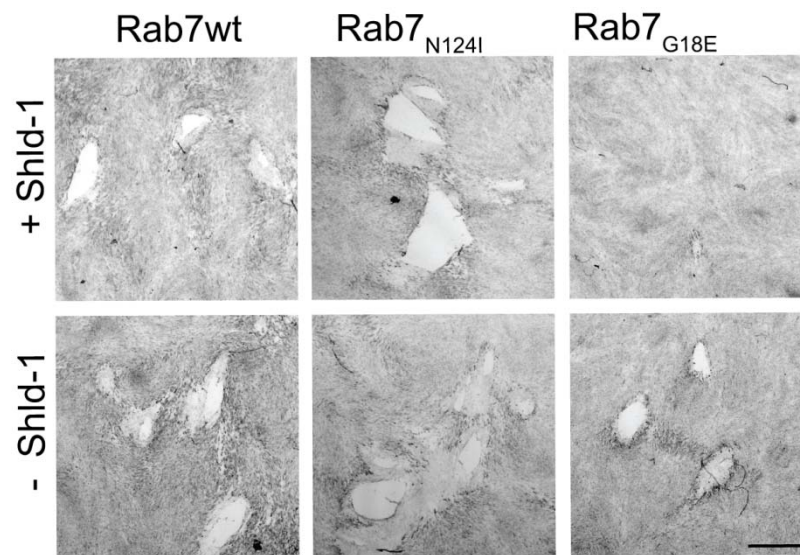


**Figure 4-7: Parasites expressing the constitutively active version of TgRab7 showed a defect in their growth ability.** Plaque assay of parasites expressing ddFKBPmycRab7(wt), ddFKBPmycRab7(N124I) or ddFKBPmycRab7(G18E) grown for 5 days with (+) and without (-) 1  $\mu$ M Shld-1. The scale bar represents 1 mm. The image was taken from (Kremer, Kamin et al. 2013).

#### 4.4.3.2. Replication analysis

To investigate if intracellular replication is causing the growth phenotype seen in Figure 4-7, replication assays were performed. Within this assay confluent HFF monolayers growing on glass coverslips in "24 well plate" wells were inoculated with parasites of the analysed strains and incubated with or without Shld-1 for 24 to 36 hours. During that time parasites invaded the host cells and replicated within the cells. After the respective incubation time the infected monolayers were fixed with 4% PFA and immunolabeled with  $\alpha$ -Sag1 or  $\alpha$ -IMC to label the surface or the inner membrane complex of the parasites so that the number of parasitophorous vacuoles (PVs) and the amount of parasites within one PV could be determined under a fluorescent microscope. 10 random fields per view were counted for each assay. Figure 4-8 displays the results of one out of 2 independent experiments. RH<sup>hxgprt</sup> parasites, TgRab7 wild type (wt) and constitutively active (G18E) TgRab7 expressing parasites were analysed. In each case, each strain was either incubated with (+) or without (-) 1 $\mu$ M Shld-1 for 36 hours before fixation. The highest number of PVs for RH and for wt parasites

was detected within the 16 cell stage. Around 10% of the PVs had already 32 parasites for RH and wt and only parasites of the RH strain showed some vacuoles with 64 parasites. Compared with RH parasites, parasites overexpressing the wild type version of TgRab7 showed a tendency of reduced replication ability after four rounds of replication (16 cell stage). No parasites of the ddFKBPmycRab7(G18E) strain reached the 32 parasite stage and most of the PVs contained 8 or 16 parasites. Interestingly, in both of these stages as well as in the single parasite stage of this strain more PVs for parasites treated with Shld-1 were detected as for parasites without Shld-1.

In summary, expression of the constitutively active version of TgRab7 is affecting the replication ability of *T.gondii* tachyzoites after four rounds of replication.

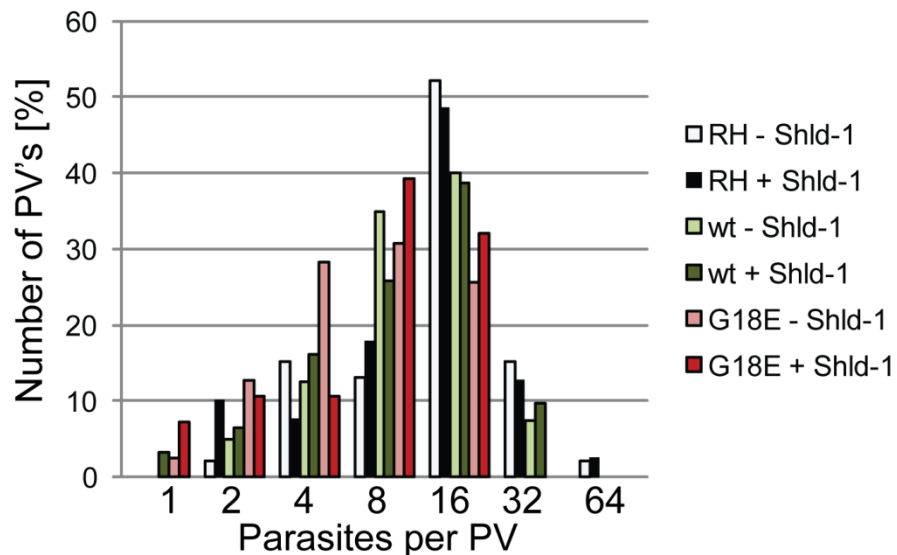


**Figure 4-8 : Parasites expressing ddFKBPmycRab7(G18E) were affected in their replication ability.** Replication assay of RH<sup>hxgprt</sup> parasites and parasites expressing ddFKBPmycRab7(wt) or ddFKBPmycRab7(G18E) grown for 36hours in presence or absence of 1 $\mu$ M Shld-1 prior to fixation. Average number of parasites per PV was determined.

#### 4.4.3.3. Egress analysis

To analyse if intracellular parasites are able to lyse and leave the host cell to infect the next cell, an egress assay was performed. Here confluent HFF monolayers were infected with an equal amount of parasites expressing ddFKBPmycRab7(wt) and ddFKBPmycRab7G18E and RH<sup>hxgprt-</sup> parasites as a control. After incubation with and without Shld-1 for 36 hours under normal growth conditions the Calcium ionophore (A23187; 1µM) was added to the medium 5-10 minutes prior to fixation. "A23187" was shown to trigger egress of intracellular parasites by increasing the intracellular Ca<sup>2+</sup> level of the parasites (Endo, Sethi et al. 1982; Black, Arrizabalaga et al. 2000; Arrizabalaga and Boothroyd 2004). After fixation, extracellular parasites were labelled with α-Sag1 before permeabilisation. After the monolayers were permeabilised, extracellular and intracellular parasites were labelled with α-IMC. By labelling α-Sag1 with a red fluorescent secondary antibody and α-IMC with a green fluorescent antibody, extracellular parasites (stained with α-Sag-1 and α-IMC) appeared yellow and intracellular parasites (only stained with α-IMC) appeared green under the fluorescent microscope. This enabled counting of egressed vacuoles under a fluorescence microscope, where the parasites were extracellularly scattered around the lysed host cell. 10 fields of view were counted per parasite strain treated with and without Shld-1. The number of egressed vacuoles was normalised with untreated RH<sup>hxgprt-</sup> parasites. The results of 2 independent experiments are displayed in Figure 4-9. For both parasite strains [ddFKBPmycRab7(wt) and ddFKBPmycRab7(G18E)] no significant reduction in egress was detected either for parasites grown in presence or absence of Shld-1. Compared with RH (100%) for both parasite strains nearly 100% of egressed vacuoles were detected, which indicated a normal ability to leave their host cells.

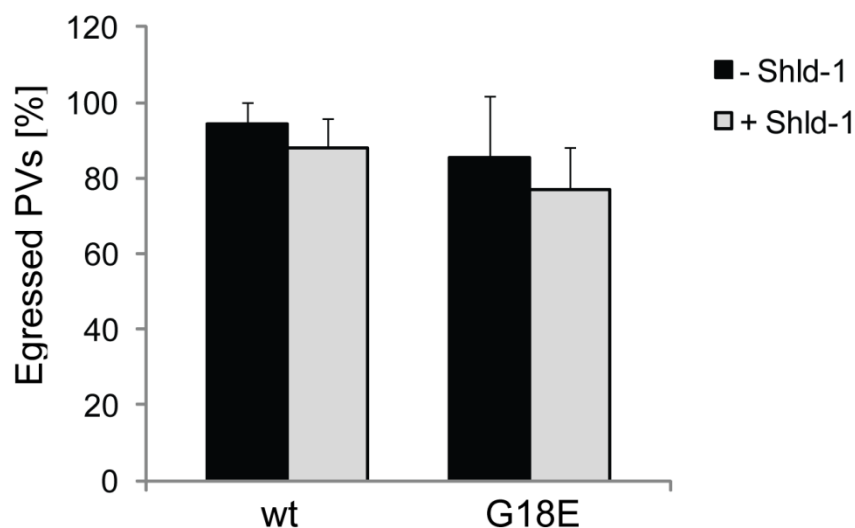


**Figure 4-9: Neither overexpression of wild type Rab7 (wt) nor expression of its constitutively active version (G18E) was affecting the ability to egress host cells.** Egress assay of RHxgprt-parasites and parasites expressing ddFKBPmycRab7(wt) or ddFKBPmycRab7(G18E) treated for 36 hours with (+) and without (-) 1 $\mu$ M Shld-1 before egress was triggered with A23187. Host cell lysis was determined 8min after induction of egress and normalised with Shld-1 untreated RH xgprt-parasites. Mean values and the respective standard deviation of two independent experiments are presented.

#### 4.4.3.4. Invasion analysis

Since no effect on egress could be detected for ddFKBPmycRab7(G18E) expressing parasites, the ability of host cell invasion was tested. Therefore invasion assays were performed. Within this assay parasites expressing ddFKBPmycRab7(wt) and ddFKBPmycRab7(G18E) were grown with and without Shld-1 for 24 hours. After that intracellular parasites were mechanically extracted from host cells. These fresh extracellular parasites were transferred onto HFF monolayer's grown on cover slips within a "24 well plate" well. An equal amount of RH<sup>hxgprt</sup>-, ddFKBPmycRab7(wt) and ddFKBPmycRab7(G18E) parasites were used for inoculation. Under normal growth conditions parasites were allowed to invade the host cells for 2 hours. After that the cover slips were washed 5 times with PBS, to remove extracellular parasites, and fixed with 4% PFA. Immunofluorescence analysis was followed to mark intracellular parasites. For each cover slip, the amount of invaded intracellular single parasites were counted within 10 fields of view. The results of 2 independent experiments are displayed in Figure 4-10. The number of parasites of ddFKBPmycRab7(wt) and ddFKBPmycRab7(G18E) expressing parasites were normalised with the number of parasites detected for RH<sup>hxgprt</sup>-. No significant difference was observed for

parasites expressing Rab7(wt) either in presence or absence of Shld-1. Compared to RH (100%) a slight general tendency of invasion reduction could be observed for parasites overexpressing Rab7(wt). Both with and without Shld-1 induction resulted in a 90% invasion rate. For parasites expressing the constitutively active mutant, a much stronger tendency of invasion reduction could be observed in presence of Shld-1. Here the parasites grown in medium without Shld-1 prior to invasion showed a normal invasion ability compared to RH<sup>hxgprt</sup> parasites, whereas treatment with Shld-1 led to an invasion reduction by nearly 50%.

In summary, expression of ddfKBPmycRab7(G18E), but not overexpression of the TgRab7(wt) in *T.gondii* tachyzoites is reducing the ability of the parasites to invade host cells.

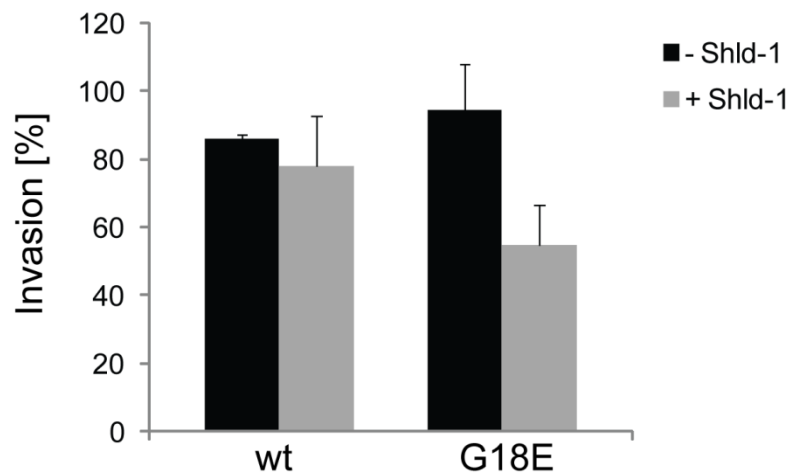


**Figure 4-10. Parasites expressing the constitutively active version of TgRab7 showed a reduced invasion ability.** Invasion assay of RH<sup>hxgprt</sup> parasites and parasites expressing ddfKBPmycRab7(wt) or ddfKBPmycRab7(G18E) treated for 24 hours with (+) and without (-) 1 $\mu$ M Shld-1, scratched and inoculated on fresh HFF cells. Subsequently invasion was determined and normalised with RH<sup>hxgprt</sup> parasites. Mean values and the respective standard deviation of two independent experiments are presented.

#### 4.4.3.5. Analysis of secretory organelles

To investigate if the detected reduction of invasion is linked with secretory organelles and their proteins, IFAs were performed to check for exemplary localisation signals of microneme and rhoptry proteins. The procedure of this assay was conducted as for TgRab7(wt) within the overexpression screen part II (chapter 4.3.). The results are displayed in Figure 4-11. Compared with the localisation signal in RH parasites, microneme proteins MIC3 and MIC2 and rhoptry proteins ROP2-4 showed their normal apical localisation signal.

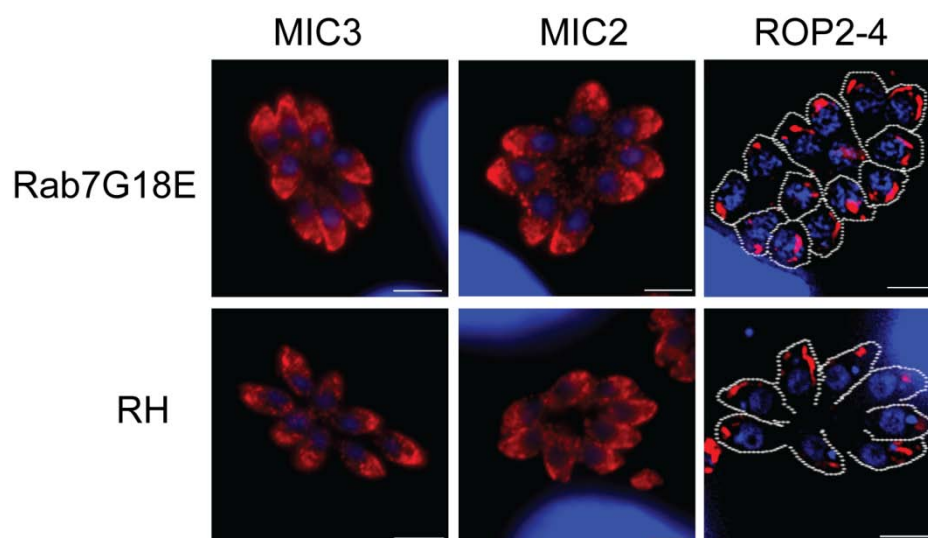


**Figure 4-11: Expression of the constitutively active version of TgRab7 was not affecting micronemes or rhoptries.** Immunofluorescence analysis of intracellular parasites expressing ddFKBPmycRab7(G18E) and RH<sup>hxgprt</sup> parasites treated for 24hours with 1 $\mu$ M Shld-1 and probed with  $\alpha$ -MIC3,  $\alpha$ -MIC2 or  $\alpha$ -ROP2-4 antibody (red) and Dapi (blue). The dashed line in the ROP2-4 images is indicating the parasites surface within the vacuole (performed from differential interference contrast (DIC) images merged with the fluorescence image of the same vacuole and outlined in Photoshop CS4). The scale bars represent 5 $\mu$ m. The images were taken with the Delta Vision Core System.

#### 4.4.3.6. Analysis of ELCs

In collaboration with the group of Vern Carruthers, additional analyses of the parasite strain ddFKBPmycRab7(G18E) were performed. They could confirm our investigations regarding the regulation, plaque assays and secretory organelles/proteins. Since this group has a special interest in ELCs and established assays to analyse protein processing in the ELCs, they had a closer look on the localisation pattern of ELC proteins TgCPL and TgVP1 in parasites expressing the constitutively active TgRab7 mutant compared to RH<sup>hxgprt</sup>

parasites. They also inoculated HFF monolayers with the respective parasite strain and incubated it with Shld-1 for 24 hours. After that they fixed the cells and performed IFAs with antibodies for microneme proteins ( $\alpha$ -MIC3 and  $\alpha$ -M2AP), and for proteins of ELCs ( $\alpha$ -TgCPL and  $\alpha$ -TgVP1). Their results are displayed in Figure 4-12. They showed that the microneme proteins MIC3 and M2AP are not affected by the expression of ddFKBpmycRab7(G18E). Also the endosomal-like compartment TgVP1 exhibits no difference in localisation pattern compared to RH<sup>hxgprt</sup> parasites. For TgCPL a more concentrated signal was detected in ddFKBpmycRab7(G18E) parasites treated with Shld-1 compared to untreated parasites.

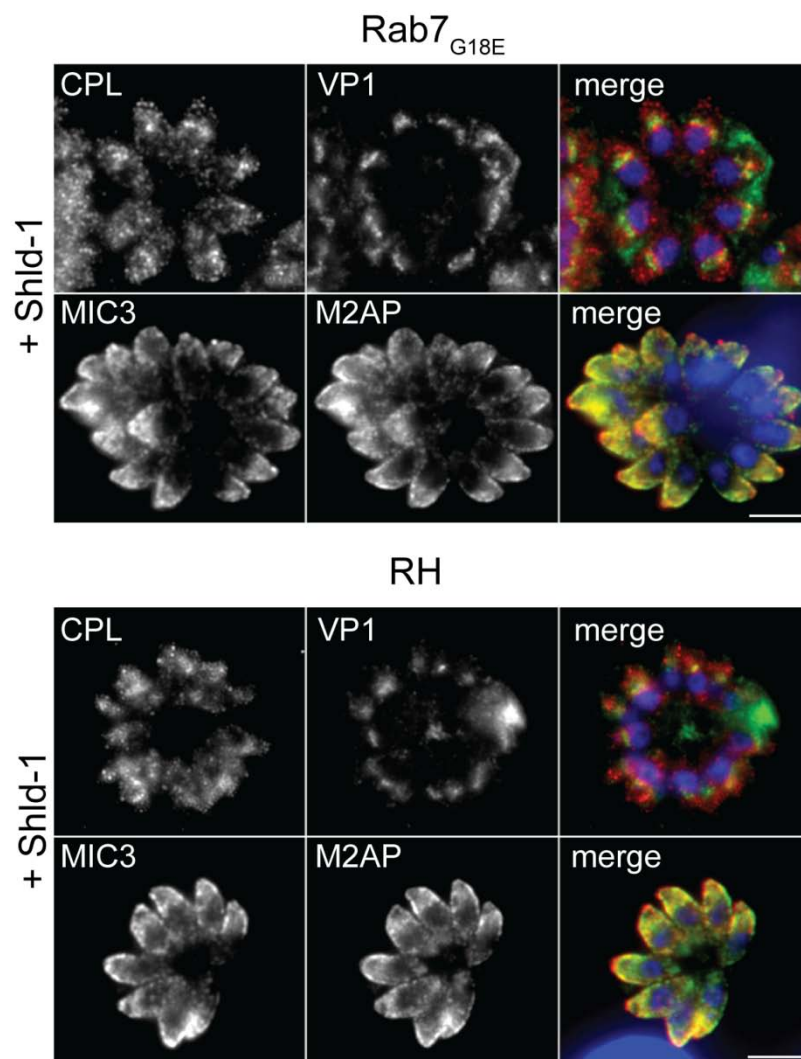


**Figure 4-12: Expression of ddFKBpmycRab7(G18E) led to a small effect on CPL localisation.** Immunofluorescence analysis of micronemes (MIC3, M2AP) and ELCs (CPL, VP1) in RH<sup>hxgprt</sup> and ddFKBpmycRab7(G18E) expressing parasites using indicated antibodies. Parasites were grown in 1  $\mu$ M Shld-1 for 24hours. Dapi is shown in blue. The scale bars represent 5 $\mu$ m. Assays were performed and images were taken by Halley Flammer. The images were taken from (Kremer, Kamin et al. 2013).

To assess, if the maturation of CPL is affected by the expression of constitutively active TgRab7, pulse-chase experiments followed by immunoprecipitation were also conducted by Vern Carruthers' group. Here ddFKBPmycRab7(G18E) and RH<sup>hxgprt</sup> parasites were grown for 24 hours with and without 1 $\mu$ M ShId-1 under normal growth conditions. Immediately prior to labelling the normal growth medium was exchanged with methionine and cysteine free DMEM. By adding <sup>35</sup>S-methionine and cysteine to the medium and incubating for 15 minutes under normal growth conditions, dividing parasites were metabolically labelled. Every protein synthesised during this time will insert these two radiolabelled amino acids. Afterwards the parasites were treated again with normal growth medium, incubated under normal growth conditions and fixed after different time points. This period is the so called "chasing" period. During that time all synthesised proteins are not labelled anymore and the maturation of labelled proteins can be analysed by immunoprecipitation followed by SDS-PAGE. The infected monolayers were washed twice with prewarmed DMEM growth medium and chased in growth medium for 0, 20, 40 and 60 minutes. After that the monolayers were washed with PBS to stop the process and intracellular parasites were extracted from host cells. Afterwards CPL was segregated from other proteins by immunoprecipitation using  $\alpha$ -CPL. The resulting immunoprecipitation was run on a SDS-PAGE, incubated in a fluorographic enhancer, dried in cellophane and exposed on X-ray films for 4 days. Two CPL bands were detectable, one presenting the processed CPL and the other one the immature unprocessed CPL. Signals of processed CPL of two independent experiments, where quantified and results are displayed in Figure 4-13. No significant differences in the amount of processed CPL could be detected at each time point either between RH and G18E or between parasites treated with and without ShId-1 prior to labelling.

In summary, one can say, that the slight effect on the CPL localisation signal in ddFKBPmycRab7(G18E) expressing parasites, seen in Figure 4-12, is not due to affected CPL maturation.

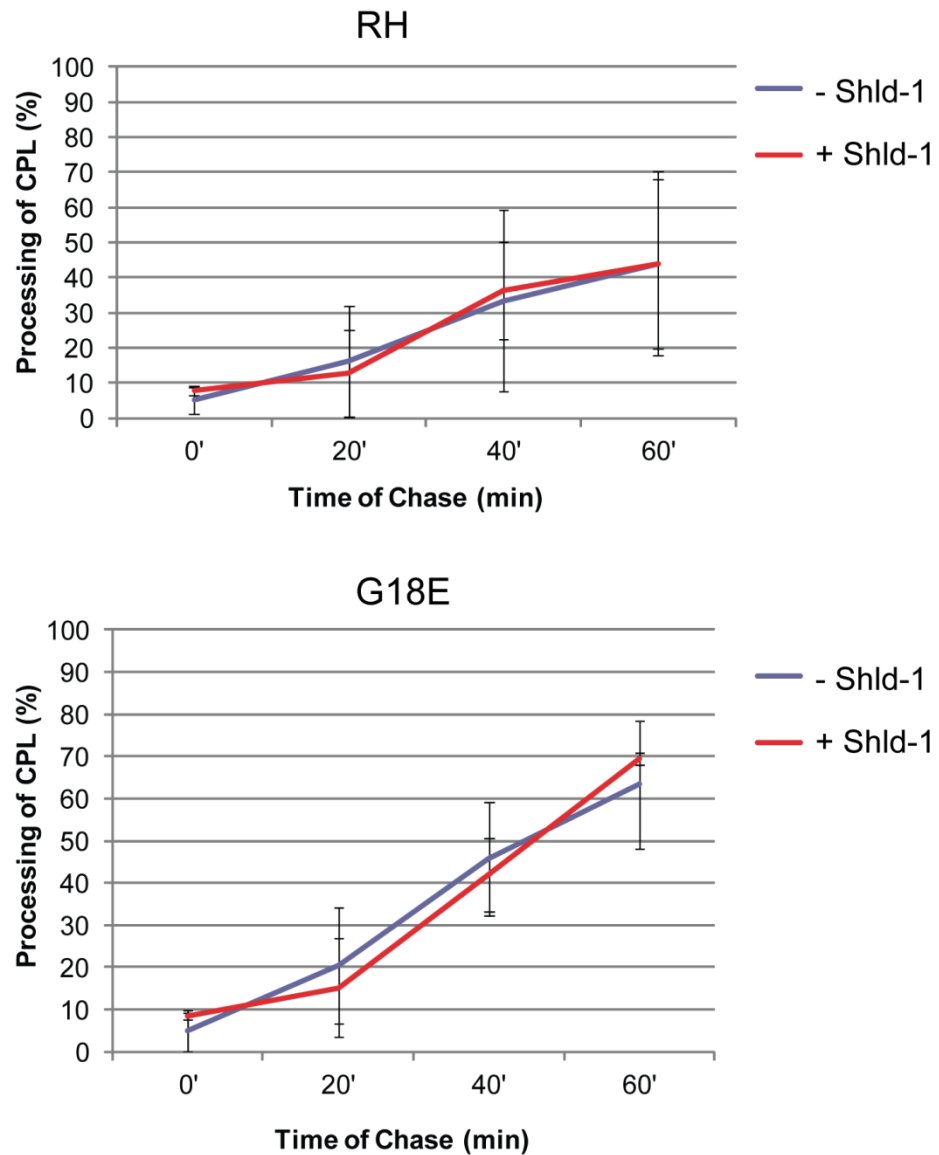


**Figure 4-13: CPL processing is unaffected in *ddFKBPmycRab7(G18E)* expressing parasites.** Quantification of pulse metabolically labelled *RH<sup>hxgprt-</sup>* and *ddFKBPmycRab7(G18E)* expressing parasites treated 24 hours with (+) and without (-) 1 $\mu$ M Shld-1 prior to labelling. After labelling parasites of the respective strain were either kept on ice (0') or chased with unlabelled methionine and cysteine containing medium for 20, 40 and 60 minutes. Signals of processed CPL were quantified after immunoprecipitation, SDS-PAGE and autoradiography. Mean values and the respective standard deviation of two independent experiments are presented. Experiments and analysis was performed by Halley Flammer.

#### **4.4.4 Characterisation of dominant negative TgRab5B**

While overexpression of TgRab5B had no effects on MIC3, MIC2 and ROP2-4, due to its post-Golgi localisation (Figure 3-8) and its potential to be an alveolate specific Rab protein (see 1.6.), TgRab5B was characterised in more detail. As described in the beginning of this chapter (4.4.) a clonal parasite strain expressing the dominant negative version of TgRab5B [ddFKBPmycRab5B(N152I)] was generated. As expected the dominant negative TgRab5B had the typical GDP-locked cytosolic localisation pattern, which was detectable in IFAs with  $\alpha$ -myc shown in Figure 4-14. To test if the expression of ddFKBPmycRab5B(N152I) is regulatable with the ddFKBP system, a western blot and IFA were performed as described for the wild type TgRab5B (see chapter 3.5.) The results are displayed in Figure 4-14. Detection of ddFKBPmycRab5B(N152I) occurred via  $\alpha$ -ddFKBP (western blot) and  $\alpha$ -myc (IFA) antibodies. A faint signal could be detected in absence of Shld-1, but compared to that a clear upregulation of the ddFKBPRab5B(N152I) fusion protein was apparent in presence of Shld-1 (Figure 4-14A). According to this, a regulation of the dominant negative Rab5B version with the ddFKBP system could be confirmed to continue with its further analysis.

##### **4.4.4.1. Growth analysis**

To test if expression of the dominant negative TgRab5B is affecting the infectivity of tachyzoites, growth analysis was conducted. The procedure of the plaque assay was the same as described for wild type TgRab5B (see chapter 4.2.). Compared with the effect on plaque formations in host cell monolayers infected with RH<sup>hxgprt</sup>- parasites, parasites expressing the dominant negative version of TgRab5B, incubated for 5 days with Shld-1, a clear effect on plaque formation could be observed (Figure 4-14B). Parasites having the dominant negative TgRab5B version upregulated showed significantly smaller plaques than parasites of the same strain without Shld-1 or RH<sup>hxgprt</sup>- parasites. The observation, that interference with the TgRab5B pathway is affecting the infectivity of *T.gondii* tachyzoites could be confirmed accordingly.

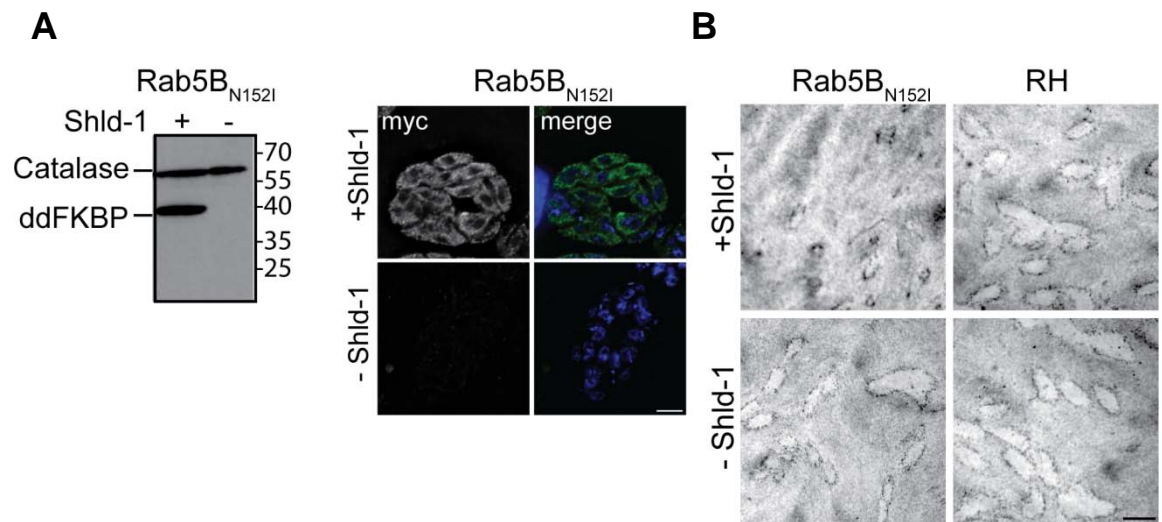


**Figure 4-14: Parasites expressing ddFKBpmycRab5B(N152I) showed a defect in their growth ability.** (A) Western blot (right panel) and immunofluorescence (left panel) analysis of ddFKBpmyc-Rab5B(N152I) expressing parasites. For the western blot freshly egressed parasites were treated for 4hours +/- 1 μM Shld-1 and for the immunofluorescence analysis intracellular parasites were treated for 18hours +/- 1 μM Shld-1. Indicated antibodies were used. Dapi is shown in blue. As an internal control for the western blot α-catalase antibodies were used. The scale bar represents 5 μm. (B) Growth analysis of the indicated parasite strains for 5 days in +/- 1 μM Shld-1. The scale bar represents 1 mm. The IFA images were taken with the Delta Vision Core System.

#### 4.4.4.2. Analysis of secretory organelles

To investigate if the decreased growth ability is directly linked with the transport of secretory proteins to their target organelles, immunofluorescence analysis was performed with the ddFKBPRab5B(N152I) strain. HFF monolayers were infected, incubated for 24 hours with (+) and without (-) Shld-1 and immunostained after fixation. Antibodies against dense granule, rhoptry and microneme proteins (microneme proteins: α-MIC2, co-stain with α-MIC3 and α-M2AP, dense granule protein: α-GRA9, rhoptry proteins: α-ROP2-4) were used exemplary to detect effects on those secretory proteins. The results are displayed in Figure 4-15. Comparing the localisation signals of the tested secretory proteins, no difference between the parasites treated with and without Shld-1 could be detected for the tested microneme, rhoptry or dense granule proteins.

In summary, expression of the dominant negative mutant of TgRab5B resulted in the same phenotype as seen for the wild type TgRab5. Parasites expressing ddFKBpmycRab5B(N152I) were nearly blocked in growth, but proteins of the

secretory proteins (MIC3, MIC2, M2AP, Rop2-4 and GRA9) remained unaffected over the tested time period.

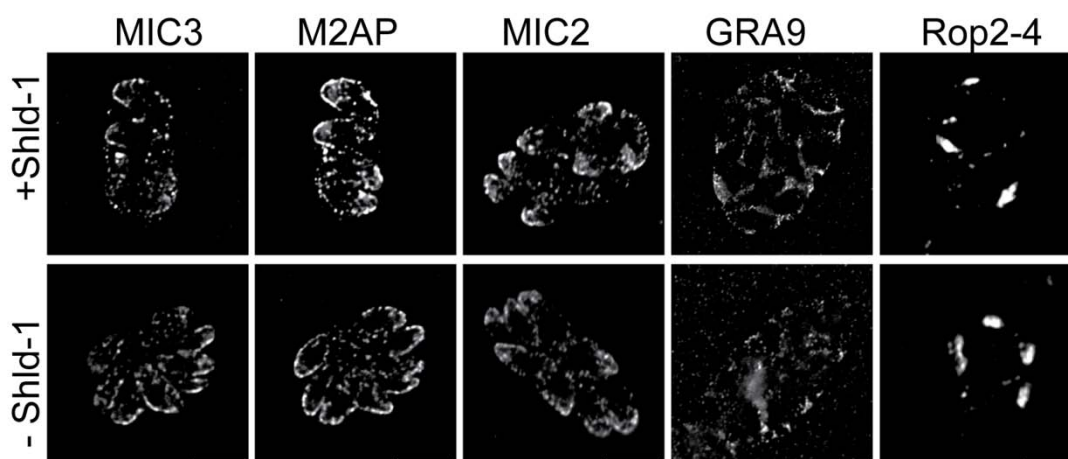


**Figure 4-15: Expression of dominant negative TgRab5B causes no mislocalisation of microneme and rhoptry proteins.** Immunofluorescence analysis of intracellular parasites expressing ddFKBPmycRab5B(N152I) treated for 24hours +/- 1  $\mu$ M Shld-1 and immunolabelled with the indicated antibodies. The scale bars represent 5  $\mu$ m. IFAs were performed by Joanne Heng. The Images were taken with the Axioscope 2 microscope.

## 4.5. Summary and Conclusions

Within this chapter further analyses were undertaken with the generated TgRab overexpressing strains described in chapter 3. Furthermore parasite strains expressing trans-dominant mutants of TgRab proteins being potentially involved in the late-secretory pathway were generated and analysed.

### 4.5.1. Overexpression screens

To investigate if the proliferation ability of the parasite strain is affected when the respective ddFKBP-tagged TgRab protein is stabilised in presence of 1  $\mu$ M Shield-1 (Herm-Gotz, Agop-Nersesian et al. 2007) it was started to perform growth analyses with these parasite strains. This showed that parasite growth was ablated for TgRab2,4 5A,5B and 5C (Figure 4-1). TgRab1A and TgRab1B displayed a severe growth defect, while in contrast for TgRab7 and TgRab18 no significant differences in parasite growth were detected (Figure 4-1).

In order to identify TgRab proteins that play a crucial role in vesicular transport to the apicomplexan-specific secretory organelles, parasites overexpressing TgRab2,4,5A,5B and 5C were grown for 24 hours in presence of ShId-1 and analysed for the location of their microneme proteins MIC2 and MIC3 and of their rhoptry proteins ROP2,3 and 4 (Figure 4-2). In parasites overexpressing TgRab2, Rab4 and Rab5B, the tested secretory proteins showed normal localisation patterns. Overexpression of TgRab5A and 5C resulted in an aberrant localisation of rhoptry proteins and MIC3 in the lumen of the parasitophorous vacuole. This indicates that MIC3 and ROP2-4 have entered the constitutive secretory pathway in these parasites. Interestingly no similar defect in trafficking of MIC2 was detected, which displayed a normal microneme location in all lines (Figure 4-2). In conclusion, overexpression of TgRab5A and 5C results in a specific trafficking defect to rhoptries and micronemes and the different behaviour of MIC2 and MIC3 suggest that specific transport pathways exist for a subset of microneme proteins. Further analyses to investigate this were performed and presented in chapter 5.

As shown in chapter 3, the localisations of TgRab2 and TgRab4 were different to higher eukaryotes. Together with the observations, that growth was blocked (Figure 4-1), but secretory proteins were not affected due to overexpression of TgRab2 and TgRab4 (Figure 4-2) these Rab proteins are not involved in vesicular transport to the micronemes or rhoptries and not further characterised within this work.

#### **4.5.2. Analysis of inducible parasite strains expressing trans-dominant Rab proteins**

All Rab proteins localised at the Golgi (TgRab4) or post-Golgi region (TgRab1A,5A,B,C and 7) were further analysed by generating parasite strains expressing a dominant negative mutant of the respective Rab protein fused with the ddfKBP domain (4.4.1.).

**Rab4:** Since TgRab4 showed a new localisation (at the Golgi) compared with other higher eukaryotes and is not conserved in *Plasmodium* (Table 3-1) it is an interesting candidate to study. Analyses with parasites expressing the wild type or dominant negative version of TgRab4 were performed under my supervision by Sabine Mahler. The results of her work are not presented in this thesis but in her

diploma thesis. In summary, she could not detect any phenotype for parasites expressing the dominant negative version of TgRab4, but parasites overexpressing TgRab4 showed a tendency of decreased invasion and replication ability. No effect on egress could be detected, when a calcium ionophore was used to induce the egress. Parasites expressing ddFKBPmycRab4 incubated with ShId-1 for 48 hours or longer showed normal localisation signals for secretory proteins, but a decreased ability to egress their host cells naturally. These results indicate that TgRab4 is not directly involved in regulated secretory trafficking. A functional role of TgRab4 in endocytosis as seen in higher eukaryotes (van der Sluijs, Hull et al. 1992) could also be an explanation, but needs to be further investigated.

**Rab1A:** Since no proliferation defect was detected for parasites expressing the dominant negative version of TgRab1A (Figure 4-4), no further analysis were performed with this mutant. To investigate the interesting and unclear function of this Rab protein other mutants need to be generated or better KO studies could be applied.

**Rab7:** Besides parasites expressing the dominant negative version of TgRab7 (N124I), parasites expressing a constitutively active version of TgRab7 (G18E) (4.4.3.) were generated to analyse TgRab7 function. While expression of ddFKBPmycRab7(N124I) did not affect parasite proliferation, expression of ddFKBPmycRab7(G18E) blocked growth (Figure 4-7). It should be noted that the destabilised (treated without ShId-1) constitutively active mutant did not form as big plaques as parasites destabilising the dominant negative or wild type (wt) version of TgRab7. This could be explained by a higher background expression for ddFKBPmycRab7(G18E) detected in IFAs and western blots (Figure 4-5). Replication assays with parasites expressing ddFKBPmycRab7(wt) and ddFKBPmycRab7(G18E) revealed a late effect on the replication ability of parasites expressing the constitutively active TgRab7 (Figure 4-8). It should be also noted that more parasitophorous vacuoles having 8 or 16 parasites were detected for parasites stabilising the ddFKBPmycTgRab7(G18E) fusion protein than parasites where it was degraded. This could mean that the presence of additional constitutively active TgRab7 is positively affecting intracellular replication. After that this effect is maybe turning into the opposite, because no PVs bigger than 16 parasites could be observed, which could mean that the

parasites die after four rounds of replication. To analyse this observation, more replication assays need to be performed under the presented conditions to confirm the results and their statistical significance. In summary, one can say that replication is not directly affected by overexpression of the wild type or expression of a dominant negative or constitutively active mutant of TgRab7. To analyse a direct role in invasion and egress, the respective assays were performed. No effect on induced egress (Figure 4-9), but a reduction by nearly 50% of invasion ability could be detected for parasites expressing ddFKBpmycRab7(G18E) (Figure 4-10). This invasion deficiency was apparently not linked to vesicle targeting to secretory organelles, since markers tested, M2AP (Figure 4-12), MIC2, MIC3, Rop2-4 (Figure 4-11) showed a normal localisation in parasites expressing TgRab7(G18E). Also tested markers for ELCs like proM2AP (Figure 4-6) and TgVP1 (Figure 4-12) showed no significant effect. A slight change of the localisation pattern for TgCPL was detected when parasites were expressing the constitutively active version of TgRab7. Here TgCPL appeared more concentrated (Figure 4-12). If this observation is statistically significant, it needs to be further analysed. However, no effect on TgCPL maturation could be detected when pulse chase experiments were performed with parasites expressing TgRab7(G18E) (Figure 4-13). This indicates that if TgRab7 is playing a role in host cell invasion, it is not due to its direct effect on vesicular trafficking to the secretory organelles or to the ELCs, proM2AP, TgVP1 and TgCPL. Since no other markers for the ELCs were available, it was not possible to define the precise trafficking step regulated by TgRab7 during the asexual life cycle of *T.gondii*.

**Rab5B:** TgRab5B could be localised at ELCs (Figure 3-8C) and may play a regulatory role in the secretory traffic of *T.gondii*. A clear growth defect was detected in parasites overexpressing TgRab5B (Figure 4-1), but the localisation of tested microneme and rhoptry proteins was unaffected (Figure 4-2). Performance of growth analyses with the dominant negative version of TgRab5B, ddFKBpmycRab5B(N124I), revealed a similar phenotype. Here, parasite proliferation was almost blocked (Figure 4-14) and no effect on the location of analysed microneme and rhoptry proteins (MIC2, M2AP, MIC3 and ROP2-4) could be detected (Figure 4-15). This indicates that Rab5B does not have a direct function in the secretory traffic of microneme and rhoptry proteins.

## 5. Characterisation of TgRab5A and TgRab5C

### 5.1. Introduction

As shown above, only overexpression of TgRab5A or 5C showed an effect on the localisation of some secretory proteins (Figure 4-1 and 4-2). Within this chapter further characterisation studies are presented to analyse the role of TgRab5A and TgRab5C in the regulated secretory pathway. Therefore parasites expressing the dominant negative versions, TgRab5A(N158I), TgRab5C(N153I), and parasites overexpressing TgRab5A and 5C were analysed for their replication, invasion and egress ability. Also the effects on microneme and rhoptry proteins were further characterised. Within IFAs and electron microscopy it was also analysed if the secretory organelles and other organelles within the affected parasites exhibited structural/ biosynthetic differences.

### 5.2. Inducibility and proliferation ability of parasites expressing dominant negative TgRab5A and TgRab5C

Dominant negative mutants [TgRab5A(N158I), TgRab5C(N153I)] were generated as described in chapter 4.4.1.. To test, if the expression of TgRab5A(N158I) and TgRab5C(N153I) was regulatable with the ddFKBP system, western blots and IFAs were performed as described for wild type TgRab5A and 5C (see chapter 3.5.). The results are displayed in Figure 5-1. Detection of ddFKBPMycRab5A(N158I) and ddFKBPMycRab5C(N153I) occurred via  $\alpha$ -ddFKBP (western blot) and  $\alpha$ -myc (IFA) antibodies. Some background expression could be detected on IFA level in absence of Shld-1. A high upregulation of the fusion protein was apparent in presence of Shld-1 seen by the strong cytosolic signal of  $\alpha$ -ddFKBP in Figure 5-1. Within the western blot it is clearly detectable, that with Shld-1 the fusion protein is stabilised (upregulated) and degraded in absence of Shld-1.

According to this, the regulation of the dominant negative TgRab5A or TgRab5C version with the ddFKBP system could be confirmed to continue with further analyses.

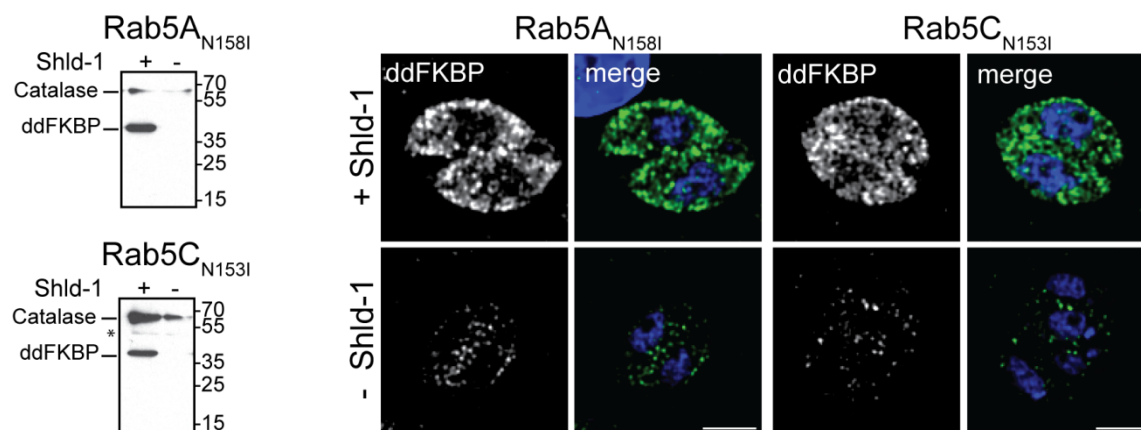


**Figure 5-1: The presence of ddFKBPMycRab5A(N158I) or ddFKBPMycRab5C(N153I) within *T.gondii* tachyzoites is regulable.** Western blot (left panel) and IFA (right panel) of parasites expressing dominant negative versions of ddFKBPMycRab5A(N158I) or ddFKBPMycRab5C(N153I). For the western blot freshly egressed parasites were treated for 4hours in presence (+), or absence (-) of 1  $\mu$ M Shld-1 and for the IFA intracellular parasites were treated for 18hours +/- 1  $\mu$ M Shld-1. The respective, mutated Rab protein was detected by  $\alpha$ -ddFKBP antibodies (in IFA:green). As an internal control for the western blot  $\alpha$ -catalase antibodies were used. Dapi is shown in blue. The scale bars represent 5  $\mu$ m. The images were taken with the Nikon TE2000 inverted microscope.

### 5.2.1. Growth analysis

As a first step to analyse the phenotype of parasites expressing the dominant negative mutants, the ability to proliferate was determined. This was performed within plaque assays, conducted as described for wild type TgRab5A and 5C (see chapter 4.2.). A clear difference in the ability of plaque formation could be observed when HFF cells were inoculated with parasites expressing the ddFKBPMycRab5A(N158I) or ddFKBPMycRab5C(N153I) construct and were treated either with or without Shld-1 for 6 days. Compared with the growth ability of RH<sup>hxp<sub>prt</sub>-</sup> parasites or the untreated (-) strains, parasites expressing the dominant negative version of TgRab5A or 5C showed a severe effect on plaque formation. Parasites expressing ddFKBPMycRab5A(N158I) exhibited a complete block of growth in presence of Shld-1. Whereas ddFKBPMycRab5C(N153I) expressing parasites showed a clear growth defect with the ability to form few small plaques (Figure 5-2).

In summary, decreased growth ability to the point of growth defect could be detected for parasites expressing the dominant negative version of TgRab5A or

5C. This correlates with the results seen in plaque assays of parasites overexpressing TgRab5A or 5C (Figure 4-1).

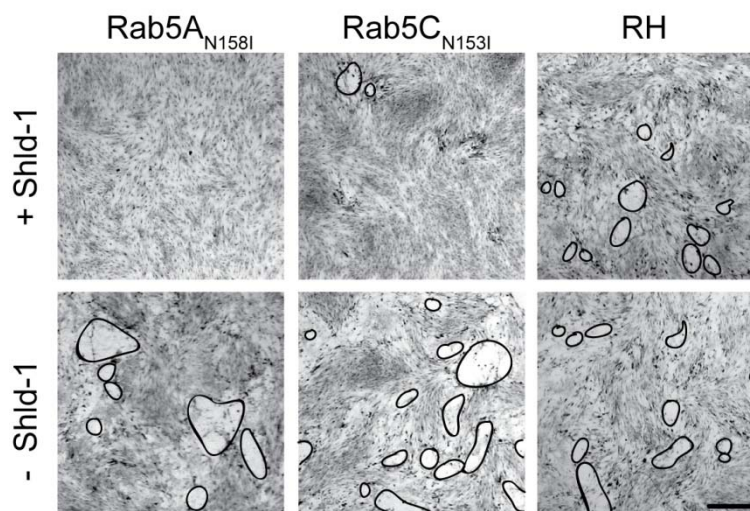


**Figure 5-2 : Expression of ddFKBPmycRab5A(N158I) and ddFKBPmycRab5C(N153I) results in a severe growth phenotype.** Plaque assay with RH parasites and parasites expressing ddFKBPmycRab5A(N158I) or ddFKBPmycRab5A(N153I) were inoculated on HFF cells and incubated for 5-6 days +/- 1 $\mu$ M Shld-1. Single plaques are indicated by black edging (bordered with ImageJ). The scale bar represents 1 mm. Images were taken from (Kremer, Kamin et al. 2013).

### 5.3. Phenotypic characterisation of parasites expressing ddFKBPmycRab5A(wt), 5C(wt), 5A(N158I) and 5C(N153I)

Both overexpression and expression of the dominant negative version of TgRab5A and 5C resulted in a significant growth defect of *T.gondii* tachyzoites. To investigate if this was due to effects on replication, invasion or egress and finally due to affected secretory organelles or their proteins, all four parasites strains were further analysed.

#### 5.3.1. Replication

To investigate if the disability to run through three to four replication cycles is causing the growth phenotype seen in Figure 5-2, replication assays were performed. Confluent HFF monolayers were inoculated with parasites expressing ddFKBPmycRab5A, 5C, 5A(N158I) or 5C(N153I) and incubated with or without Shld-1 for 24 hours. After fixation, IFAs were performed to detect single parasites and vacuoles under a fluorescent microscope. The number of parasites per vacuole was counted for 100 to 150 vacuoles for each assay. Figure 5-3

displays the results of 3 independent experiments. If overexpression or expression of the dominant negative version of TgRab5A or C has an impact on replication, formation of daughter parasites would be affected. This would mean that less parasites per vacuole would be detectable compared to RH<sup>hxgprt</sup>-parasites. For ddFKBPmycRab5A and C as well as for ddFKBPmycRab5A(N158I) and Rab5C(N153I), there was no significant difference in the formation of vacuoles containing one, two, four, eight or sixteen parasites in presence (+) or absence (-) of 1 $\mu$ M Shld-1 compared with RH<sup>hxgprt</sup>- parasites (Figure 5-3).

In summary, neither overexpression of TgRab5A, 5C or expression of their dominant negative version had an direct effect on the proliferation ability of *T.gondii* tachyzoites.

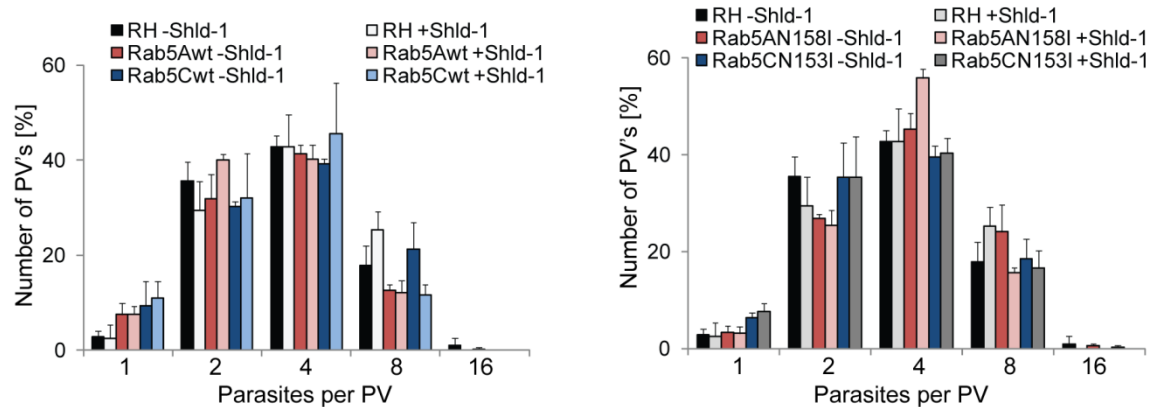


**Figure 5-3 : No significant differences in replication were detected when parasites expressing ddFKBPmycRab5A(wt),5C(wt),5A(N158I) and 5C(N153I) were analysed.** Replication assay of indicated parasites grown for 24hours in presence (+) or absence (-) of 1 $\mu$ M Shld-1 prior to fixation. Average number of parasites per parasitophorous vacuole (PV) was determined. Mean values and the respective standard deviation of three independent experiments are presented. The images were taken from (Kremer, Kamin et al. 2013).

### 5.3.2. Egress

After it was observed that intracellular replication was not directly affected in the four analysed parasite strains, egress abilities were further investigated. Egress assays were performed as described for TgRab7 (see chapter 4.4.3.3.). Confluent HFF monolayers were infected with an equal amount of RH<sup>hxgprt</sup>-parasites and parasites expressing ddFKBPmycRab5A or C or ddFKBPmycRab5A(158I) or Rab5C(153I). After an incubation time of 36 hours with and without Shld-1, a Calcium ionophore (A 23187; 1 $\mu$ M) was added to the

medium 5-10 minutes prior fixation. After fixation, IFAs were performed to enable counting of lysed and intact vacuoles under a fluorescence microscope with 100x magnification. 10 fields of view were counted per parasite strain induced or uninduced with Shld-1 and the results were normalised with RH<sup>hxgprt</sup>-. For all four parasites strains, normal (100%) egress ability could be detected in absence of Shld-1. If overexpression or expression of dominant negative TgRab5A or 5C became stabilized by adding Shld-1, the egress ability was decreased by over 50%.

Both overexpression of wild type and expression of dominant negative ddFKBpmycRab5A or C caused a significant reduction in egress ability compared to RH<sup>hxgprt</sup>- parasites.

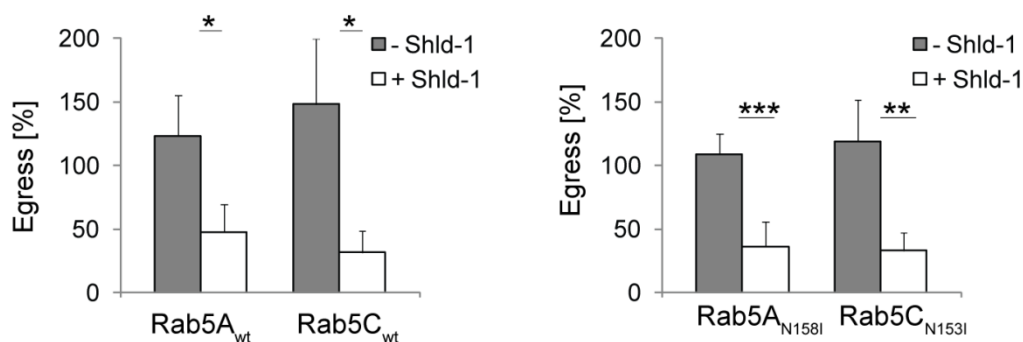


**Figure 5-4 : Both overexpression and dominant negative expression of TgRab5A and TgRab5C led to a decrease in the egress ability.** Egress assay of RH<sup>hxgprt</sup>- parasites, ddFKBpmycRab5A, ddFKBpmycRab5C, ddFKBpmycRab5A(158I) and ddFKBpmycRab5C(N153I) expressing parasites grown for 36hours +/- 1  $\mu$ M Shld-1 before egress was triggered with A23187. Host cell lysis was determined 8 min after induction of egress and normalised with RH<sup>hxgprt</sup>- parasites. Mean values and the respective standard deviation of three independent experiments are presented (\*\*\*)indicates p-value of  $P \leq 0.01$ , \*\*indicates  $P \leq 0.02$  and \*indicates  $P \leq 0.07$  in a two tailed Student's test). The images were taken from (Kremer, Kamin et al. 2013).

### 5.3.3. Invasion

To investigate if the decreased egress ability is the sole cause of the growth defects, or if the invasion ability contributes to it as well, it was continued with invasion assays. Therefore "Red/Green invasion" assays (Huynh, Rabenau et al. 2003) were performed for ddFKBpmycRab5A, 5C, 5A(N158I) and 5C(N153I) expressing parasites and RH<sup>hxgprt</sup>- parasites. Parasites were grown on HFF cells and treated with and without Shld-1 for 12 or 24 hours. Intracellular parasites were extracted from host cells by scratching and passage three times through a 0.7mm needle. HFF monolayers growing on glass cover slips on "24 well plate"

wells were infected with an equal amount of the resulting fresh extracellular parasites. The parasites were allowed to invade host cells under normal growth conditions for 1-2 hours prior to fixation. Immunofluorescence without the permeabilisation step was performed for extracellular parasites using  $\alpha$ -Sag1-  $\alpha$ -mouse Alexa Fluor 594 antibody combination. For intracellular a second standard immunofluorescence was performed with permeabilisation and with  $\alpha$ -IMC- $\alpha$ -rabbit Alexa Fluor 488 antibody combination.  $\alpha$ -SAG1 binds to the outer surface of the parasite and does not require a permeabilisation step. Whereas  $\alpha$ -IMC binds to the inner membrane complex (IMC) of the parasite and for this reason requires permeabilisation. Consequently extracellular parasites (stained with  $\alpha$ -Sag-1 and  $\alpha$ -IMC) appeared yellow and intracellular parasites (only stained with  $\alpha$ -IMC) appeared green under the fluorescent microscope. This enabled counting of intra- and extracellular parasites separately for each parasite strain in presence and absence of ShId-1. The ratios of yellow versus green fluorescent parasites were calculated and normalised with RH<sup>hxgprt-</sup> parasites. The results are displayed in Figure 5-5. Compared to RH (100%) all parasite strains showed a normal invasion ability, when they were grown without ShId-1 prior to invasion. Except for ddFKBPmycRab5C(N153I) expressing parasites, an invasion rate of nearly 100% could be detected. For ddFKBPmycRab5C(N153I) expressing parasites a slight reduction by 10% could be detected in the assays where the parasites were pre-treated without ShId-1 for 12 hours. This tendency couldn't be observed for parasites incubated for 24 hours without ShId-1. All overexpressing and dominant negative expressing TgRab5A and TgRab5C parasite strains showed an invasion reduction by 60-50% within the invasion assays after 12 hours pre-treatment with ShId-1. ShId-1 treatment of these parasite strains for 24 hours intensified this effect. All parasite strains showed a reduction of invasion by 90% when the ShId-1 incubation time was increased from 12 hours to 24 hours prior to invasion.

In summary, a severe decrease of host cell invasion could be observed for parasites overexpressing or expressing a dominant negative version of TgRab5A and TgRab5C. The longer TgRab5A or TgRab5C were overexpressed, or TgRab5A(N158I) or TgRab5C(N153I) were expressed in the parasites, the stronger the observed effect. After 24 hours, overexpression or expression of dominant negative TgRab5A or TgRab5C resulted nearly in a complete invasion block.

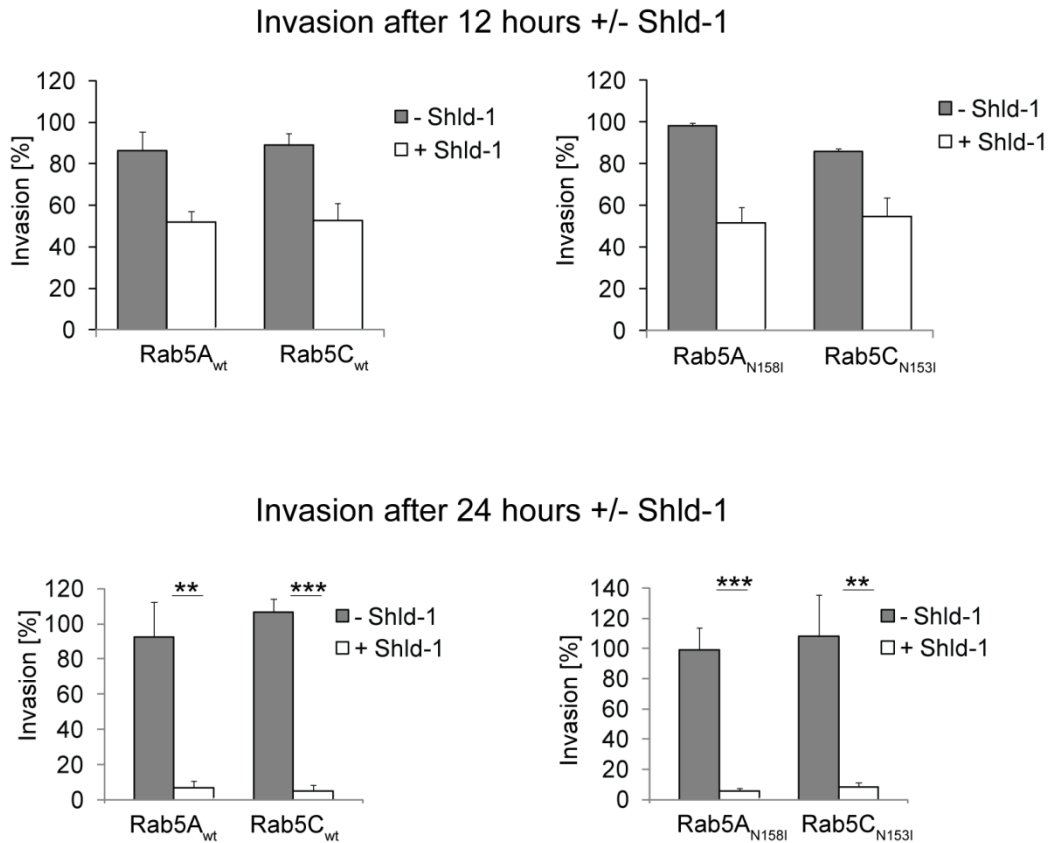


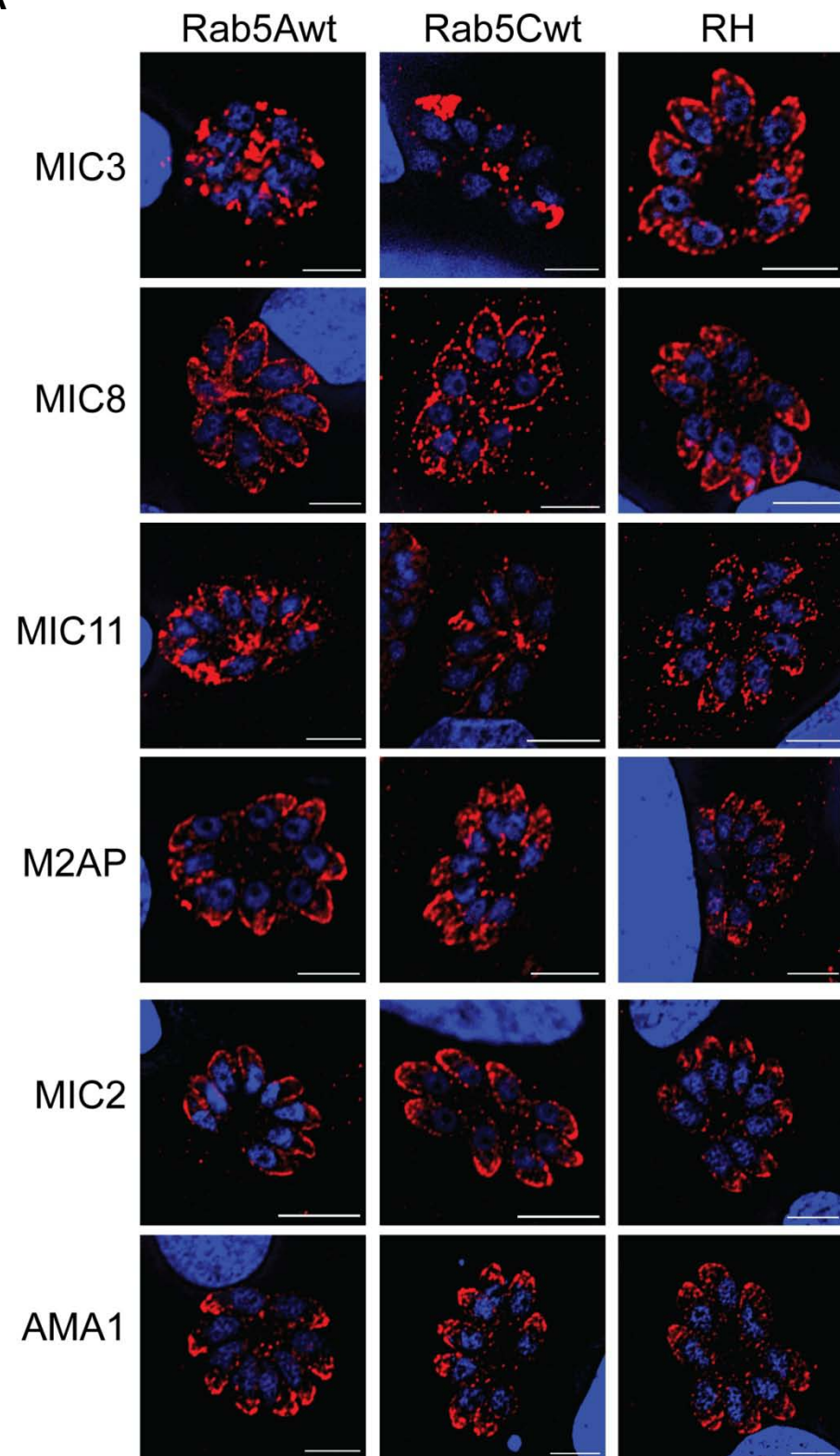
**Figure 5-5: Both overexpression and dominant negative expression of TgRab5A and TgRab5C led to a severe invasion defect.** A Red/Green-Invasion assay was performed with pre-treated (12 and 24 hours +/- 1uM Shld-1) extracellular parasites, which were allowed to invade HFF monolayer for 1- 2hours before fixation. In total 150 -250 parasites were counted. The ratios of intra- and extracellular were calculated for each parasite strain with (+) and without (-) Shld-1 and normalised with RH<sup>hxgprt-</sup> parasites. Mean values and the respective standard deviation of two independent 12 hours pre-treatment experiments and of three independent 24 hours pre-treatment experiments are presented (\*\*\*)indicates p-value of  $P \leq 0.01$  and \*\*indicates  $P \leq 0.02$  in a two tailed Student's test). The images were taken from (Kremer, Kamin et al. 2013).

### 5.3.4. Analysis of secretory organelles

#### 5.3.4.1. Microneme proteins

After it could be shown that both overexpression of ddFKBPmycRab5A or 5C and expression of their dominant negative versions led to decreased egress ability and nearly an invasion block, the question appears if the expression of the mutants also affects the localisation of only a subset of microneme proteins as observed for the overexpressing parasites (Figure 4-2). Therefore immunofluorescence analysis of intracellular parasites expressing ddFKBPmycRab5A or ddFKBPmycRab5C and ddFKBPmycRab5A(N158I) or

ddFKBPmycRab5C(N153I), treated for 24 hours with Shld-1, were performed. Antibodies against different microneme proteins ( $\alpha$ -MIC3,  $\alpha$ -MIC8,  $\alpha$ -MIC11,  $\alpha$ -M2AP,  $\alpha$ -MIC2 and  $\alpha$ -AMA1) were employed. The results for both overexpressing and dominant negative expressing TgRab5A and TgRab5C parasites are displayed in Figure 5-6. For all microneme proteins, the normal apical localisation signal was detected within RH<sup>hxgprt</sup>- parasites. Confirming the observation made in chapter 4.3., a normal localisation signal for MIC2 was observed, whereas MIC3 was mislocalised in parasites overexpressing TgRab5A and TgRab5C (Figure 4-2; Figure 5-6). This could also be detected for parasites expressing the dominant negative version of TgRab5A or TgRab5C (Figure 5-6). In all four parasite strains the  $\alpha$ -MIC3 signal was not at the apical tip of the parasites, but in the parasitophorous vacuole (PV). Additionally, shown in Figure 5-6 and observed within this assay were mislocalisations of MIC8 and MIC11 and normal localisation signals for M2AP and AMA1 for all tested TgRab5A and TgRab5C parasite strains. Here MIC8, which is a trans-membrane protein, was detected at the entire membrane of every single parasite within one PV, instead of its normal apical localisation. MIC11, which is a soluble protein like MIC3, was mislocalised into the PV as observed for MIC3.

**A**

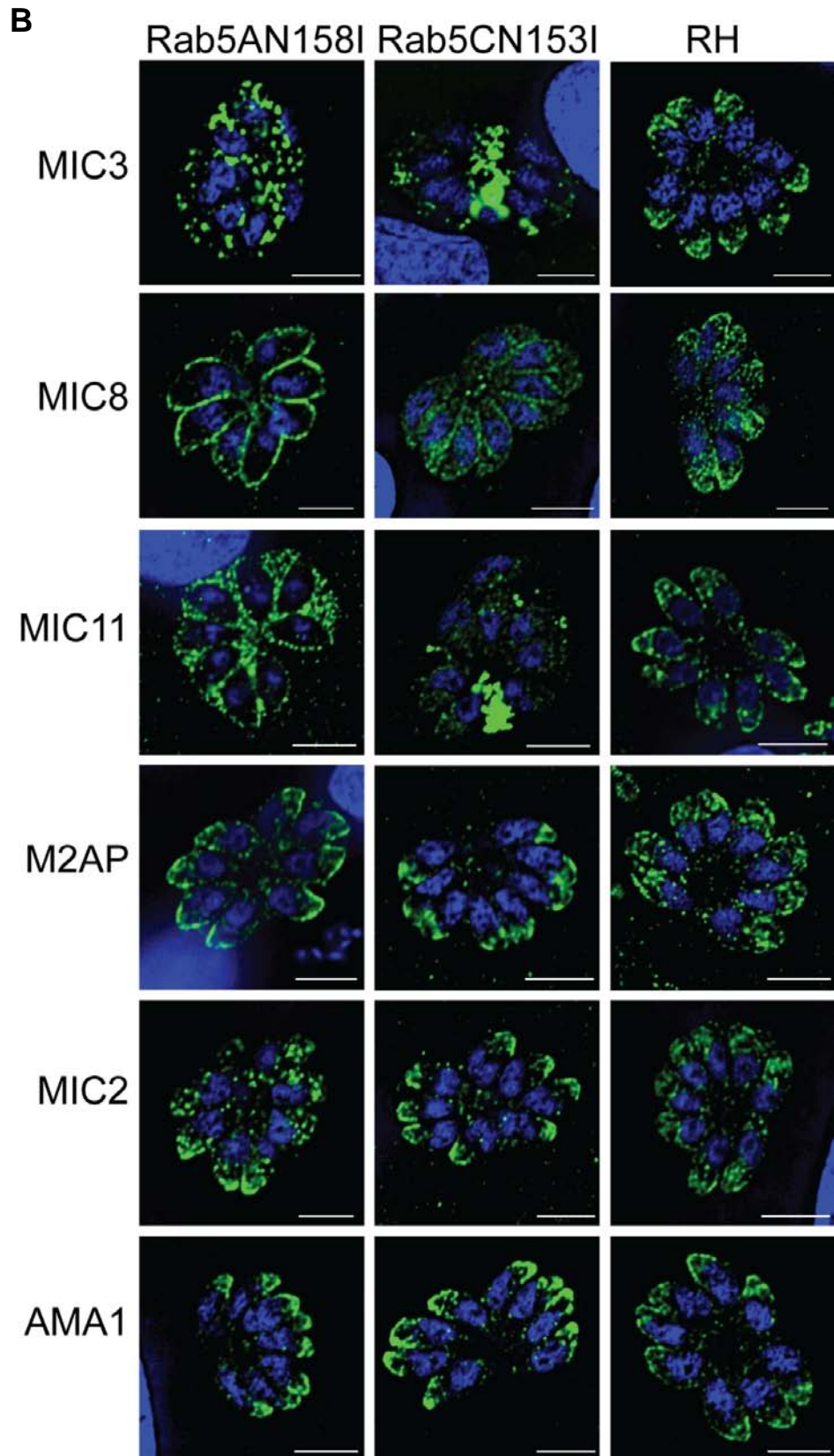


**Figure 5-6: Parasites overexpressing ddFKBpmycRab5A, ddFKBpmycRab5C, ddFKBpmycRab5A(N158I) or ddFKBpmycRab5C(N153I) led to mislocalisation of only a subset of microneme proteins (MIC3, MIC8 and MIC11).** IFAs of intracellular parasites stably expressing the indicated Rab protein version fused with ddFKBpmyc and RH<sup>hxgprt</sup> treated for 24hours with 1  $\mu$ M Shld-1 and probed with indicated microneme antibodies (left panel of each image series). For parasites overexpressing wild type (wt) Rab5A and 5C micronemal stain is shown in red (A) and parasites expressing the dominant negative versions micronemal stain is shown in green (B). Dapi is shown in blue. Scale bars represent 5 $\mu$ m. The images were taken with the Delta Vision Core System.

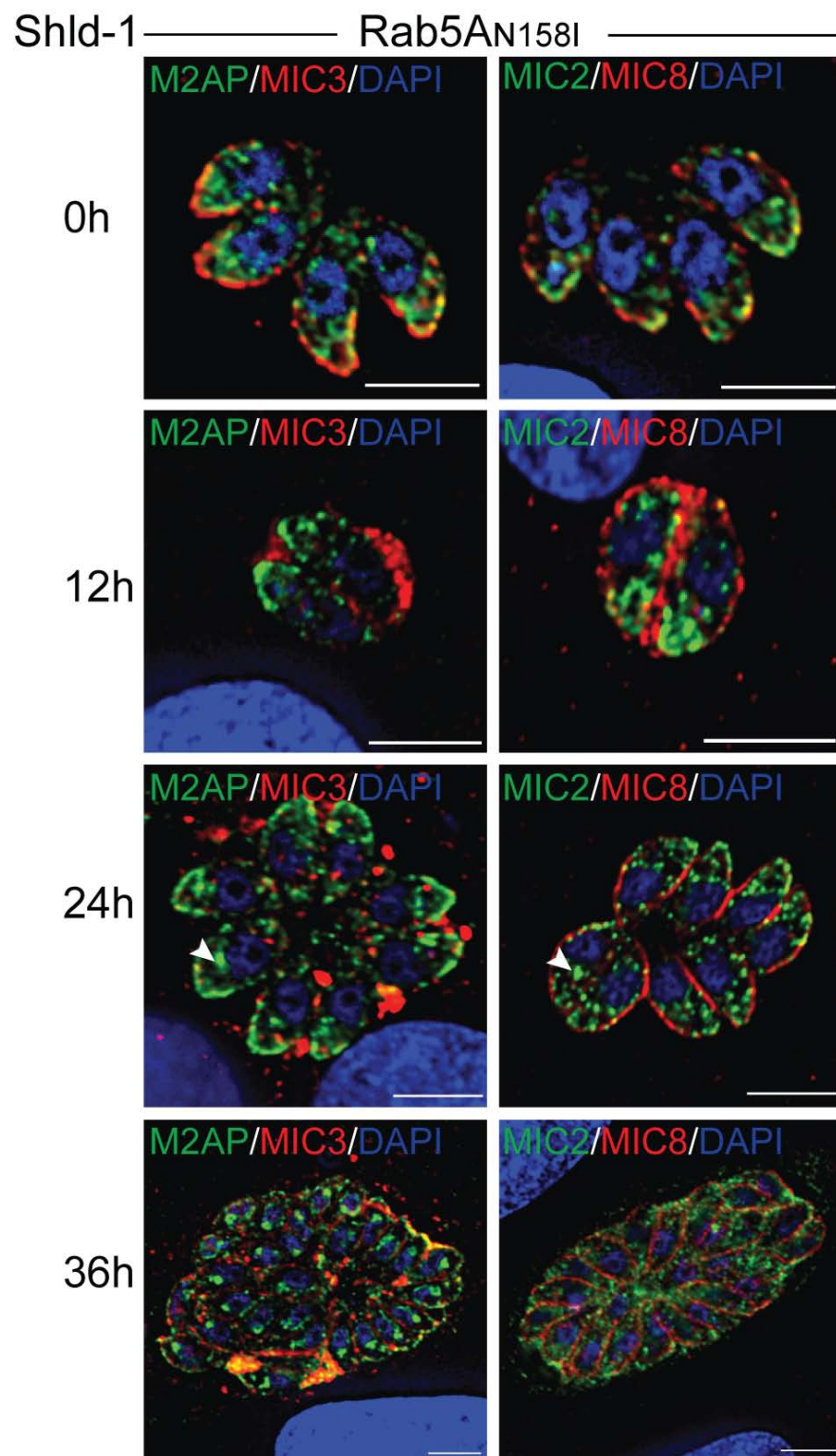
### 6.3.4.1. Time course of microneme protein localisation signals

The majority of parasites of all four TgRab5 strains showed a normal localisation pattern for the microneme proteins M2AP, MIC2 and AMA1 after 24 hours, shown in Figure 5-6. But in some parasites an intracellular accumulation, in the post-Golgi region, of M2AP and MIC2 could be observed besides the apical localisation pattern (arrowheads in Figure 5-7). To analyse if these observations were significant, immunofluorescence analyses with different Shld-1 incubation times were performed and localisation signals of microneme protein were quantified. Therefore intracellular RH<sup>hxgprt-</sup> parasites and parasites expressing ddFKBpmycRab5A, ddFKBpmycRab5C, ddFKBpmycRab5A(N158I) and ddFKBpmycRab5C(153I) were treated with Shld-1 for 12, 24 and 36 hours prior to fixation. Immunofluorescence analysis was performed using the antibodies  $\alpha$ -MIC3,  $\alpha$ -MIC8,  $\alpha$ -M2AP,  $\alpha$ -MIC2 and  $\alpha$ -AMA1. The results for ddFKBpmycRab5A(N158I) expressing parasites treated with Shld-1 for the indicated time and immunolabelled with  $\alpha$ -MIC3/  $\alpha$ -M2AP and  $\alpha$ -MIC8/  $\alpha$ -MIC2 co-stains are displayed in Figure 5-7A. Additionally, the localisation patterns of microneme proteins within 300-400 PVs of all analysed strains were counted and normalised with the signals seen in RH<sup>hxgprt-</sup> parasites. In Figure 5-7B the results of two independent assays for each parasite strain are displayed. Parasites with a normal localisation signal for MIC3 and MIC8 could only be detected, when parasites were only treated without (Figure 5-7A) or with Shld-1 for 12 hours. Here, MIC3 showed either the normal apical localisation or the signal within the PV (green framed in Figure 5-7B) and MIC8 showed either a normal apical localisation or the membranous localisation (green framed 5-7B). In both cases, the majority (over 50%) of MIC3 and MIC8 was already mislocalised within 12 hours incubation with Shld-1 (Figure 5-7A,B). A longer incubation time resulted in an increase in MIC3 and MIC8 mislocalisation. No normal localisation signal could be detected for both microneme proteins after 24 and 36 hours treatment with Shld-1 (Figure 5-7A,B).

For M2AP, MIC2 and AMA1, the quantification showed that nearly 100% of these microneme proteins were normally localised after 12 hours treatment with Shld-1 for M2AP and MIC2 in ddFKBpmycRab5(N158I) parasites (see Figure 5-7A). After 24 hours the majority of M2AP, MIC2 and AMA1 signals were still normal (60 to 80% for M2AP and MIC2 and 70 to 90% for AMA1), but a tendency for intracellular

accumulation could be observed for M2AP and MIC2 (arrowheads in Figure 5-7A and blue framed images in Figure 5-7B). For both microneme proteins circa 40 to 20% of the detected signals were additionally intracellular accumulated. Also AMA1 showed a slight tendency of different localisation. In this case 10-30% of the parasites had a punctuate accumulation at the apical tip (blue framed image for AMA1 in Figure 5-7B). After 36 hours incubation with ShId-1, nearly half of the counted PVs exhibit a mislocalisation signal for M2AP, which was then mainly in the PV (Figure 5-7A and green framed image in Figure 5-7B). Circa 20 to 30% were intracellular accumulated and normally localised. For MIC2 this effect could be seen only for ddFKBPmycRab5A(N158I) expressing parasites (Figure 5-7A). The other parasite strains exhibited similar localisation patterns as seen for the 24 hour time point. For AMA1, an increase accumulation in punctate apical staining was observed after 36hours ShId-1 incubation.

A



B

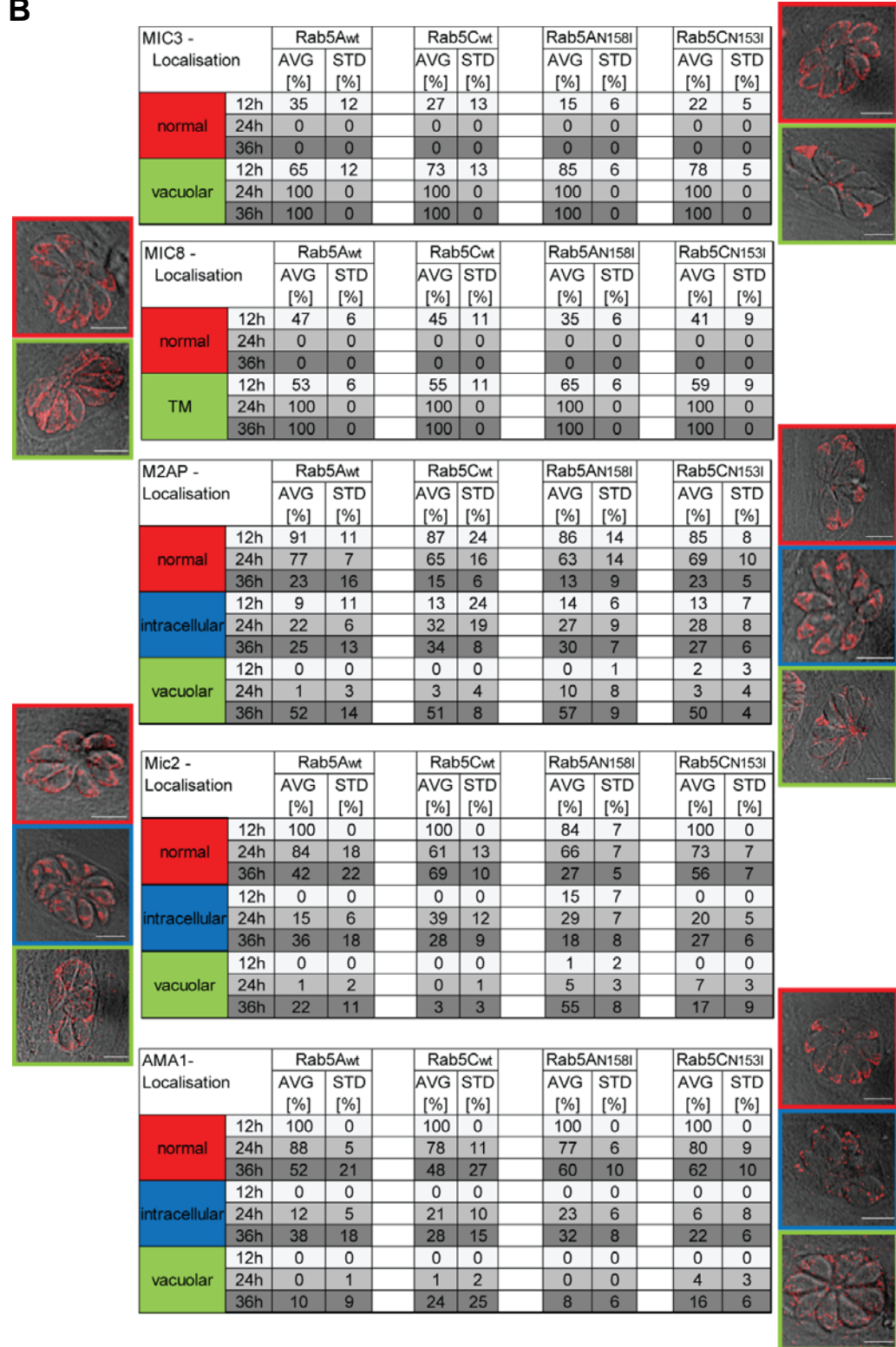


**Figure 5-7: Time course analysis of parasites expressing ddFKBpmycRab5A, ddFKBpmycRab5C, ddFKBpmycRab5A(N158I) and ddFKBpmycRab5C(N153I).** (A) Immunofluorescence analysis of intracellular parasites stably expressing ddFKBpmycRab5A(N158I) treated for 0, 12, 24 and 36 hours with 1  $\mu$ M Shld-1 and co-stained with the indicated microneme antibodies (green/red) and Dapi (blue). The arrowheads indicate an intracellular mislocalisation signal for MIC2 and M2AP seen after 24 hours Shld-1 induction. (B) Quantification of localisations of indicated microneme proteins of intracellular RH<sup>h<sub>x</sub>gprt</sup> parasites and parasites expressing ddFKBpmycRab5A, ddFKBpmycRab5C, ddFKBpmycRab5A(N158I) and ddFKBpmycRab5C(N153I) treated for 12, 24 and 36 hours with 1  $\mu$ M Shld-1. 300-400 PVs of two independent experiments were analysed and normalised with RH<sup>h<sub>x</sub>gprt</sup> parasites. Mean values and the respective standard deviation are presented. The Images were taken with the Delta Vision Core System.

### 6.3.4.2. Rhoptry proteins

It was shown that the rhoptry proteins ROP 2,3,4 were mislocalised when TgRab5A and 5C were overexpressed (Figure 4-2). To analyse if the dominant negative mutants exhibit the same phenotype, IFAs of intracellular parasites induced for 24 hours with Shld-1 prior to fixation and probed with  $\alpha$ -ROP2-4 and  $\alpha$ -ROP5 antibodies were performed. Within both parasite strains expressing ddFKBpmycRab5A(N158I) and ddFKBpmycRab5C(N153I), the tested rhoptry proteins were mainly located outside of the parasites in the PV (Figure 5-8) instead of a normal punctual to elongated signal as seen in RH<sup>hxgprt</sup> parasites.

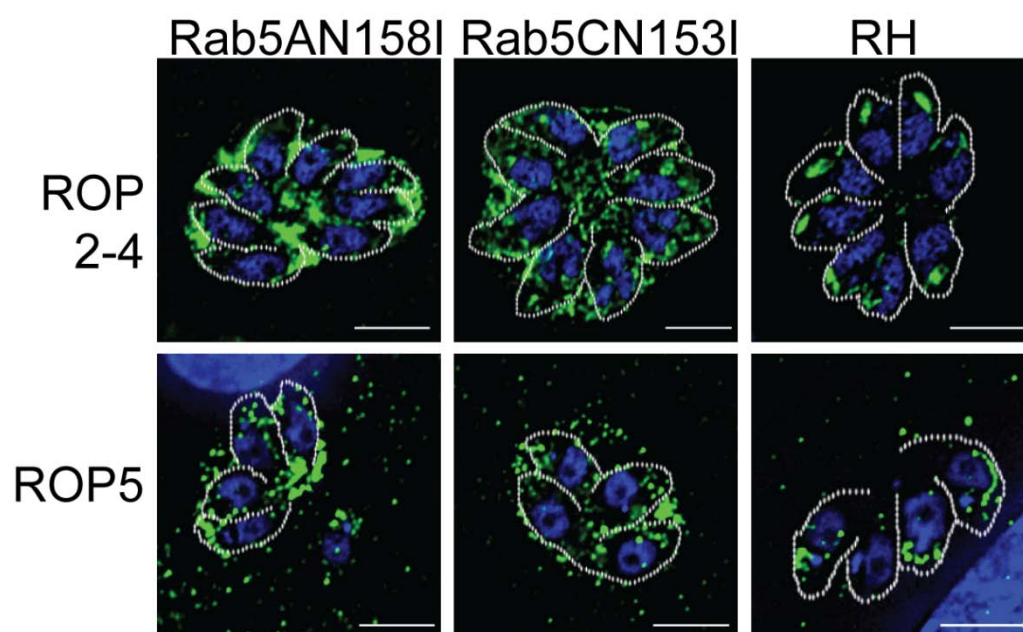


**Figure 5-8: Expression of the dominant negative version of TgRab5A or TgRab5C is causing mislocalisation of rhoptry proteins.** IFA of intracellular parasites stably expressing ddFKBpmycRab5A(N158I), ddFKBpmycRab5C(N153I) or RH<sup>hxgprt</sup> parasites treated for 24 hours with 1  $\mu$ M Shld-1 and probed with indicated rhoptry antibodies (left panel). Dapi is shown in blue. The scale bars represent 5 $\mu$ m. The Images were taken with the Delta Vision Core System.

In summary, for all analysed secretory proteins, all four strains [ddFKBpmycRab5A, ddFKBpmycRab5C, ddFKBpmycRab5A(N158I) and ddFKBpmycRab5C(N153I)] exhibited exactly the same phenotype. The microneme proteins MIC3, MIC8, MIC11 and the tested rhoptry proteins were all mislocalised in presence of Shld-1. They were either concentrated at the PM of the parasites or within the PV, depending if they are soluble or transmembrane proteins. MIC2, its associated proteins, M2AP and AMA1, did not show these effects. Up to 24 hours the majority exhibited normal localisations. However intracellular accumulation (within the post-Golgi region for MIC2 and M2AP and

at the apical tip for AMA1) appeared more and more the longer the parasite strains were treated with ShId-1. For MIC2 and M2AP, where the signals were mainly within the parasite mislocalisation could also be detected after 36 hours.

## **5.4. Further characterisation of TgRab5A(N158I)**

Since overexpression and expression of the dominant negative version of both TgRab5A and TgRab5C had the same phenotypes, from now on, only results for the dominant negative mutant of TgRab5A will be displayed. This parasite strain, expressing ddFKBPmycRab5A(N158I), exhibited the strongest growth phenotype.

### ***5.4.1. MIC3 processing in ddFKBPRab5A(N158I) expressing parasites***

It is known that some microneme proteins (e.g. MIC3 and M2AP) undergo proteolytic processing within the ELCs (Harper, Huynh et al. 2006; El Hajj, Papoin et al. 2008; Parussini, Coppens et al. 2010). Since MIC3 is mislocalised when the function of TgRab5A or TgRab5C was influenced by either overexpression of the wild type or expression of a dominant negative version, it was interesting to investigate if the unprocessed (immature) MIC3 is affected as well. Therefore immunofluorescence analysis was performed with ddFKBPmycRab5A(N158I) expressing parasites induced with and without ShId-1 for 18 hours, in collaboration with the group of Vern Carruthers. Antibodies against the propeptide of MIC3,  $\alpha$ -proMIC3, and the protein previously shown to be involved in MIC3 processing,  $\alpha$ -CPL (Parussini, Coppens et al. 2010), were employed. The results are displayed in Figure 5-9A. In untreated parasites, proMIC3 and CPL exhibited their typical post-Golgi localisation signal. Interestingly a mislocalisation of proMIC3 could be observed when this parasite strain was treated with ShId-1. However this didn't affect localisation of CPL. Therefore, stabilised expression of the dominant negative version of TgRab5A led to a mistargeting of the unprocessed MIC3, but had no effect on ELC or CPL.

To assess if processing of MIC3 was affected, pulse chase experiments were conducted by Vern Carruthers's group in the same way as described for TgRab7(G18E) (see chapter 4.4.3.6.). ddFKBPmycRab5A(N158I) and RH<sup>hxgprt</sup>-

parasites were grown for 24 hours with and without 1 $\mu$ M Shld-1 under normal growth conditions. Immediately prior to labelling, the normal growth medium was exchanged with methionine and cysteine free DMEM. Dividing parasites were metabolically labelled with  $^{35}$ S-methionine and cysteine for 15 minutes and then "chased" for 0, 20, 40 and 60 minutes. After that the monolayers were washed with PBS to stop the process and intracellular parasites were extracted from host cells. Afterwards MIC3 was segregated from other proteins by immunoprecipitation using  $\alpha$ -MIC3. The resulting immunoprecipitation was loaded on a SDS-PAGE, incubated in a fluorographic enhancer, dried in cellophane and exposed on X-ray films for 4 days. Two MIC3 bands were detectable, one presenting the processed MIC3 and the other one the immature unprocessed MIC3. The signal of processed MIC3 of three independent experiments were quantified. The immunoblot of one representative experiment and the results of the quantification of three independent experiments are displayed in Figure 5-9B. No significant differences in the amount of processed MIC3 could be detected at each time point either between RH<sup>hxgprt-</sup> or ddFKBPmycRab5A(N158I) expressing parasites or between parasites treated with and without Shld-1 prior to labelling. For both strains and under both conditions, maturation (processing) of MIC3 was increasing over the time.

In summary, unprocessed MIC3 was mislocalised into the PV, but neither processing of MIC3 nor the "CPL compartment" were affected when the dominant negative mutant of Rab5(N158I) was expressed in *T.gondii* tachyzoites.

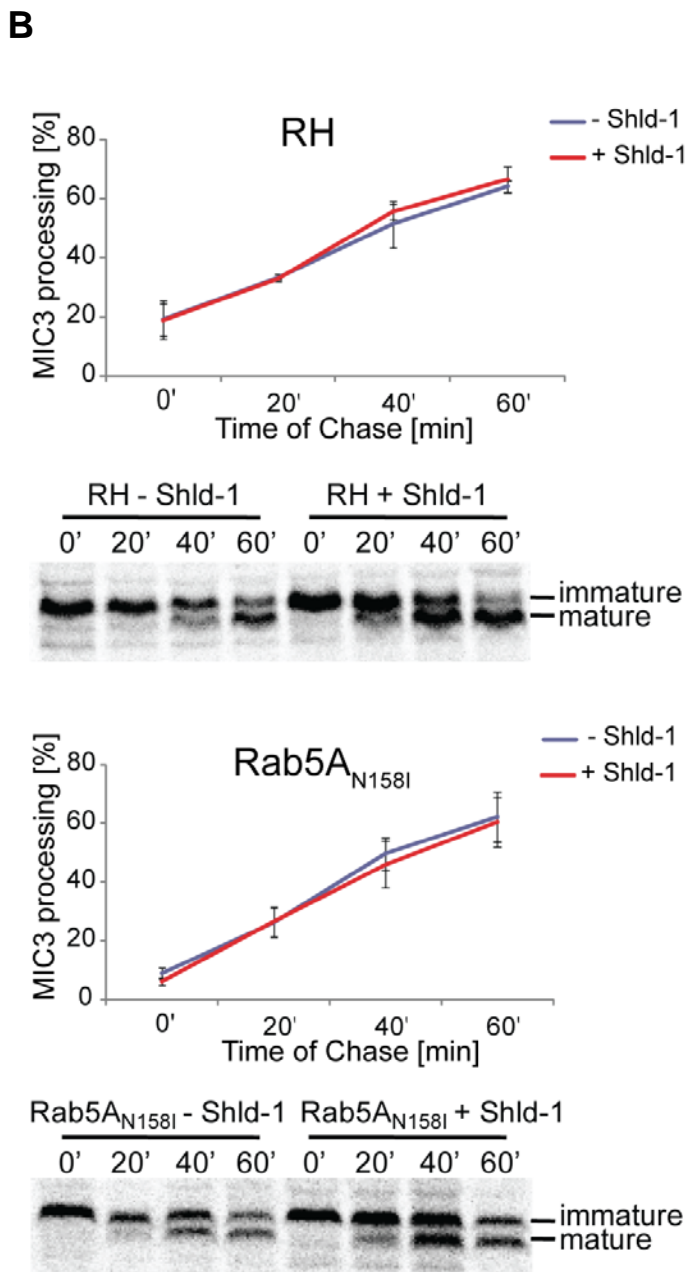
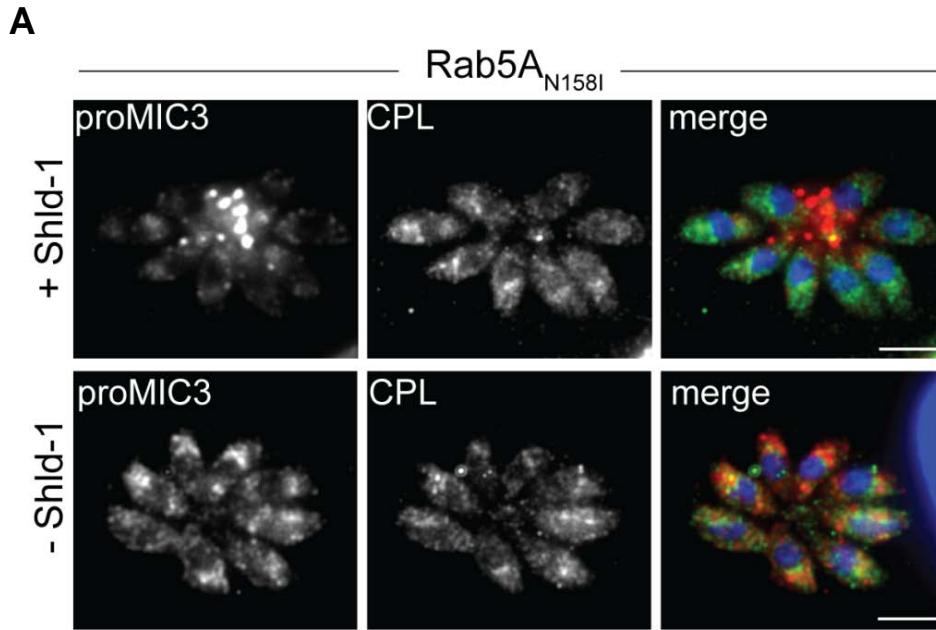


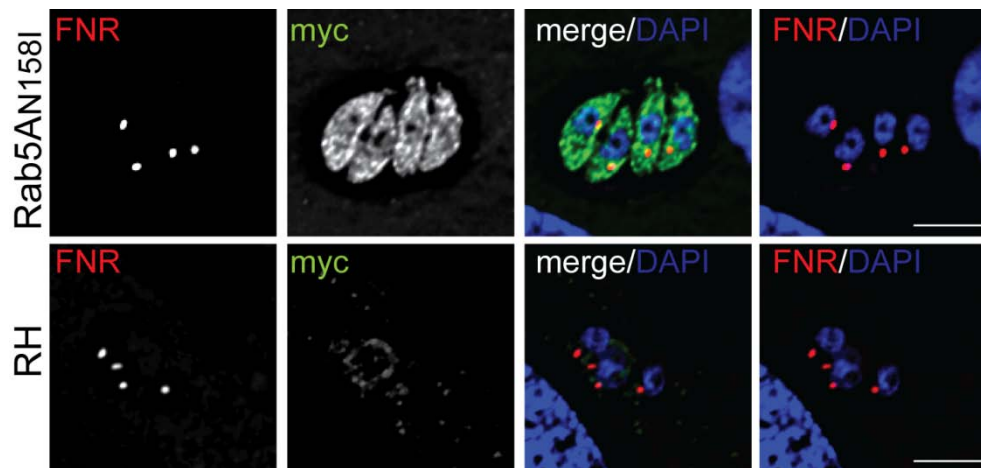
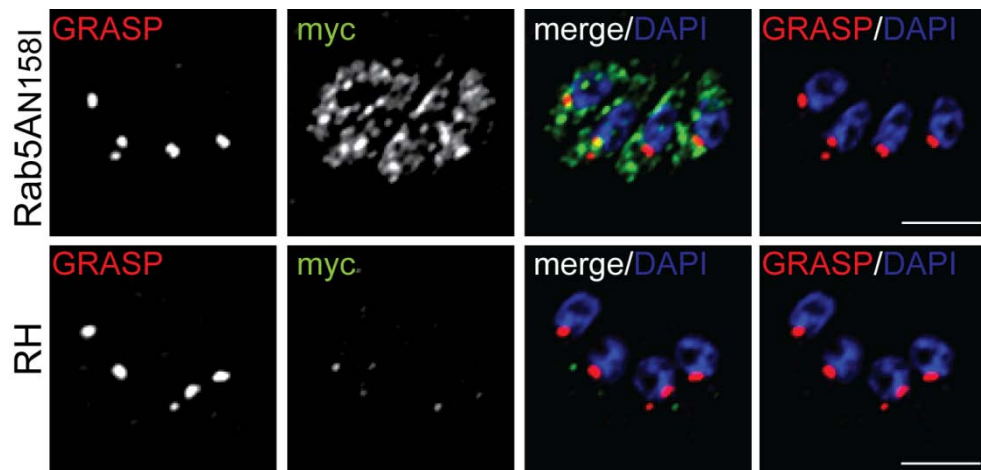
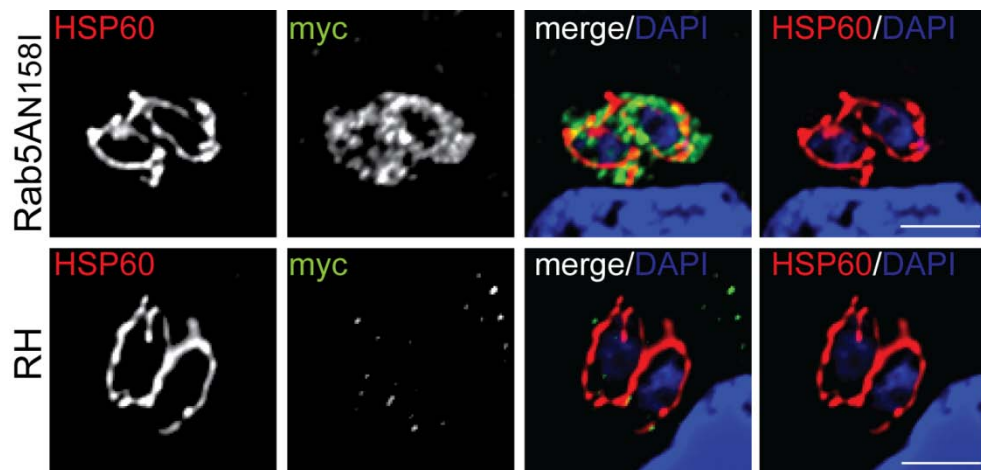
**Figure 5-9: Microneme processing and organisation of the ELC, CPL, is unaffected in ddFKBPmycRab5A(N158I) expressing parasites.**

(A) Immunofluorescence analysis of ddFKBPmycRab5A(N158I) parasites grown for 18hours +/- 1 $\mu$ M Shld-1 and probed with proMIC3 (red) and CPL (green) antibodies. Dapi is shown in blue. The scale bar represents 5  $\mu$ m. (B) Quantification and the respective Immuno blots of pulse chased experiments of MIC3 maturation in RH<sup>hxgprt</sup> and ddFKBPmycRab5A(N158I) parasites are shown. Mean values and the respective standard deviation of three independent experiments are presented. The images were taken from (Kremer, Kamin et al. 2013).

### **5.4.2. Other organelles**

To test if other organelles were affected in dominant negative mutants immunofluorescence analysis with different organellar markers and antibodies were performed. Therefore RH<sup>hxgprt-</sup> and ddfKBPmycRab5A(N158I) expressing parasites were either treated for 24 hours with Shld-1 prior to fixation and probed with  $\alpha$ -IMC or  $\alpha$ -GRA9 (a dense granule protein) within immunofluorescence analysis or co-transfected with an apicoplast marker (FNR-RFP), a Golgi marker (GRASP-RFP) or with a mitochondrion marker (HSP60-RFP) before being transferred onto HFF cells and incubated with Shld-1 for 24 hours prior to fixation. For all immunofluorescence analyses the  $\alpha$ -myc antibody was used to detect the expression of ddfKBPmycRab5A(N158I). The results of the co-transfections are displayed in Figure 5-10A,B,C and the results for the immunofluorescence analysis with  $\alpha$ -IMC and  $\alpha$ -GRA9 are displayed in Figure 5-10D,E. As expected, for all IFAs no signal was detected with  $\alpha$ -myc in RH<sup>hxgprt-</sup> parasites and for ddfKBPmycRab5A(N158I) expressing parasites the typical cytosolic stain could be observed. For FNR-RFP (a Ferredoxin NADP<sup>+</sup> Reductase within the apicoplast) and GRASP-RFP the normal punctual localisation signal could be detected in both RH<sup>hxgprt-</sup> parasites and ddfKBPmycRab5A(N158I) expressing parasites. For HSP60, a mitochondrial chaperonin, the typical shape of the mitochondrion could be detected for both parasite strains. Also normally located were the IMC and the dense granule protein GRA9 in parasites expressing the dominant negative version of TgRab5A compared to RH<sup>hxgprt-</sup> parasites.

In summary, other organelles appear to be not affected by the expression of the dominant negative TgRab5A mutant.

**A****B****C**

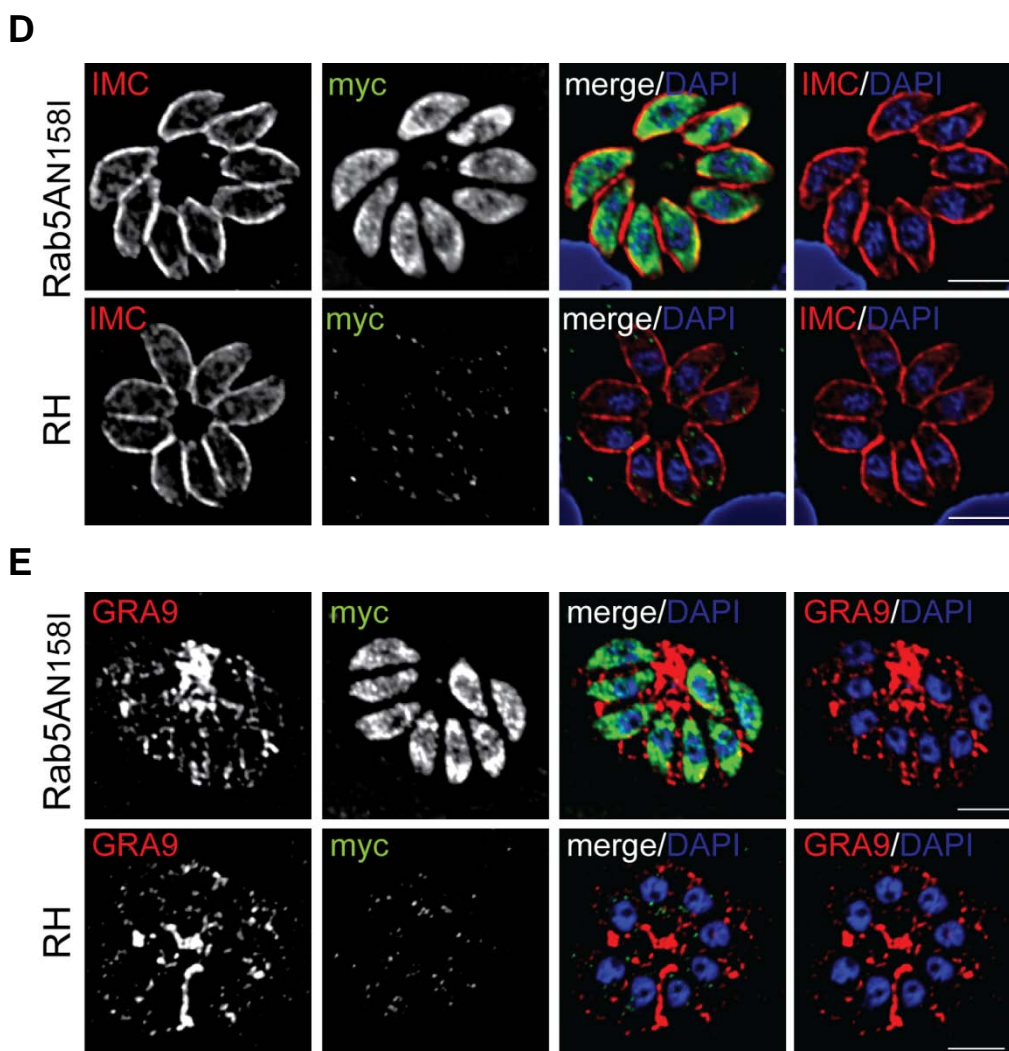


**Figure 5-10 : Expression of dominant negative ddfKBPmycRab5A(N158I) shows no negative effects on organelle formation and distribution.** Immunofluorescence analysis of intracellular parasites stably expressing the dominant negative ddfKBPmycRab5A(N158I) and RH<sup>hxgprt</sup> parasites treated for 24hours with 1  $\mu$ M Shld-1 co-expressed with organellar markers for the (A) apicoplast (FNR-RFP), (B) the Golgi (GRASP-RFP), (C) the Mitochondrion (HSP60-RFP), or co-stained with (D)  $\alpha$ -IMC (inner membrane complex) and (E)  $\alpha$ -GRA9 (dense granules) antibodies. To detect the expression of ddfKBPmycRab5A(N158I) samples were additionally probed with  $\alpha$ -myc antibodies. Dapi is stained in blue. Scale bars represent 5  $\mu$ m. The Images were taken with the Nikon TE2000 inverted microscope.

### 5.4.3. Organellar effects on ultrastructural level

To assess how expression of the dominant negative mutant of TgRab5 is affecting tachyzoites on the ultrastructural level, electron microscopy was applied in collaboration with David Ferguson. Confluent HFF monolayers were infected with ddfKBPmycRab5A(N158I) and ddfKBPmycRab5C(N153I) expressing parasites so that 80% of the host cells were infected. Before fixation intracellular parasites were treated with and without Shld-1 for 24 hours. Afterwards infected host cells were fixed, embedded and cut into ultrathin sections for transmission

electron microscopy. David Ferguson examined several samples and came to the conclusion, that both parasite strains were able to fully form daughter cells by undergoing repeated endodyogeny. He could also observe that both strains lack rhoptries and rhoptry precursors within the daughter parasites. Both strains showed also a reduction in the amount of micronemes, when they were pre-treated with ShId-1. According to David Ferguson, this effect was stronger for parasites expressing ddFKBPmycRab5A(N158I). Except for the secretory organelles, other organelles looked normal, but he could also observe expansions of the Golgi area with numerous naked and coated vesicles in both parasite strains.

In Figure 5-11, EM-images of the apical half of single parasites expressing ddFKBPmycRab5A(N158I) treated with and without ShId-1 are displayed. Readily identifiable are the missing rhoptries (R) and the reduced amount of micronemes (arrowheads) in the parasite treated with ShId-1 compared to the untreated parasite. Differences in the Golgi (G) and post-Golgi regions are also distinguishable. Within the lower panel, the apical half of a treated parasite is displayed. Some enlarged vesicle adjacent to the Golgi and within the post-Golgi region are indicated with arrows. The absence of rhoptries and micronemes is also observable in this image.

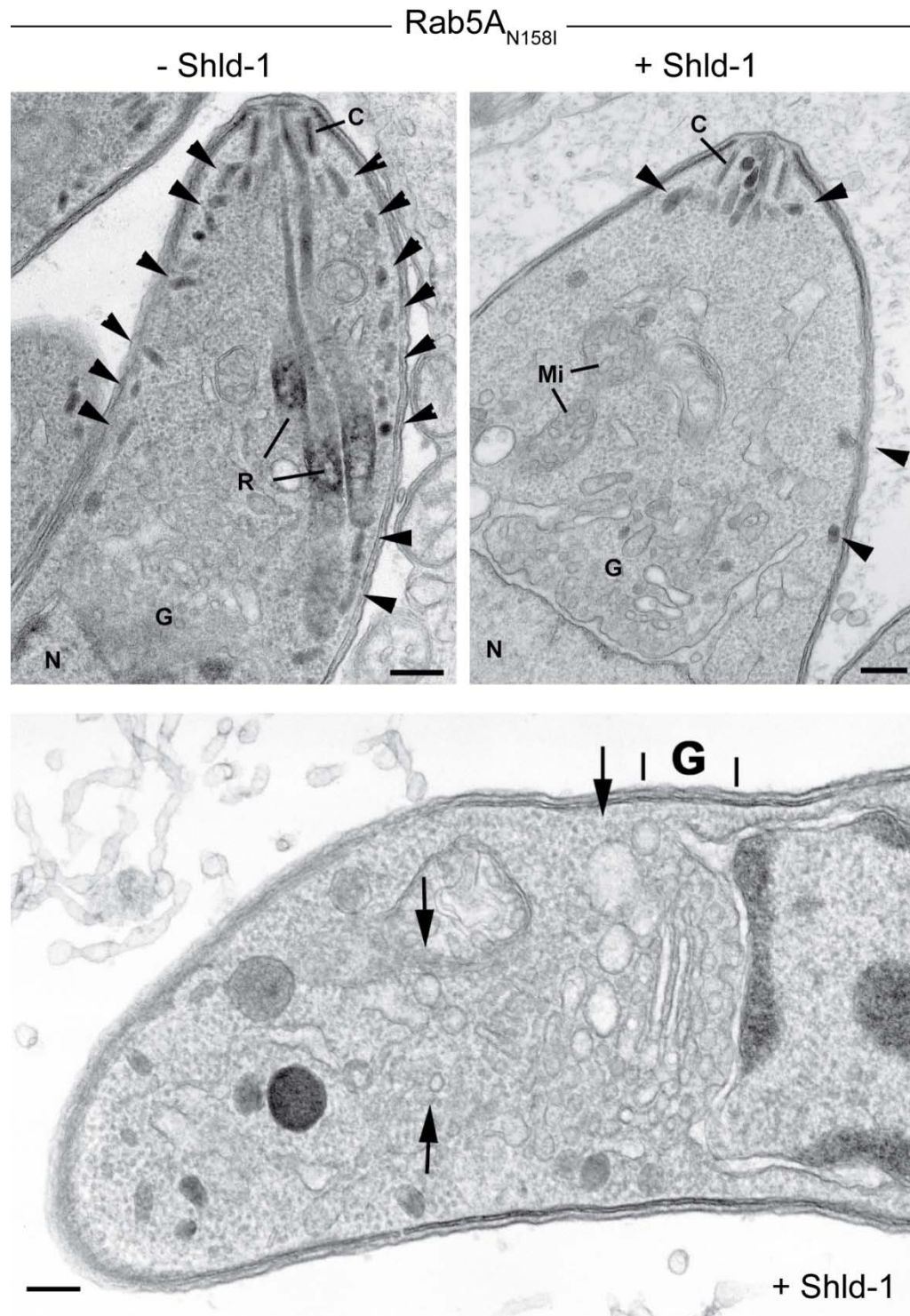


**Figure 5-11: Less micronemes and no rhoptries were detectable in ddFKBpmycRab5A(N158I) parasites grown in presence of Shield-1 in electron microscopic samples.** Accumulation and enlargement of post-Golgi vesicles were also observed. Electron microscopy was performed by David Ferguson with intracellular ddFKBpmycRab5A(N158I) expressing parasites treated with (+) and without (-) Shld-1 for 24hours. Scale bars represent 0.5 $\mu$ m. The apical half of a treated parasite shows no rhoptries (R) or micronemes (arrowheads) but enlarged vesicles in the post-Golgi region (arrows). C: Conoid, G: Golgi, Mi: Mitochondrion, N: Nucleus. EM imaging was performed by David Ferguson.

Since David Ferguson could not detect any rhoptries in Shld-1 treated parasites, but a reduction of micronemes, he quantified the amount of micronemes in 20 ddFKBPmycRab5A(N158I) expressing parasites. The results are displayed in Figure 5-12. More than 50% less micronemes could be detected in ddFKBPmycRab5A(N158I) expressing parasites treated with Shld-1 compared to parasites without Shld-1.

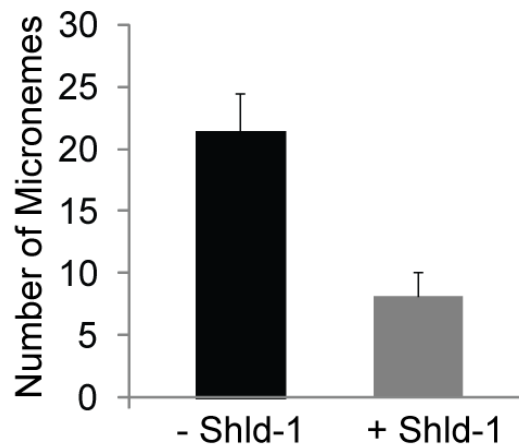


**Figure 5-12: Over 50% less micronemes were detected when expressed ddFKBPmycRab5A(N158I) is stabilised in *T.gondii* tachyzoites.** Electron microscopy quantification of micronemes present in longitudinal sections passing through the conoid and nucleus. 20 parasites per situation were quantified. Quantification of EM images was performed by David Ferguson. The diagram was taken from (Kremer, Kamin et al. 2013).

After effects on the secretory organelles (rhoptries and micronemes) were confirmed within EM, further analyses were undertaken to access microneme proteins in immuno EM in collaboration with David Ferguson. HFF monolayers were infected with ddFKBPmycRab5A(N158I)-expressing parasites as described for EM sample preparation and treated with and without Shld-1 for 24 hours. Afterwards infected host cells were fixed, embedded, cut into ultrathin sections and treated with primary antibodies against microneme proteins and colloidal gold labelled secondary antibodies before transmission electron microscopy was applied. Antibodies against MIC3, MIC8 and M2AP were used. Unfortunately no analysable samples could be gained for MIC3 and MIC8 labelling. Only  $\alpha$ -M2AP probing resulted in IEM images where the microneme protein was detected. Figure 5-13 shows the apical half of two ddFKBPmycRab5A(N158I) expressing parasites, one treated with and the other one without Shld-1. As expected no

differences could be observed for M2AP. Both samples showed an intracellular localisation of M2AP (arrowheads), within micronemes.

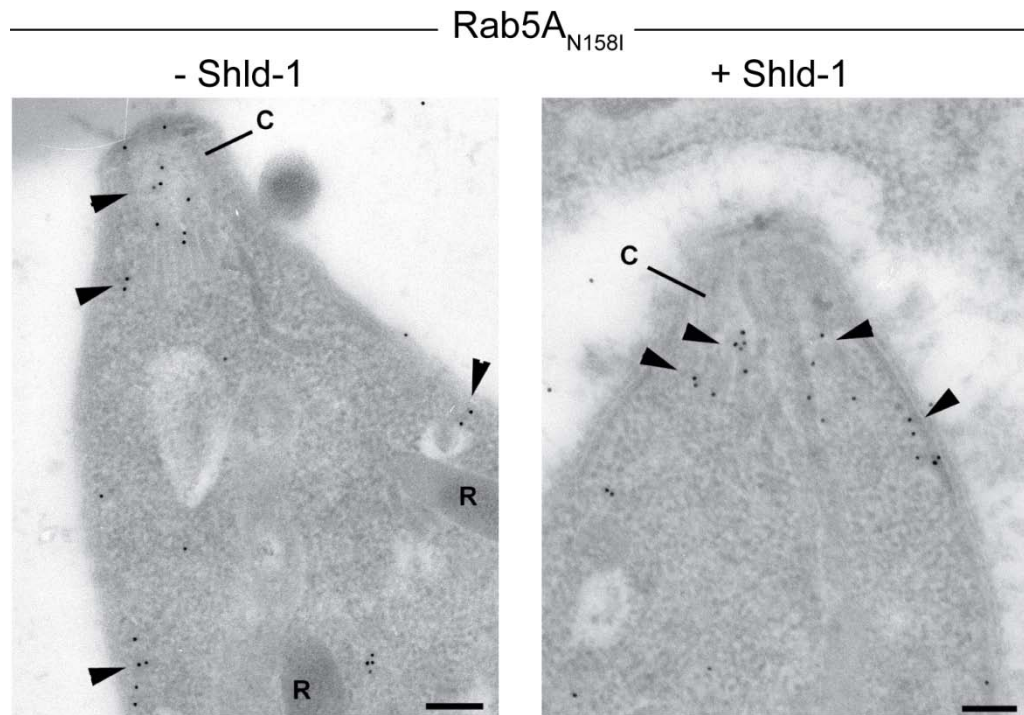


**Figure 5-13: M2AP distribution in ddFKBPmycRab5A(N158I) expressing parasites imaged with ImmunoEM.** ImmunoEM performed on ddFKBPmycRab5A(N158I) expressing parasites treated with (+) and without (-) Shld-1 for 24 hours using  $\alpha$ -M2AP as a primary antibody. The arrowheads indicate  $\alpha$ -M2AP signals within micronemes. Scale bars represent 0.5 $\mu$ m. C: Conoid, R: rhoptry. IEM was performed by David Ferguson.

In summary, the effect on rhoptry and micronemes (see chapter 6.3.4.) could be confirmed in EM for parasites expressing the stabilised dominant negative version of TgRab5A. Here, no rhoptries could be detected and a reduced set of micronemes were observed. Within IEM analyses it could be confirmed, that the microneme protein M2AP remained unaffected in parasites expressing the stabilised dominant negative version of Rab5A.

## 5.5. Summary and Conclusions

In chapter 3 it was observed, that TgRab5A and TgRab5C showed an identical localisation (Figure 3-9), which led to the assumption, that both proteins are involved in the same pathway. In chapter 4 it was shown, that the overexpression of TgRab5A or TgRab5C was blocking the parasites' growth (Figure 4-1). Additionally, it was found that rhoptry proteins and only a subset of microneme proteins were mislocalised due to the overexpression of TgRab5A and TgRab5C (Figure 4-2). To further investigate the functions of these two proteins in more detail, parasites expressing dominant negative versions of TgRab5A and TgRab5C were generated (see chapter 4.4.1.) and analysed together with parasites overexpressing TgRab5A and TgRab5C. For all performed assays [growth, replication and invasion analysis (Figure 5-2,-3,-4)] expression of dominant negative Rab5A(N158I) and Rab5C(N153I) resulted in a phenotype identical to that observed for overexpression of their wild type versions. In all four parasite strains, it was detected that intracellular replication displayed no defect (Figure 5-2), while host cell egress was significantly decreased (Figure 5-3) and invasion was significantly blocked (Figure 5-4). Analysing the localisation of rhoptry proteins (ROP 2-4,5) and microneme proteins MIC2,3,8,11,M2AP and AMA1 again all four strains exhibited the same phenotype. All analysed rhoptry proteins and only a subset (MIC3, 8, 11) of microneme proteins were mainly mislocalised within 12 hours, when TgRab5A or TgRab5C were overexpressed or their respective dominant negative version was expressed. Here all affected soluble secretory proteins (MIC3, MIC11, ROP2-4,5) could be detected within the PV and the transmembrane MIC8 was detected at the parasite's PM (Figure 5-7). This could indicate that the interference in the TgRab5A or TgRab5C cycle is causing constitutive secretion of rhoptry proteins and some microneme proteins. Other microneme proteins (M2AP, MIC2 and AMA1) remained unaffected, but the longer TgRab5A,C were overexpressed or their dominant negative versions were expressed, the more apparent the differences in the localisation of M2AP, MIC2 and AMA1. After 24 hours, some parasites showed additional intracellular accumulation of the respective microneme protein (Figure 5-7). For M2AP and MIC2 this additional intracellular signal was most likely within the post-Golgi region, probably the ELCs, whereas AMA1 exhibited a signal at the very apical tip, probably the conoid, of the parasite. To determine the exact localisation,

further co-localisation studies with the respective antibodies need to be applied in the future. After 36 hours M2AP, was mainly secreted into the PV. This could also be detected for MIC2 in ddFKBPmycRab5A(N158I) expressing parasites (Figure 5-7) and to a weaker extend in their wild type overexpressing parasites. For TgRab5C parasites, the signal of MIC2 was mainly normal for overexpressing and dominant negative expressing parasites. AMA1 showed more intracellular accumulation after 36 hours than after 24 hours, but it was mainly normal localised in all four parasite strains. It should be noted that the standard deviation values for some counting were very high and therefore further assays should be performed. Nevertheless, these observations indicate a tendency of M2AP, MIC2 and AMA1 to be indirectly affected by the overexpression of TgRab5A,C or expression of their dominant negative versions. Here it appeared, that the effect especially on M2AP and MIC2 resulted first in intracellular accumulation, probably in the ELC area, and then in secretion.

Many microneme proteins, such as MIC3 and M2AP undergo proteolytic maturation during their transit through the ELCs (Harper, Huynh et al. 2006; El Hajj, Papoin et al. 2008; Parussini, Coppens et al. 2010). Since MIC3, but not M2AP is constitutively secreted in parasites expressing dominant negative TgRab5A, it was further investigated at which step this rerouting occurs. If rerouting occurred directly at the Golgi, MIC3 would be secreted as an immature proMIC3. In contrast, if rerouting occurred at the ELCs, processing of the propeptide would take place, resulting in secretion of mature MIC3. Therefore, pulse-chase experiments were performed to compare pro-peptide processing of MIC3 in RH<sup>hxgprt</sup>- parasites and parasites expressing ddFKBPmycRab5A(N158I) in presence and absence of Shield-1 (Figure 5-9A). Since no differences in propeptide processing could be detected, it can be assumed that the rerouting of MIC3 occurs post-Golgi, after processing in the ELCs (Figure 5-9B).

It could also be shown in this chapter, that other organelles, such as Golgi, apicoplast, mitochondrion, dense granules and IMC were not affected by expression of dominant negative TgRab5A. This could be confirmed in electron microscopy (Figure 5-11). Although the Golgi exhibited a normal appearance, an accumulation of enlarged vesicles adjacent to the Golgi and in the post-Golgi region was detected in ultrastructural samples. In good agreement with the IFA data parasites expressing ddFKBPmycRab5A(N158I) are devoid of rhoptries and

only very few micronemes are identified (Figure 5-11). If the rhoptries were absent or without proteins and for that reason not detectable needs to be further investigated. In particular, interference with Rab5A function resulted in a significant loss of micronemes (~70%) (Figure 5-12). Performance of immuno EM with different microneme proteins in ShId-1 treated ddfKBPmycRab5A(N158I) expressing parasites could confirm that M2AP remained unaffected. No intracellular accumulation as seen for some parasites on IFA level was mentioned by David Ferguson assuming that this effect wasn't very striking. Nevertheless, it needs to be further investigated, if the enlarged vesicles next to the Golgi and within the post-Golgi region are connected with the intracellular mislocalisation signal observed for M2AP and MIC2 in IFAs.

Finally, the observation made in this chapter, that only a subset of microneme proteins is constitutively secreted as a direct effect of interference within the Rab5A,C cycle leads to the suggestion that microneme proteins reach their destination using at least two distinct transport routes with one depending on functional Rab5A and/or Rab5C. Consequently one can speculate that micronemes might be organised into different subsets with different protein content.

## 6. Stimulated Emission Depletion (STED) microscopy on RH<sup>hxgprt-</sup> parasites to investigate, if subpopulations of micronemes exist

### 6.1. Introduction

The observations made and described in chapter 4.3 and 5 that the localisation of only a subset (MIC11, MIC3, MIC8) of microneme proteins were affected by the overexpression of TgRab5A and 5C and the expression of their dominant negative versions (Figure 5-6), could indicate that microneme proteins reach their destinations using at least two distinct transport routes, with one depending on functional Rab5A and/or Rab5C. Consequently it is possible, that micronemes might be organised into different subsets with different protein content. Dense clustering of secretory organelles within the apical complex of the parasite and limitations in optical resolution made it difficult to differentiate individual compartments using standard microscopy techniques. For these reasons super-resolution STED (Stimulated Emission Depletion) microscopy (Hell and Wichmann 1994) was used to finely pinpoint the subcellular localisation of microneme proteins in RH<sup>hxgprt-</sup> parasites.

The STED microscopy uses two synchronized laser pulses: the excitation pulse and the depletion pulse (STED-pulse). Whereas the excitation pulse is adjusted to the absorption spectrum of the sample's dye, the STED pulse is red-shifted in frequency to the emission spectrum of the dye. Thereby lower energy photons of the excited dye are depleted to their ground state by stimulated emission. As a consequence these excited molecules cannot fluoresce. Arranging the STED pulse as a doughnut leads to depletion of the molecules at the periphery of the spot. The fluorescence in the centre remains unaffected. In this way resolutions of lower than 30nm (depending on employed fluorescent dye) can be achieved. Compared to confocal microscopy, STED microscopy could be an application, which theoretically allows a resolution of single micronemes within IFAs in *T.gondii*.

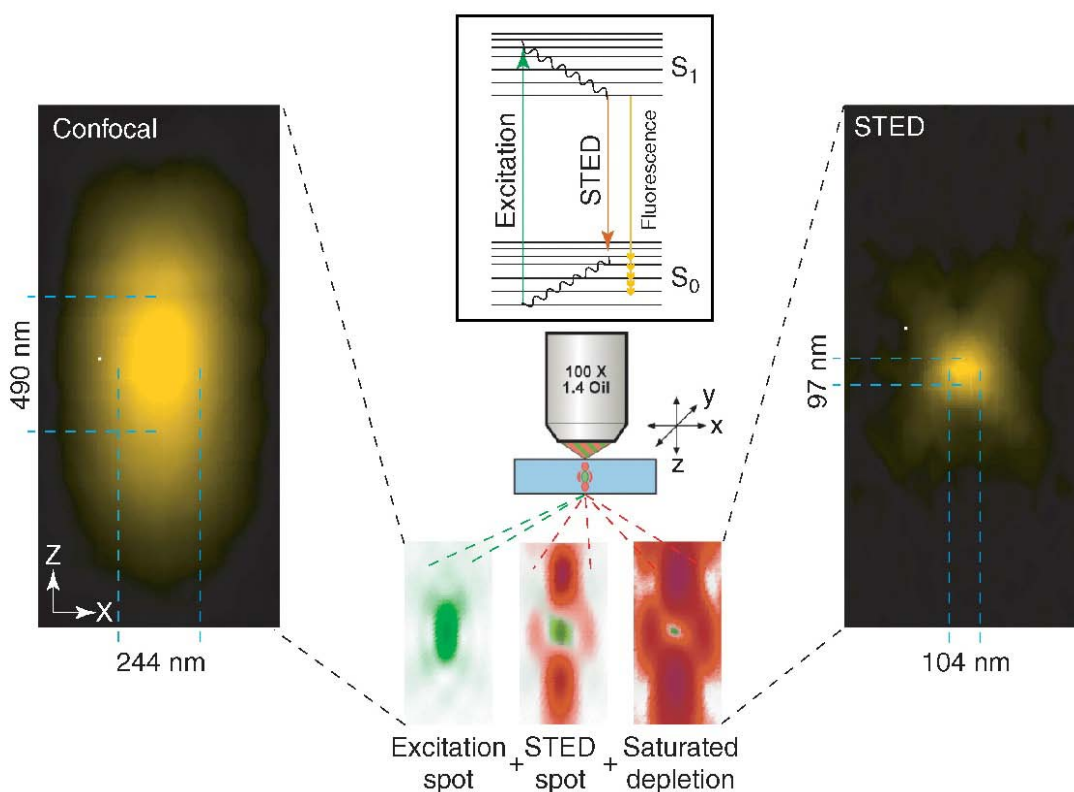


**Figure 6-1: STED-microscopy.** In STED microscopy two synchronized laser pulses are used. One laser pulse excites molecules in their fluorescent state ( $S_1$ ) (green arrow). These molecules return to their ground state ( $S_0$ ) by fluorescence emission (yellow arrow) spontaneously. Detecting this fluorescence would result in a confocal image (left panel). In STED analysis an additional laser pulse is arranged around the excitation spot in a donut-shaped way. This laser pulse enforces the molecules to return from their  $S_1$  state to the  $S_0$  state via stimulated emission (red arrow). No fluorescence can be detected in this area due to depletion. Since saturated reduction of fluorescence is at any coordinate but the focal point the resolution of a STED image (right panel) is much improved. The image was modified from (Hell, Dyba et al. 2004)

## 6.2. Single-colour STED analysis

Single-colour STED was performed to optimise the conditions for “two-colour STED analysis” to gain best possible resolutions. Therefore it was important to establish optimal dilutions for primary and secondary antibodies. Single labelled IFA samples were prepared with different antibody dilutions to reach similar emission intensities for antibodies which should be combined in dual-labelling (“two-colour STED analysis”) later. Therefore, samples were prepared in the same way as for immunofluorescence analysis for confocal imaging, except for additional treatment with  $\text{NH}_4\text{Cl}$  directly after fixation to quench autofluorescence of host cells and washing with high salt PBS (PBS with 500mM NaCl) after labelling with the secondary antibody. For “single-colour STED” single stains using  $\alpha\text{-MIC3}$ ,  $\alpha\text{-MIC8}$ ,  $\alpha\text{-MIC2}$  and  $\alpha\text{-M2AP}$  as primary antibodies and

anti-rabbit-DY 485 XL or anti-mouse-ATTO 565 as secondary antibodies were employed. The samples were fixed in Mowiol 4-88/ DABCO mounting media. The STED-imaging was performed by Eva Rittweger from Stefan Hell's group in Heidelberg. The results of optimised sample preparation and STED analysis of intracellular RH<sup>hxgprt</sup>- parasites are displayed in Figure 6-2. Differences in resolution between confocal and STED microscopy were readily identifiable. Since the apical halves, especially the tips, of the tachyzoites were densely packed with micronemes, it was not possible to distinguish between single micronemes in confocal images. After application of STED analysis the resolution could be improved (Figure 6-2A). An additional deconvolution step (STED<sup>+</sup>), shown in Figure 6-2B for MIC2 could additionally improve the resolution up to 40-30 nm. Still, the apical tips were too packed with micronemes to resolve them individually. However, with STED analysis it was possible to detect single micronemal signals within the rest of the apical half of the parasites compared with confocal imaging. Different localisation patterns for  $\alpha$ -MIC3,  $\alpha$ -MIC8,  $\alpha$ -M2AP and  $\alpha$ -MIC2 became identifiable (Figure 6-2). Interestingly a similar pattern for M2AP and MIC2 could be detected. Here the signals appeared sometimes as arranged in a line (see arrows in Figure 6-2). For MIC8, a diffuse distribution of signals was observed. STED analysis of MIC3 resulted in signals, which were arranged in dots, which again were arranged in lines mainly spread over the apical half of the parasite.

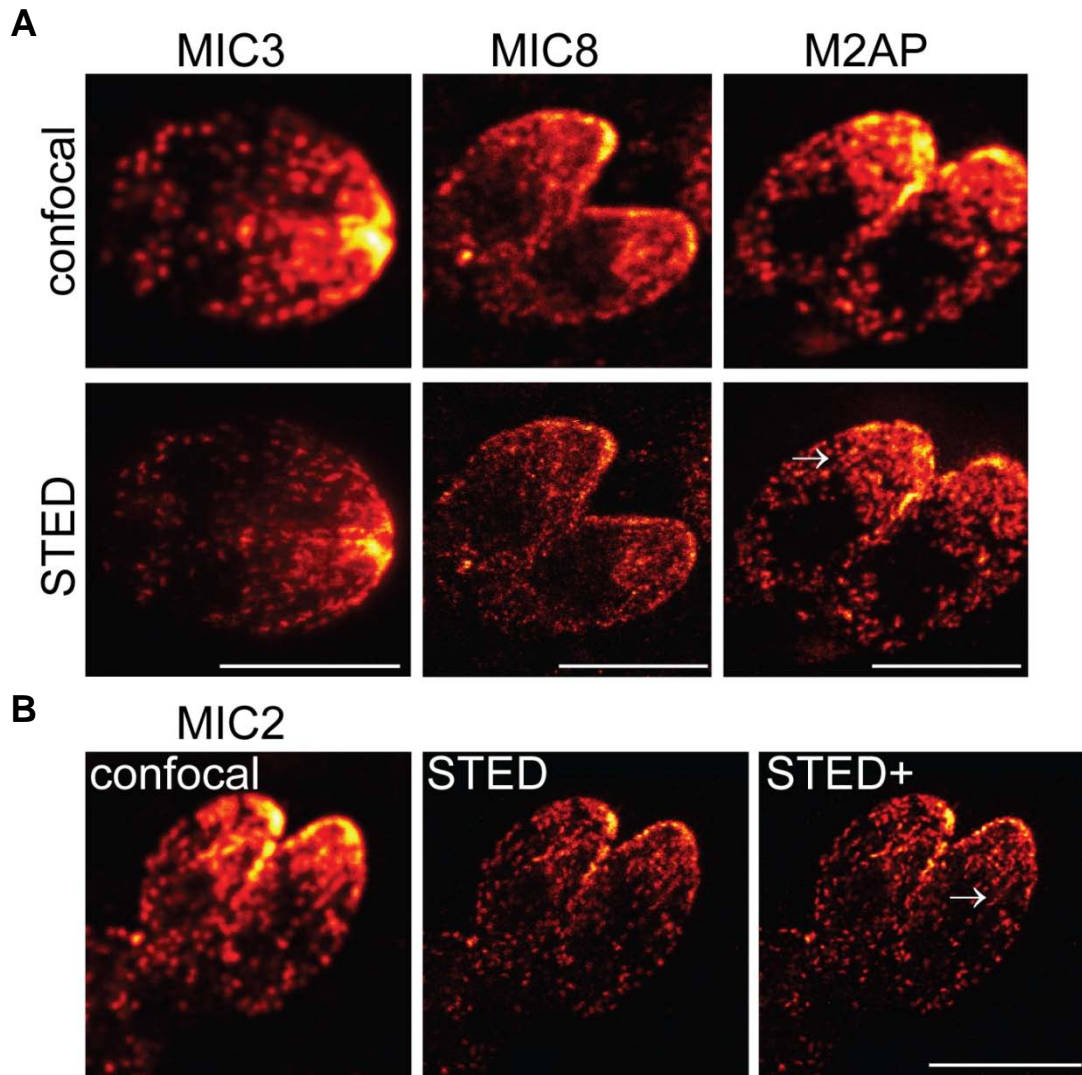


**Figure 6-2: Single-colour STED analysis reveals different localisation patterns of microneme proteins in  $RH^{hxgprt-}$  parasites.** Single-colour STED measurements on  $RH^{hxgprt-}$  parasites labelling MIC3, MIC8, M2AP and MIC2. Resolution obtained in confocal, STED microscopy and STED<sup>+</sup> (linear deconvoluted) is compared as indicated. The arrows show, where signals appeared to be arranged in a line. Scale bars represent 5  $\mu\text{m}$ . STED imaging was performed by Eva Rittweger.

### 6.3. Two-colour STED analysis

To investigate if the different localisation patterns of microneme proteins observed in STED images of Figure 6-2 are due to different subsets of micronemes, “two-colour STED analysis” was performed. Therefore IFA samples were prepared, applying the optimised conditions, for dual-labelling with different microneme antibodies established in single-colour STED (5.2). Here intracellular  $RH^{hxgprt-}$  parasites were co-stained with  $\alpha$ -M2AP- anti rabbit DY 485 XL /  $\alpha$ -MIC2- anti mouse ATTO 565 or  $\alpha$ -M2AP- anti rabbit DY 485 XL /  $\alpha$ -MIC3- anti mouse ATTO 565. STED imaging was done by Eva Rittweger. The results for

confocal and STED<sup>+</sup> analysis are displayed in Figure 6-3. Again a clear difference in resolution between confocal and STED analysis could be detected. Comparing the confocal sections of the two different co-stains (M2AP/MIC2 and M2AP/MIC3) it was difficult to recognise a difference. Since M2AP and MIC2 form a complex one would expect, that both proteins end up in the same microneme in case different subsets of micronemes exist. In this case an identical localisation signal for  $\alpha$ -M2AP and  $\alpha$ -MIC2 was expected. Analysing the STED images it became obvious that M2AP and MIC2 were co-localising, as expected, whereas M2AP and MIC3 exhibited different localisation signals.

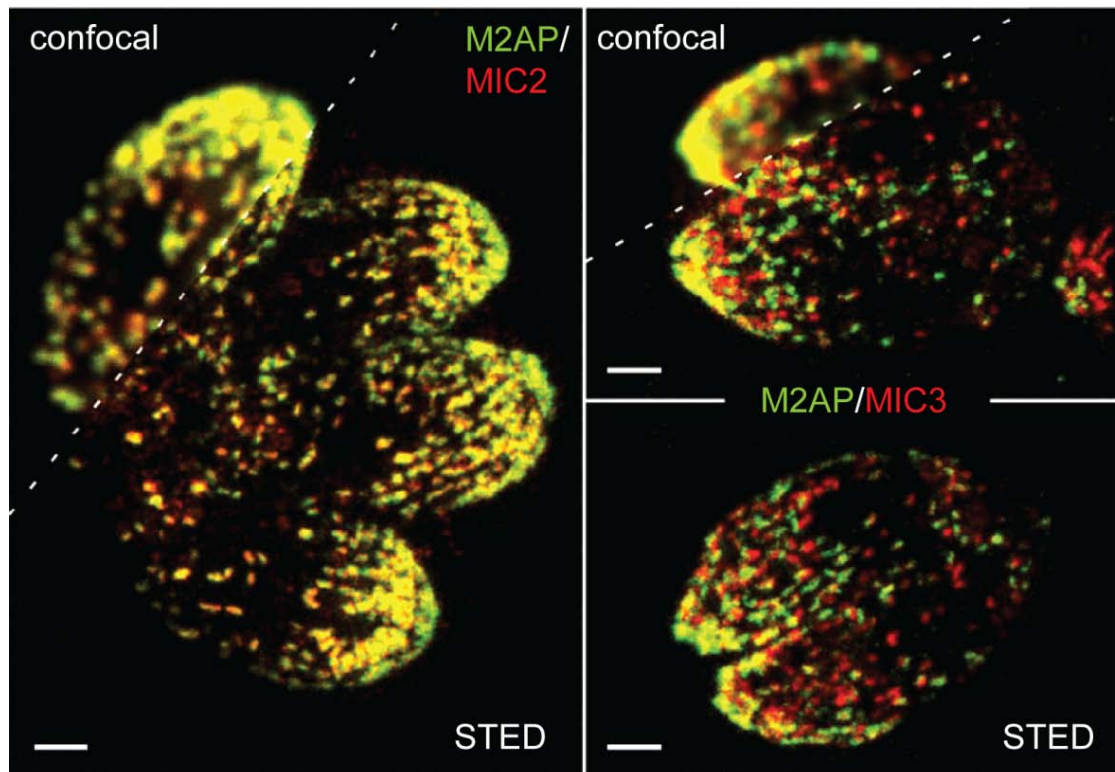


**Figure 6-3: Two-colour STED analysis reveals different localisations of microneme proteins in RH<sup>hxgprt</sup> parasites.** Two-colour STED measurements on RH<sup>hxgprt</sup> parasites. Dual labelling of MIC2 and M2AP (left) and M2AP and MIC3 (right) has been performed. Resolution obtained in confocal and STED<sup>+</sup> microscopy is compared as indicated. Scale bar 1  $\mu$ m.

### 6.3. Two-colour STED analysis with thin-sectioned samples

The previous STED analyses showed the signals of the respective microneme proteins signals of whole parasites, since z-sectioning is not applicable for STED analysis. Imaging of one z-section would already bleach the next section and the single images of one stack would not be comparable anymore and the final image set would be not analysable. To better resolve the apical part and especially the tip of the parasites, thin-sectioning of intracellular RH<sup>hxgprt</sup>-parasites and followed STED analysis were performed by Dirk Kamin from Stefan Hell's group in Goettingen. Therefore samples were prepared as described for two-colour STED analysis. The following antibody combinations were employed: M2AP- anti rabbit ATTO 594/MIC2- anti mouse ATTO 647, M2AP- anti rabbit ATTO 594/MIC3- anti mouse ATTO 647, MIC8- anti rabbit ATTO 594/AMA1- anti mouse ATTO 647, MIC8- anti rabbit ATTO 594/MIC3- anti mouse ATTO 647 and as a control M2AP-anti rabbit ATTO 594/M2AP-anti rabbit ATTO 647. After immunostaining, the infected host cell layers were embedded in melamine. Subsequent to polymerisation, cell layers were detached from the glass coverslip and cut into 100nm thin-sections with an ultramicrotome. The thin-sections were then embedded in Mowiol 4-88/DABCO mounting media and STED analysis with an additional deconvolution step (STED<sup>+</sup>) was followed. The results and quantification of the co-localisation are displayed in Figure 6-4. M2AP was dually labelled with both fluorescent dyes (ATTO 594 and ATTO 647) as a positive control for co-localisation. As expected nearly 100% co-localisation could be observed, reflected in a Pearson correlation coefficient of almost 1. Comparing the co-localisation of M2AP and MIC2, a high degree of co-localisation could be observed as well. This confirmed former observations (Figure 6-3). For the co-stain of M2AP and MIC3 it could be detected that the two signals were not overlapping and did not co-localise, as seen for M2AP/MIC2. The same could be detected for the co-stains with MIC8/AMA1 and MIC8/MIC3. However, for these three co-stains, overlapping regions could be detected close to the parasite's surface. Since quantification was performed with whole images the correlation coefficients were all above 0.5, which indicate partial co-localisation.

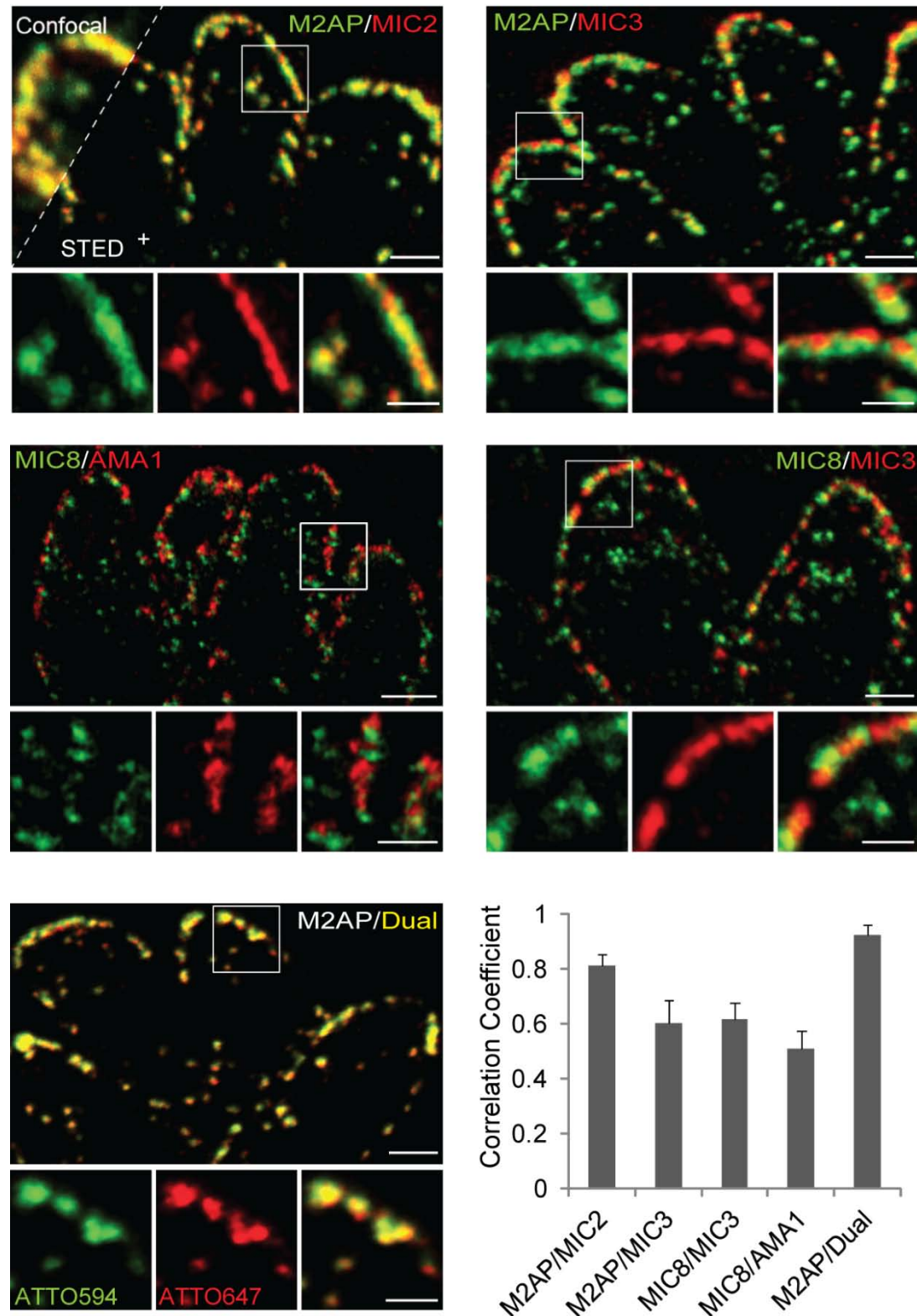


**Figure 6-4: Two-colour STED images of typical microneme co-localisation patterns in 100nm ultrathin sections.** (A) Intracellular RH<sup>hxcprt</sup> parasites were immunolabelled with indicated antibody combinations. Confocal and STED<sup>+</sup> (linear deconvoluted) resolution is shown for M2AP/MIC2. As a positive co-localisation control dual labelling of M2AP with a mixture of ATTO 594- and ATTO 647N-labelled secondary antibodies (M2AP/Dual) was performed. Scale bars for the overview images represent 1  $\mu$ m and for close-up images 0.5  $\mu$ m. (B) Quantification of the correlation between indicated micronemal marker proteins from (A) by calculating the Pearson's correlation coefficient. Thin-sectioning, STED imaging and quantification was performed by Dirk Kamin. The Images were taken from (Kremer, Kamin et al. 2013).

## 6.4. Summary and conclusions

Within this chapter it was analysed if micronemes are organised into different subsets with different protein contents in *T. gondii* tachyzoites. According to the observations made in chapter 4 and 5, it was assumed, that at least two different subsets of micronemes could exist. One subset would contain microneme proteins (MIC2, M2AP, AMA1) taking a TgRab5A,5C independent trafficking pathway, and another subset would contain proteins with an TgRab5A,5C dependent transport pathway to their target organelles (MIC3, MIC8 and MIC11). In consequence, microneme proteins of different subsets would show different localisation patterns. Since the resolution of confocal microscopic imaging is not sufficient to examine this, STED microscopy was applied on RH<sup>hxppt</sup> parasites in collaboration with the group of Stefan Hell in Heidelberg and Goettingen.

First, “single-colour STED analysis” was performed to optimise the conditions for sample preparation and STED setups to gain the best possible resolution. Performing “single-colour STED” with different combinations of dilutions for primary and secondary antibodies resulted in images with a resolution of up to 30nm. By that, a clear improvement in resolving single micronemes in the apical part of the parasites could be reached compared to confocal images (Figure 6-2). Here, different localisation patterns for different microneme proteins became detectable. The localisation patterns for MIC2 and its associating protein M2AP were noticeably similar, whereas MIC3 and MIC8 exhibited different signal patterns. Interestingly MIC3 showed a signal with lots of spots, probably single micronemes, arranged in lines along the apical half of the parasites. This arrangement is reminiscent of the organisation of subpellicular microtubules of the apical complex (Hu, Johnson et al. 2006).

Performing “two-colour STED analysis” with parasites dually labelled with  $\alpha$ -MIC2/ $\alpha$ -M2AP and  $\alpha$ -MIC3/ $\alpha$ -M2AP could confirm the observations made in “single-colour STED”. The complex forming proteins MIC2 and M2AP exhibited the same localisation signals, resulting in co-localisation signals, whereas for MIC3 and M2AP no significant co-localisation could be detected except for the area of the apical tip. There the resolution was not high enough to distinguish between individual signals. The observations made for single- and two-colours

STED analysis could be confirmed again in “two-colour STED analysis” with 100nm thin sectioned parasites. In most parts, especially in the apical half, of the parasites, M2AP and MIC2 showed perfect co-localisation. Dual-labelling of parasites with  $\alpha$ -MIC8/  $\alpha$ -AMA1 and  $\alpha$ -MIC3/  $\alpha$ -M2AP showed mainly no co-localisation. This could indicate that M2AP and MIC2 share the same transport pathway. The different localisations for MIC8 and AMA1 could indicate different transport routes and/or different target organelles. This also applies for M2AP and MIC3. Interestingly, no co-localisation could be observed for  $\alpha$ -MIC3 and  $\alpha$ -MIC8. This could indicate that there are more than two subsets of micronemes or microneme proteins and that more than two trafficking pathways for microneme proteins could exist in *T.gondii*. However, microneme signals close to the parasite’s surface could not be resolved properly. Whether these signals were microneme proteins within micronemes close to the surface or already secreted micronemes at the plasma membrane needs to be further investigated. Co-localisation within this region could be detected for all antibody combinations, but significantly less for  $\alpha$ -MIC8/  $\alpha$ -AMA1,  $\alpha$ -MIC3/  $\alpha$ -M2AP,  $\alpha$ -MIC8/  $\alpha$ -MIC3 than for  $\alpha$ -MIC2/ $\alpha$ -M2AP. This tendency is reflecting what could be seen in areas, which didn’t show a high signal density. So it is most likely, that these signals could be microneme protein signals located within micronemes next to the surface.

The internal dimensions of micronemes ranges from 75nm to 150nm (Carruthers and Tomley 2008). With a resolution of 30nm it is possible that detected non-co localising signals were coming from proteins located within one organelle. So if different microneme proteins are equally distributed to micronemal organelles, then the observations made in this chapter indicate, that microneme proteins are clustered in different membrane domains within the micronemal membrane. This kind of compartmentalisation of organelles or vesicles is also known from endosomes (Sonnichsen, De Renzis et al. 2000).

Taken the different localisation signals of different microneme proteins observed in this chapter one can say, that at least two different trafficking pathways exist for microneme proteins. Either microneme proteins are transported to micronemal organelles with different protein contents and/or they are arranged in different membrane compartments within the micronemes.

## 7. Discussion

In this study, vesicular trafficking in *Toxoplasma gondii*, focusing on the trafficking of microneme and rhoptry proteins and the biogenesis of their organelles, TgRab GTPases were analysed. In order to investigate this, the ddFKBP system (Herm-Gotz, Agop-Nersesian et al. 2007) was utilised. This system allows for the rapid regulation of protein levels of a protein of interest (POI) and has been successfully applied for TgRab11A (Agop-Nersesian, Naissant et al. 2009) and TgRab11B (Agop-Nersesian, Egarter et al. 2010). As recently shown for these two TgRab proteins, the regulated overexpression of Rab wild type (wt) and dominant negative (DN) allows localisation and functional studies.

The presence of 15 Rab proteins in the *T.gondii* genome (Langsley, van Noort et al. 2008) was confirmed in this work (Figure 3-1). Three Rab genes were excluded from our analysis (chapter 3.3.). Since the function of TgRab6, TgRab11A and TgRab11B have previously been characterised (Stedman, Sussmann et al. 2003; Agop-Nersesian, Naissant et al. 2009; Agop-Nersesian, Egarter et al. 2010), it was decided to analyse the remaining 9 TgRab proteins. In order to determine the function of these genes, stable transfected parasites expressing ddFKBPMyc-tagged versions of TgRab1A, 1B, 2, 4, 5A, 5C, 7, 18 and TgRab5B-HAddFKBP were generated and co-localisation studies performed. For all experiments, Shield-1 dependent regulation of protein levels was confirmed (Figure 3-2) and the Shield-1 concentration was adjusted to the lowest functional level in order to minimise the risk of artefacts due to overexpression of the respective protein.

Interestingly, none of the Rabs could be found to co-localise with the apical secretory organelles. Instead, TgRab1B, TgRab2 and TgRab18 could be identified to localise to the early secretory pathway (Figure 3-4), TgRab4 to the Golgi (Figure 3-5) and TgRab5A, TgRab5B, TgRab5C and TgRab7 to the late secretory pathway (Figure 3-7, 3-8). No exact localisation of TgRab1A could be determined (Figure 3-6).

Screening for phenotypes caused by overexpression of the different ddFKBPMyc/HA-tagged Rabs, revealed that parasite growth was ablated for TgRab2, 4 5A,5B and 5C (Figure 4-1). To identify Rabs that play a crucial role in vesicular transport to the apicomplexan-specific secretory organelles, the

localisation of the microneme proteins MIC2 and MIC3 and of the rhoptry proteins ROP2,3,4 were analysed in parasites overexpressing TgRab2,4 5A,5B and 5C. Only overexpression of TgRab5A and 5C resulted in a specific trafficking defect to rhoptries and micronemes (Figure 4-2). This indicates that TgRab2, 4 and 5B are essential for *T.gondii* tachyzoites, but are not directly involved in the secretory pathway of these microneme or rhoptry proteins.

## **7.1 Rab proteins and their potential functions in *T.gondii***

Within the next paragraphs I summarise our investigations and published data to present a model how and where I propose Rab proteins regulate vesicular trafficking in *T.gondii*.

### **7.1.1. Rab proteins of the early secretory pathway and the Golgi**

Localisation analysis of TgRab1B and TgRab2 led to the suggestion that these TgRab proteins play a role in the transport of vesicles between the ER and the Golgi, as has been established in higher eukaryotes. Rab1 proteins are involved in the regulation of the anterograde transport between ER and cis-Golgi and also in intra-Golgi vesicle transport in plants (Batoko, Zheng et al. 2000), mammals (Plutner, Cox et al. 1991; Tisdale, Bourne et al. 1992) and yeast (Jedd, Richardson et al. 1995). Rab2 has been shown to be involved in COPI vesicle trafficking between ER and Golgi in mammalian (Tisdale, Bourne et al. 1992; Tisdale and Jackson 1998) and plant cells (Cheung, Chen et al. 2002). No Rab2 homolog is present in yeast. In recent studies it was shown that Rab1 and Rab2 show distinct localisations, phenotypes and functions in *Trypanosoma brucei* (Dhir, Goulding et al. 2004). Reduction in Rab protein level led to delayed export of the variant surface glycoprotein (VSG) from the parasite. It was suggested that both Rab proteins act sequentially in the same early secretory pathway. TbRab1 was suggested to be involved in the maintenance of the Golgi and TbRab2 involved in the maturation of pre-Golgi intermediates, as predicted from mammalian studies (Tisdale and Balch 1996). This indicates a conserved function of these two Rab proteins between mammals and single celled eukaryotes, suggesting that this role may be maintained in *T.gondii*. In plants, Rab2 was shown to be essential for secreted proteins in tip growth cells (Cheung, Chen et

al. 2002). These data were suggested to support the hypothesis that activities performed by Rab2 are specific for cells with a high demand on secretion, offering a suggestion as to why Rab2 is not present in yeast. Since secretion is important in *T.gondii* tachyzoites and TgRab2 was shown to be essential for their growth (Figure 4-1), a similar role within the early secretory pathway, as found in plants and *Trypanosoma brucei*, could be suggested. No effect on microneme or rhoptry protein localisation could be detected when TgRab2 was overexpressed (Figure 4-2), leading to the assumption that TgRab2 is not directly involved in their secretory pathway. Since further investigations, including dominant negative mutants and knock out studies are still pending; the functions of TgRab1B and TgRab2 remain hypothetical.

Among higher eukaryotes, Rab18 exhibits various functions. Its main appearance is in vesicular transport between ER and Golgi (Dejgaard, Murshid et al. 2008). As TgRab18 could be localised at the ER-Golgi area in *T.gondii* tachyzoites (Figure 3-4), a similar functional role is posited. Nevertheless, the involvement of Rab18 in lipid transport pathways in mammalian cells (Martin, Driessen et al. 2005; Ozeki, Cheng et al. 2005) and the existence of membrane contact sites (MCS) between the ER and the apicoplast in *T.gondii* (Tomova, Humbel et al. 2009) would make TgRab18 an interesting candidate to study lipid transport in *T.gondii*. Overexpression of TgRab18 did not result in a significant growth defect. However, Rab18 is only present in apicomplexan parasites that build a parasitophorous vacuole membrane (PVM), which can be seen as an additional specialised "organelle" important for the parasites survival in terms of nutrient acquisition and protection from innate defense (Sinai 2008; Spielmann, Montagna et al. 2012), emphasising the benefit of further studies investigating the function of TgRab18 via trans-dominant mutants or knock-out studies.

Rab4 is associated with early endosomes in higher eukaryotes and involved in endocytosis, especially in the receptor recycling pathway (Van Der Sluijs, Hull et al. 1991; Conti, Sertic et al. 2009). No Rab4 homolog has been identified in plant cells and interestingly, Rab4 has been shown to be involved in lysosomal traffic in *Trypanosoma brucei* (Hall, Pal et al. 2004) demonstrating that its function is not strictly conserved. This was confirmed with my data, where Rab4 localises predominantly at the Golgi and only rarely with the endosomal-like compartment (ELC) in *T.gondii* (Figure 3-5). We have shown that overexpression

of TgRab4 causes a block in growth; however microneme and rhoptry proteins remained unaffected. No phenotype was observed for parasites expressing a dominant negative version of TgRab4 (Diploma thesis of Sabine Mahler, University of Heidelberg). Sabine Mahler also showed that overexpression of TgRab4 did not affect dense granule proteins and that parasites showed a reduced ability to egress host cells naturally. Further analyses needs to be undertaken to investigate the functional role of TgRab4. The absence of a Rab4 homolog in *Plasmodium*, *Theileria* and *Babesia* makes Rab4 an interesting candidate to study how Rab proteins and vesicular trafficking are different in protozoan parasites, reflecting different environmental challenges.

Another TgRab localised at the Golgi is TgRab6. This Rab protein was not analysed in this study as it has already been described in the literature to be involved in retrograde transport from post-Golgi secretory granules to the Golgi (Stedman, Sussmann et al. 2003). Recently, Rab6 was shown to act within trans-Golgi trafficking of clathrin coated and COPI-coated vesicles and suggested to be important for the maintenance of Golgi homeostasis in human cells (Storrie, Micaroni et al. 2012). Unpublished data (Breinich et al. submitted) utilising the *T.gondii* clathrin heavy chain I (CHCI) indicates an essential role for clathrin in the formation of vesicles at the trans-Golgi network and for Golgi function and segregation. Since clathrin was also shown to be required for constitutive secretion in *T.gondii* (Breinich et al. submitted), a regulating role for TgRab6 in these clathrin coated vesicles is possible.

### **7.1.2. Rab proteins of the late secretory pathway**

TgRab11A has been shown to localise to rhoptries and the Inner Membrane Complex (IMC) during replication (Bradley, Ward et al. 2005; Agop-Nersesian, Naissant et al. 2009). Both TgRab11A and 11B are required for IMC biogenesis with TgRab11B appearing to act prior to TgRab11A during replication (Agop-Nersesian, Naissant et al. 2009; Agop-Nersesian, Egarter et al. 2010).

Rab1A and Rab1B share a high sequence homology (Touchot, Zahraoui et al. 1989). However, it has been shown that both paralogs exhibit different functions in mammalian cells and yeast (Plutner, Cox et al. 1991; Tisdale, Bourne et al. 1992; Jedd, Richardson et al. 1995; Sclafani, Chen et al. 2010; Mukhopadhyay, Nieves et al. 2011). In *Plasmodium*, a Rab1 paralog was identified as alveolate

specific and named Rab1A. Functional differences between PfRab1A and PfRab1B were assumed (Elias, Patron et al. 2009). In our studies we could confirm this alveolate specific phylogenetic pattern for Rab1A (Kremer, Kamin et al. 2013). Furthermore, we identified a different localisation for TgRab1A compared to TgRab1B, suggesting different functional roles of these Rab proteins in *T.gondii* (Figure 3-4, 3-6). Overexpression of TgRab1A led to a severe growth defect (Figure 4-1), however since this effect could not be observed with expression of a dominant negative mutant (Figure 4-4), TgRab1A was not further analysed and its role remains unexplored. However, due to its unique localisation pattern (Figure 3-6), knock-out studies and further characterisation of TgRab1A would be worthwhile to uncover the function of Rab1A.

In higher eukaryotes, Rab7 is found to be localised at early and late endosomes and is important for the maintenance of endocytic organelles. Rab7 also plays a key role in vesicular trafficking between early and late endosomes and between late endosomes and lysosomes (Chavrier, Parton et al. 1990; Meresse, Gorvel et al. 1995; Mukhopadhyay, Funato et al. 1997; Bucci, Thomsen et al. 2000; Vonderheit and Helenius 2005; Stenmark 2009; Vanlandingham and Ceresa 2009). In *T.gondii* TgRab7 was shown to localise at compartments, which are thought to be endosomal-like compartments (ELCs) (Miranda, Pace et al. 2010; Parussini, Coppens et al. 2010). This could be confirmed within this work (Figure 3-7). Miranda and colleagues observed that overexpressed haemagglutinin (HA) epitope tagged TgRab7 localised as a ring around TgVP1 in intracellular parasites. Interestingly this wasn't detected by Parussini and colleagues and I could not confirm this specific observation either. This difference in TgRab7 localisation might be due to different conditions during the assays or due to the use of different host cell lines and the exact cause remains to be investigated.

Since overexpression of the wild type Rab7 or expression of trans-dominant mutants has been shown to effect vesicular trafficking between endosome organelles or trafficking between endosomes and lysosomes in other organisms (Chavrier, Parton et al. 1990; Meresse, Gorvel et al. 1995; Mukhopadhyay, Funato et al. 1997; Bucci, Thomsen et al. 2000; Vonderheit and Helenius 2005; Stenmark 2009; Vanlandingham and Ceresa 2009), one would expect that overexpression or expression of a trans-dominant mutant of TgRab7 is affecting proteins within (TgVP1, proM2AP or TgCPL) or transported via the ELCs (M2AP or

MIC3). Except for TgCPL ELCs, microneme and rhoptry proteins remained unaffected (Figure 4-2, 4-11, 4-12). TgCPL exhibited a slightly denser localisation signal, when the dominant active version of TgRab7 was expressed, but pulse chase experiments showed, that CPL maturation remained normal in these parasites (Figure 4-13). Growth-, replication-, induced egress- and invasion- analysis revealed that a growth block, a late effect on replication and a significant reduction in invasion ability (Figure 4-7, 4-8, 4-9, 4-10) were only observed, when the dominant active version of TgRab7 was expressed. In summary one can say, that TgRab7 is not directly involved in vesicular trafficking of microneme or rhoptry proteins or in the biogenesis of their secretory organelles. Since Rab7 has been shown in other eukaryotes to be involved in trafficking of proteins from the late endosomes to the lysosome (see above) this pathway might have been adapted, in the case of apicomplexan parasites, to target overexpressed proteins to a lysosome-like compartment.

A potential role of TgRab7 in autophagy could not be investigated within this work due to lack of time. The role of Rab7 in maturation of autophagosomes and its impact on autophagy in higher eukaryotes were reported over the last years (Gutierrez, Munafo et al. 2004; Hyttinen, Niittykoski et al. 2013). Also in apicomplexans autophagy became an increasing subject to study. By using an autophagosome membrane marker, TgATG8, autophagic vesicles could be detected in dividing tachyzoites (Besteiro 2012). It would be interesting to study, if TgRab7 plays a similar role in final maturation of autophagic vacuoles as reported in HeLa cells (Jager, Bucci et al. 2004). A conditional knock-down mutant of the TgATG8 interacting protein TgATG3 was causing growth arrest and revealed a function of TgATG3 in mitochondrion homeostasis (Besteiro, Brooks et al. 2011). Rhoptries and micronemes remained unaffected in these parasites. In *Plasmodium berghei* and *Plasmodium falciparum* ATG8 was localised at the apicoplast (Kitamura, Kishi-Itakura et al. 2012; Eickel, Kaiser et al. 2013). Future knock-out studies with TgRab7 could be useful to investigate its role in autophagy and to study if autophagy is linked with lipid remodelling and vice versa as seen in higher eukaryotes (Dall'Armi, Devereaux et al. 2013; Lapierre, Silvestrini et al. 2013).

Rab7 and Rab5 are both involved in endocytosis in higher eukaryotes and assumed to act sequentially (Mukhopadhyay, Barbieri et al. 1997; Bottanelli,

Gershlick et al. 2011). There are three isoforms of Rab5 (Rab5A, Rab5B and Rab5C), which are involved in endocytosis and endosome biogenesis in mammalian cells (Zeigerer, Gilleron et al. 2012). Also three isoforms of Rab5 could be found in yeast and plants. The yeast Rab5 homologues Vps21/Ypt51p, Ypt52p, Ypt53p can be grouped together and are also involved in endocytic membrane traffic and responsible for correct sorting of vacuolar hydrolases (Singer-Kruger, Stenmark et al. 1994). Interestingly, two classes of Rab5 proteins were identified in plants. Rha1 and Ara7 share a very high sequence homology (Sohn, Kim et al. 2003), whereas Ara6 is a Rab5 protein only found in plant cells. Rha1 and Ara7 exhibit the typical prenylation motif at the C-terminus, which Ara6 does not have. Therefore a N-terminal myristoylation site could be identified (Ueda, Yamaguchi et al. 2001). Since both Rab5 classes show partial but no identical co-localisation at endosomes they are thought to function differently (Ebine, Fujimoto et al. 2011). All these observation on plant Rab5 proteins could reflect a similar situation in *T.gondii*. In our studies, we could also identify two classes of Rab5 proteins in Toxoplasma, TgRab5A and TgRab5C, which would correspond to Rha1 and Ara7, and TgRab5B, which would correspond to Ara6. Like in plants, TgRab5A and 5C share high sequence homology and exhibit a C-terminal prenylation motif, whereas TgRab5B has a N-terminal myristoylation site (Figure 3-1). In our localisation studies we came to the conclusion, that both *T.gondii* classes (TgRab5A,5C and TgRab5B) could exhibit different functions in tachyzoites. In plants, Rab5 proteins are mainly involved in vesicular trafficking to the vacuole, an organelle of the secretory pathway (Sohn, Kim et al. 2003; Bolte, Brown et al. 2004; Kotzer, Brandizzi et al. 2004; Bottanelli, Gershlick et al. 2011). Since all three TgRab5 proteins were mainly detected in the area of the endosomal-like compartments (Figure 3-8) an involvement in vesicular trafficking of microneme and/or rhoptry proteins was assumed. Overexpression or expression of a dominant negative version of all three TgRab5 proteins confirmed again, that TgRab5A and Rab5C are involved in the same pathway, as opposed to TgRab5B (Figure 4-2, 4-15, 5-2). No direct effect on microneme or rhoptry proteins could be detected for parasites overexpressing TgRab5B or expressing its dominant negative version, but proliferation was severely decreased or blocked (Figure 4-14, 4-15). Both overexpression of TgRab5A, 5C or expression of their dominant negative versions (TgRab5A(N158I), TgRab5C(N153I)) exhibited identical phenotypes. Here rhoptry

proteins (ROP5, ROP2,3,4) and only a subset of microneme proteins (MIC3, MIC8 and MIC11) were constitutively secreted into the PV or the PM respectively, whereas AMA1, MIC2 and M2AP were not directly affected (Figure 5-6, 5-7, 5-8)). By that we identified for the first time that a Rab protein is involved in the regulation of the transport of microneme and rhoptry proteins.

TgRab5A was earlier reported as TgRab51 to be localised at a compartment, which is thought to be an early endosome. All later publications are referring to this, when they were talking about early endosomes in *T.gondii*. TgRab51 was assumed to be involved in Golgi-endosome transport and being involved in host-cholesterol uptake (Robibaro, Stedman et al. 2002). We cannot rule out an indirect effect of TgRab5A,5C in Golgi-Endosome transport as suggested from Robibaro and colleagues (Robibaro, Stedman et al. 2002), but since our data show rerouting of MIC3 after processing in the ELCs (Figure 5-9), we assume that TgRab5A and 5C act at a later step. How the parasite is maintaining the balance of membrane components of organelles involved in biosynthesis and secretory organelles remains a mystery. Since no working tool was established so far to show or investigate endocytosis in *T.gondii*, endocytosis remains a controversial topic in this field. Gaining more information about the function of TgRab5 proteins could certainly help to understand the situation of post-Golgi organelles (ELCs), since more and more data reveals, that proteins classically known to be involved in endocytosis in higher eukaryotes are essential for the biogenesis of apicomplexan unique organelles micronemes, rhoptries and the apicoplast (Agop-Nersesian, Naissant et al. 2009; Breinich, Ferguson et al. 2009; van Dooren, Reiff et al. 2009; Agop-Nersesian, Egarter et al. 2010; Tawk, Dubremetz et al. 2011; Sloves, Delhaye et al. 2012). A potential connection between TgRab5 proteins and apicoplast biogenesis cannot be excluded. In yeast and mammalian cells Rab5 or VPS21 are assumed to be involved in the PI(3)P synthesis (Bridges, Fisher et al. 2012). In apicomplexans PI(3)P was detected at the apicoplast and at apicoplast protein-shuttling vesicles in apicomplexa (Tawk, Chicanne et al. 2010; Tawk, Dubremetz et al. 2011). Inhibition of the PI3P synthesising kinase, which is a Rab5 effector (VPS34) in higher eukaryotes, interfered with the biogenesis of the apicoplast, known for its crucial role in lipid synthesis. Recently cholesterol acquired from the host cell was also found in apicoplast membranes in *Plasmodium falciparum* (Botte, Yamaro-Botte et al.

2013). Although except for the rhoptries and micronemes, all other organelles, including the apicoplast remained unaffected, when TgRab5A function was interfered (Figure 5-10) an indirect involvement of TgRab5 proteins in vesicular trafficking to the apicoplast cannot be excluded. From there, lipids could be transported via membrane contact sites (Tomova, Humbel et al. 2009) to the ER to supply the ER with membrane components needed for further secretory pathways. This would put TgRab5 in a key position of the biosynthetic processes of secretory proteins. Here TgRab5B would be an especially interesting candidate for further functional characterisation. Its occasional localisation at the plasma membrane (Figure 3-8) could be an indication of crucial lipid and protein transfer via exocytosis or endocytosis.

## **7.2. Distinct transport routes to the micronemes**

In good agreement with our data, all microneme and rhoptry trafficking mutants described so far correspond to homologues of the yeast VPS (vacuolar protein sorting) system. The dynamin related protein B (DrpB) is a homologue of VPS1 (Breinich, Ferguson et al. 2009), Sortilin (TgSORTLR) of VPS10 and Rab5A and RabC are homologues of VPS21. In yeast these mutants were identified by screening for transport defects of carboxypeptidase Y (CPY) to the yeast vacuole, which is analogous to the lysosome (Rothman and Stevens 1986; Valls, Hunter et al. 1987; Robinson, Kliensky et al. 1988). Interestingly, their abrogation in yeast leads to the constitutive secretion of CPY, a phenotype observed here for rhoptry and microneme proteins. Similarities between rhoptries and secretory lysosomes have been pointed out (Ngo, Yang et al. 2004) and it is tempting to speculate that micronemes and rhoptries are derived from lysosomal organelles. Therefore the data presented in this study is consistent with the parasite modifying parts of its endocytic system, giving rise to the formation of unique organelles, required for intracellular parasitism.

Based on the localisation studies, I assume TgRab5A,B and C to function at the ELCs. From there TgRab5A and C are directly involved in the regulation of the transport of rhoptry proteins and microneme proteins. Due to the lack of data, I cannot say, if immature micronemes or rhoptries are formed first to mature into their final organelles and if TgRab5A and 5C are involved in their formation.

Since I showed, that overexpression of TgRab5A and TgRab5C and expression of their dominant negative mutants is causing constitutive secretion of rhoptry proteins (ROP5, ROP2,3,4) and only a subset of microneme proteins (MIC3, MIC8 and MIC11) I also identified for the first time that at least two different subsets of microneme proteins exist in *T.gondii*. This observation led me to the assumption, that different pathways for microneme protein trafficking might exist. Although it is possible that redundant pathways are in place that can complement functional abrogation of Rab5A and C, I assume at least one TgRab5A,5C dependent (for MIC3, MIC8 and MIC11) and one TgRab5A,5C independent (for AMA1, MIC2 and M2AP) pathway. Unfortunately I was not able to identify the trafficking pathways involved in the transport of the second subset of microneme proteins (MIC2, M2AP and AMA1).

We also showed that no rhoptries and 70% less micronemes were detectable on ultrastructural level, when TgRab5A function was impaired (Figure 5-11). As I know from the Dynamin B mutant, where all microneme and rhoptry proteins were constitutively secreted and no rhoptry or micronemes could be detected on ultrastructural level, affected parasites could replicate normally and exhibited blocked invasion and egress ability (Breinich, Ferguson et al. 2009). As expected, overexpression of TgRab5A,5C or expression of their dominant negative versions didn't affect intracellular replication (Figure 5-3). No clear block, but a significant decrease of the egress ability and an invasion block could be detected in these parasite lines (Figure 5-4, 5-5). Comparing the DrpB phenotype with our observations I hypothesise that, besides different transport pathways for different subsets of microneme proteins, the possibility exist, that micronemes consist of different and functionally distinct organelles. Invasion and egress was blocked, when all microneme proteins were secreted in DrpB dominant negative parasites (Breinich, Ferguson et al. 2009), but egress was only decreased and not blocked when TgRab5A,5C was overexpressed or the dominant negative version expressed, while invasion was blocked. In conclusion, it might be possible, that the TgRab5A,5C dependent subset would be exclusively necessary for invasion and the other subset would be necessary for egress and probably for gliding too. Recent data from our group, which shows that MIC2 (Andenmatten, Egarter et al. 2013) and AMA1(Andenmatten et al. under preparation) are not required for

invasion, strengthens this theory. However further investigations to functionally group microneme proteins and to show their different localisation are required.

To test whether micronemes are in fact made up of multiple subsets we employed two-colour STED measurements on ultra-thin sections to finely pinpoint the location of different microneme proteins. We found that only few microneme proteins, such as MIC2 and M2AP that are known to form a complex (Huynh, Rabenau et al. 2003), co-localise (Figure 6-3, 6-4). In contrast substantially less co-localisation was observed for several other microneme proteins (Figure 6-4), suggesting the presence of different subsets of micronemes with independent protein content. Alternatively, the differential localisation could reflect organisation of micronemal proteins into sub-compartments, similar to the rhoptries, where proteins are either localised in the bulb, or the neck of the organelle (Boothroyd and Dubremetz 2008). Further investigations to clarify the composition of micronemes would give a clearer picture of the organisation and regulation of host cell invasion, especially since the traditional model might need to be reconsidered (see chapter 1.4.1).

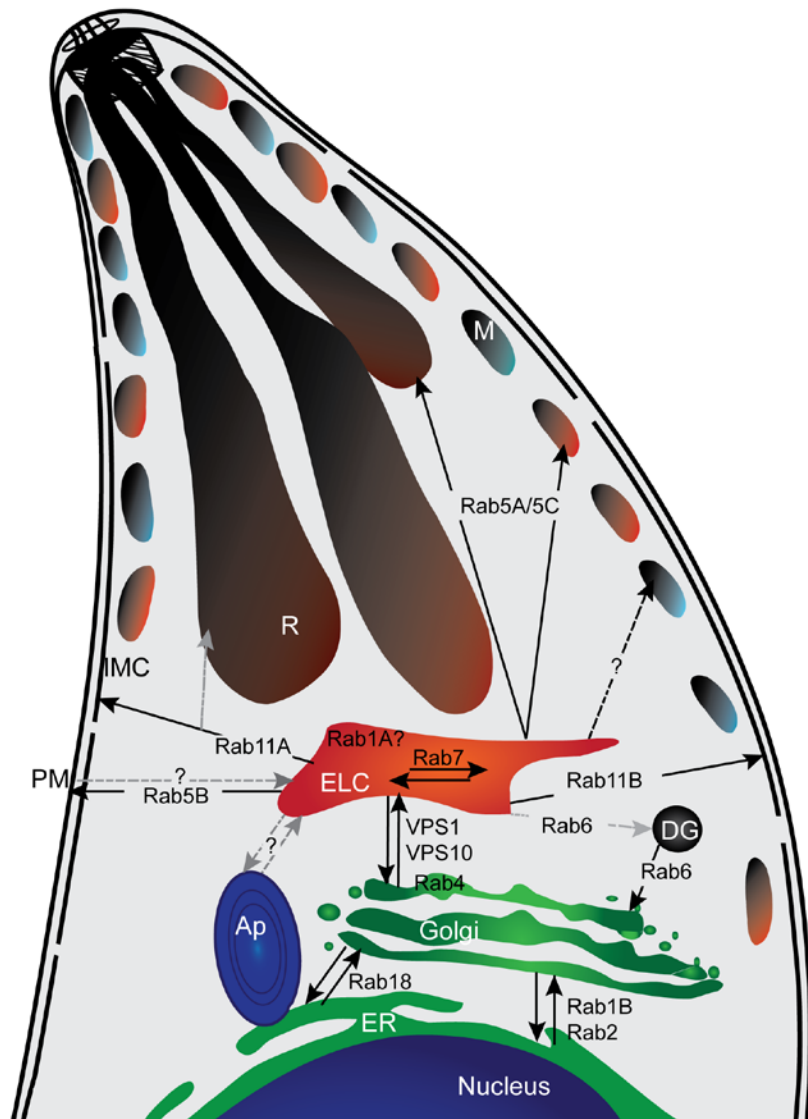


**Figure 7-1: Model of Rab locations and potential functions in *T.gondii*.** The cartoon is showing the apical half of a *T.gondii* tachyzoite with its organelles and Rab proteins, where I propose them to regulate vesicles. Rab18, Rab1B and Rab2 are cycling between the endoplasmic reticulum (ER) and Golgi. Rab1B and Rab2 are thought to be sequentially involved in the same pathway. Rab4 is probably regulating intra-Golgi transfer, but could also be involved in vesicular trafficking between endosomal like compartments (ELCs) and the Golgi, like VPS1 (DrpB) and VPS10 (SORTLR). Rab7 is probably involved in trafficking between ELCs. Rab6 is thought to regulate the retrograde transport between post-Golgi secretory granules and the Golgi (Stedman, Sussmann et al. 2003). It is not clear, if these granules are dense granules or their precursors, which could mature to dense granules (DG). To simplify the model, I just labelled them as DG. Since Rab6 could also be localised at the ELCs, I assume Rab6 regulated transport from there to the DGs (dashed arrow line in grey). I also assume vesicular trafficking between the Apicoplast (Ap) and ELCs. Rab11A and Rab11B are reported to be involved in transport to the inner membrane complex (IMC) (Agop-Nersesian, Naissant et al. 2009; Agop-Nersesian, Egarter et al. 2010). Rab11A was also localised at and found in the rhoptries (R) (Bradley, Ward et al. 2005), but if and how trafficking to the rhoptries is Rab11A regulated is not clear (grey dashed arrow line). Rab5A,B and C were all localised at the ELCs. Rab5B is probably involved in vesicular transport to the plasma membrane (PM). An endocytic pathway from there to the ELCs is controversial, but cannot be excluded (grey dashed arrowline, questionmark). Rab5A and C are involved in vesicular trafficking to the rhoptries and one subset of microneme proteins (MIC3, MIC8, MIC11), whereas another subset of microneme proteins (AMA1, M2AP, MIC2) would be Rab5A,C independently transported to the micronemes (M). I don't know via which pathway and how it is regulated so far (dashed arrow line and questionmark). I also hypothesise that at least two different types of micronemal organelles with different protein content exist. One subset would contain RabA and C dependently transported proteins (black/red) and the other subset (black/blue) the Rab5A,C independently transported proteins.

## 7.3 Future work

### 7.3.1. Investigating TgRab functions

The localisation studies presented in this work were giving us a general impression of Rab proteins and their potential functions in *T.gondii*. They can be taken as starting points to analyse the protein and lipid transports in the parasite. To draw any conclusions from the localisation of TgRab proteins to their functions the Rab protein of interest (ROI) should be endogenously tagged. Here the introduced method (Huynh and Carruthers 2009) would provide a fast strategy for C-terminal YFP-tagging, which would also enable live cell imaging to follow vesicles labelled with the respective Rab proteins. Another option to C-terminally tag the ROI would be the strategy established in *T.gondii* by Manuela Breinich (Breinich et al, submitted). Here the ROI becomes endogenously HA-tagged and could be conditionally knocked out, at the same time, to study its function. It should be noted that C-terminal tagging could interfere with the prenylation motif of most Rab proteins and it may be possible that it cannot be used indiscriminately. If interference with the prenylation motif can be excluded by detecting the correct localisation of the HA tagged ROI, this strategy might still be an option to analyse potential interacting proteins like effector proteins or Rab activators via immunoprecipitations. It might also be possible to purify HA-Rab labelled vesicles or organelles to analyse their contents as recently shown for apicoplast purification in *Plasmodium falciparum* (Botte, Yamaro-Botte et al. 2013). This would give us more ideas of the function of the respective Rab protein and would be a potential tool to analyse the composition and nature of post-Golgi organelles.

A more elegant way to tag a ROI and to generate a knock-out mutant at the same time would be the recently established gene swap strategy (Andenmatten, Egarter et al. 2013). Here the Rab protein can also be N-terminally expressed to perform interaction studies.

Another and more classical approach to gain more information about the function of a Rab protein would be to bioinformatically assess the databases for homologs of effector proteins in the *T.gondii* genome, similar to what was done for *Plasmodium* Rab interaction factors (Rached, Ndjembo-Ezougou et al. 2011), and to continue with specific knock-outs. Yeast-two hybrid screens could be an

option as well to identify TgRab interacting proteins but wouldn't be the tool of our first choice, since the used Rab proteins are not in their natural environment and false identifications are most likely.

### **7.3.2. Functionally different microneme subset**

In our studies we showed, that TgRab5A and 5C are directly involved in the trafficking of rhoptry and some microneme proteins. More detailed time course experiments could be performed to investigate, which organelles are first affected, rhoptries or micronemes. It is known that rhoptries are formed before micronemes (Nishi, Hu et al. 2008) and since conditional knock-out studies with TgMIC8 showed, that the rhoptry protein RON4 could not be secreted anymore (Kessler, Herm-Gotz et al. 2008), secretion of rhoptry proteins affecting microneme secretion or vice versa could be a scenario.

After some microneme proteins (PFROM1, PFSUB1) were identified to be present in additional secretory organelles (mononemes and exonemes) in *Plasmodium* (Singh, Plassmeyer et al. 2007; Yeoh, O'Donnell et al. 2007), we could show for the first time that at least two different subsets of microneme proteins exist in *T.gondii*. We conclude that one subset (MIC8, MIC3 and MIC11) is transported TgRab5A,5C dependently to the micronemes and that the other subset (MIC2, M2AP and AMA1) is TgRab5A,5C independent. We also hypothesised that at least two different subsets of functionally different micronemes exist. Unfortunately we were not able to proof the existence of micronemes with different protein contents by using STED. With STED it would be very time-consuming to generate 3D high resolution images of the apical tip of the parasite. Since Z-stack imaging is not applicable thin sections need to be made, imaged and reconstructed to a 3D whole parasite image. Due to the thickness (100nm) of the sections, the resulting image would be less detailed than z-stack images. Also live cell imaging with STED is not applicable, since image taking would be too slow for processes in vesicular trafficking. Here imaging techniques like FRAP (fluorescence recovery after photobleaching) or the application of photoactivatable proteins (Patterson and Lippincott-Schwartz 2002) might be combined with high resolution imaging like SIM (Structured Illumination Microscopy) to follow fluorescent labelled microneme proteins on its way through the late secretory pathway in *T.gondii* tachyzoites.

The distance between two different microneme proteins could be measured by using FRET (Fluorescence resonance energy transfer), but since micronemes are sometimes arranged so close to each other that different MICs localised in different micronemes would be as close as MICs localised within one microneme our possibilities to investigate micronemes with different protein content via fluorescent imaging techniques are limited. Also Immuno-EM was not very successful for microneme proteins so far and double labelled immuno EM even less. To proof our hypothesis of micronemes equipped with different microneme proteins, tools to sort and purify differently labelled micronemes to analyse their protein contents need to be established.

## REFERENCES

- Agop-Nersesian, C., S. Egarter, et al. (2010). "Biogenesis of the inner membrane complex is dependent on vesicular transport by the alveolate specific GTPase Rab11B." PLoS Pathog **6**(7): e1001029.
- Agop-Nersesian, C., B. Naissant, et al. (2009). "Rab11A-controlled assembly of the inner membrane complex is required for completion of apicomplexan cytokinesis." PLoS Pathog **5**(1): e1000270.
- Ahn, H. J., S. Kim, et al. (2006). "Interactions between secreted GRA proteins and host cell proteins across the parasitophorous vacuolar membrane in the parasitism of *Toxoplasma gondii*." Korean J Parasitol **44**(4): 303-312.
- Ahn, H. J., S. Kim, et al. (2005). "Host cell binding of GRA10, a novel, constitutively secreted dense granular protein from *Toxoplasma gondii*." Biochem Biophys Res Commun **331**(2): 614-620.
- Alexander, D. L., J. Mital, et al. (2005). "Identification of the moving junction complex of *Toxoplasma gondii*: a collaboration between distinct secretory organelles." PLoS Pathog **1**(2): e17.
- Altschul, S. F., W. Gish, et al. (1990). "Basic local alignment search tool." J Mol Biol **215**(3): 403-410.
- Andenmatten, N., S. Egarter, et al. (2013). "Conditional genome engineering in *Toxoplasma gondii* uncovers alternative invasion mechanisms." Nat Methods **10**(2): 125-127.
- Armstrong, C. M. and D. E. Goldberg (2007). "An FKBP destabilization domain modulates protein levels in *Plasmodium falciparum*." Nat Methods **4**(12): 1007-1009.
- Arrizabalaga, G. and J. C. Boothroyd (2004). "Role of calcium during *Toxoplasma gondii* invasion and egress." Int J Parasitol **34**(3): 361-368.
- Arvan, P. and D. Castle (1998). "Sorting and storage during secretory granule biogenesis: looking backward and looking forward." Biochem J **332** ( Pt 3): 593-610.
- Arvan, P., R. Kuliawat, et al. (1991). "Protein discharge from immature secretory granules displays both regulated and constitutive characteristics." J Biol Chem **266**(22): 14171-14174.
- Ashton, N. (1979). "Ocular toxoplasmosis in wallabies (*Macropus rufogriseus*)." Am J Ophthalmol **88**(3 Pt 1): 322-332.
- Banaszynski, L. A., C. W. Liu, et al. (2005). "Characterization of the FKBP.rapamycin.FRB ternary complex." J Am Chem Soc **127**(13): 4715-4721.
- Barlowe, C., L. Orci, et al. (1994). "COPII: a membrane coat formed by Sec proteins that drive vesicle budding from the endoplasmic reticulum." Cell **77**(6): 895-907.
- Batoko, H., H. Q. Zheng, et al. (2000). "A rab1 GTPase is required for transport between the endoplasmic reticulum and golgi apparatus and for normal golgi movement in plants." Plant Cell **12**(11): 2201-2218.
- Beck, J. R., I. A. Rodriguez-Fernandez, et al. (2010). "A novel family of *Toxoplasma* IMC proteins displays a hierarchical organization and functions in coordinating parasite division." PLoS Pathog **6**(9): e1001094.
- Beckers, C. J., T. Wakefield, et al. (1997). "The expression of *Toxoplasma* proteins in *Neospora caninum* and the identification of a gene encoding a novel rhoptry protein." Mol Biochem Parasitol **89**(2): 209-223.
- Besteiro, S. (2012). "Which roles for autophagy in *Toxoplasma gondii* and related apicomplexan parasites?" Mol Biochem Parasitol **184**(1): 1-8.
- Besteiro, S., C. F. Brooks, et al. (2011). "Autophagy protein Atg3 is essential for maintaining mitochondrial integrity and for normal intracellular development of *Toxoplasma gondii* tachyzoites." PLoS Pathog **7**(12): e1002416.
- Besteiro, S., A. Michelin, et al. (2009). "Export of a *Toxoplasma gondii* rhoptry neck protein complex at the host cell membrane to form the moving junction during invasion." PLoS Pathog **5**(2): e1000309.

- Black, M., F. Seeber, et al. (1995). "Restriction enzyme-mediated integration elevates transformation frequency and enables co-transfection of *Toxoplasma gondii*." Mol Biochem Parasitol **74**(1): 55-63.
- Black, M. W., G. Arrizabalaga, et al. (2000). "Ionophore-resistant mutants of *Toxoplasma gondii* reveal host cell permeabilization as an early event in egress." Mol Cell Biol **20**(24): 9399-9408.
- Bolte, S., S. Brown, et al. (2004). "The N-myristoylated Rab-GTPase m-Rabmc is involved in post-Golgi trafficking events to the lytic vacuole in plant cells." J Cell Sci **117**(Pt 6): 943-954.
- Bonifacino, J. S. and B. S. Glick (2004). "The mechanisms of vesicle budding and fusion." Cell **116**(2): 153-166.
- Bonifacino, J. S. and J. Lippincott-Schwartz (2003). "Coat proteins: shaping membrane transport." Nat Rev Mol Cell Biol **4**(5): 409-414.
- Boothroyd, J. C. and J. F. Dubremetz (2008). "Kiss and spit: the dual roles of *Toxoplasma* rhoptries." Nat Rev Microbiol **6**(1): 79-88.
- Bottanelli, F., D. C. Gershlick, et al. (2011). "Evidence for sequential action of Rab5 and Rab7 GTPases in prevacuolar organelle partitioning." Traffic **13**(2): 338-354.
- Botte, C. Y., Y. Yamaryo-Botte, et al. (2013). "Atypical lipid composition in the purified relict plastid (apicoplast) of malaria parasites." Proc Natl Acad Sci U S A **110**(18): 7506-7511.
- Bougdour, A., E. Durandau, et al. (2013). "Host cell subversion by *Toxoplasma* GRA16, an exported dense granule protein that targets the host cell nucleus and alters gene expression." Cell Host Microbe **13**(4): 489-500.
- Bradley, P. J. and J. C. Boothroyd (2001). "The pro region of *Toxoplasma* ROP1 is a rhoptry-targeting signal." Int J Parasitol **31**(11): 1177-1186.
- Bradley, P. J., N. Li, et al. (2004). "A GFP-based motif-trap reveals a novel mechanism of targeting for the *Toxoplasma* ROP4 protein." Mol Biochem Parasitol **137**(1): 111-120.
- Bradley, P. J., C. Ward, et al. (2005). "Proteomic analysis of rhoptry organelles reveals many novel constituents for host-parasite interactions in *Toxoplasma gondii*." J Biol Chem **280**(40): 34245-34258.
- Brecht, S., V. B. Carruthers, et al. (2001). "The *Toxoplasma* micronemal protein MIC4 is an adhesin composed of six conserved apple domains." J Biol Chem **276**(6): 4119-4127.
- Breinich, M. S., D. J. Ferguson, et al. (2009). "A dynamin is required for the biogenesis of secretory organelles in *Toxoplasma gondii*." Curr Biol **19**(4): 277-286.
- Bridges, D., K. Fisher, et al. (2012). "Rab5 proteins regulate activation and localization of target of rapamycin complex 1." J Biol Chem **287**(25): 20913-20921.
- Brighouse, A., J. B. Dacks, et al. (2010). "Rab protein evolution and the history of the eukaryotic endomembrane system." Cell Mol Life Sci **67**(20): 3449-3465.
- Brossier, F., T. J. Jewett, et al. (2003). "C-terminal processing of the *Toxoplasma* protein MIC2 is essential for invasion into host cells." J Biol Chem **278**(8): 6229-6234.
- Brown, M. S. and J. L. Goldstein (1979). "Receptor-mediated endocytosis: insights from the lipoprotein receptor system." Proc Natl Acad Sci U S A **76**(7): 3330-3337.
- Brydges, S. D., G. D. Sherman, et al. (2000). "Molecular characterization of TgMIC5, a proteolytically processed antigen secreted from the micronemes of *Toxoplasma gondii*." Mol Biochem Parasitol **111**(1): 51-66.
- Bucci, C., R. G. Parton, et al. (1992). "The small GTPase rab5 functions as a regulatory factor in the early endocytic pathway." Cell **70**(5): 715-728.
- Bucci, C., P. Thomsen, et al. (2000). "Rab7: a key to lysosome biogenesis." Mol Biol Cell **11**(2): 467-480.
- Buguliskis, J. S., F. Brossier, et al. (2010). "Rhomboïd 4 (ROM4) affects the processing of surface adhesins and facilitates host cell invasion by *Toxoplasma gondii*." PLoS Pathog **6**(4): e1000858.
- Burgess, T. L. and R. B. Kelly (1987). "Constitutive and regulated secretion of proteins." Annu Rev Cell Biol **3**: 243-293.
- Burnette, W. N. (1981). "Western blotting": electrophoretic transfer of proteins from sodium dodecyl sulfate--polyacrylamide gels to unmodified nitrocellulose and radiographic detection with antibody and radioiodinated protein A." Anal Biochem **112**(2): 195-203.

- Carey, K. L., A. M. Jongco, et al. (2004). "The *Toxoplasma gondii* rhopty protein ROP4 is secreted into the parasitophorous vacuole and becomes phosphorylated in infected cells." Eukaryot Cell **3**(5): 1320-1330.
- Carpenter, G. (1987). "Receptors for epidermal growth factor and other polypeptide mitogens." Annu Rev Biochem **56**: 881-914.
- Carroll, K. S., J. Hanna, et al. (2001). "Role of Rab9 GTPase in facilitating receptor recruitment by TIP47." Science **292**(5520): 1373-1376.
- Carruthers, V. and J. C. Boothroyd (2007). "Pulling together: an integrated model of *Toxoplasma* cell invasion." Curr Opin Microbiol **10**(1): 83-89.
- Carruthers, V. B. (1999). "Armed and dangerous: *Toxoplasma gondii* uses an arsenal of secretory proteins to infect host cells." Parasitol Int **48**(1): 1-10.
- Carruthers, V. B., S. N. Moreno, et al. (1999). "Ethanol and acetaldehyde elevate intracellular [Ca<sup>2+</sup>] and stimulate microneme discharge in *Toxoplasma gondii*." Biochem J **342** ( Pt 2): 379-386.
- Carruthers, V. B. and L. D. Sibley (1997). "Sequential protein secretion from three distinct organelles of *Toxoplasma gondii* accompanies invasion of human fibroblasts." Eur J Cell Biol **73**(2): 114-123.
- Carruthers, V. B. and F. M. Tomley (2008). "Microneme proteins in apicomplexans." Subcell Biochem **47**: 33-45.
- Casavola, E. C., A. Catucci, et al. (2008). "Ypt32p and Mlc1p bind within the vesicle binding region of the class V myosin Myo2p globular tail domain." Mol Microbiol **67**(5): 1051-1066.
- Cerede, O., J. F. Dubremetz, et al. (2002). "The *Toxoplasma gondii* protein MIC3 requires pro-peptide cleavage and dimerization to function as adhesin." EMBO J **21**(11): 2526-2536.
- Cesbron-Delauw, M. F., C. Gendrin, et al. (2008). "Apicomplexa in mammalian cells: trafficking to the parasitophorous vacuole." Traffic **9**(5): 657-664.
- Chandramohanadas, R., P. H. Davis, et al. (2009). "Apicomplexan parasites co-opt host calpains to facilitate their escape from infected cells." Science **324**(5928): 794-797.
- Chaturvedi, S., H. Qi, et al. (1999). "Constitutive calcium-independent release of *Toxoplasma gondii* dense granules occurs through the NSF/SNAP/SNARE/Rab machinery." J Biol Chem **274**(4): 2424-2431.
- Chavrier, P., R. G. Parton, et al. (1990). "Localization of low molecular weight GTP binding proteins to exocytic and endocytic compartments." Cell **62**(2): 317-329.
- Cheung, A. Y., C. Y. Chen, et al. (2002). "Rab2 GTPase regulates vesicle trafficking between the endoplasmic reticulum and the Golgi bodies and is important to pollen tube growth." Plant Cell **14**(4): 945-962.
- Christoforidis, S., M. Miaczynska, et al. (1999). "Phosphatidylinositol-3-OH kinases are Rab5 effectors." Nat Cell Biol **1**(4): 249-252.
- Colicelli, J. (2004). "Human RAS superfamily proteins and related GTPases." Sci STKE **2004**(250): RE13.
- Collins, C. R. and M. J. Blackman (2011). "Apicomplexan AMA1 in host cell invasion: a model at the junction?" Cell Host Microbe **10**(6): 531-533.
- Conti, F., S. Sertic, et al. (2009). "Intracellular trafficking of the human oxytocin receptor: evidence of receptor recycling via a Rab4/Rab5 "short cycle"." Am J Physiol Endocrinol Metab **296**(3): E532-542.
- Dall'Armi, C., K. A. Devereaux, et al. (2013). "The role of lipids in the control of autophagy." Curr Biol **23**(1): R33-45.
- de Castro, F. A., G. E. Ward, et al. (1996). "Identification of a family of Rab G-proteins in *Plasmodium falciparum* and a detailed characterisation of pfrab6." Mol Biochem Parasitol **80**(1): 77-88.
- Dejgaard, S. Y., A. Murshid, et al. (2008). "Rab18 and Rab43 have key roles in ER-Golgi trafficking." J Cell Sci **121**(Pt 16): 2768-2781.
- Dhir, V., D. Goulding, et al. (2004). "TbRAB1 and TbRAB2 mediate trafficking through the early secretory pathway of *Trypanosoma brucei*." Mol Biochem Parasitol **137**(2): 253-265.

- Di Cristina, M., R. Spaccapelo, et al. (2000). "Two conserved amino acid motifs mediate protein targeting to the micronemes of the apicomplexan parasite *Toxoplasma gondii*." Mol Cell Biol **20**(19): 7332-7341.
- Dobrowolski, J. M., V. B. Carruthers, et al. (1997). "Participation of myosin in gliding motility and host cell invasion by *Toxoplasma gondii*." Mol Microbiol **26**(1): 163-173.
- Docampo, R., W. de Souza, et al. (2005). "Acidocalcisomes - conserved from bacteria to man." Nat Rev Microbiol **3**(3): 251-261.
- Donahue, C. G., V. B. Carruthers, et al. (2000). "The *Toxoplasma* homolog of Plasmodium apical membrane antigen-1 (AMA-1) is a microneme protein secreted in response to elevated intracellular calcium levels." Mol Biochem Parasitol **111**(1): 15-30.
- Donald, R. G., D. Carter, et al. (1996). "Insertional tagging, cloning, and expression of the *Toxoplasma gondii* hypoxanthine-xanthine-guanine phosphoribosyltransferase gene. Use as a selectable marker for stable transformation." J Biol Chem **271**(24): 14010-14019.
- Donald, R. G. and D. S. Roos (1993). "Stable molecular transformation of *Toxoplasma gondii*: a selectable dihydrofolate reductase-thymidylate synthase marker based on drug-resistance mutations in malaria." Proc Natl Acad Sci U S A **90**(24): 11703-11707.
- Drozdowicz, Y. M., M. Shaw, et al. (2003). "Isolation and characterization of TgVP1, a type I vacuolar H<sup>+</sup>-translocating pyrophosphatase from *Toxoplasma gondii*. The dynamics of its subcellular localization and the cellular effects of a diphosphonate inhibitor." J Biol Chem **278**(2): 1075-1085.
- Dubey, J. P., D. S. Lindsay, et al. (1998). "Structures of *Toxoplasma gondii* tachyzoites, bradyzoites, and sporozoites and biology and development of tissue cysts." Clin Microbiol Rev **11**(2): 267-299.
- Dubey, J. P., N. L. Miller, et al. (1970). "Characterization of the new fecal form of *Toxoplasma gondii*." J Parasitol **56**(3): 447-456.
- Dubey, J. P., J. P. Sundberg, et al. (1981). "Toxoplasmosis associated with abortion in goats and sheep in Connecticut." Am J Vet Res **42**(9): 1624-1626.
- Dubremetz, J. F. (2007). "Rhoptries are major players in *Toxoplasma gondii* invasion and host cell interaction." Cell Microbiol **9**(4): 841-848.
- Dubremetz, J. F., N. Garcia-Reguet, et al. (1998). "Apical organelles and host-cell invasion by Apicomplexa." Int J Parasitol **28**(7): 1007-1013.
- Dunn, J. D., S. Ravindran, et al. (2008). "The *Toxoplasma gondii* dense granule protein GRA7 is phosphorylated upon invasion and forms an unexpected association with the rhoptry proteins ROP2 and ROP4." Infect Immun **76**(12): 5853-5861.
- Dziadek, B. and A. Brzostek (2012). "Recombinant ROP2, ROP4, GRA4 and SAG1 antigen-cocktails as possible tools for immunoprophylaxis of toxoplasmosis: What's next?" Bioengineered **3**(6): 358-364.
- Ebine, K., M. Fujimoto, et al. (2011). "A membrane trafficking pathway regulated by the plant-specific RAB GTPase ARA6." Nat Cell Biol **13**(7): 853-859.
- Edwards, S. L., N. K. Charlie, et al. (2009). "Impaired dense core vesicle maturation in *Caenorhabditis elegans* mutants lacking Rab2." J Cell Biol **186**(6): 881-895.
- Eickel, N., G. Kaiser, et al. (2013). "Features of autophagic cell death in Plasmodium liver-stage parasites." Autophagy **9**(4): 568-580.
- El Hajj, H., M. Lebrun, et al. (2007). "Inverted topology of the *Toxoplasma gondii* ROP5 rhoptry protein provides new insights into the association of the ROP2 protein family with the parasitophorous vacuole membrane." Cell Microbiol **9**(1): 54-64.
- El Hajj, H., J. Papoin, et al. (2008). "Molecular signals in the trafficking of *Toxoplasma gondii* protein MIC3 to the micronemes." Eukaryot Cell **7**(6): 1019-1028.
- Elias, M., A. Brighouse, et al. (2012). "Sculpting the endomembrane system in deep time: high resolution phylogenetics of Rab GTPases." J Cell Sci **125**(Pt 10): 2500-2508.
- Elias, M., N. J. Patron, et al. (2009). "The RAB family GTPase Rab1A from Plasmodium falciparum defines a unique paralog shared by chromalveolates and rhizaria." J Eukaryot Microbiol **56**(4): 348-356.
- Endo, T., K. K. Sethi, et al. (1982). "*Toxoplasma gondii*: calcium ionophore A23187-mediated exit of trophozoites from infected murine macrophages." Exp Parasitol **53**(2): 179-188.

- Fentress, S. J., T. Steinfeldt, et al. (2012). "The arginine-rich N-terminal domain of ROP18 is necessary for vacuole targeting and virulence of *Toxoplasma gondii*." Cell Microbiol **14**(12): 1921-1933.
- Foth, B. J., S. A. Ralph, et al. (2003). "Dissecting apicoplast targeting in the malaria parasite *Plasmodium falciparum*." Science **299**(5607): 705-708.
- Foussard, F., M. A. Leriche, et al. (1991). "Characterization of the lipid content of *Toxoplasma gondii* rhoptries." Parasitology **102 Pt 3**: 367-370.
- Fox, B. A., J. G. Ristuccia, et al. (2009). "Efficient gene replacements in *Toxoplasma gondii* strains deficient for nonhomologous end joining." Eukaryot Cell **8**(4): 520-529.
- Frenal, K., V. Polonais, et al. (2010). "Functional dissection of the apicomplexan glideosome molecular architecture." Cell Host Microbe **8**(4): 343-357.
- Fujita-Yoshigaki, J., Y. Dohke, et al. (1999). "Presence of a complex containing vesicle-associated membrane protein 2 in rat parotid acinar cells and its disassembly upon activation of cAMP-dependent protein kinase." J Biol Chem **274**(33): 23642-23646.
- Garcia-Reguet, N., M. Lebrun, et al. (2000). "The microneme protein MIC3 of *Toxoplasma gondii* is a secretory adhesin that binds to both the surface of the host cells and the surface of the parasite." Cell Microbiol **2**(4): 353-364.
- Gardner, M. J., N. Hall, et al. (2002). "Genome sequence of the human malaria parasite *Plasmodium falciparum*." Nature **419**(6906): 498-511.
- Gaskins, E., S. Gilk, et al. (2004). "Identification of the membrane receptor of a class XIV myosin in *Toxoplasma gondii*." J Cell Biol **165**(3): 383-393.
- Gerdes, H. H. (2008). "Membrane traffic in the secretory pathway." Cell Mol Life Sci **65**(18): 2779-2780.
- Ghelis, T., O. Dellis, et al. (2000). "Abscisic acid specific expression of RAB18 involves activation of anion channels in *Arabidopsis thaliana* suspension cells." FEBS Lett **474**(1): 43-47.
- Ghosh, P., N. M. Dahms, et al. (2003). "Mannose 6-phosphate receptors: new twists in the tale." Nat Rev Mol Cell Biol **4**(3): 202-212.
- Gilbert, L. A., S. Ravindran, et al. (2007). "*Toxoplasma gondii* targets a protein phosphatase 2C to the nuclei of infected host cells." Eukaryot Cell **6**(1): 73-83.
- Giovannini, D., S. Spath, et al. (2011). "Independent roles of apical membrane antigen 1 and rhoptry neck proteins during host cell invasion by apicomplexa." Cell Host Microbe **10**(6): 591-602.
- Girod, A., B. Storrie, et al. (1999). "Evidence for a COP-I-independent transport route from the Golgi complex to the endoplasmic reticulum." Nat Cell Biol **1**(7): 423-430.
- Goud, B., A. Zahraoui, et al. (1990). "Small GTP-binding protein associated with Golgi cisternae." Nature **345**(6275): 553-556.
- Grant, B. D. and J. G. Donaldson (2009). "Pathways and mechanisms of endocytic recycling." Nat Rev Mol Cell Biol **10**(9): 597-608.
- Gray, M. W., B. F. Lang, et al. (2004). "Mitochondria of protists." Annu Rev Genet **38**: 477-524.
- Griffiths, G. and K. Simons (1986). "The trans Golgi network: sorting at the exit site of the Golgi complex." Science **234**(4775): 438-443.
- Gruenberg, J. (2003). "Lipids in endocytic membrane transport and sorting." Curr Opin Cell Biol **15**(4): 382-388.
- Gruenberg, J. and H. Stenmark (2004). "The biogenesis of multivesicular endosomes." Nat Rev Mol Cell Biol **5**(4): 317-323.
- Gutierrez, M. G., D. B. Munafo, et al. (2004). "Rab7 is required for the normal progression of the autophagic pathway in mammalian cells." J Cell Sci **117**(Pt 13): 2687-2697.
- Hakansson, S., A. J. Charron, et al. (2001). "*Toxoplasma* evacuoles: a two-step process of secretion and fusion forms the parasitophorous vacuole." EMBO J **20**(12): 3132-3144.
- Hales, C. M., J. P. Vaerman, et al. (2002). "Rab11 family interacting protein 2 associates with Myosin Vb and regulates plasma membrane recycling." J Biol Chem **277**(52): 50415-50421.
- Hall, B. S., A. Pal, et al. (2004). "Rab4 is an essential regulator of lysosomal trafficking in trypanosomes." J Biol Chem **279**(43): 45047-45056.

- Harper, J. M., M. H. Huynh, et al. (2006). "A cleavable propeptide influences Toxoplasma infection by facilitating the trafficking and secretion of the TgMIC2-M2AP invasion complex." *Mol Biol Cell* **17**(10): 4551-4563.
- Harper, J. M., X. W. Zhou, et al. (2004). "The novel coccidian micronemal protein MIC11 undergoes proteolytic maturation by sequential cleavage to remove an internal propeptide." *Int J Parasitol* **34**(9): 1047-1058.
- Haugwitz, M., O. Nourzaie, et al. (2008). "ProteoTuner: a novel system with rapid kinetics enables reversible control of protein levels in cells and organisms." *Biotechniques* **44**(3): 432-433.
- Heasman, S. J. and A. J. Ridley (2008). "Mammalian Rho GTPases: new insights into their functions from in vivo studies." *Nat Rev Mol Cell Biol* **9**(9): 690-701.
- Hebert, D. N. and M. Molinari (2007). "In and out of the ER: protein folding, quality control, degradation, and related human diseases." *Physiol Rev* **87**(4): 1377-1408.
- Hehl, A. B., C. Lekutis, et al. (2000). "Toxoplasma gondii homologue of plasmodium apical membrane antigen 1 is involved in invasion of host cells." *Infect Immun* **68**(12): 7078-7086.
- Hell, S. W., M. Dyba, et al. (2004). "Concepts for nanoscale resolution in fluorescence microscopy." *Curr Opin Neurobiol* **14**(5): 599-609.
- Hell, S. W. and J. Wichmann (1994). "Breaking the diffraction resolution limit by stimulated emission: stimulated-emission-depletion fluorescence microscopy." *Opt Lett* **19**(11): 780-782.
- Herm-Gotz, A., C. Agop-Nersesian, et al. (2007). "Rapid control of protein level in the apicomplexan Toxoplasma gondii." *Nat Methods* **4**(12): 1003-1005.
- Hilfiker, S., A. J. Czernik, et al. (2001). "Tonically active protein kinase A regulates neurotransmitter release at the squid giant synapse." *J Physiol* **531**(Pt 1): 141-146.
- Hill, D. E., S. Chirukandoth, et al. (2005). "Biology and epidemiology of Toxoplasma gondii in man and animals." *Anim Health Res Rev* **6**(1): 41-61.
- Hoepfner, S., F. Severin, et al. (2005). "Modulation of receptor recycling and degradation by the endosomal kinesin KIF16B." *Cell* **121**(3): 437-450.
- Howell, S. A., F. Hackett, et al. (2005). "Distinct mechanisms govern proteolytic shedding of a key invasion protein in apicomplexan pathogens." *Mol Microbiol* **57**(5): 1342-1356.
- Hu, K., J. Johnson, et al. (2006). "Cytoskeletal components of an invasion machine--the apical complex of Toxoplasma gondii." *PLoS Pathog* **2**(2): e13.
- Hu, K., D. S. Roos, et al. (2002). "A novel polymer of tubulin forms the conoid of Toxoplasma gondii." *J Cell Biol* **156**(6): 1039-1050.
- Hutagalung, A. H. and P. J. Novick (2011). "Role of Rab GTPases in membrane traffic and cell physiology." *Physiol Rev* **91**(1): 119-149.
- Huynh, M. H. and V. B. Carruthers (2006). "Toxoplasma MIC2 is a major determinant of invasion and virulence." *PLoS Pathog* **2**(8): e84.
- Huynh, M. H. and V. B. Carruthers (2009). "Tagging of endogenous genes in a Toxoplasma gondii strain lacking Ku80." *Eukaryot Cell* **8**(4): 530-539.
- Huynh, M. H., K. E. Rabenau, et al. (2003). "Rapid invasion of host cells by Toxoplasma requires secretion of the MIC2-M2AP adhesive protein complex." *EMBO J* **22**(9): 2082-2090.
- Hyttinen, J. M., M. Niittykoski, et al. (2013). "Maturation of autophagosomes and endosomes: a key role for Rab7." *Biochim Biophys Acta* **1833**(3): 503-510.
- Itzen, A. and R. S. Goody (2010). "GTPases involved in vesicular trafficking: structures and mechanisms." *Semin Cell Dev Biol* **22**(1): 48-56.
- Jager, S., C. Bucci, et al. (2004). "Role for Rab7 in maturation of late autophagic vacuoles." *J Cell Sci* **117**(Pt 20): 4837-4848.
- Janoo, R., A. Musoke, et al. (1999). "A Rab1 homologue with a novel isoprenylation signal provides insight into the secretory pathway of Theileria parva." *Mol Biochem Parasitol* **102**(1): 131-143.
- Jedd, G., C. Richardson, et al. (1995). "The Ypt1 GTPase is essential for the first two steps of the yeast secretory pathway." *J Cell Biol* **131**(3): 583-590.
- Jewett, T. J. and L. D. Sibley (2004). "The toxoplasma proteins MIC2 and M2AP form a hexameric complex necessary for intracellular survival." *J Biol Chem* **279**(10): 9362-9369.

- Kaasch, A. J. and K. A. Joiner (2000). "Protein-targeting determinants in the secretory pathway of apicomplexan parasites." *Curr Opin Microbiol* **3**(4): 422-428.
- Kafsack, B. F. and V. B. Carruthers (2010). "Apicomplexan perforin-like proteins." *Commun Integr Biol* **3**(1): 18-23.
- Kafsack, B. F., J. D. Pena, et al. (2009). "Rapid membrane disruption by a perforin-like protein facilitates parasite exit from host cells." *Science* **323**(5913): 530-533.
- Kalanon, M., C. J. Tonkin, et al. (2009). "Characterization of two putative protein translocation components in the apicoplast of *Plasmodium falciparum*." *Eukaryot Cell* **8**(8): 1146-1154.
- Karsten, V., H. Qi, et al. (1998). "The protozoan parasite *Toxoplasma gondii* targets proteins to dense granules and the vacuolar space using both conserved and unusual mechanisms." *J Cell Biol* **141**(6): 1323-1333.
- Kashiwazaki, J., T. Iwaki, et al. (2009). "Two fission yeast rab7 homologs, ypt7 and ypt71, play antagonistic roles in the regulation of vacuolar morphology." *Traffic* **10**(7): 912-924.
- Katz, B. and R. Miledi (1967). "The timing of calcium action during neuromuscular transmission." *J Physiol* **189**(3): 535-544.
- Keeley, A. and D. Soldati (2004). "The glideosome: a molecular machine powering motility and host-cell invasion by Apicomplexa." *Trends Cell Biol* **14**(10): 528-532.
- Kessler, H., A. Herm-Gotz, et al. (2008). "Microneme protein 8--a new essential invasion factor in *Toxoplasma gondii*." *J Cell Sci* **121**(Pt 7): 947-956.
- Kim, K., D. Soldati, et al. (1993). "Gene replacement in *Toxoplasma gondii* with chloramphenicol acetyltransferase as selectable marker." *Science* **262**(5135): 911-914.
- Kirchhausen, T. (2000). "Three ways to make a vesicle." *Nat Rev Mol Cell Biol* **1**(3): 187-198.
- Kitamura, K., C. Kishi-Itakura, et al. (2012). "Autophagy-related Atg8 localizes to the apicoplast of the human malaria parasite *Plasmodium falciparum*." *PLoS One* **7**(8): e42977.
- Köhler, S., C. F. Delwiche, et al. (1997). "A plastid of probable green algal origin in Apicomplexan parasites." *Science* **275**(5305): 1485-1489.
- Kornfeld, S. (1987). "Trafficking of lysosomal enzymes." *FASEB J* **1**(6): 462-468.
- Kotzer, A. M., F. Brandizzi, et al. (2004). "AtRabF2b (Ara7) acts on the vacuolar trafficking pathway in tobacco leaf epidermal cells." *J Cell Sci* **117**(Pt 26): 6377-6389.
- Kremer, K., D. Kamin, et al. (2013). "An Overexpression Screen of *Toxoplasma gondii* Rab-GTPases Reveals Distinct Transport Routes to the Micronemes." *PLoS Pathog* **9**(3): e1003213.
- Kuliawat, R. and P. Arvan (1994). "Distinct molecular mechanisms for protein sorting within immature secretory granules of pancreatic beta-cells." *J Cell Biol* **126**(1): 77-86.
- Labruyere, E., M. Lingnau, et al. (1999). "Differential membrane targeting of the secretory proteins GRA4 and GRA6 within the parasitophorous vacuole formed by *Toxoplasma gondii*." *Mol Biochem Parasitol* **102**(2): 311-324.
- Laemmli, U. K. (1970). "Cleavage of structural proteins during the assembly of the head of bacteriophage T4." *Nature* **227**(5259): 680-685.
- Lagal, V., E. M. Binder, et al. (2010). "*Toxoplasma gondii* protease TgSUB1 is required for cell surface processing of micronemal adhesive complexes and efficient adhesion of tachyzoites." *Cell Microbiol* **12**(12): 1792-1808.
- Lamarque, M., S. Besteiro, et al. (2011). "The RON2-AMA1 interaction is a critical step in moving junction-dependent invasion by apicomplexan parasites." *PLoS Pathog* **7**(2): e1001276.
- Langsley, G., V. van Noort, et al. (2008). "Comparative genomics of the Rab protein family in Apicomplexan parasites." *Microbes Infect* **10**(5): 462-470.
- Lapierre, L. R., M. J. Silvestrini, et al. (2013). "Autophagy genes are required for normal lipid levels in *C. elegans*." *Autophagy* **9**(3): 278-286.
- Lebrun, M., A. Michelin, et al. (2005). "The rhoptry neck protein RON4 re-localizes at the moving junction during *Toxoplasma gondii* invasion." *Cell Microbiol* **7**(12): 1823-1833.
- Lee, M. T., A. Mishra, et al. (2009). "Structural mechanisms for regulation of membrane traffic by rab GTPases." *Traffic* **10**(10): 1377-1389.
- Letourneur, F., E. C. Gaynor, et al. (1994). "Coatomer is essential for retrieval of dilysine-tagged proteins to the endoplasmic reticulum." *Cell* **79**(7): 1199-1207.

- Liendo, A., T. T. Stedman, et al. (2001). "Toxoplasma gondii ADP-ribosylation factor 1 mediates enhanced release of constitutively secreted dense granule proteins." *J Biol Chem* **276**(21): 18272-18281.
- Lipatova, Z., A. A. Tokarev, et al. (2008). "Direct interaction between a myosin V motor and the Rab GTPases Ypt31/32 is required for polarized secretion." *Mol Biol Cell* **19**(10): 4177-4187.
- Lovett, J. L. and L. D. Sibley (2003). "Intracellular calcium stores in Toxoplasma gondii govern invasion of host cells." *J Cell Sci* **116**(Pt 14): 3009-3016.
- Luo, S., M. Vieira, et al. (2001). "A plasma membrane-type Ca(2+)-ATPase co-localizes with a vacuolar H(+)-pyrophosphatase to acidocalcisomes of Toxoplasma gondii." *EMBO J* **20**(1-2): 55-64.
- Luzio, J. P., P. R. Pryor, et al. (2007). "Lysosomes: fusion and function." *Nat Rev Mol Cell Biol* **8**(8): 622-632.
- Mann, T. and C. Beckers (2001). "Characterization of the subpellicular network, a filamentous membrane skeletal component in the parasite Toxoplasma gondii." *Mol Biochem Parasitol* **115**(2): 257-268.
- Martin, S. (2001). "Congenital toxoplasmosis." *Neonatal Netw* **20**(4): 23-30.
- Martin, S., K. Driessen, et al. (2005). "Regulated localization of Rab18 to lipid droplets: effects of lipolytic stimulation and inhibition of lipid droplet catabolism." *J Biol Chem* **280**(51): 42325-42335.
- Maxfield, F. R. and T. E. McGraw (2004). "Endocytic recycling." *Nat Rev Mol Cell Biol* **5**(2): 121-132.
- McBride, H. M., V. Rybin, et al. (1999). "Oligomeric complexes link Rab5 effectors with NSF and drive membrane fusion via interactions between EEA1 and syntaxin 13." *Cell* **98**(3): 377-386.
- McLauchlan, H., J. Newell, et al. (1998). "A novel role for Rab5-GDI in ligand sequestration into clathrin-coated pits." *Curr Biol* **8**(1): 34-45.
- Meissner, M., D. Schluter, et al. (2002). "Role of Toxoplasma gondii myosin A in powering parasite gliding and host cell invasion." *Science* **298**(5594): 837-840.
- Mercier, C., M. F. Cesbron-Delauw, et al. (1998). "The amphipathic alpha helices of the toxoplasma protein GRA2 mediate post-secretory membrane association." *J Cell Sci* **111** (Pt 15): 2171-2180.
- Meresse, S., J. P. Gorvel, et al. (1995). "The rab7 GTPase resides on a vesicular compartment connected to lysosomes." *J Cell Sci* **108** ( Pt 11): 3349-3358.
- Messina, M., I. Niesman, et al. (1995). "Stable DNA transformation of Toxoplasma gondii using phleomycin selection." *Gene* **165**(2): 213-217.
- Miller, S. A., V. Thathy, et al. (2003). "TgSUB2 is a Toxoplasma gondii rhoptry organelle processing proteinase." *Mol Microbiol* **49**(4): 883-894.
- Miranda, K., D. A. Pace, et al. (2010). "Characterization of a novel organelle in Toxoplasma gondii with similar composition and function to the plant vacuole." *Mol Microbiol* **76**(6): 1358-1375.
- Mital, J., M. Meissner, et al. (2005). "Conditional expression of Toxoplasma gondii apical membrane antigen-1 (TgAMA1) demonstrates that TgAMA1 plays a critical role in host cell invasion." *Mol Biol Cell* **16**(9): 4341-4349.
- Mittenhuber, G. (2001). "Comparative genomics of prokaryotic GTP-binding proteins (the Era, Obg, EngA, ThdF (TrmE), YchF and YihA families) and their relationship to eukaryotic GTP-binding proteins (the DRG, ARF, RAB, RAN, RAS and RHO families)." *J Mol Microbiol Biotechnol* **3**(1): 21-35.
- Miyagishima, S. Y. (2005). "Origin and evolution of the chloroplast division machinery." *J Plant Res* **118**(5): 295-306.
- Morisaki, J. H., J. E. Heuser, et al. (1995). "Invasion of Toxoplasma gondii occurs by active penetration of the host cell." *J Cell Sci* **108** ( Pt 6): 2457-2464.
- Morrisette, N. S., J. M. Murray, et al. (1997). "Subpellicular microtubules associate with an intramembranous particle lattice in the protozoan parasite Toxoplasma gondii." *J Cell Sci* **110** ( Pt 1): 35-42.

- Morrisette, N. S. and L. D. Sibley (2002). "Cytoskeleton of apicomplexan parasites." Microbiol Mol Biol Rev **66**(1): 21-38; table of contents.
- Mukhopadhyay, A., A. M. Barbieri, et al. (1997). "Sequential actions of Rab5 and Rab7 regulate endocytosis in the *Xenopus* oocyte." J Cell Biol **136**(6): 1227-1237.
- Mukhopadhyay, A., K. Funato, et al. (1997). "Rab7 regulates transport from early to late endocytic compartments in *Xenopus* oocytes." J Biol Chem **272**(20): 13055-13059.
- Mukhopadhyay, A., E. Nieves, et al. (2011). "Proteomic analysis of endocytic vesicles: Rab1a regulates motility of early endocytic vesicles." J Cell Sci **124**(Pt 5): 765-775.
- Murray, J. T. and J. M. Backer (2005). "Analysis of hVps34/hVps15 interactions with Rab5 in vivo and in vitro." Methods Enzymol **403**: 789-799.
- Nam, H. W. (2009). "GRA proteins of *Toxoplasma gondii*: maintenance of host-parasite interactions across the parasitophorous vacuolar membrane." Korean J Parasitol **47 Suppl**: S29-37.
- Ngo, H. M., M. Yang, et al. (2004). "Are rhoptries in Apicomplexan parasites secretory granules or secretory lysosomal granules?" Mol Microbiol **52**(6): 1531-1541.
- Ngo, H. M., M. Yang, et al. (2003). "AP-1 in *Toxoplasma gondii* mediates biogenesis of the rhoptry secretory organelle from a post-Golgi compartment." J Biol Chem **278**(7): 5343-5352.
- Nichols, B. A. and M. L. Chiappino (1987). "Cytoskeleton of *Toxoplasma gondii*." J Protozool **34**(2): 217-226.
- Nicolle, C. and L. Manceaux (1908). "Sur une infection a corps de Leishman (ou organismes voisins) du gondi." CR Acad Sci **146**: 2207-2209.
- Nielsen, E., S. Christoforidis, et al. (2000). "Rabenosyn-5, a novel Rab5 effector, is complexed with hVPS45 and recruited to endosomes through a FYVE finger domain." J Cell Biol **151**(3): 601-612.
- Nishi, M., K. Hu, et al. (2008). "Organellar dynamics during the cell cycle of *Toxoplasma gondii*." J Cell Sci **121**(Pt 9): 1559-1568.
- Oksanen, A., M. Tryland, et al. (1998). "Serosurvey of *Toxoplasma gondii* in North Atlantic marine mammals by the use of agglutination test employing whole tachyzoites and dithiothreitol." Comp Immunol Microbiol Infect Dis **21**(2): 107-114.
- Opitz, C., M. Di Cristina, et al. (2002). "Intramembrane cleavage of microneme proteins at the surface of the apicomplexan parasite *Toxoplasma gondii*." EMBO J **21**(7): 1577-1585.
- Ossorio, P. N., J. F. Dubremetz, et al. (1994). "A soluble secretory protein of the intracellular parasite *Toxoplasma gondii* associates with the parasitophorous vacuole membrane through hydrophobic interactions." J Biol Chem **269**(21): 15350-15357.
- Ossorio, P. N., J. D. Schwartzman, et al. (1992). "A *Toxoplasma gondii* rhoptry protein associated with host cell penetration has unusual charge asymmetry." Mol Biochem Parasitol **50**(1): 1-15.
- Ozeki, S., J. Cheng, et al. (2005). "Rab18 localizes to lipid droplets and induces their close apposition to the endoplasmic reticulum-derived membrane." J Cell Sci **118**(Pt 12): 2601-2611.
- Pagano, A., P. Crottet, et al. (2004). "In vitro formation of recycling vesicles from endosomes requires adaptor protein-1/clathrin and is regulated by rab4 and the connector rabaptin-5." Mol Biol Cell **15**(11): 4990-5000.
- Palade, G. (1975). "Intracellular aspects of the process of protein synthesis." Science **189**(4200): 347-358.
- Pantazopoulou, A. and M. A. Penalva (2011). "Characterization of *Aspergillus nidulans* RabC/Rab6." Traffic **12**(4): 386-406.
- Parsons, M., A. DeRocher, et al. (2007). Protein targeting to the apicoplast. Toxoplasma molecular and cellular biology. J. W. Ajioka and D. Soldati. Norfolk, UK, Horizon Biosciences.
- Parussini, F., I. Coppens, et al. (2010). "Cathepsin L occupies a vacuolar compartment and is a protein maturase within the endo/exocytic system of *Toxoplasma gondii*." Mol Microbiol **76**(6): 1340-1357.
- Parussini, F., Q. Tang, et al. (2012). "Intramembrane proteolysis of *Toxoplasma* apical membrane antigen 1 facilitates host-cell invasion but is dispensable for replication." Proc Natl Acad Sci U S A **109**(19): 7463-7468.

- Patterson, G. H. and J. Lippincott-Schwartz (2002). "A photoactivatable GFP for selective photolabeling of proteins and cells." *Science* **297**(5588): 1873-1877.
- Pelissier, A., J. P. Chauvin, et al. (2003). "Trafficking through Rab11 endosomes is required for cellularization during *Drosophila* embryogenesis." *Curr Biol* **13**(21): 1848-1857.
- Pereira-Leal, J. B. and M. C. Seabra (2000). "The mammalian Rab family of small GTPases: definition of family and subfamily sequence motifs suggests a mechanism for functional specificity in the Ras superfamily." *J Mol Biol* **301**(4): 1077-1087.
- Pfeffer, S. R. (2005). "Structural clues to Rab GTPase functional diversity." *J Biol Chem* **280**(16): 15485-15488.
- Pflugger, S. L., H. V. Goodson, et al. (2005). "Receptor for retrograde transport in the apicomplexan parasite *Toxoplasma gondii*." *Eukaryot Cell* **4**(2): 432-442.
- Piper, R. C. and D. J. Katzmman (2007). "Biogenesis and function of multivesicular bodies." *Annu Rev Cell Dev Biol* **23**: 519-547.
- Plutner, H., A. D. Cox, et al. (1991). "Rab1b regulates vesicular transport between the endoplasmic reticulum and successive Golgi compartments." *J Cell Biol* **115**(1): 31-43.
- Ponnambalam, S. and S. A. Baldwin (2003). "Constitutive protein secretion from the trans-Golgi network to the plasma membrane." *Mol Membr Biol* **20**(2): 129-139.
- Pryor, P. R. and J. P. Luzio (2009). "Delivery of endocytosed membrane proteins to the lysosome." *Biochim Biophys Acta* **1793**(4): 615-624.
- Quevillon, E., T. Spielmann, et al. (2003). "The *Plasmodium falciparum* family of Rab GTPases." *Gene* **306**: 13-25.
- Rabenau, K. E., A. Sohrabi, et al. (2001). "TgM2AP participates in *Toxoplasma gondii* invasion of host cells and is tightly associated with the adhesive protein TgMIC2." *Mol Microbiol* **41**(3): 537-547.
- Rached, F. B., C. Ndjembo-Ezougou, et al. (2011). Construction of a *Plasmodium falciparum* Rab-interactome identifies CK1 and PKA as Rab-effector kinases in malaria parasites. *Biol Cell* **104**: 34-47.
- Reiss, M., N. Viebig, et al. (2001). "Identification and characterization of an escorter for two secretory adhesins in *Toxoplasma gondii*." *J Cell Biol* **152**(3): 563-578.
- Riglar, D. T., D. Richard, et al. (2011). "Super-resolution dissection of coordinated events during malaria parasite invasion of the human erythrocyte." *Cell Host Microbe* **9**(1): 9-20.
- Robert-Gangneux, F. and M. L. Darde (2012). "Epidemiology of and diagnostic strategies for toxoplasmosis." *Clin Microbiol Rev* **25**(2): 264-296.
- Robibaro, B., T. T. Stedman, et al. (2002). "*Toxoplasma gondii* Rab5 enhances cholesterol acquisition from host cells." *Cell Microbiol* **4**(3): 139-152.
- Robinson, J. S., D. J. Klionsky, et al. (1988). "Protein sorting in *Saccharomyces cerevisiae*: isolation of mutants defective in the delivery and processing of multiple vacuolar hydrolases." *Mol Cell Biol* **8**(11): 4936-4948.
- Rodrigues, C. O., F. A. Ruiz, et al. (2002). "Characterization of isolated acidocalcisomes from *Toxoplasma gondii* tachyzoites reveals a novel pool of hydrolyzable polyphosphate." *J Biol Chem* **277**(50): 48650-48656.
- Rodriguez-Boulan, E. and A. Musch (2005). "Protein sorting in the Golgi complex: shifting paradigms." *Biochim Biophys Acta* **1744**(3): 455-464.
- Roiko, M. S. and V. B. Carruthers (2009). "New roles for perforins and proteases in apicomplexan egress." *Cell Microbiol* **11**(10): 1444-1452.
- Roos, D. S. (1999). "The apicoplast as a potential therapeutic target in *Toxoplasma* and other apicomplexan parasites: some additional thoughts." *Parasitol Today* **15**(1): 41.
- Rosowski, E. E., D. Lu, et al. (2011). "Strain-specific activation of the NF-kappaB pathway by GRA15, a novel *Toxoplasma gondii* dense granule protein." *J Exp Med* **208**(1): 195-212.
- Rothman, J. E. (1986). "Life without clathrin." *Nature* **319**(6049): 96-97.
- Rothman, J. E. (1994). "Intracellular membrane fusion." *Adv Second Messenger Phosphoprotein Res* **29**: 81-96.
- Rothman, J. H. and T. H. Stevens (1986). "Protein sorting in yeast: mutants defective in vacuole biogenesis mislocalize vacuolar proteins into the late secretory pathway." *Cell* **47**(6): 1041-1051.

- Russell, M. R., D. P. Nickerson, et al. (2006). "Molecular mechanisms of late endosome morphology, identity and sorting." *Curr Opin Cell Biol* **18**(4): 422-428.
- Saeij, J. P., J. P. Boyle, et al. (2006). "Polymorphic secreted kinases are key virulence factors in toxoplasmosis." *Science* **314**(5806): 1780-1783.
- Saftig, P. and J. Klumperman (2009). "Lysosome biogenesis and lysosomal membrane proteins: trafficking meets function." *Nat Rev Mol Cell Biol* **10**(9): 623-635.
- Saito-Nakano, Y., B. N. Mitra, et al. (2007). "Two Rab7 isoforms, EhRab7A and EhRab7B, play distinct roles in biogenesis of lysosomes and phagosomes in the enteric protozoan parasite *Entamoeba histolytica*." *Cell Microbiol* **9**(7): 1796-1808.
- Santos, J., A. Graindorge, et al. (2012). "New insights into parasite rhomboid proteases." *Mol Biochem Parasitol* **182**(1-2): 27-36.
- Santos, J. M., D. J. Ferguson, et al. (2011). "Intramembrane cleavage of AMA1 triggers *Toxoplasma* to switch from an invasive to a replicative mode." *Science* **331**(6016): 473-477.
- Saouros, S., B. Edwards-Jones, et al. (2005). "A novel galectin-like domain from *Toxoplasma gondii* micronemal protein 1 assists the folding, assembly, and transport of a cell adhesion complex." *J Biol Chem* **280**(46): 38583-38591.
- Saraste, J. and K. Svensson (1991). "Distribution of the intermediate elements operating in ER to Golgi transport." *J Cell Sci* **100** ( Pt 3): 415-430.
- Sarkar, G. and S. S. Sommer (1990). "The "megaprimer" method of site-directed mutagenesis." *Biotechniques* **8**(4): 404-407.
- Sasidharan, N., M. Sumakovic, et al. (2012). "RAB-5 and RAB-10 cooperate to regulate neuropeptide release in *Caenorhabditis elegans*." *Proc Natl Acad Sci U S A* **109**(46): 18944-18949.
- Schmidt, D. J., D. J. Rose, et al. (2005). "Functional analysis of cytoplasmic dynein heavy chain in *Caenorhabditis elegans* with fast-acting temperature-sensitive mutations." *Mol Biol Cell* **16**(3): 1200-1212.
- Sclafani, A., S. Chen, et al. (2010). "Establishing a role for the GTPase Ypt1p at the late Golgi." *Traffic* **11**(4): 520-532.
- Seabra, M. C., E. H. Mules, et al. (2002). "Rab GTPases, intracellular traffic and disease." *Trends Mol Med* **8**(1): 23-30.
- Seaman, M. N., M. E. Harbour, et al. (2009). "Membrane recruitment of the cargo-selective retromer subcomplex is catalysed by the small GTPase Rab7 and inhibited by the Rab-GAP TBC1D5." *J Cell Sci* **122**(Pt 14): 2371-2382.
- Seeber, F., J. Limenitakis, et al. (2008). "Apicomplexan mitochondrial metabolism: a story of gains, losses and retentions." *Trends Parasitol* **24**(10): 468-478.
- Seeber, F. and D. Soldati (2007). The metabolic functions of the mitochondrion and the apicoplast. *Toxoplasma molecular and cellular biology*. J. W. Ajioka and D. Soldati. Norfolk, UK, Horizon Biosciences.
- Semerdjieva, S., B. Shortt, et al. (2008). "Coordinated regulation of AP2 uncoating from clathrin-coated vesicles by rab5 and hRME-6." *J Cell Biol* **183**(3): 499-511.
- Shao, S. and R. S. Hegde (2011). "Membrane protein insertion at the endoplasmic reticulum." *Annu Rev Cell Dev Biol* **27**: 25-56.
- Sheffield, H. G. and M. L. Melton (1968). "The fine structure and reproduction of *Toxoplasma gondii*." *J Parasitol* **54**(2): 209-226.
- Sheiner, L., J. M. Santos, et al. (2010). "*Toxoplasma gondii* transmembrane microneme proteins and their modular design." *Mol Microbiol*.
- Sheiner, L. and D. Soldati-Favre (2008). "Protein trafficking inside *Toxoplasma gondii*." *Traffic* **9**(5): 636-646.
- Sheiner, L. and B. Striepen (2012). "Protein sorting in complex plastids." *Biochim Biophys Acta*.
- Shin, H. W., M. Hayashi, et al. (2005). "An enzymatic cascade of Rab5 effectors regulates phosphoinositide turnover in the endocytic pathway." *J Cell Biol* **170**(4): 607-618.
- Sibley, L. D. and J. C. Boothroyd (1992). "Virulent strains of *Toxoplasma gondii* comprise a single clonal lineage." *Nature* **359**(6390): 82-85.

- Sibley, L. D., M. Messina, et al. (1994). "Stable DNA transformation in the obligate intracellular parasite *Toxoplasma gondii* by complementation of tryptophan auxotrophy." Proc Natl Acad Sci U S A **91**(12): 5508-5512.
- Sinai, A. P. (2008). "Biogenesis of and activities at the *Toxoplasma gondii* parasitophorous vacuole membrane." Subcell Biochem **47**: 155-164.
- Sinai, A. P. and K. A. Joiner (2001). "The *Toxoplasma gondii* protein ROP2 mediates host organelle association with the parasitophorous vacuole membrane." J Cell Biol **154**(1): 95-108.
- Singer-Kruger, B., H. Stenmark, et al. (1994). "Role of three rab5-like GTPases, Ypt51p, Ypt52p, and Ypt53p, in the endocytic and vacuolar protein sorting pathways of yeast." J Cell Biol **125**(2): 283-298.
- Singh, S., M. Plassmeyer, et al. (2007). "Mononeme: a new secretory organelle in *Plasmodium falciparum* merozoites identified by localization of rhomboid-1 protease." Proc Natl Acad Sci U S A **104**(50): 20043-20048.
- Skop, A. R., D. Bergmann, et al. (2001). "Completion of cytokinesis in *C. elegans* requires a brefeldin A-sensitive membrane accumulation at the cleavage furrow apex." Curr Biol **11**(10): 735-746.
- Sloves, P. J., S. Delhay, et al. (2012). "*Toxoplasma* sortilin-like receptor regulates protein transport and is essential for apical secretory organelle biogenesis and host infection." Cell Host Microbe **11**(5): 515-527.
- Soares, H. S., A. H. Minervino, et al. (2011). "Occurrence of *Toxoplasma gondii* antibodies in *Dasyprocta aguti* from Brazil: comparison of diagnostic techniques." J Zoo Wildl Med **42**(4): 763-765.
- Sohn, E. J., E. S. Kim, et al. (2003). "Rha1, an Arabidopsis Rab5 homolog, plays a critical role in the vacuolar trafficking of soluble cargo proteins." Plant Cell **15**(5): 1057-1070.
- Soldati, D. and J. C. Boothroyd (1993). "Transient transfection and expression in the obligate intracellular parasite *Toxoplasma gondii*." Science **260**(5106): 349-352.
- Soldati, D. and J. C. Boothroyd (1995). "A selector of transcription initiation in the protozoan parasite *Toxoplasma gondii*." Mol Cell Biol **15**(1): 87-93.
- Soldati, D., A. Lassen, et al. (1998). "Processing of *Toxoplasma* ROP1 protein in nascent rhoptries." Mol Biochem Parasitol **96**(1-2): 37-48.
- Soldati, D. and M. Meissner (2004). "*Toxoplasma* as a novel system for motility." Curr Opin Cell Biol **16**(1): 32-40.
- Sonnichsen, B., S. De Renzis, et al. (2000). "Distinct membrane domains on endosomes in the recycling pathway visualized by multicolor imaging of Rab4, Rab5, and Rab11." J Cell Biol **149**(4): 901-914.
- Spielmann, T., G. N. Montagna, et al. (2012). "Molecular make-up of the *Plasmodium* parasitophorous vacuolar membrane." Int J Med Microbiol **302**(4-5): 179-186.
- Spira, D., J. Stypmann, et al. (2007). "Cell type-specific functions of the lysosomal protease cathepsin L in the heart." J Biol Chem **282**(51): 37045-37052.
- Stedman, T. T., A. R. Sussmann, et al. (2003). "*Toxoplasma gondii* Rab6 mediates a retrograde pathway for sorting of constitutively secreted proteins to the Golgi complex." J Biol Chem **278**(7): 5433-5443.
- Stenmark, H. (2009). "Rab GTPases as coordinators of vesicle traffic." Nat Rev Mol Cell Biol **10**(8): 513-525.
- Stenmark, H. and V. M. Olkkonen (2001). "The Rab GTPase family." Genome Biol **2**(5): REVIEWS3007.
- Storrie, B., M. Micaroni, et al. (2012). "Electron tomography reveals Rab6 is essential to the trafficking of trans-Golgi clathrin and COPI-coated vesicles and the maintenance of Golgi cisternal number." Traffic **13**(5): 727-744.
- Straub, K. W., E. D. Peng, et al. (2011). "The moving junction protein RON8 facilitates firm attachment and host cell invasion in *Toxoplasma gondii*." PLoS Pathog **7**(3): e1002007.
- Striepen, B., C. N. Jordan, et al. (2007). "Building the perfect parasite: cell division in apicomplexa." PLoS Pathog **3**(6): e78.

- Struck, N. S., S. Herrmann, et al. (2008). "Spatial dissection of the cis- and trans-Golgi compartments in the malaria parasite *Plasmodium falciparum*." *Mol Microbiol* **67**(6): 1320-1330.
- Surolia, A., T. N. Ramya, et al. (2004). "'FAS't inhibition of malaria." *Biochem J* **383**(Pt. 3): 401-412.
- Takahashi, N., T. Kadowaki, et al. (1999). "Post-priming actions of ATP on Ca<sup>2+</sup>-dependent exocytosis in pancreatic beta cells." *Proc Natl Acad Sci U S A* **96**(2): 760-765.
- Tawk, L., G. Chicanne, et al. (2010). "Phosphatidylinositol 3-phosphate, an essential lipid in *Plasmodium*, localizes to the food vacuole membrane and the apicoplast." *Eukaryot Cell* **9**(10): 1519-1530.
- Tawk, L., J. F. Dubremetz, et al. (2011). "Phosphatidylinositol 3-monophosphate is involved in toxoplasma apicoplast biogenesis." *PLoS Pathog* **7**(2): e1001286.
- Thompson, J. D., D. G. Higgins, et al. (1994). "CLUSTAL W: improving the sensitivity of progressive multiple sequence alignment through sequence weighting, position-specific gap penalties and weight matrix choice." *Nucleic Acids Res* **22**(22): 4673-4680.
- Tilney, L. G. and M. S. Tilney (1996). "The cytoskeleton of protozoan parasites." *Curr Opin Cell Biol* **8**(1): 43-48.
- Tisdale, E. J. and W. E. Balch (1996). "Rab2 is essential for the maturation of pre-Golgi intermediates." *J Biol Chem* **271**(46): 29372-29379.
- Tisdale, E. J., J. R. Bourne, et al. (1992). "GTP-binding mutants of rab1 and rab2 are potent inhibitors of vesicular transport from the endoplasmic reticulum to the Golgi complex." *J Cell Biol* **119**(4): 749-761.
- Tisdale, E. J. and M. R. Jackson (1998). "Rab2 protein enhances coatamer recruitment to pre-Golgi intermediates." *J Biol Chem* **273**(27): 17269-17277.
- Tomova, C., B. M. Humbel, et al. (2009). "Membrane contact sites between apicoplast and ER in *Toxoplasma gondii* revealed by electron tomography." *Traffic* **10**(10): 1471-1480.
- Tonkin, M. L., M. Roques, et al. (2011). "Host cell invasion by apicomplexan parasites: insights from the co-structure of AMA1 with a RON2 peptide." *Science* **333**(6041): 463-467.
- Tooze, S. A. (1998). "Biogenesis of secretory granules in the trans-Golgi network of neuroendocrine and endocrine cells." *Biochim Biophys Acta* **1404**(1-2): 231-244.
- Touchot, N., A. Zahraoui, et al. (1989). "Biochemical properties of the YPT-related rab1B protein. Comparison with rab1A." *FEBS Lett* **256**(1-2): 79-84.
- Towbin, H., T. Staehelin, et al. (1979). "Electrophoretic transfer of proteins from polyacrylamide gels to nitrocellulose sheets: procedure and some applications." *Proc Natl Acad Sci U S A* **76**(9): 4350-4354.
- Turetzky, J. M., D. K. Chu, et al. (2010). "Processing and secretion of ROP13: A unique *Toxoplasma* effector protein." *Int J Parasitol* **40**(9): 1037-1044.
- Tyler, J. S., M. Treeck, et al. (2011). "Focus on the ringleader: the role of AMA1 in apicomplexan invasion and replication." *Trends Parasitol* **27**(9): 410-420.
- Ueda, T., M. Yamaguchi, et al. (2001). "Ara6, a plant-unique novel type Rab GTPase, functions in the endocytic pathway of *Arabidopsis thaliana*." *EMBO J* **20**(17): 4730-4741.
- Vaishnav, S. and B. Striepen (2006). "The cell biology of secondary endosymbiosis--how parasites build, divide and segregate the apicoplast." *Mol Microbiol* **61**(6): 1380-1387.
- Valls, L. A., C. P. Hunter, et al. (1987). "Protein sorting in yeast: the localization determinant of yeast vacuolar carboxypeptidase Y resides in the propeptide." *Cell* **48**(5): 887-897.
- van der Goot, F. G. and J. Gruenberg (2006). "Intra-endosomal membrane traffic." *Trends Cell Biol* **16**(10): 514-521.
- van der Sluijs, P., M. Hull, et al. (1992). "The small GTP-binding protein rab4 controls an early sorting event on the endocytic pathway." *Cell* **70**(5): 729-740.
- Van Der Sluijs, P., M. Hull, et al. (1991). "The small GTP-binding protein rab4 is associated with early endosomes." *Proc Natl Acad Sci U S A* **88**(14): 6313-6317.
- van Dooren, G. G., S. B. Reiff, et al. (2009). "A novel dynamin-related protein has been recruited for apicoplast fission in *Toxoplasma gondii*." *Curr Biol* **19**(4): 267-276.
- van Dooren, G. G., C. Tomova, et al. (2008). "*Toxoplasma gondii* Tic20 is essential for apicoplast protein import." *Proc Natl Acad Sci U S A* **105**(36): 13574-13579.

- Vanlandingham, P. A. and B. P. Ceresa (2009). "Rab7 regulates late endocytic trafficking downstream of multivesicular body biogenesis and cargo sequestration." *J Biol Chem* **284**(18): 12110-12124.
- Vazquez-Martinez, R., D. Cruz-Garcia, et al. (2007). "Rab18 inhibits secretory activity in neuroendocrine cells by interacting with secretory granules." *Traffic* **8**(7): 867-882.
- Vazquez-Martinez, R., A. Diaz-Ruiz, et al. (2012). "Revisiting the regulated secretory pathway: from frogs to human." *Gen Comp Endocrinol* **175**(1): 1-9.
- Vežina, C., A. Kudelski, et al. (1975). "Rapamycin (AY-22,989), a new antifungal antibiotic. I. Taxonomy of the producing streptomycete and isolation of the active principle." *J Antibiot (Tokyo)* **28**(10): 721-726.
- Vonderheit, A. and A. Helenius (2005). "Rab7 associates with early endosomes to mediate sorting and transport of Semliki forest virus to late endosomes." *PLoS Biol* **3**(7): e233.
- Vutova, K., Z. Peicheva, et al. (2002). "Congenital toxoplasmosis: eye manifestations in infants and children." *Ann Trop Paediatr* **22**(3): 213-218.
- Waller, R. F., P. J. Keeling, et al. (1998). "Nuclear-encoded proteins target to the plastid in *Toxoplasma gondii* and *Plasmodium falciparum*." *Proc Natl Acad Sci U S A* **95**(21): 12352-12357.
- Waller, R. F., P. J. Keeling, et al. (2003). "Comment on "A green algal apicoplast ancestor"." *Science* **301**(5629): 49; author reply 49.
- Waller, R. F., M. B. Reed, et al. (2000). "Protein trafficking to the plastid of *Plasmodium falciparum* is via the secretory pathway." *EMBO J* **19**(8): 1794-1802.
- Werk, R. (1985). "How does *Toxoplasma gondii* enter host cells?" *Rev Infect Dis* **7**(4): 449-457.
- Wetzel, D. M., S. Hakansson, et al. (2003). "Actin filament polymerization regulates gliding motility by apicomplexan parasites." *Mol Biol Cell* **14**(2): 396-406.
- WHO (2012). "World Malaria Report."
- Whyte, J. R. and S. Munro (2002). "Vesicle tethering complexes in membrane traffic." *J Cell Sci* **115**(Pt 13): 2627-2637.
- Wilson, R. J., P. W. Denny, et al. (1996). "Complete gene map of the plastid-like DNA of the malaria parasite *Plasmodium falciparum*." *J Mol Biol* **261**(2): 155-172.
- Wilson, R. J. and D. H. Williamson (1997). "Extrachromosomal DNA in the Apicomplexa." *Microbiol Mol Biol Rev* **61**(1): 1-16.
- Xu, P., G. Widmer, et al. (2004). "The genome of *Cryptosporidium hominis*." *Nature* **431**(7012): 1107-1112.
- Yeoh, S., R. A. O'Donnell, et al. (2007). "Subcellular discharge of a serine protease mediates release of invasive malaria parasites from host erythrocytes." *Cell* **131**(6): 1072-1083.
- Yudowski, G. A., M. A. Puthenveedu, et al. (2009). "Cargo-mediated regulation of a rapid Rab4-dependent recycling pathway." *Mol Biol Cell* **20**(11): 2774-2784.
- Zeigerer, A., J. Gilleron, et al. (2012). "Rab5 is necessary for the biogenesis of the endolysosomal system in vivo." *Nature* **485**(7399): 465-470.
- Zhou, X. W., B. F. Kafsack, et al. (2005). "The opportunistic pathogen *Toxoplasma gondii* deploys a diverse legion of invasion and survival proteins." *J Biol Chem* **280**(40): 34233-34244.
- Zuleger, N., A. R. Kerr, et al. (2012). "Many mechanisms, one entrance: membrane protein translocation into the nucleus." *Cell Mol Life Sci* **69**(13): 2205-2216.